

Copyright  
by  
Dimitri Mikhailovich Khramov  
2008

**The Dissertation Committee for Dimitri Mikhailovich Khramov Certifies that this is  
the approved version of the following dissertation:**

**Novel N-Heterocyclic Carbenes: Applications in Materials Chemistry  
and Catalysis**

**Committee:**

---

Christopher W. Bielawski, Supervisor

---

C. Grant Willson

---

Eric V. Anslyn

---

Alan H. Cowley

---

Sean M. Kerwin

**Novel N-Heterocyclic Carbenes: Applications in Materials Chemistry  
and Catalysis**

**by**

**Dimitri Mikhailovich Khramov, B.S.**

**Dissertation**

Presented to the Faculty of the Graduate School of  
The University of Texas at Austin  
in Partial Fulfillment  
of the Requirements  
for the Degree of

**Doctor of Philosophy**

**The University of Texas at Austin  
May, 2008**

## **Dedication**

To Anastasia Grega: I met you the first week I moved to Texas and ever since you have been by my side, always supporting me and making me laugh when my spirits were down. Without your support and encouragement, this would not have been possible.

And to my family for everything they have done for me.

Thank you.

## Acknowledgements

First, I would like to thank my advisor Prof. Chris Bielawski. I joined his group in my 3<sup>rd</sup> year as a graduate student. On my first day at work, on my first project, I promptly threw away 5 grams of analytically pure product straight into the trash can. Thankfully, that has not been the case since then. Working for Chris has been an amazing experience. With Chris' unique vision and approach to mentoring, I have been able to take charge of my career and develop it with unimaginable freedom. I feel that working for Chris pushed my professional abilities as a chemist to level that will be hard to surpass for many years to come.

The entire Bielawski group deserves a very warm thank you for many memorable years in the graduate school. While the daily routine of graduate school, at times, is very rough, I always looked forward to coming in to work because of them. Their energy and scientific curiosity have generated many great ideas, many of which ultimately transformed into very successful projects.

Dr. Vince Lynch was another great co-worker that I have met at UT. I want to thank him for solving numerous X-Ray structures and being patient enough to answer my questions about crystallography. With his seemingly magical ability to find X-ray quality crystals in my samples, I am almost convinced that amorphous materials do not exist.

Michael Ronalter is the glass-blower at UT and a great person that I was fortunate enough to meet during my time here. Besides fixing my broken glass, and keeping the boss happy with low bills for new flasks, I have learned a lot of interesting things from Mike about the art of glass-blowing.

I am grateful for the support of my committee members, Prof. Willson, Prof. Anslyn, Prof. Cowley, and Prof. Kerwin. I cannot even fathom how much you have taught me through formal classes and personal advice. Special thanks to Prof. Willson, his advices helped me to get through a rough start in my graduate school career. Also, I would like to extend special thanks to Jeff Gorman, Julie Le, Hongda Zhao, and Darren Engers. With their help I managed to avoid lots (though not all) pitfalls that I encountered at the beginning of my graduate school career.

**Novel N-Heterocyclic Carbenes: Applications in Materials Chemistry  
and Catalysis**

Publication No. \_\_\_\_\_

Dimitri Mikhailovich Khramov, Ph.D.

The University of Texas at Austin, 2008

Supervisor: Christopher W. Bielawski

A unifying theme of the chemistry presented is the synthesis, study, and application of a novel N-heterocyclic carbenes. Pursuit of these materials has resulted in new advances in carbene structure and bonding, the discovery of highly-efficient reactions, and the development of new polymers with unusual properties.

## Table of Contents

Chapter 1: Introduction .....	1
N-Heterocyclic Carbenes .....	1
References.....	7
Chapter 2: Triazene formation via reaction of imidazol-2-ylidenes with azide ....	11
Abstract.....	11
Introduction.....	11
Results.....	11
Conclusion .....	16
Experimental .....	16
References.....	24
Chapter 3: Highly Efficient Synthesis and Solid-State Characterization of 1,2,4,5-Tetrakis(alkyl- and arylamino)benzenes and Cyclization to their Respective Benzobis(imidazolium) Salts .....	27
Abstract.....	27
Introduction.....	27
Results.....	29
Conclusion .....	34
Experimental .....	35
References.....	42
Chapter 4: An alternative synthesis of benzobis(imidazolium) salts via a “one-pot” cyclization/oxidation reaction sequence .....	46
Abstract.....	46
Introduction.....	46
Results.....	48
Conclusion .....	50
References.....	51

Chapter 5: Synthesis and Study of Janus Bis(carbene)s and Their Transition Metal Complexes.....	55
Introduction.....	55
Results.....	55
Conclusion .....	61
Experimental .....	62
References.....	71
Chapter 6: Donor-Acceptor Triazenes: Synthesis, Characterization, and Study of Their Electronic and Thermal Properties.....	75
Abstract.....	75
Introduction.....	76
Results.....	79
Conclusion .....	96
Experimental .....	98
References.....	113
Chapter 7: N-Heterocyclic Carbene – Transition Metal Complexes: Spectroscopic and Crystallographic Analyses of $\pi$ -Backbonding Interactions .....	119
Abstract.....	119
Introduction.....	120
Results.....	125
Conclusion .....	135
Experimental .....	136
References.....	143
Chapter 8: Diaminocarbene[3]ferrocenophanes and Their Transition Metal Complexes.....	148
Introduction.....	148
Results.....	148
Conclusion .....	155
Experimental .....	156
References.....	165

Chapter 9: N-Heterocyclic carbenes: Deducing $\sigma$ - and $\pi$ - contributions in Rh-mediated hydroboration and Pd-mediated coupling reactions.....	170
Abstract.....	170
Introduction.....	170
Results.....	175
Conclusion .....	194
Experimental .....	195
References.....	201
Appendix A: Synthesis of Methyl 2-(trifluoromethyl)acrylate .....	206
Experimental .....	206
References.....	207
Vita .....	208

## List of Tables

Table 2.1: Synthesis of substituted imidazol-2-ylidenes.....	13
Table 3.1: Synthesis of 1,2,4,5-tetrakis(alkyl- and arylamino)benzenes .....	32
Table 6.1: Synthesis of donor-acceptor triazenes bearing bulky N- <i>tert</i> -butyl groups .....	81
Table 6.2: Summary of key UV-Vis absorbance data for triazenes <b>6.1</b> .....	84
Table 6.3: Synthesis and UV-Vis data of crystalline triazenes bearing N-methyl groups.....	87
Table 6.4: Selected bond lengths (Å) and angles (°) for triazenes <b>6.3</b> .....	90
Table 6.5: Selected bond crystal data for triazenes <b>6.3</b> .....	91
Table 6.6: Steric and electronic effects on triazene stability .....	93
Table 6.S1: Rate constants for a variety of triazene forming reactions. ....	105
Table 6.S2: Absolute energy, calculated dipole moment, and coordinates for triazene <b>6.3-H-H</b> ( <i>cf.</i> Table 6.3, Entry 1) at B3LYP/6-31G*-level of theory.....	108
Table 6.S3: Absolute energy, calculated dipole moment, and coordinates for triazene <b>6.3-H-NO<sub>2</sub></b> ( <i>cf.</i> Table 6.3, Entry 2) at B3LYP/6-31G*-level of theory.....	109
Table 6.S4: Absolute energy, calculated dipole moment, and coordinates for triazene <b>6.3-OCH<sub>3</sub>-H</b> ( <i>cf.</i> Table 6.3, Entry 3) at B3LYP/6-31G*-level of theory.....	110
Table 6.S5: Absolute energy, calculated dipole moment, and coordinates for triazene <b>6.3-OCH<sub>3</sub>-NO<sub>2</sub></b> ( <i>cf.</i> Table 6.3, Entry 4) at B3LYP/6-31G*-level of theory. <sup>48</sup> .....	111

Table 7.1: Selected IR stretching frequencies of CN groups in a variety of NHC-metal complexes.....	127
Table 7.2: $^1\text{H}$ NMR chemical shifts of the protons on the olefin <i>trans</i> to the NHC ligand.....	130
Table 7.3: Selected carbonyl stretching frequencies for a series of (NHC)Rh(CO) <sub>2</sub> Cl complexes.....	131
Table 7.4: Selected crystal data for Rh complexes <b>7.9</b> .....	135
Table 9.1: Spectroscopic properties of various NHC-Rh complexes. ....	177
Table 9.2: Hydroboration of alkynes catalyzed by various Rh complexes.....	181
Table 9.3: Selected bond lengths ( $\text{\AA}$ ) and angles ( $^\circ$ ) for Pd complexes <b>9.8</b> ....	188
Table 9.4: Yields of products obtained by coupling <i>tert</i> -butyl acrylate with various aryl halides using NHC-Pd complexes <b>9.8</b> as catalysts and NaOAc as base. .....	189
Table 9.5: Yields of products obtained by coupling phenylboronic acid with various aryl halides using NHC-Pd complexes <b>9.8</b> as catalysts and K <sub>2</sub> CO <sub>3</sub> as base.....	193

## List of Figures

Figure 1.1: Singlet and triplet carbenes.....	1
Figure 1.2: Persistent carbene.....	2
Figure 1.3: Lemals cross-dimer experiment.....	3
Figure 1.4: Representative examples of an N-heterocyclic carbene (NHC) ( <b>1.2</b> ) and catalytically-active transition metal complexes bearing NHCs ( <b>1.3</b> and <b>1.4</b> ).....	4
Figure 1.5: Representative examples of heteroatom carbenes.....	5
Figure 2.1: ORTEP representation of the X-ray crystal structure of (Z)-N-benzyl 1,3-dimesitylimidazol-2-ylidenetriazene ( <b>2.3</b> ).....	15
Figure 2.2: ORTEP representation of the X-ray crystal structure of (E)-N-benzyl 1,3-dimesitylimidazol-2-ylidenetriazene ( <b>2.3</b> ).....	15
Figure 3.1: Reduced and oxidized states of 1,2,4,5-tetraaminobenzene.....	28
Figure 3.2: ORTEP representations of the X-ray crystal structures of 1,2,4,5-tetrakis( <i>tert</i> -butylamino)benzene ( <b>3.4</b> ) (left) and N,N',N'',N'''-tetrakis( <i>tert</i> -butyl) 1,4-diamino-2,5-benzoquinone-diimine ( <b>3.5</b> ) (right) .....	31
Figure 4.1: ORTEP drawing of <b>4.7b</b> .....	50
Figure 5.1: ORTEP view of <b>5.2a</b> .....	57
Figure 5.2: ORTEP view of <b>5.3a</b> .....	58
Figure 5.3: ORTEP view of <b>5.3c</b> .....	59
Figure 5.4: ORTEP view of <b>5.5</b> .....	61
Figure 6.1: Triazene formation via coupling of a N-heterocyclic carbene with an azide.....	77

Figure 6.2: UV-Vis absorbance spectra (left) color coded with their respective compound (right).	83
Figure 6.3: (top) Illustration of two resonance structures for triazenes containing donor (D) and acceptor (A) groups. (bottom) Key bond lengths for 1-(1,3-dimesityl-imidazol-2-ylidene)-3-benzyl-triazene.	86
Figure 6.4: UV-Vis absorbance spectra (left) color coded with their respective compound (right)	88
Figure 6.5: ORTEP diagrams for (a) <b>6.3-H-H</b> , (b) <b>6.3-H-NO<sub>2</sub></b> , (c) <b>6.3-OCH<sub>3</sub>-H</b> , (d) <b>6.3-OCH<sub>3</sub>-NO<sub>2</sub></b> .	89
Figure 6.6: Guanidine formation from triazene <i>via</i> loss of nitrogen	92
Figure 6.7: Illustration of the Staudinger reaction	95
Figure 6.8: Proposed mechanism of thermally-induced triazene decomposition based on a <sup>15</sup> N-labeling experiment	96
Figure 6.S1: Plot of 1/[substrate] versus time for the reaction of 1,3-di- <i>tert</i> -butylbenzimidazol-2-ylidene with phenylazide	106
Figure 6.S2: Plot of 1/[substrate] versus time for the reaction of 1,3-di- <i>tert</i> -butylbenzimidazol-2-ylidene with para-methoxyphenyl azide	106
Figure 6.S3: Plot of 1/[substrate] versus time for the reaction of 1,3-di- <i>tert</i> -butylbenzimidazol-2-ylidene with para-nitrophenyl azide	107
Figure 7.1: Examples of metal complexes used to study $\pi$ -backbonding in NHCs..	122
Figure 7.2: Basic design for evaluating $\pi$ -backbonding in a range of NHC metal complexes using IR and NMR spectroscopies	124
Figure 7.3: Synthesis of various metal complexes containing 4,5-disubstituted-imidazol-2-ylidenes	126

Figure 7.4: Dominant resonance contributors for complexes 9-CN (left) and 10-CN (right).....	127
Figure 7.5: (a) Expected changes in key bond lengths as the $\pi$ -backbonding ability of the NHC ligand increases. (b) Summary of key bond lengths observed for a series of (NHC)Rh(cod)Cl complexes with NHC ligands of varying degrees of $\pi$ -acidity.....	132
Figure 7.6: ORTEP diagrams of (A) 7.9-H, (B) 7.9-Cl, (C) 7.9-NO <sub>2</sub> and (D) 7.9-CN. ....	133
Figure 8.1: ORTEP view of <b>8.1a</b> .....	151
Figure 8.2: ORTEP view of <b>8.3a</b> .....	152
Figure 8.3: ORTEP view of <b>8.4a</b> .....	153
Figure 8.4: ORTEP view of <b>8.3b</b> .....	154
Figure 8.5: (top) Superimposed difference FT-IR spectra showing (bottom) the disappearance of <b>8.4a</b> ( $\nu_{CO} = 2070, 1992 \text{ cm}^{-1}$ ) with concomitant formation of <b>8.4a</b> <sup>+</sup> ( $\nu_{CO} = 2088, 2015 \text{ cm}^{-1}$ ). .....	155
Figure 8.6: Cyclic voltammograms for <b>8.1a</b> (left) and <b>8.1b</b> (right). ....	163
Figure 8.7: Cyclic voltammograms for <b>8.3a</b> (left) and <b>8.3b</b> (right). ....	164
Figure 8.8: Cyclic voltammograms for <b>8.4a</b> (left) and <b>8.4b</b> (right). ....	164
Figure 8.9: Spectroelectrochemical cell in pieces (left) and assembled (right).165	
Figure 9.1: Representative examples of an N-heterocyclic carbene (NHC) ( <b>9.1</b> ) and catalytically-active transition metal complexes bearing NHCs ( <b>9.2</b> and <b>9.3</b> ). ....	172
Figure 9.2: Representative complexes used for examining the electron donating properties of N-heterocyclic carbenes. ....	173

Figure 9.3: Suzuki cross coupling reactions using Pd complexes ligated to electronically-different N-heterocyclic carbenes .....	174
Figure 9.4: Structures of Rh olefin ( <b>9.6</b> ) and carbonyl ( <b>9.7</b> ) complexes.....	176
Figure 9.5: ORTEP drawing of <b>9.6-CF<sub>3</sub></b> .....	178
Figure 9.6: Proposed general reaction scheme for the hydroborations of alkynes catalyzed by Rh-NHC complexes.....	184
Figure 9.7: Synthesis of Pd-NHC complexes <b>9.8</b> .....	187
Figure 9.8: ORTEP diagram of <b>9.8-Cl</b> .....	187
Figure 9.9: Generally accepted mechanism for Pd-catalyzed cross-coupling reactions.....	191
Figure 9.10: Plots of yield versus time for the Heck reaction of tert-butylacrylate with 4-bromoanisole, as catalyzed by <b>9.8-H</b> and <b>9.8-CN</b> .....	192
Figure A.1: Esterification of 2-(trifluoromethyl)acrylic acid.....	206

## List of Schemes

Scheme 1.1: NHCs in organic chemistry.....	6
Scheme 3.1: Synthesis of 1,2,4,5-tetrakis(tert-butylamino)benzene ( <b>3.4</b> ) and its related 2,5-diamino-1,4-quinonediimine ( <b>3.5</b> ).....	29
Scheme 3.3: Synthesis of tetrakis(aryl amino)arenes .....	38
Scheme 3.4: Cyclization of tetraamines to give bis(azolium) salts .....	34
Scheme 4.1: The <i>o</i> -tautomer of 2,5-diamino-1,4-benzoquinonediimine ( <b>4.1-o</b> ). .	47
Scheme 4.2: Conversion of 2,5-diamino-1,4-quinonediimines to their respective benzobis(imidazolium) salts using a “one-pot” cyclization/ oxidation reaction sequence.....	49
Scheme 5.1: Synthesis of benzobis(imidazolylidene)s and their related transition metal complexes.....	55
Scheme 5.2: Selective dimerization and oxidation of a desymmetrized Janus bis(carbene) precursor.....	61
Scheme 8.1: Synthesis of diaminocarbene[3]ferrocenophanes and related bimetallic complexes.....	150

## List of Abbreviations

Ad	adamantyl
Bn	benzyl
Bu	butyl
cat.	catalytic
d	doublet
DMF	N,N-dimethylformamide
DMSO	dimethyl sulfoxide
equiv.	equivalents
HRMS	high resolution mass spectrometry
Imid.	imidazole
IPr	1,3-bis(2,6-diisopropylphenyl)imidazole-2-ylidene
IPr•HCl	1,3-bis(2,6-diisopropylphenyl)imidazolium chloride
IR	infrared
KHMDS	potassium bis(trimethylsilyl)amide
LDA	lithium diisopropylamide
<i>m</i>	meta
M	molar
<i>m</i>	multiplet
m.p.	melting point
Me	methyl
Mes	mesityl
mol	mole
NaHMDS	sodium bis(trimethylsilyl)amide
NHC	N-heterocyclic carbene
<i>o</i>	ortho
<i>p</i>	para
Ph	phenyl
Pyr	pyridine
<i>q</i>	quartet
RT	room temperature
<i>s</i>	singlet
<i>t</i>	triplet'
<i>t</i> Bu	<i>tert</i> -butyl
THF	tetrahydrofuran

## Chapter 1: Introduction

### N-HETEROCYCLIC CARBENES

Carbenes are defined as divalent 6-electron carbon atoms of general formula  $R_1R_2C$ . Carbenes can be classified into two groups: singlet carbenes and triplet carbenes (figure 1.1). The singlet type has its carbon atom  $sp^2$  hybridized with an empty p-orbital. Triplet carbenes have two unpaired electrons each occupying a separate orbital. For simple hydrocarbons, triplet carbenes usually have energies lower than singlet carbenes. However, inclusion of substituents that can donate electron pairs may stabilize the singlet state by delocalizing the electron pair into an empty p-orbital, thus making the singlet state more stable than the triplet state.

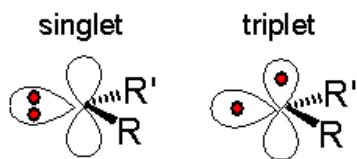


Figure 1.1 Singlet and triplet carbenes.

A specific subset of carbenes that are covered in this dissertation is a so-called persistent N-heterocyclic carbenes **1.1** (figure 1.2). This particular class of carbenes was chosen due to their remarkable stability despite being reactive intermediates. Due to the presence of electron donating atoms around the carbene center, NHCs adopt a singlet state with a lone pair in a  $sp^2$  hybridized orbital and an empty p-orbital. The remarkable stability of the carbene comes from bulky N-groups that prevent homodimerization due to electrostatic repulsion and electron lone pairs on the nitrogen atoms flanking the carbene center. Formally, a 5-center, 6-electron system, NHCs possess a significant delocalization of electrons in the ring, thus further lowering their reactivity due aromatic stabilization.

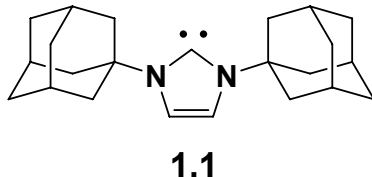


Figure 1.2 Persistent carbene.

Although first proposed by Breslow in the 1957<sup>1</sup>, a significant amount of work on NHC dimers has been performed by Wanzlick in 1960s,<sup>2</sup> followed by isolation of a stable carbene by Bertrand<sup>3</sup>. Finally, isolation of a crystalline, air-stable NHC by Arduengo et al<sup>4</sup> has demonstrated how remarkably stable the NHCs really are. Over the years most of the published work on the NHC chemistry can be categorized into 3 distinct areas: 1) Dimerization chemistry (i.e. “Wanzlick equilibrium”); 2) Organometallic chemistry (i.e. Grubbs 2<sup>nd</sup> generation metathesis catalyst); 3) Adducts with electrophiles (i.e. organocatalysis).

### “Wanzlick” Equilibrium

The term “Wanzlick equilibrium” has been created following the extensive work by Wanzlick in the area of carbene dimerization. Wanzlick *et al.* believed that once prepared, these carbenes existed in an unfavorable equilibrium with its corresponding dimer. This assertion was based on reactivity studies which they believed showed that the free carbene was the active species, reacting with electrophiles, while the dimer was inactive to these electrophiles, and merely acted as a stable carbene reservoir.<sup>5</sup> Lemal<sup>6</sup> has tested Wanzlick’s claims of a carbene-dimer equilibrium by heating together two differently N-aryl substituted tetraaminoethylenes. This reaction did not produce a mixed dimeric product, and thus indicated that carbene-dimer equilibrium does not exist for dihydroimidazol-2-ylidenes.

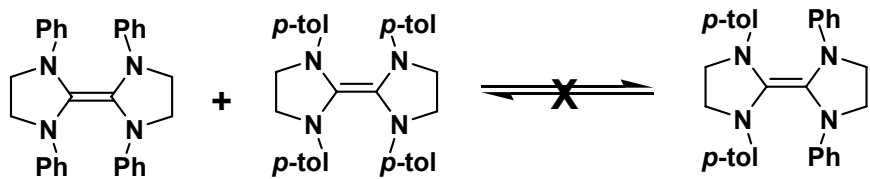


Figure 1.3 Lemals cross-dimer experiment.

Recently, refuting some of the earlier work, the reversible nature of Wanzlick equilibrium has been demonstrated in the work describing new class of dynamic reversible materials.<sup>7</sup> The report conclusively showed the dependence on molecular weight as a function of concentration, thus providing evidence of the dynamic nature of Wanzlick equilibrium. Furthermore, addition of differentially substituted mono-functional carbenes provided a first example of elusive cross-dimer while limiting the molecular weight of the polymer in the studies. Overall, while great strides of progress have been made in studies of reversible nature of the carbene dimers, their extreme air sensitivity<sup>7</sup> has limited their practical applications.<sup>8</sup>

### Carbenes in Organometallic Chemistry

Over the past 40 years,<sup>9</sup> N-heterocyclic carbenes (NHCs) (**1.2**)<sup>10</sup> have blossomed into a class of ligands that have proven to be useful for a broad range of transition metals.<sup>11,12</sup> As strong, two-electron donors, they generally coordinate to metals in a fashion that is analogous to phosphines;<sup>13</sup> however, in many instances, they often produce complexes which are more thermally-stable<sup>14</sup> and/or exhibit higher catalytic activities.<sup>11</sup> NHCs are often the ligand of choice for applications ranging from metal-mediated catalysis to organometallic materials.<sup>11,15</sup> Prime examples include the Grubbs 2<sup>nd</sup> generation (**1.3**)<sup>16</sup> and PEPPSI<sup>17</sup> catalysts (**1.3**) (see Figure 1.4), both of which show

higher catalytic activities in olefin metathesis and cross-coupling reactions, respectively, than many of their phosphine-ligated counterparts.

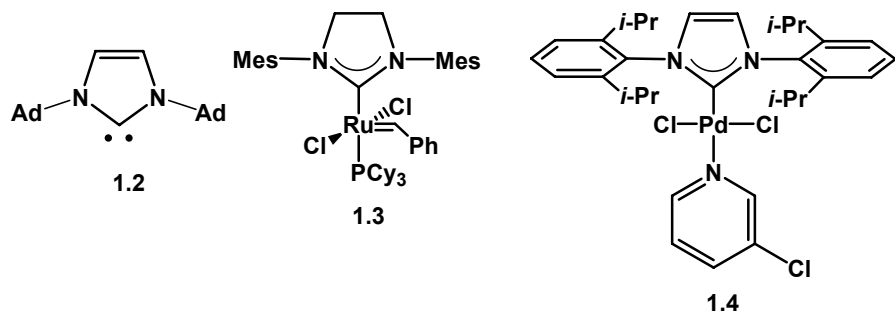


Figure 1.4 Representative examples of an N-heterocyclic carbene (NHC) (**1.2**) and catalytically-active transition metal complexes bearing NHCs (**1.3** and **1.4**). Ad = adamantyl, Mes = 2,4,6-trimethylbenzene, i-Pr = *iso*-propyl.

Considering the number of synthetic methods known to prepare these compounds,<sup>18</sup> NHCs are often the ligand of choice for applications ranging from metal-mediated catalysis to organometallic materials.<sup>11,19</sup> In addition to imidazole-2-ylidenes, many variations of NHCs have appeared in the literature such as imidazol-2-ylidenes (**1.5**), triazol-5-ylidenes (**1.6**)<sup>20</sup>, cyclic (**1.7**)<sup>21</sup> and acyclic diaminocarbenes (**1.8**)<sup>22</sup>, heteroamino carbenes (**1.9**)<sup>23</sup> and other nucleophilic carbenes (**1.10**)<sup>24</sup>. The synthesis of these novel systems is driven by the desire to explore structure-activity relationship in organic or organometallic catalysis.

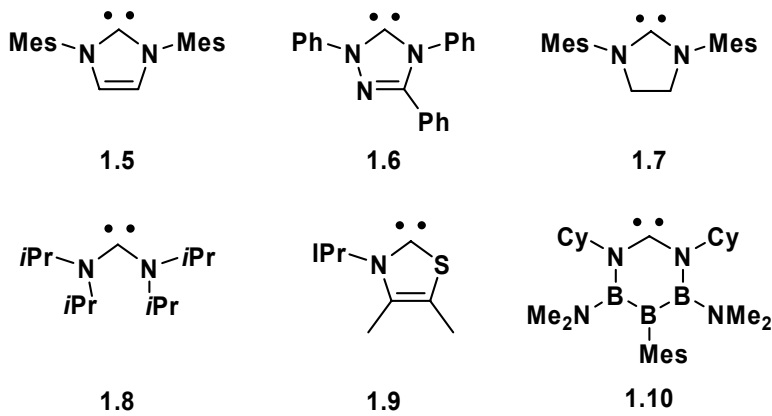


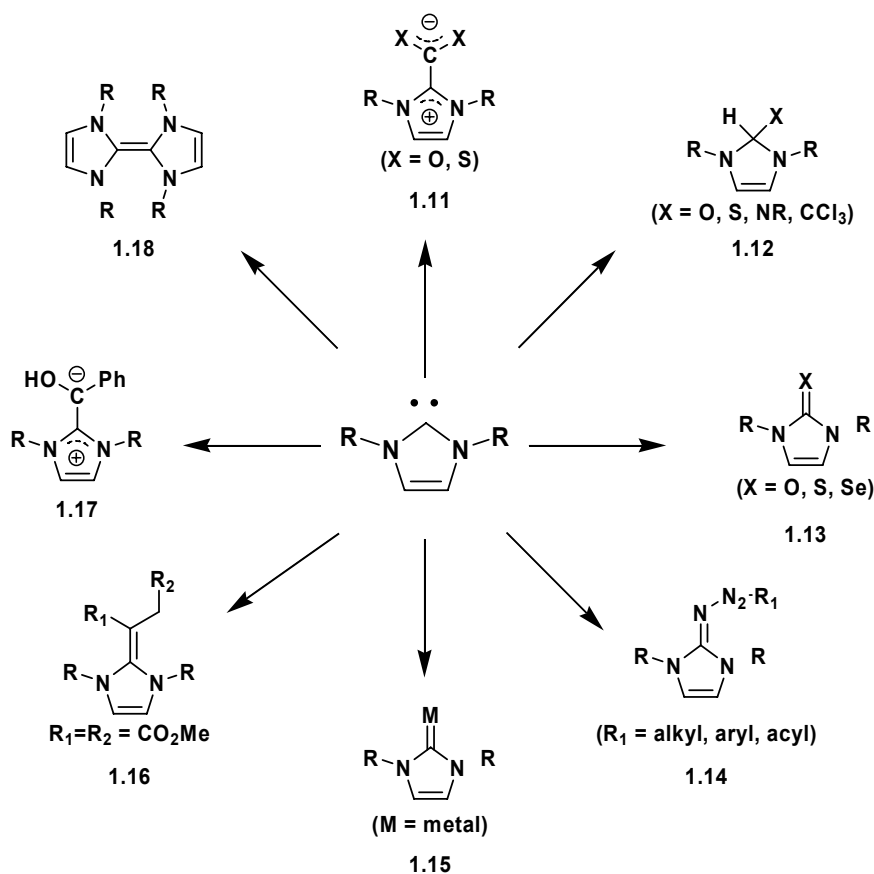
Figure 1.5 Representative examples of heteroatom carbenes. Mes = mesityl, IPr = 2,6-diisopropyl phenyl, Cy = cyclohexyl.

### Carbenes in Organic Chemistry.

Due to the lone pairs present on nitrogen atoms next to the carbene carbon, the p-orbital of the carbene is mostly filled; therefore NHCs predominantly act as strong nucleophiles. While the chemistry of NHCs with organic coupling partners has not been fully explored, numerous adducts have been reported to date. Examples of rich chemistry of NHCs are illustrated in scheme 1.1. Carbenes undergo reactions with CO<sub>2</sub> and CS<sub>2</sub>, forming near quantitative zwitterionic salts **1.11**. CO<sub>2</sub> adducts have found utility as stable intermediates that at elevated temperatures decompose to their constituents and release the reactive carbene,<sup>25</sup> while CS<sub>2</sub> adducts have been utilized as intermediates in the synthesis of novel chain-transfer reagents for RAFT polymerization.<sup>26</sup> Moving in a clockwise direction (Scheme 1.1), NHC form adducts with compounds possessing acidic proton (i.e. water, amine, chloroform) **1.12**. Many of these adducts are bench-stable compounds that undergo quantitative reverse reactions upon vacuum pyrolysis,<sup>27</sup> therefore this class of adducts complements CO<sub>2</sub> adducts **1.11** as a source of free carbene generated *in situ*. While adducts **1.11** and **1.12** are used to release stable carbenes, adducts **1.13** are frequently relied upon as trapping agents when carbenes are not stable

and undergo decomposition reactions.<sup>28</sup> These trapping experiments generally serve as an indirect proof that carbene formation has occurred. Alternatively stable carbenes can also be isolated as their sulfur adducts, which can undergo reduction with strong reducing agents such as  $\text{KC}_8$  to generate the free carbene.<sup>29</sup>

The rich chemistry of NHCs continues with discoveries of new adducts such as **1.14**<sup>30</sup> and ever increasing number of publications describing organometallic complexes **1.15**<sup>31</sup>. Furthermore, carbenes can undergo Michael additions **1.16**<sup>32</sup> and serve as metal free catalysts **1.17**<sup>33</sup> (i.e. benzoin condensation). Recently ene-tetramine adducts **1.18** have found use as strong reducing agents in organic chemistry.<sup>8</sup>



Scheme 1.1 NHCs in organic chemistry.

With such versatile chemistry of NHCs, it is clear that these compounds possess tremendous potential in chemistry. However, several areas of NHC chemistry have been severely underrepresented. Prior to our endeavor in this field, there were no publications describing applications of carbenes in materials chemistry.<sup>34</sup> Also, the burgeoning area of organometallic chemistry of NHCs had an unanswered fundamental question on the nature of carbene-metal bond.<sup>35</sup> Overall, the tremendous utility and versatility of NHCs, along with many unanswered questions about the fundamental nature of NHCs, have made this area of chemistry an attractive topic for further studies. In this dissertation, a unifying theme of the chemistry presented is the synthesis, study, and application of a novel class of biscarbenes. Pursuit of these versatile materials has resulted in new advances in carbene structure and bonding, discovery of highly-efficient reactions, and new polymers with unusual properties.

## REFERENCES

- 1 (a) Breslow, R. *Chem. and Ind.* **1957**, 893; (b) Breslow, R. *J. Am. Chem. Soc.* **1957**, *79*, 1762.
- 2 (a) Wanzlick, H. W.; Schikora, E. *Angew. Chem.* **1960**, *72*, 494. (b) H. W. Wanzlick and E. Schikora, *Angew. Chem.* **1960**, *72*, 2389.
- 3 (a) Igau, A. Grutzmacher, H. Baceiredo, A.; Bertrand, G. *J. Am. Chem. Soc.* **1988**, *110*, 6463.; (b) Bertrand, G.; R. Reed, R. *Coord. Chem. Rev.* **1994**, *137*, 323.
- 4 Arduengo, A. J.; Dias, H. V. R.; Harlow, R. L.; Kline, M. *J. Am. Chem. Soc.* **1992**, *114*, 5530.
- 5 Wanzlick, H. W. *Angew. Chem., Int. Ed. Engl.* **1962**, *1*, 75.
- 6 Lemal, D. M.; Lovald, R. A.; Kawano, K. I. *J. Am. Chem. Soc.* **1964**, *86*, 2518.
- 7 Kamplain, J. W.; Bielawski, C.W. *Chem. Comm.* **2006**, 1727.
- 8 For use of ene-tetramines as reducing agents, see: (a) Khan, T.; McGlacken G. P. *Angew. Chem. Int. Ed.* **2008**, *47*, 1819; (b) For synthesis and electrochemical

- studies of substituted ene-tetramines, see: Kamplain, J. W.; Lynch, V. M.; Bielawski C. W. *Org. Lett.* **2007**, *9*, 5401.
- 9 (a) Wanzlick, H. W.; Schönherr, H. J. *Angew. Chem. Int. Ed.* **1968**, *7*, 141. (b) Öfele, K. *J. Organomet. Chem.* **1968**, *12*, P42. (c) Cardin, D. J.; Çetinkaya, B.; Çetinkaya, E.; Lappert, M. F. *J. Chem. Soc., Dalton Trans.* **1973**, 514.
- 10 Arduengo, A. J. ; Harlow, R. L.; Kline, M. *J. Am. Chem. Soc.* **1991**, *113*, 361.
- 11 For recent reviews of catalytically-active transition metal complexes containing N-heterocyclic carbenes, see: (a) Peris, E.; Crabtree, R. H. *Coord. Chem. Rev.* **2004**, *248*, 2239. (b) Cavell, K. J.; McGuiness, D. S. *Coord. Chem. Rev.* **2004**, *248*, 671. (c) Herrmann, W. A. *Angew. Chem., Int. Ed.* **2002**, *41*, 1290. (d) Hillier, A. C.; Gasa, G. A.; Viciu, M. S.; Lee, H. M.; Yang, C. L.; Nolan, S. P. *J. Organomet. Chem.* **2002**, *653*, 69. (e) Herrmann, W. A.; Elison, M.; Fischer, J.; Köcher, C.; Artus, G. R. *Angew. Chem. Int. Ed.* **1996**, *34*, 2371. (f) Díez-González, S.; Nola, S. P. *Top Organomet. Chem.* **2007**, *21*, 47. (g) Bourissou, D.; Guerret, O.; Gabbaï, F. P. *Chem. Rev.* **2000**, *100*, 39.
- 12 For representative examples, see: (a) Marion, N.; Navarro, O.; Mei, J.; Stevens, E. D.; Scott, N. M.; Nolan, S. P. *J. Am. Chem. Soc.* **2006**, *128*, 4101. (b) Navarro, O.; Marion, N.; Oonishi, Y.; Kelly, R. A., III; Nolan, S. P. *J. Org. Chem.* **2006**, *71*, 685. (c) Louie, J.; Gibby, J. E.; Farnworth, M. V.; Tekavec, T. N. *J. Am. Chem. Soc.* **2002**, *124*, 15188. (d) Jørgensen, M.; Lee, S.; Liu, X.; Wolkowski, J. P.; Hartwig, J. F. *J. Am. Chem. Soc.* **2002**, *124*, 12557. (e) Trnka, T. M.; Grubbs, R. H. *Acc. Chem. Res.* **2001**, *34*, 18.
- 13 Herrmann, W. A.; Mihalios, D.; Ofele, K.; Kipfor, P.; Belmedjahed, F. *Chem. Ber.* **1992**, *125*, 1795.
- 14 Jafarpour, L.; Stevens, E. D.; Nolan, S. P. *J. Organomet. Chem.* **2000**, *606*, 2000.
- 15 (a) Boydston, A. J.; Williams, K. A.; Bielawski, C. W. *J. Am. Chem. Soc.* **2005**, *127*, 12496. (b) Khramov, D. M.; Boystron, A. J.; Bielawski, C. W. *Angew. Chem. Int. Ed.* **2006**, *45*, 6186. (c) Boydston, A. J.; Bielawski, C. W. *Dalton Trans.* **2006**, 4073. (d) Boydston, A. J.; Rice, J. D.; Sanderson, M. D.; Dykhno, O. L.; Bielawski, C. W. *Organometallics* **2006**, *25*, 6087.
- 16 Scholl, M.; Ding, S.; Lee, C. W.; Grubbs, R. H. *Org. Lett.* **1999**, *1*, 953.
- 17 O'Brien, C. J.; Kantchev, E. A. B.; Valente, C.; Hadei, N.; Chass, G. A.; Lough, A.; Hopkinson, A. C.; Organ, M. G. *Chem. Eur. J.* **2006**, *12*, 4743.
- 18 (a) Herrmann, W. A.; Schwarz, J.; Gardiner, M. G. *Organometallics* **1999**, *18*, 4082. (b) Voutchkova, A. M.; Feliz, M.; Clot, E.; Eisenstein, O.; Crabtree, R. H.

- J. Am. Chem. Soc.* **2007**, *129*, 12834. (c) Lin, I. J. B.; Vasam, C. S. *Coord. Chem. Rev.* **1998**, *251*, 642. (d) Wang, H. M. J.; Lin, I. J. B. *Organometallics* **1998**, *17*, 972.
- 19 (a) Boydston, A. J.; Williams, K. A.; Bielawski, C. W. *J. Am. Chem. Soc.* **2005**, *127*, 12496. (b) Khramov, D. M.; Boystron, A. J.; Bielawski, C. W. *Angew. Chem. Int. Ed.* **2006**, *45*, 6186. (c) Boydston, A. J.; Bielawski, C. W. *Dalton Trans.* **2006**, 4073. (d) Boydston, A. J.; Rice, J. D.; Sanderson, M. D.; Dykhno, O. L.; Bielawski, C. W. *Organometallics* **2006**, *25*, 6087.
- 20 Enders, D.; Breuer, K.; Raabe, G.; Rumsink, J. Teles, J. H.; Melder, J. P.; Ebel, K.; Brode, S. *Angew. Chem., Int. Ed. Engl.*, **1995**, *34*, 1021.
- 21 (a) Arduengo, A. J.; Goerlich, J. R.; Marshall, W. J. *J. Am. Chem. Soc.* **1995**, *117*, 11027. (b) Denk, M. K. Thadani, A.; Hatano, K.; Lough A. J. *Angew. Chem., Int. Ed. Engl.* **1997**, *36*, 2607. (c) Alder, R. W.; Blake, M. E.; Bortolotti, C.; Buffali, S.; Butts, C. P.; Lineham, E.; Oliva, J. M.; Orpen, A. G.; Quayle, M. J. *Chem. Comm.* **1999**, 241.
- 22 (a) Alder, R. W.; Allen, P. R.; Murray, M.; Orpen A. G. *Angew. Chem., Int. Ed. Engl.* **1996**, *35*, 1121. (b) Alder R. W.; Blake, M. E. *Chem. Commun.*, **1997**, 1513. (c) Alder, R. W.; Blake, M. E.; Oliva, J. M. *J. Phys. Chem. A* **1999**, *103*, 11200. (d) Rosen, E. L.; Sanderson, M. D.; Saravanakumar, S.; Bielawski, C. W. *Organometallics* **2007**, *26*, 5774.
- 23 (a) Arduengo, A. J.; Goerlich, J. R.; Marshall, W. J. *Liebigs Annalen* **1997**, *2*, 365. (b) Alder, R. W.; Butts, C. P.; Orpen, A. G. *J. Am. Chem. Soc.* **1998**, *120*, 11526.
- 24 Präsang, C.; Donnadieu, B.; Bertrand, G. *J. Am. Chem. Soc.* **2005**, *127*, 10182
- 25 Voutchkova, A. M.; Feliz, M.; Clot, E.; Eisenstein, O.; Crabtree, R. H. *J. Am. Chem. Soc.* **2007**, *129*, 12834.
- 26 Coady, D. J.; Norris, B. C.; Bielawski C. W. *Marcomolecules*, In press.
- 27 Coulembier, O.; Lohmeijer, B. G. G.; Dove, A. P.; Pratt, R.C.; Mespouille, L.; Culkin, D. A.; Benight, S.J.; Dubois, P.; Waymouth, R.M.; Hedrick, J. L. *Marcomolecules* **2006**, *39*, 5617.
- 28 (a) Metallinos, C.; Barrett, F. B.; Chaytor, J.L.; Heska, M. E. A. *Org. Lett.* **2004**, *6*, 3641. (b) Bildstein, B.; Malaun, M.; Kopacka, H.; Onganria, K. -H.; Wurst, K. *J. Organomet. Chem.* **1999**, *572*, 177.
- 29 Gehrhus, B.; Hitchcock, P. B.; Lappert, M. F. *z. Anorg. Allgem. Chem.* **2005**, *631*, 1383.

- 30 Khramov, D. M.; Bielawski, C. W. *Chem. Comm.* **2005**, 4958.
- 31 Rogers, M. M; Stahl, S. S. *Top. Organomet. Chem.* **2006**.
- 32 He, L., Jian, T.-Y., Song Ye, S. *J. Org. Chem.* **2007**, 72, 7466.
- 33 (a) Sohn, S. S.; Rosen, E. L.; Bode, J. W. *J. Am. Chem. Soc.* **2004**, 126, 14370. (b) Chiang P.-C.; Kaeobamrung J.; Bode J. W . *J. Am. Chem. Soc.* **2007**, 129, 3520.
- 34 (a) Boydston, A. J.; Williams, K. A.; Bielawski, C. W. *J. Am. Chem. Soc.* **2005**, 127, 12496; (b) Boydston, A. J.; Bielawski, C. W. *Dalton Trans.* **2006**, 4073; (c) Boydston, A. J.; Rice, J. D.; Sanderson, M. D.; Dykhno, O. L.; Bielawski C. W. *Organometallics*, **2006**, 25, 6087.
- 35 (a) Öfele, K.; Herberhold, M. *Z. Naturforsch.* **1973**, 28b, 306. (b) Öfele, K.; Kreiter, C. G. *Chem. Ber.* **1972**, 105, 529. (b) (a) Lee, M.; Hu, C. *Organometallics* **2004**, 23, 976. (b) Niehues, M.; Erker, G.; Kehr, G.; Schwab, P.; Fröhlich, R.; Blacque, O.; Berke, H. *Organometallics* **2002**, 21, 2905. (c) Boehme, C.; Frenking, G. *Organometallics* **1998**, 17, 5801. (d) Fröhlich, N.; Pidun, U.; Stahl, M.; Frenking, G. *Organometallics* **1997**, 16, 442. (c) Díez-González, S.; Nolan, S. P. *Coord. Chem. Rev.* **2007**, 251, 874.

## **Chapter 2: Triazene formation via reaction of imidazol-2-ylidenes with azide<sup>†</sup>**

### **ABSTRACT**

Treatment of N-heterocyclic carbenes (as their free carbenes or generated in situ) with alkyl, aryl, acyl, or tosyl azides afforded the respective substituted triazenes in excellent yields.

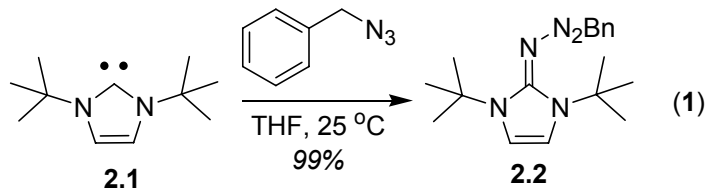
### **INTRODUCTION**

Triazenes<sup>1</sup> have found use as alkylating agents in tumor therapy,<sup>2</sup> as iodo-masking groups in the synthesis of small-<sup>3</sup> and macromolecules,<sup>4</sup> and in the preparation of N-containing heterocycles.<sup>5</sup> The two most utilized methods of synthesizing triazenes has been through azo coupling of aryl diazonium salts and through the addition of organometallic reagents (RMgBr, RLi, etc.) to alkyl azides.<sup>6</sup> Herein, we report a new and operationally simple method of preparing substituted triazenes in high yields *via* the reaction of neutral nucleophilic N-heterocyclic carbenes with alkyl, aryl, acyl, and tosylated azides.

### **RESULTS**

Phosphines are well-known to react with azides to afford the corresponding phosphazide which subsequently loses N<sub>2</sub> and yields an azaylide. In the presence of water, the azaylide hydrolyzes to the respective primary amine (i.e., the Staudinger reaction).<sup>7</sup> Spectroscopic studies suggest that imidazolylidenes are principally strong σ-donors with poor π-acceptor capabilities; thus they often share similar reactivity profiles as phosphines.<sup>8</sup> As such, we reasoned that reaction of an azide with an imidazolylidene would ultimately afford a 2-iminoimidazoline in lieu of the azaylide.<sup>9,10</sup> However, as

shown in Equation 1, we found that by adding benzyl azide to 1,3-di-*t*-butylimidazol-2-ylidene (**2.1**) in tetrahydrofuran at ambient temperature afforded the respective triazene **2.2**. Analysis of the crude reaction mixture by  $^1\text{H}$  NMR spectroscopy indicated that the reaction was essentially quantitative with an estimated product purity of greater than 95%. Alternatively, we discovered that the free carbene can be generated *in situ* through combination of the more stable and readily accessible 1,3-di-*t*-butylimidazolium chloride with potassium *t*-butoxide or sodium hydride and reacted with benzyl azide without suffering any loss in yield of product.



entry	imidazolium salt	azide	product	isolated yield <sup>b</sup>
1				60%
2				94%
3				75%
4				81%
5				54%
6				83%
7				60%
8				74%
9				92%

Table 2.1 Synthesis of substituted imidazol-2-ylidenes. Reaction conditions: THF or toluene, temp = 25 °C, ratios: imidazolium salt (1.00 eq.)/ azide (1.05 eq.)/ KOtBu (0.95 eq.) or NaH(0.95 eq.) <sup>b</sup>Isolated yield based on limiting reagent.

Crystallization of N-benzyl 1,3-dimesitylimidazol-2-ylidenetriazene (**2.3**) (see Table 1.1, Entry 6) from ethyl acetate by slow evaporation afforded single crystals suitable for X-ray structure determination. Unexpectedly, as shown in Figure 2.1, the triazene was found to be the *Z*-isomer. To the best of our knowledge, this is the first example of a non-heteroatom stabilized triazene with a *cis* configuration about the N=N bond.<sup>11</sup> Curiously, when the crystallization was repeated, the *E*-isomer was found. Factors governing the preferential formation of one isomer over the other remain unclear and are currently under investigation. Notably, the triazeno moiety in the *Z* isomer has a shorter N-N single bond (N6-N7, 1.34 Å) and a longer N-N double bond (N7-N8, 1.28 Å) when compared to the *E* isomer (1.36 Å and 1.26 Å, respectively), which may reflect a long-range interaction between the 2-imino and the benzyl moieties (*vide infra*). In both isomers, the exocyclic 2-imino bond is significantly polarized as evidenced by its increased length (1.33 – 1.34 Å) relative to typical C-N double bonds (1.29 Å).<sup>12</sup>

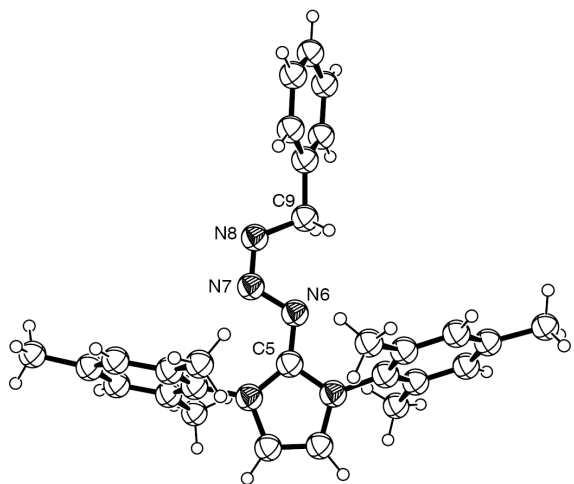


Figure 2.1 ORTEP representation of the X-ray crystal structure of (Z)-N-benzyl 1,3-dimesitylimidazol-2-ylidenetriazene (**2.3**), showing non-hydrogen atoms as 50% thermal ellipsoids. Selected bond distances (Å) and angles (°): C5–N6, 1.330(3); N6-N7, 1.342(4); N7-N8, 1.278(3); N8-C9, 1.431(5); C5-N6-N7, 114.7(3); N6-N7-N8, 116.2(2); N7-N8-C9, 116.4(2); N6-N7-N8-C9, 2.3(5).

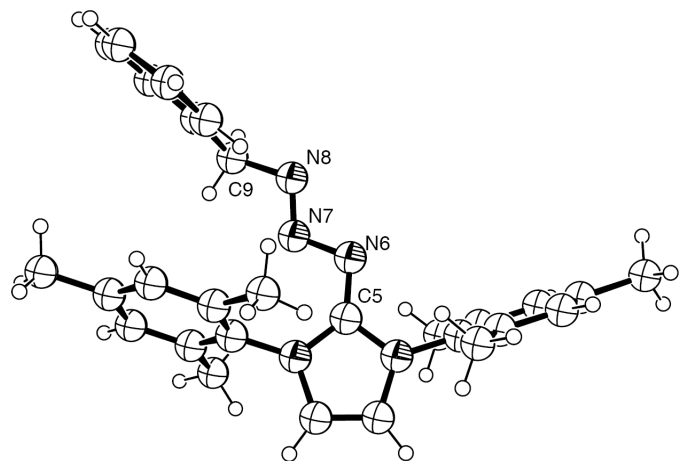
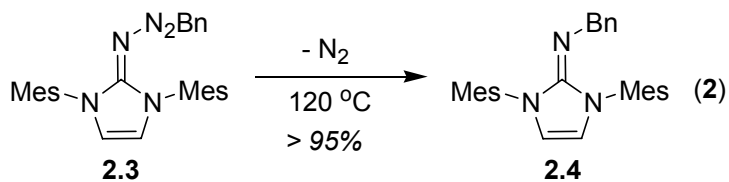


Figure 2.2 ORTEP representation of the X-ray crystal structure of (E)-N-benzyl 1,3-dimesitylimidazol-2-ylidenetriazene (**2.3**), showing non-hydrogen atoms as 50% thermal ellipsoids. Selected bond distances (Å) and angles (°): C5–N6, 1.339(3); N6-N7, 1.370(2); N7-N8, 1.261(2); N8-C9, 1.468(2); C5-N6-N7, 109.4(2); N6-N7-N8, 112.1(2); N7-N8-C9, 109.8(2); N6-N7-N8-C9, 179.2(2).

Since both *E* and *Z* stereoisomers were discovered in the solid-state, focus shifted toward identifying them in solution. Resonances attributable to discrete isomers of **2.3** were not resolved at -80 °C in the <sup>1</sup>H NMR spectrum (solvent: toluene-*d*<sub>8</sub>).<sup>13</sup> However, we discovered that heating to >120 °C (in DMSO-*d*<sub>6</sub>) cleanly extruded N<sub>2</sub> and formed N-benzyl 1,3-dimesityl-2-iminoimidazoline (**2.4**) in >95% yield. The scope and mechanism of this reaction is currently under investigation.



## CONCLUSION

In summary, we report a simple and effective route to substituted triazenes by treatment of imidazol-2-ylidenes with various azides. The utility of this triazenetation reaction in the synthesis of small molecules and macromolecular materials will be reported in due course.

## EXPERIMENTAL

**General Information.** Representative procedure for the synthesis of N-benzyl 1,3-dimesitylimidazol-2-ylidenetriazene (**2.3**): Benzyl azide (0.79 mmol, 105 mg) was added in one portion using a 1 mL syringe to a slurry of mesityl imidazolium chloride (0.53 mmol, 180 mg) in dry THF (3 mL). In one portion, KOtBu (0.58 mmol, 65 mg) was added to the reaction vessel and the resulting mixture was stirred under argon for 2 hours. Excess hexanes (1 mL) were then added and the reaction mixture was filtered through Celite. The crude product was concentrated and purified using flash chromatography (70% EtOAc/Hexanes) to afford N-benzyl 1,3-dimesitylimidazol-2-ylidenetriazene as off-white crystals (192 mg, 83%). Crystals suitable for X-ray analysis were grown by

slow evaporation from ethyl acetate.  $R_f = 0.33$  (70% EtOAc/Hexanes);  $^1\text{H}$  NMR (400 MHz,  $\text{CDCl}_3$ ):  $\delta$  7.18-7.09 (m, 3H), 6.89 (br s, 6H), 6.44 (s, 2H), 4.04 (s, 2H), 2.28 (s, 6H), 2.14 (s, 12H);  $^{13}\text{C}$  NMR (100 MHz,  $\text{CDCl}_3$ ):  $\delta$  152.1, 138.5, 138.3, 135.6, 124.3, 128.9, 128.8, 127.8, 126.3, 116.0, 65.4, 21.0, 18.0; HRMS calcd for  $\text{C}_{28}\text{H}_{31}\text{N}_5$  [ $\text{M}+\text{H}^+$ ]: 438.2658; found: 438.2659.

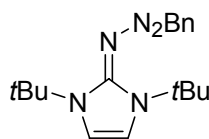
Crystal data for (Z)-N-benzyl 1,3-dimesitylimidazol-2-ylidenetriazene ( $\text{C}_{28}\text{H}_{31}\text{N}_5$ ):  $M = 437.58$ ,  $T = 153$  (2) K, triclinic, space group P-1,  $a = 9.1191(1)$ ,  $b = 15.4148(2)$ ,  $c = 18.4677(3)$  Å,  $\alpha = 104.680(1)$ ,  $\beta = 92.260(1)$ ,  $\gamma = 90.110(1)^\circ$ ,  $V = 2509.10(6)$  Å<sup>3</sup>,  $Z = 4$ ,  $D_x = 1.158$  mg m<sup>-3</sup>,  $\mu = 0.070$  mm<sup>-1</sup>,  $\lambda = 0.71073$  Å,  $\theta_{\text{max}} = 27.48^\circ$ , 19912 measured reflections, 11357 independent reflections, 612 refined parameters,  $\text{GOF} = 1.152$ ,  $R[\text{F}2 > 2\sigma(\text{F}2)] = 0.0576$ ,  $wR(\text{F}2) = 0.1163$ . The intensity data were collected on a Nonius Kappa CCD diffractometer. The structure was solved by direct methods using SIR9714 and refined by full-matrix least-squares on F2 with anisotropic displacement parameters for the non-H atoms using SHELXL-97.14. The hydrogen atoms were calculated in ideal positions with isotropic displacement parameters set to 1.2 x Ueq of the attached atom (1.5 x Ueq for methyl hydrogen atoms). There were two crystallographically unique molecules in the asymmetric unit. In one molecule, the orientation of the triaza portion was disordered about two orientations. The disorder was modeled by assigning the variable x to the site occupancy factors of one component of the disorder composed of atoms N6, N7, N8 and C9. The site occupancy factor of the alternate component, composed of atoms N6A, N7A, N8A and C9A, had a site occupancy factor of 1-x. A common isotropic displacement parameter was assigned to the relevant atoms while refining x. The variable, x, refined to 0.82(2). The geometry of the disordered moieties were restrained to be approximately equal throughout the

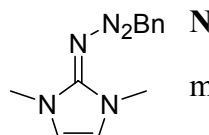
refinement. The atoms of the minor component of the disorder were refined isotropically. CCDC 275072.

Crystal data for (*E*)-N-benzyl 1,3-dimesitylimidazol-2-ylidenetriazene ( $C_{28}H_{31}N_5$ ):  $M = 437.58$ ,  $T = 153$  (2) K, monoclinic, space group P21/c,  $a = 14.6396(3)$ ,  $b = 12.1965(2)$ ,  $c = 28.0462(5)$  Å,  $\alpha = 90$ ,  $\beta = 90.634(1)$ ,  $\gamma = 90^\circ$ ,  $V = 5007.40(16)$  Å<sup>3</sup>,  $Z = 8$ ,  $D_x = 1.161$  mg m<sup>-3</sup>,  $\mu = 0.070$  mm<sup>-1</sup>,  $\lambda = 0.71073$  Å,  $\theta_{\max} = 25.00^\circ$ , 16441 measured reflections, 8809 independent reflections, 596 refined parameters, GOF = 1.002,  $R[F^2 > 2\sigma(F^2)] = 0.0525$ ,  $wR(F^2) = 0.0974$ . The intensity data were collected on a Nonius Kappa CCD diffractometer. The structure was solved by direct methods using SIR97<sup>14</sup> and refined by full-matrix least-squares on  $F^2$  with anisotropic displacement parameters for the non-H atoms using SHELXL-97.<sup>15</sup> The hydrogen atoms were calculated in ideal positions with isotropic displacement parameters set to 1.2 x Ueq of the attached atom (1.5 x Ueq for methyl hydrogen atoms). There were two crystallographically unique molecules in the asymmetric unit. These two molecules differed only slightly in conformation. CCDC 275071.

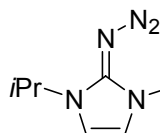
All reactions were performed under an atmosphere of argon at ambient temperature. Flasks were dried and cooled under atmosphere of nitrogen prior to use. Unless otherwise noted, solvents and reagents were purchased from Aldrich or Acros and used as received. Thin-layer chromatography was performed on EM 250 Kieselgel 60 F254 silica gel. The plates were developed by staining with Ceric Ammonium Nitrate (CAM) or I<sub>2</sub>. <sup>1</sup>H-NMR and <sup>13</sup>C-NMR data was obtained on a Varian Unity Plus 300 or a Varian INOVA 400. Chemical shifts ( $\delta$ ) are expressed in ppm downfield from tetramethylsilane using the residual protonated solvent as an internal standard (CDCl<sub>3</sub>, <sup>1</sup>H 7.24 ppm and <sup>13</sup>C 77.0 ppm; (DMSO-*d*6) <sup>1</sup>H 2.49 ppm and <sup>13</sup>C 39.5 ppm; C<sub>6</sub>D<sub>6</sub>, <sup>1</sup>H 7.15 ppm and <sup>13</sup>C 128.0 ppm). Coupling constants ( $J$ ) are expressed in hertz. <sup>13</sup>C-NMR

spectra were routinely run with broadband  $^1\text{H}$  decoupling. Where appropriate, descriptions of signals include singlet (s), doublet (d), triplet (m), multiplet (m), and broad (br). HRMS (ESI, CI) were obtained with a VG analytical ZAB2-E instrument.

 **N-Benzyl 1,3-di-*t*-butylimidazol-2-ylidenetriazene (2.2).** Benzyl azide (0.33 mmol, 44 mg) was added in one portion using a 1 mL syringe to a solution of *t*-butyl imidazolium carbene (0.33 mmol, 60 mg) in dry THF (1 mL). The solution was stirred overnight and solvent was removed to give pure product (102 mg, 99%) as yellow solid.  $^1\text{H}$ -NMR (400 MHz,  $\text{C}_6\text{D}_6$ ):  $\delta$  7.58 (d,  $J = 9.2$  Hz, 2H), 7.22 (t,  $J = 9.2$  Hz, 2H), 7.12-7.06 (m, 1H), 6.11 (s, 2H), 5.19 (s, 2H), 1.41 (s, 18H);  $^{13}\text{C}$ -NMR (100 MHz,  $\text{C}_6\text{D}_6$ ):  $\delta$  141.7, 129.1, 128.5, 126.6, 110.9, 65.2, 58.0, 29.7; HRMS calcd for  $\text{C}_{18}\text{H}_{27}\text{N}_5$  [ $\text{M}+\text{H}^+$ ]: 314.2345, found: 314.2340.

 **N-Benzyl 1,3-dimethylimidazol-2-ylidenetriazene.** Benzyl azide (1.95 mmol, 257 mg) was added in one portion using a 1 mL syringe to a slurry of methyl imidazolium iodide (0.97 mmol, 218 mg) in dry THF (4 mL). In one portion, NaH (1.07 mmol, 43 mg, 60% in mineral oil) was added to the reaction vessel and the resulting mixture was stirred for 12 h. After hexanes (1 mL) were added, the reaction mixture was filtered through Celite. Solvent was removed and pure product was obtained as a yellow solid (134 mg, 60%).  $^1\text{H}$ -NMR (400 MHz,  $\text{CDCl}_3$ ):  $\delta$  7.21-7.10 (m, 5H), 6.31 (s, 2H), 4.71 (s, 2H), 3.40 (s, 6H);  $^{13}\text{C}$ -NMR (100 MHz,  $\text{CDCl}_3$ ):  $\delta$  152.01, 138.7, 128.7, 128.1, 126.5, 115.9, 64.7, 35.4; HRMS calcd for  $\text{C}_{12}\text{H}_{15}\text{N}_5$  [ $\text{M}+\text{H}^+$ ]: 230.1406, found: 230.1408.

**N-Butyl 1,3-dimethylimidazol-2-ylidenetriazene.** Butyl azide (0.95 mmol, 94 mg) was added in one portion using a 1 mL syringe to a slurry of methyl imidazolium iodide (0.79 mmol, 177 mg) in dry THF (3 mL). In one portion, KO*t*Bu (0.71 mmol, 80 mg) was added to the reaction vessel and the resulting mixture was stirred for 90 minutes. Excess hexanes (1 mL) were then added and the reaction mixture was filtered through Celite. Solvent was removed and pure product was obtained as a pale yellow solid (128 mg, 94 %). <sup>1</sup>H-NMR (400 MHz, C<sub>6</sub>D<sub>6</sub>): δ 5.47 (s, 2H), 3.89 (t, *J* = 7.2 Hz, 2H), 3.03 (s, 6H), 1.87 (pentet, *J* = 7.2, 2H), 1.51 (sextet, *J* = 7.2 Hz, 2H), 0.93 (t, *J* = 7.2 Hz, 3H); <sup>13</sup>C-NMR (100 MHz C<sub>6</sub>D<sub>6</sub>): δ 153.3, 114.9, 61.6, 34.8, 32.0, 21.2, 14.3; HRMS calcd for C<sub>9</sub>H<sub>15</sub>N<sub>5</sub> [M+H<sup>+</sup>]: 196.1562, found: 196.1564.

 **N-Butyl 1,3-diisopropylimidazol-2-ylidenetriazene.** Butyl azide (0.5 mmol, 50 mg) was added in one portion using a 1 mL syringe to a slurry of isopropyl imidazolium chloride (0.5 mmol, 90 mg) in dry THF (3 mL). In one portion, KO*t*Bu (0.55 mmol, 47 mg) was added to the reaction vessel and the resulting mixture was stirred for 90 minutes. Hexanes (1 mL) were then added and the reaction mixture was filtered through Celite. Solvent was removed and pure product was obtained as white crystals (94 mg, 75 %). <sup>1</sup>H-NMR (400 MHz, C<sub>6</sub>D<sub>6</sub>): δ 5.98 (s, 2H), 5.08 (septet, *J* = 6.8 Hz, 2H), 3.94 (t, *J* = 6.8 Hz, 2H), 1.90 (pentet, *J* = 6.8 Hz, 2H), 1.52 (sextet, *J* = 7.2 Hz, 2H), 0.98 (d, *J* = 6.8 Hz, 12H), 0.92 (t, *J* = 7.2 Hz, 3H); <sup>13</sup>C-NMR (100 MHz C<sub>6</sub>D<sub>6</sub>): δ 151.5, 109.9, 61.7, 47.6, 32.2, 22.0, 21.2, 14.3; HRMS calcd for C<sub>13</sub>H<sub>25</sub>N<sub>5</sub> [M+H<sup>+</sup>]: 252.2188, found: 252.2186.

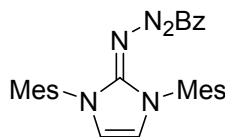
**N-s-Butyl 1,3-diisopropylimidazol-2-ylidenetriazene.** *s*-Butyl azide (1.01 mmol, 99 mg) was added in one portion using a 1 mL syringe to a slurry of isopropyl imidazolium chloride (0.84 mmol, 158 mg) in dry THF (3 mL). In one portion, KO*t*Bu (0.75 mmol, 84 mg) was added to the reaction vessel and the resulting mixture was stirred for 180 minutes. Hexanes (1 mL) were then added and the reaction mixture was filtered through Celite. Solvent was removed and pure product was obtained as white crystals (150 mg, 81 %). <sup>1</sup>H-NMR (400 MHz, C<sub>6</sub>D<sub>6</sub>): δ 6.00 (s, 2H), 5.08 (septet, *J* = 6.8 Hz, 2H), 3.66 (sextet, *J* = 6.4 Hz, 1H), 2.05-1.94 (m, 1H), 1.77-1.67 (m, 1H), 1.40 (d, *J* = 6.4 Hz, 3H), 1.04 (t, *J* = 7.6 Hz, 3H), 0.98 (d, *J* = 6.8 Hz, 12H); <sup>13</sup>C-NMR (100 MHz C<sub>6</sub>D<sub>6</sub>): δ 151.6, 109.9, 67.1, 47.5, 30.1, 21.998, 21.952, 20.7, 11.6; HRMS calcd for C<sub>13</sub>H<sub>25</sub>N<sub>5</sub> [M+H<sup>+</sup>]: 252.2188, found: 252.2188.

**N-Phenyl 1,3-diisopropylimidazol-2-ylidenetriazene.** Phenyl azide (1.12 mmol, 130 mg) was added in one portion using a 1 mL syringe to a slurry of isopropyl imidazolium chloride (0.93 mmol, 148 mg) in dry THF (3 mL). In one portion, KO*t*Bu (0.93 mmol, 105 mg) was added to the reaction vessel and the resulting mixture was stirred under argon for 4 hours. Hexanes (1 mL) were then added and the reaction mixture was filtered through Celite. Solvent was removed and pure product was obtained as a yellow solid (135 mg, 54%). <sup>1</sup>H-NMR (400 MHz, CDCl<sub>3</sub>): δ 7.50 (d, *J* = 9.6, 2H), 7.31 (t, *J* = 7.6 Hz, 1H), 7.11 (t, *J* = 7.2 Hz), 6.65 (s, 2H), 5.17 (septet, *J* = 6.4 Hz, 2H), 1.40 (d, *J* = 6.4 Hz, 12H); <sup>13</sup>C-NMR (100 MHz CDCl<sub>3</sub>): δ 152.3, 150.2, 128.7, 125.1, 120.9, 111.3, 48.0, 22.5 HRMS calcd for C<sub>15</sub>H<sub>21</sub>N<sub>5</sub> [M+H<sup>+</sup>]: 272.1875, found: 272.1871.

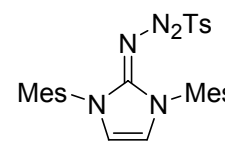
**N-Benzyl 1,3-dimesitylimidazol-2-ylidenetriazene (2.3).** Benzyl azide (0.79 mmol, 105 mg) was added in one portion using a 1 mL syringe to a slurry of mesityl imidazolium chloride (0.53 mmol, 180 mg) in dry THF (3 mL). In one portion, KOtBu (0.58 mmol, 65 mg) was added to the reaction vessel and the resulting mixture was stirred under argon for 2 hours. Excess hexanes (1 mL) were then added and the resulting mixture was filtered through Celite. After removal of solvent, the crude product was purified by flash chromatography (70% EtOAc/Hexanes) to afford product as pale yellow crystals (192 mg, 83%). Crystals suitable for X-ray analysis were grown by slow evaporation from ethyl acetate and were found to contain either the Z-isomer or the E-isomer. (Subtle factors governing the preferential formation of one geometric isomer over the other remain elusive, however the E-isomer has been found more often than the Z-isomer.)  $R_f = 0.33$  (70% EtOAc/Hexanes);  $^1\text{H-NMR}$  (400 MHz,  $\text{CDCl}_3$ ):  $\delta = 7.18\text{-}7.09$  (m, 3H), 6.89 (br s, 6H), 6.44 (s, 2H), 4.04 (s, 2H), 2.28 (s, 6H), 2.14 (s, 12H);  $^{13}\text{C-NMR}$  (100 MHz  $\text{CDCl}_3$ ):  $\delta = 152.1, 138.5, 138.3, 135.6, 134.3, 128.9, 128.8, 127.8, 126.3, 116.0, 65.4, 21.0, 18.0$ ; HRMS calcd for  $\text{C}_{28}\text{H}_{31}\text{N}_5$  [ $\text{M}+\text{H}^+$ ]: 438.2658, found: 438.2659.

**N-Adamantyl 1,3-dimesitylimidazol-2-ylidenetriazene.** Mesityl imidazolium chloride (0.46 mmol, 156 mg) was added to dry toluene (3 mL) followed by addition of KOtBu (0.46 mmol, 51 mg) in one portion. After stirring the slurry for 10 minutes, adamantyl azide (0.44 mmol, 77 mg) was added in one portion and the reaction mixture was stirred for 12 h. The solution was then filtered through Celite. Solvent was removed and the crude product was washed with hexanes (1 mL) to afford the product as light yellow crystals (0.125 g, 60%).  $R_f = 0.40$  (20% EtOAc/Hexanes);  $^1\text{H-NMR}$  (400 MHz,  $\text{CDCl}_3$ ):  $\delta = 6.89$  (s, 4H), 6.36 (s, 2H), 2.26

(s, 6H), 2.13 (s, 12H), 1.81 (br s, 3H), 1.54-1.50 (m, 3H), 1.42-1.39 (m, 3H), 1.17 (d,  $J$  = 2.4 Hz, 6H);  $^{13}\text{C}$ -NMR (100 MHz  $\text{CDCl}_3$ ):  $\delta$  152.4, 137.9, 135.6, 128.9, 115.9, 59.9, 40.9, 36.5, 29.4, 20.9, 18.0; HRMS calcd for  $\text{C}_{31}\text{H}_{39}\text{N}_5$  [ $\text{M}+\text{H}^+$ ]: 482.3248, found: 482.3315.

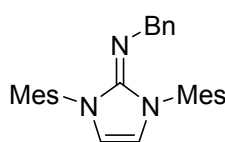


**N-Benzoyl 1,3-dimesitylimidazol-2-ylidenetriazene.**  $\text{KOtBu}$  (0.59 mmol, 1 M in THF) was added to a slurry of mesityl imidazolium chloride (0.59 mmol, 200 mg) in dry THF (3 mL). After stirring the reaction for 15 minutes, benzoyl azide (0.59 mmol, 87 mg) was added in one portion using a 1 mL syringe and the reaction mixture was stirred for 12 h. The solution was then concentrated to approximately half the original volume and the resulting slurry was purified by flash chromatography (50% EtOAc/Hexanes gradually increasing to 80% EtOAc/Hexanes) to obtain product as orange crystals (0.197 g, 74 %). A crystal suitable for X-ray analysis was grown by slow evaporation from EtOAc.  $R_f$  = 0.20 (50% EtOAc/Hexanes);  $^1\text{H}$ -NMR (400 MHz,  $\text{CDCl}_3$ ):  $\delta$  7.92 (d,  $J$  = 7.6 Hz, 2H), 7.36 (t,  $J$  = 7.6 Hz, 1H), 7.26 (t,  $J$  = 7.6 Hz, 1H), 6.87 (s, 4H), 6.75 (s, 2H), 2.25 (s, 6H), 2.11 (s, 12H);  $^{13}\text{C}$ -NMR (100 MHz  $\text{CDCl}_3$ ):  $\delta$  178.2, 151.9, 139.1, 136.2, 134.8, 132.3, 131.2, 129.9, 129.0, 127.4, 118.5, 20.9, 17.7; HRMS calcd for  $\text{C}_{28}\text{H}_{29}\text{N}_5\text{O}$  [ $\text{M}+\text{H}^+$ ]: 452.2450, found: 452.2690.



**N-Tosyl 1,3-dimesitylimidazol-2-ylidenetriazene.**  $\text{KOtBu}$  (0.71 mmol, 79 mg) was added to a slurry of mesityl imidazolium chloride (0.68 mmol, 230 mg) in dry THF (4 mL). After stirring the reaction mixture for 15 minutes, tosyl azide (0.74 mmol, 146 mg) was added in one portion using a 1 mL syringe. The reaction was then stirred for 12 h. Yellow precipitate formed which

was collected by filtration and dried, giving pure product (310 mg, 92%) as yellow crystals.  $^1\text{H-NMR}$  (400 MHz,  $\text{CDCl}_3$ ):  $\delta$  = 7.11 (d,  $J$  = 8.4 Hz, 2H), 7.08 (d,  $J$  = 8.4 Hz, 2H), 7.02 (s, 4H), 6.84 (s, 2H), 2.38-2.37 (m, 9H), 2.05 (s, 12H);  $^{13}\text{C-NMR}$  (100 MHz  $\text{CDCl}_3$ ):  $\delta$  142.8, 140.1, 137.7, 135.3, 132.6, 129.6, 129.2, 127.8, 119.5, 21.6, 21.2, 17.8, HRMS calcd for  $\text{C}_{28}\text{H}_{31}\text{N}_5\text{O}_2\text{S} [\text{M}+\text{H}^+]$ : 502.2277; found: 502.2520.



**N-Benzyl 1,3-dimesityl-2-iminoimidazoline (2.4).** Benzyl 1,3-dimesitylimidazol-2-ylidenetriazene (**2.3**) was dissolved in  $\text{DMSO}-d_6$  and heated in an NMR tube to 120 °C for 3 hours to obtain the desired product in >95% yield.  $^1\text{H-NMR}$  (400 MHz,  $(\text{CD}_3)_2\text{SO}$ ):  $\delta$  = 10.0 (s, 1H), 7.92-7.90 (m, 2H), 7.73-7.69 (m, 1H), 7.62-7.59 (m, 2H), 7.02 (s, 6H), 6.63 (s, 2H), 2.28 (s, 6H), 2.09 (s, 12H);  $^{13}\text{C-NMR}$  (100 MHz,  $(\text{CD}_3)_2\text{SO}$ ):  $\delta$  192.3, 138.0, 136.4, 136.2, 134.6, 129.4, 129.2, 128.9, 113.6, 20.6, 17.4. HRMS calcd for  $\text{C}_{28}\text{H}_{31}\text{N}_3 [\text{M}+\text{H}^+]$ : 410.2596, found: 410.2595.

## REFERENCES

- † Portions of this chapter have been previously reported, see: Khramov, D. M.; Bielawski, C. W. *Chem. Comm.* **2005**, 4958.
- 1 (a) H. Zollinger, *Diazo Chemistry, Vol. 1*, VCH, Weinheim, **1994**. (b) P. A. S. Smith, *Open Chain Nitrogen Compounds, Vol. 2*, W. A. Benjamin, New York, 1966. (c) D. B. Kimball and M. M. Haley, *Angew. Chem. Int. Ed.*, **2002**, *41*, 3338.
- 2 C. A. Rouzer, M. Sabourin, T. L. Skinner, E. J. Thompson, T. O. Wood, G. N. Chmurny, J. R. Klose, J. M. Roman, R. H. Smith, Jr. and C. J. Michejda, *Chem. Res. Toxicol.* **1996**, *9*, 172.
- 3 (a) J. S. Moore, E. J. Weinstein and Z. Wu, *Tetrahedron Lett.*, **1991**, *32*, 2465. (b) K. C. Nicolaou, C. N. C. Boddy, H. Li, A. E. Koumbis, R. Hughes, S. Natarajan, N. F. Jain, J. M. Ramanjulu, S. Bräse and M. E. Soloman, *Chem. Eur. J.*, **1999**, *5*, 2602.

- 4 (a) L. Jones, II, J. S. Schumm and J. M. Tour, *J. Org. Chem.* **1997**, *62*, 1388. (b) J. S. Moore, *Acc. Chem. Res.*, **1997**, *30*, 402.
- 5 W. Wirshun, M. Winkler, K. Lutz and J. C. Jochims, *J. Chem. Soc., Perkin Trans. 2*, **1998**, 1755.
- 6 K. H. Saunders, *The Aromatic Diazo Compounds, 2nd ed.*, Longmans, Green, and Co., New York, **1949**.
- 7 (a) H. Staudinger and I. Meyer, *Helv. Chim. Acta.*, **1919**, *2*, 635. (b) Leffler, J. E.; Temple, R. D. *J. Am. Chem. Soc.* **1967**, *89*, 5235.
- 8 W. A. Herrmann, D. Mihalios, K. Ofele, P. Kiprof and F. Belmedjahed, *Chem. Ber.*, **1992**, *125*, 1795.
- 9 It was previously reported that reaction of imidazolylidenes (*pKa* of conjugate acid ~ 24, ref: R. W. Alder, P. R. Allen and S. J. Williams, *Chem. Commun.*, 1995, 1267) with  $\text{HN}_3$  (*pKa* = 4.7) lead exclusively to the corresponding imidazolium azide salts; see: N. Kuhn, M. Göhner and Y. C. Frenking, Unusual Structures and Physical Properties in Organometallic Chemistry, in: M. Gielen, R. Willem, and R. Wrackmeyer (Eds.), *Physical Organometallic Chemistry, Vol. 3*, Wiley: The Atrium, West Sussex, U.K., **2002**.
- 10 Reaction of imidazol-2-ylidenes with TMS- $\text{N}_3$  affords mixed results: reaction with 1,3-dimesitylimidazol-2-ylidene in THF affords the respective 2-iminoimidazoline in 24% yield (see: J. M. Hopkins, M. Bowridge, K. N. Robertson, T. S. Cameron, H. A. Jenkins and J. A. C. Clyburne, *J. Org. Chem.*, **2001**, *66*, 5713) whereas reaction with 1,3-di-*t*-butylimidazol-2-ylidene in refluxing toluene affords the respective N-silylated 2-iminoimidazoline (see: M. Tamm, S. Randall, T. Bannenberg and E. Herdtweck, *Chem. Commun.*, **2004**, 876).
- 11 (*Z*)-Triazenes have been found in two thiotriazene derivatives and a stabilized phosphazide; see: R. L. Beddoes and O. S. Mills, *J. Chem. Res.*, **1981**, *132*, 1701, G. L'abbe, A. Willocx, J. P. Declercq, G. Germain and M. van Meerssche, *Bull. Soc. Chim. Belg.*, **1979**, *88*, 107, and P. Molina, C. López-Leonardo, J. Llamas-Botía, C. Foces-Foces and C. Fernández-Castano, *Tetrahedron*, **1996**, *52*, 9629.
- 12 The crystal structure of (*E*)-N-benzoyl 1,3-dimesitylimidazol-2-ylidenetriazene was also determined. Crystal data for  $\text{C}_{28}\text{H}_{29}\text{N}_5\text{O}$ :  $M = 451.56$ ,  $T = 153$  (2) K, orthorhombic, space group  $P212121$ ,  $a = 14.0109(3)$ ,  $b = 14.0230(3)$ ,  $c = 12.6469(2)$  Å,  $\alpha = 90^\circ$ ,  $\beta = 90^\circ$ ,  $\gamma = 90^\circ$ ,  $V = 2484.80(8)$  Å<sup>3</sup>,  $Z = 4$ ,  $D_x = 1.207$  mg m<sup>-3</sup>,  $\mu = 0.076$  mm<sup>-1</sup>,  $\lambda = 0.71073$  Å,  $\theta_{\max} = 27.48^\circ$ , 5434 measured reflections, 5434 independent reflections, 308 refined parameters,  $\text{GOF} = 1.191$ ,  $R[F^2 > 2\sigma(F^2)] = 0.0511$ ,  $wR(F^2) = 0.1018$ . The data were collected on a Nonius Kappa CCD diffractometer. The structure was solved by direct methods using SIR97<sup>14</sup>

- and refined by full-matrix least-squares on  $F^2$  with anisotropic displacement parameters for the non-H atoms using SHELXL-97.<sup>15</sup> The hydrogen atoms were calculated in ideal positions with isotropic displacement parameters set to 1.2 x Ueq of the attached atom (1.5 x Ueq for methyl hydrogen atoms). CCDC 275073. Selected bond distances (Å) and angles (°): C5–N6, 1.355(3); N6–N7, 1.328(2); N7–N8, 1.295(2); N8–C9, 1.414(3); C5–N6–N7, 110.4(2); N6–N7–N8, 112.3(2); N7–N8–C9, 110.4(2); N6–N7–N8–C9, -173.1(2).
- 13 E/Z isomerization in related 1,3-dialkylbenzoimidazol-2-ylidenetriazenes is known to be relatively facile, see: E. Fanghänel, R. Hänsel, and J. Hohlfeld, *J. Prakt. Chem.*, **1977**, *319*, 485.
- 14 A. Altomare, M. C. Burla, M. Camalli, G. L. Cascarano, C. Giacovazzo, A. Guagliardi, A. G. G. Moliterni, G. Polidori and R. Spagna, *J. Appl. Cryst.*, **1999**, *32*, 115.
- 15 G. M. Sheldrick, SHELXL-97, Program for refinement of crystal structures, University of Göttingen, Germany, 1997.

## **Chapter 3: Highly Efficient Synthesis and Solid-State Characterization of 1,2,4,5-Tetrakis(alkyl- and arylamino)benzenes and Cyclization to their Respective Benzobis(imidazolium) Salts<sup>†</sup>**

### **ABSTRACT**

New synthetic methodology to a variety of 1,2,4,5-tetraaminobenzenes and their corresponding benzobis(imidazolium) salts has been accomplished. Palladium catalyzed coupling of various 1,2,4,5-tetrabromo- or 1,2,4,5-tetrachlorobenzenes with aryl or *tert*-alkyl amines afforded the respective tetrakis(N-substituted)aminobenzenes in excellent yields. This enabled comparative solid-state structural analyses of this elusive class of electron rich arenes with their oxidized derivatives. The tetraamines were found to undergo formylative cyclization to the corresponding benzobis(imidazolium) salts in good to excellent yields.

### **INTRODUCTION**

We have recently launched a program on the broad study and application of benzobis(imidazolium)s and benzobis(imidazolylidene)s in organic and organometallic materials chemistry.<sup>1</sup> These difunctional compounds are readily prepared in multigram quantities and in excellent yields via formylative cyclization of their respective tetraaminoarene precursors followed by subsequent alkylation with primary alkyl halides. While modular in many regards, the inherent limitations of this methodology included incompatibility of incorporating N-aryl and bulky N-alkyl substituents into the benzobis(imidazole) nucleus. To overcome these limitations, we targeted a general and highly efficient synthetic route to a range of 1,2,4,5-tetrakis(alkyl- and arylamino)benzenes. Herein, we disclose details on these advances and include a comparative solid-state study of substituted 1,2,4,5-tetraaminobenzenes and their

respective 2,5-diamino-1,4-quinonediimines. In addition, we describe the cyclization of the tetraamines to their corresponding benzobis(imidazolium) salts.

As a general class of highly electron-rich arenes, tetraaminobenzenes have seen a rich diversity of chemical applications. For example, 1,2,4,5-tetraaminobenzene<sup>2</sup> (**3.1**) and its oxidized derivative, 2,5-diamino-1,4-quinonediimine<sup>3</sup> (**3.2**), have found great utility in organic, organometallic, and macromolecular chemistry. They have been used as ditopic ligands in coordination chemistry,<sup>4</sup> as pH-dependent chromophores,<sup>5</sup> as difunctional monomers in the synthesis of main-chain organometallic<sup>6</sup> and supramolecular polymers,<sup>7</sup> and as  $\pi$ -complexation partners in supramolecular systems.<sup>8</sup>

While **3.1**<sup>9</sup> is commercially available (as its tetrahydrochloride salt), access to its N,N',N'',N'''-tetra(alkyl and aryl) derivatives remains synthetically challenging due to the high propensity of these electron rich arenes to oxidize during isolation. For example, Braunstein obtained a variety of N,N',N'',N'''-tetraalkyl 2,5-diamino-1,4-benzoquinonediimines by reducing their respective 1,2,4,5-tetraamidobenzenes under aerobic conditions.<sup>4h,5</sup> More recently, in a breakthrough report by Harlan,<sup>10</sup> exhaustive Buchwald-Hartwig<sup>11</sup> Pd-catalyzed amination of 1,2,4,5-tetrabromobenzene with 2,6-dimethylaniline provided mixtures of the respective tetrakis(aryl amino)benzene and azophenine in a promising 26% yield.<sup>12</sup> We envisioned that the incorporation of large N-substituents could slow down (or even eliminate) undesired oxidative pathways and facilitate isolation of the targeted tetraamines.

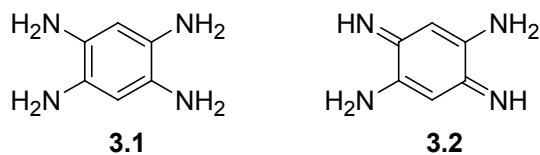
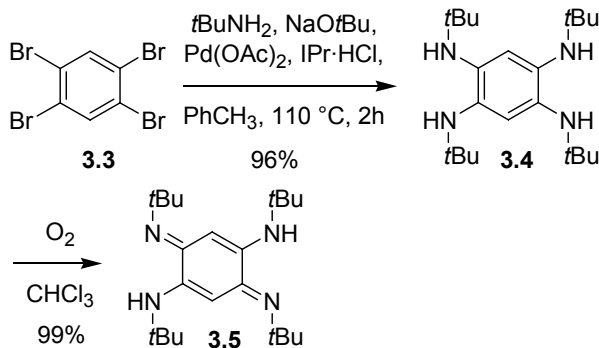


Figure 3.1 Reduced and oxidized states of 1,2,4,5-tetraaminobenzene.

## RESULTS

Inspired by Harlan's report,<sup>10</sup> we examined the Pd-catalyzed cross coupling of *tert*-butylamine with 1,2,4,5-tetrabromobenzene (**3.3**) under basic conditions as shown in Scheme 3.1. The reaction was performed in toluene (0.2 M) using 1,3-bis(2,6-diisopropylphenyl)imidazolylidene ·HCl<sup>13</sup> (IPr·HCl) : Pd(OAc)<sub>2</sub><sup>14</sup> (2:1 stoichiometry; 2 mol % Pd catalyst relative to **3.3**) as the catalyst precursor.<sup>15</sup> Surprisingly, after less than 1 h at 110 °C, a colorless solid precipitated from the reaction solution which was subsequently isolated in 96% yield via filtration under a cone of nitrogen.<sup>16</sup> The <sup>1</sup>H NMR spectrum of this compound exhibited a single, diagnostic signal at  $\delta = 6.53$  ppm (solvent = CDCl<sub>3</sub>) which was indicative of highly symmetric structure consistent with the desired 1,2,4,5-tetrakis(*tert*-butylamino)benzene (**3.4**). To confirm, a crystal suitable for X-ray crystallography was obtained by slow cooling of a hot saturated solution of **3.4** in toluene; an ORTEP diagram of the corresponding structure is shown in Figure 3.1 (left). Notably, the four nitrogen atoms were found to be co-planar with nearly equivalent N-C (1.43-1.44 Å) and aryl C-C (1.39-1.41 Å) bond distances. In addition, the *tert*-butyl groups on the nitrogen atoms were situated above and below the plane of the arene ring with dihedral angles of 100-110°.



Scheme 3.1      Synthesis of 1,2,4,5-tetrakis(*tert*-butylamino)benzene (**3.4**) and its related 2,5-diamino-1,4-quinonediimine (**3.5**)

To compare **3.4** directly with its corresponding 2,5-diamino-1,4-quinonediimine, the tetramine was dissolved in CHCl<sub>3</sub> and stirred under an atmosphere of oxygen at room temperature.<sup>17</sup> The <sup>1</sup>H NMR spectrum (solvent = CDCl<sub>3</sub>) of this compound exhibited a signal at  $\delta$  = 5.53 ppm which was consistent<sup>4h,5,10</sup> with quinoid-derivative **3.5** (Scheme 3.1). Crystals of azophenine **3.5** suitable for X-ray analysis were also obtained which allowed for direct comparison of the related species. As shown in Figure 1 (right), the ORTEP diagram of **3.5** exhibited not only co-planar *tert*-butyl groups (with dihedral angles of 175-179°), but also varied N-C (N1-C1, 1.35 Å and N2-C2, 1.29 Å) and aryl C-C (1.51 Å, 1.37 Å, and 1.44 Å) bond lengths. This type of bonding pattern has been previously described and is fully consistent with related azophenine solid-state structures.<sup>4h,5,10</sup> To our knowledge, this is the first example of a crystalline 1,2,4,5-tetrakis(alkylamino)benzene and a direct comparison with its oxidized derivative. More importantly, the collective data suggested that the synthetic methodology detailed above was successful in preparing and isolating bona fide N,N',N'',N'''-tetra(alkyl) 1,2,4,5-tetraminobenzenes.

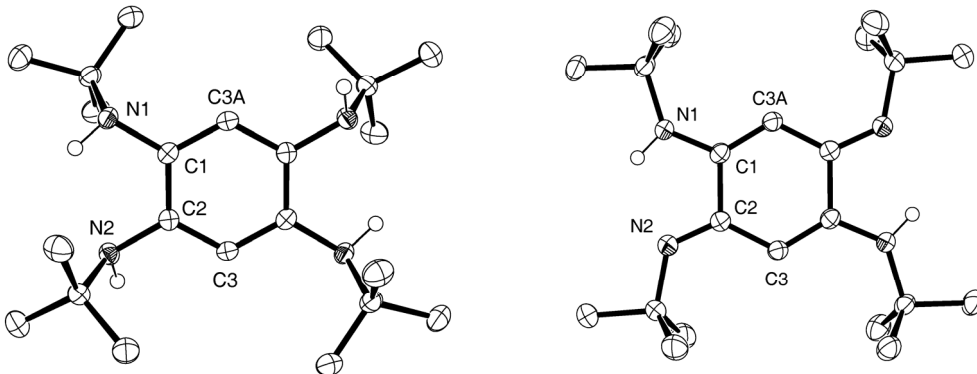
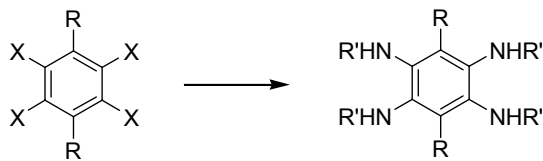


Figure 3.2 ORTEP representations of the X-ray crystal structures of 1,2,4,5-tetrakis(*tert*-butylamino)benzene (**3.4**) (left) and N,N',N'',N'''-tetrakis(*tert*-butyl) 1,4-diamino-2,5-benzoquinone-diimine (**3.5**) (right), showing non-hydrogen atoms as 50% thermal ellipsoids.<sup>18</sup>

Prompted by these results and using the protocol described above, a variety of other amines were probed for their ability to couple with **3.3**. As expected, the coupling of 1-adamantyl amine (AdNH<sub>2</sub>) with **3.3** afforded similar results as tBuNH<sub>2</sub> (90% yield; Table 3.1, Entry 2). Aryl amines including aniline, relatively bulky mesitylamine,<sup>19</sup> and electron-rich o-anisidine were also found to successfully couple to **3.3** in excellent yields (Entries 3 - 5). Unfortunately, primary alkyl (i.e., 1-butylamine), secondary alkyl (i.e., cyclohexylamine), or electron deficient aryl amines (nitro- and chloroanilines) either resulted in no reaction or afforded complex product mixtures.<sup>20</sup> It is noteworthy that cross-coupling of 2,3,5,6-tetrabromo-p-xylene and 1,2,4,5-tetrachlorobenzene with tBuNH<sub>2</sub> afforded the corresponding tetraamines in 99 and 94% yields, respectively (Entries 6 and 7). The former result suggested that the bulky IPr-ligated Pd catalyst was not impeded by the presence of steric bulk ortho to both sites of amination and the latter was a testament to the high activity of this catalyst system.



entry	tetrahalobenzene	amine	product	yield
	X	R		
1	Br	H	<i>t</i> BuNH <sub>2</sub>	<b>3.4</b>
2	Br	H	AdNH <sub>2</sub>	<b>3.6</b>
3	Br	H	PhNH <sub>2</sub>	<b>3.7</b>
4	Br	H	MesNH <sub>2</sub>	<b>3.8</b>
5	Br	H	2-MeOPhNH <sub>2</sub>	<b>3.10</b>
6	Br	Me	<i>t</i> BuNH <sub>2</sub>	<b>3.11</b>
7	Cl	H	<i>t</i> BuNH <sub>2</sub>	<b>3.4</b>

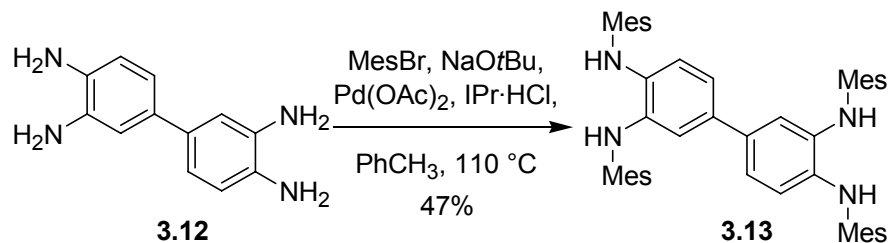
Table 3.1 Synthesis of 1,2,4,5-tetrakis(alkyl- and arylamino)benzenes. General reaction conditions: IPr•HCl (0.04 equiv); Pd(OAc)<sub>2</sub> (0.02 equiv); NaOtBu (4.1 equiv); RNH<sub>2</sub> (4.1 - 10 equiv); solvent = toluene, temp = 110 °C. Isolated yields are indicated. *t*BuNH<sub>2</sub> = *tert*-butyl amine; AdNH<sub>2</sub> = 1-adamantyl amine; PhNH<sub>2</sub> = aniline; MesNH<sub>2</sub> = 2,4,6-trimethylaniline; 2-MeOPhNH<sub>2</sub> = *o*-anisidine.

After the 1,2,4,5-tetrakis(alkyl- and arylamino)-benzenes were synthesized, their relative susceptibilities toward oxidation were qualitatively investigated.<sup>21</sup> The amines were independently dissolved in aerated CDCl<sub>3</sub> and examined by <sup>1</sup>H NMR spectroscopy periodically over time. In general, the 1,2,4,5-tetrakis(alkylamino)benzenes were found to oxidize slower ( $\tau_{1/2} \sim$  days) than their N-aryl analogues ( $\tau_{1/2} \sim$  hours). However, the electron-rich N-anisidyl derivative **3.10** was exceptional and was found to exhibit stability comparable to the N-alkyl derivatives (**3.4** and **3.6**). The most stable tetraamine was the xylene derivative **3.11** which resisted oxidation even after dissolution in aerated solvents for several weeks. These results may be rationalized by examining individual steric and electronic contributors which may kinetically and/or thermodynamically inhibit

nitrogenyl formation.<sup>22</sup> As expected, electronically rich and sterically hindered tetraamines show lower propensities to undergo oxidation.

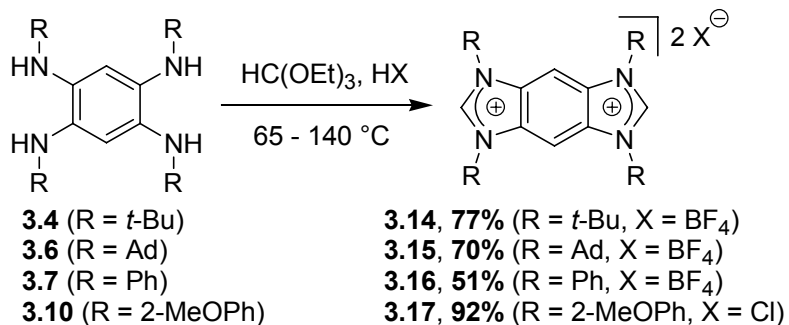
In an attempt prepare partially aminated arenes, a Pd catalyzed cross-coupling reaction was performed using two molar equivalents of *t*BuNH<sub>2</sub> relative to 1,2,4,5-tetrabromobenzene. To our surprise, only the tetraaminated product (**3.4**) and unreacted starting materials were observed, even in crude reaction mixtures. In fact, identical results were obtained when sub-stoichiometric amounts of *t*BuNH<sub>2</sub> or AdNH<sub>2</sub> were used which suggested that reactivity enhancements were occurring upon subsequent aminations. In contrast, the use of aniline as a coupling partner in the Pd-catalyzed reaction afforded a complex mixture of aminated products.<sup>23</sup>

Thus far we have demonstrated that various tetrakis(alkyl- and arylamino)arenes can be prepared via aryl amination from their corresponding tetrahaloarene. However, in situations when the requisite polyhalogenated arenes are not readily available (e.g., 3,3',4,4'-tetrachlorobiphenyl<sup>24</sup>), a complementary route to the respective tetrakis(amino)arenes would be desirable. As shown in Scheme 3.3, mesityl bromide was coupled to commercially available 3,3'-diaminobenzidine **3.12** using the catalyst system and conditions discussed above to afford the corresponding N,N',N'',N'''-tetramesityl 3,3'-diaminobenzidine (**3.13**) in 47% yield (Scheme 3.3).<sup>25</sup>



Scheme 3.3      Synthesis of tetrakis(aryl amino)arenes

With the tetraamines in hand, we were poised to prepare the corresponding N-aryl and N-alkyl benzobis(imidazolium) salts through a formylative cyclization methodology.<sup>26</sup> As shown in Scheme 3.4, ring closure was effected by subjecting tetraamines noted above to acidified (HCl or HBF<sub>4</sub>)<sup>27</sup> HC(OEt)<sub>3</sub> solutions at elevated temperatures (the N-alkylated derivatives **3.4** and **3.6** required 65 °C whereas the N-arylated derivatives **3.7** and **3.10** required 140 °C). Although cyclizations were sluggish (reaction time: 24 h), good to excellent yields of product were obtained.<sup>28</sup> Notably the electron rich N-anisidyl substrate **3.10** underwent clean cyclization to afford product in only 2 h (92% yield). Unfortunately, mesitylated derivatives **3.8** and **3.12** were reluctant to undergo cyclization under these conditions.



Scheme 3.4     Cyclization of tetraamines to give bis(azolium) salts

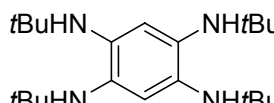
## CONCLUSION

In summary, we have developed an efficient synthetic and isolation protocol for preparing 1,2,4,5-tetrakis(alkyl- and arylamino)benzenes, two elusive classes of electron rich arenes. Their structures were unambiguously proven using X-ray crystallography and compared with their oxidized derivatives. Immediate efforts will concentrate on expanding the substrate scope of this reaction and elucidating its unique substitution pattern. The tetraamines were successfully cyclized to give the desired bis(azolium)

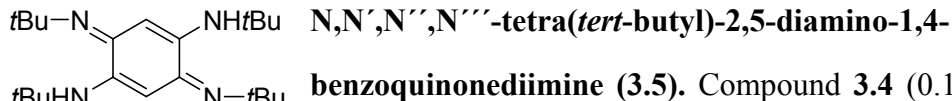
compounds in good to excellent yields. Currently we are also investigating applications of bis(azolium) salts for direct formation of non-chelating bis(carbene)s and their respective bimetallic complexes.<sup>29</sup>

## EXPERIMENTAL

All reactions were conducted under an atmosphere of nitrogen using standard Schlenk techniques or in a nitrogen-filled glove-box. CHCl<sub>3</sub> was degassed by two freeze-pump-thaw cycles and stored over 4Å molecular sieves and K<sub>2</sub>CO<sub>3</sub>. Hexanes were distilled from CaH<sub>2</sub> and degassed by two freeze-pump-thaw cycles. THF and toluene were freshly distilled from Na/benzophenone and degassed by two freeze-pump-thaw cycles. All reagents were purchased from Aldrich or Acros and were used without further purification. <sup>1</sup>H NMR spectra were recorded using a Varian Gemini (300 MHz or 400 MHz) spectrometer. Chemical shifts are reported in delta ( $\delta$ ) units, expressed in parts per million (ppm) downfield from tetramethylsilane using the residual protonated solvent as an internal standard (CDCl<sub>3</sub>, 7.24 ppm; C<sub>6</sub>D<sub>6</sub>, 7.15 ppm; DMSO-d<sub>6</sub>, 2.49 ppm). <sup>13</sup>C NMR spectra were recorded using a Varian Gemini (100 MHz) spectrometer. Chemical shifts are reported in delta ( $\delta$ ) units, expressed in parts per million (ppm) downfield from tetramethylsilane using the solvent as an internal standard (CDCl<sub>3</sub>, 77.0 ppm; C<sub>6</sub>D<sub>6</sub>, 128 ppm; DMSO-d<sub>6</sub>, 39.5 ppm). <sup>13</sup>C NMR spectra were routinely run with broadband decoupling. High-resolution mass spectra (HRMS) were obtained with a VG analytical ZAB2-E or a Karatos MS9 instrument and are reported as m/z (relative intensity)

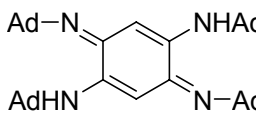
 **1,2,4,5-Tetrakis-N-tert-butylaminobenzene (3.4).** A catalyst for mediating aryl-amination coupling reaction was prepared by charging a 20 mL vial with 1,3-bis(2,6-

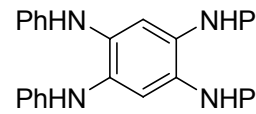
diisopropylphenyl)imidazolium chloride (0.085 g, 0.2 mmol), NaOtBu (0.03 g, 0.3 mmol), Pd(OAc)<sub>2</sub> (0.025 g, 0.1 mmol), toluene (5 mL), and a stir bar followed by stirring this mixture at 80 °C for 10 minutes. The catalyst solution was added to a 250 mL flask containing 1,2,4,5-tetrabromobenzene (2.22 g, 5.64 mmol) suspended in toluene (100 mL). *tert*-Butyl amine (1.73 g, 23.7 mmol) and NaOtBu (2.65 g, 27.6 mmol) were then added and the resulting mixture was sealed and stirred at 110 °C overnight. After cooling to ambient temperature, precipitated solids were collected by filtration under a cone of nitrogen, dissolved in degassed CHCl<sub>3</sub> (100 mL), and filtered to remove residual NaBr salts. Solvent was then removed under reduced pressure to afford 1.96 g (96% yield) of the desired product as a gray solid. Note: the product slowly oxidizes to the corresponding benzoquinonediimine over several days in aerated solutions. As a solid, the product is bench stable for >months. <sup>1</sup>H NMR (CDCl<sub>3</sub>): δ 6.53 (s, 2H), 3.73 (br, 4H), 1.22 (s, 36H). <sup>13</sup>C NMR (CDCl<sub>3</sub>): δ 131.7, 115.5, 52.0, 30.0. HRMS: [M]<sup>+</sup> calcd for C<sub>22</sub>H<sub>42</sub>N<sub>4</sub>: 362.3409; Found, 362.3406.



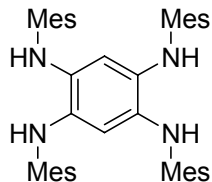
**benzoquinonediimine (3.5).** Compound **3.4** (0.1 g, 0.28 mmol) was dissolved in CHCl<sub>3</sub> (3 mL) and stirred under a balloon of oxygen for 24 h followed by removal of solvent to obtain a yellow powder (0.1 g) in quantitative yield. Alternatively, oxidations can be accomplished in less than 5 minutes by adding an excess of H<sub>2</sub>O<sub>2</sub>. <sup>1</sup>H NMR (CDCl<sub>3</sub>): δ 5.53 (s, 2H), 1.35 (s, 36H). <sup>13</sup>C NMR (CDCl<sub>3</sub>): δ 138, 90.8, 52.0, 29.8. HRMS: [M]<sup>+</sup> calcd for C<sub>24</sub>H<sub>41</sub>N<sub>4</sub>: 361.3331; Found: 361.3326.

**1,2,4,5-Tetrakis-N-adamantylaminobenzene (3.6).** The aryl amination was performed in a manner analogous to the synthesis of **3.4** using 1,2,4,5-tetrabromobenzene (13.97 g, 35.5 mmol) and adamantyl amine (22.5 g, 149 mol). Upon completion, the cooled reaction mixture was filtered in a drybox to afford a beige solid. The solids were rinsed with toluene and extracted with degassed  $\text{CHCl}_3$  and the extract was concentrated under reduced pressure to afford 21.5 g (90% yield) of the desired product as a white powder. Note: the product slowly oxidizes to the corresponding benzoquinone-diimine over several days in aerated solutions. As a solid, the product is bench stable for >months.  $^1\text{H}$  NMR ( $\text{CDCl}_3$ ):  $\delta$  6.59 (s, 2H), 2.06 (br, 12H), 1.81 (br, 24H), 1.66-1.58 (br, 24H).  $^{13}\text{C}$  NMR ( $\text{CDCl}_3$ ):  $\delta$  131.3, 117.8, 52.5, 43.7, 36.6, 29.8. HRMS:  $[\text{M}]^+$  calcd for  $\text{C}_{46}\text{H}_{66}\text{N}_4$ , 674.5287; Found, 674.5286.

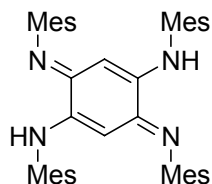
 **N,N',N'',N'''-tetra(adamantyl)-2,5-diamino-1,4-benzoquinone-diimine.** Compound **3.4** (0.1 g, 0.15 mmol) was dissolved in  $\text{CH}_2\text{Cl}_2$  (3 mL) and stirred under a balloon of oxygen for 24 h followed by removal of solvent to obtain a yellow powder (0.1 g) in quantitative yield.  $^1\text{H}$  NMR ( $\text{CDCl}_3$ ):  $\delta$  6.69 (br, 2H), 5.77 (s, 2H), 2.10 (br, 12H), 1.97 (br, 24H), 1.68 (br, 24H).  $^{13}\text{C}$  NMR ( $\text{CDCl}_3$ ):  $\delta$  138, 92.2, 52.7, 42.6, 36.9, 29.8. HRMS:  $[\text{M}+\text{H}]^+$  calcd for  $\text{C}_{46}\text{H}_{64}\text{N}_4$ , 673.5209; Found, 673.5209.

 **1,2,4,5-Tetrakis-N-phenylbenzene (3.7).** The aryl amination was performed in a manner analogous to the synthesis of **3.4** using 1,2,4,5-tetrabromobenzene (2.39 g, 5.84 mol) and aniline (2.8 g, 30 mol). Upon completion, the cooled reaction mixture was filtered in a drybox to afford a beige solid. The solids were rinsed with excess hexanes and extracted with degassed  $\text{CHCl}_3$ . The

extract was then concentrated under reduced pressure to afford 1.78 g (76 %) of the desired product as a light pink powder.  $^1\text{H}$  NMR ( $\text{CDCl}_3$ ):  $\delta$  7.24-7.19 (br m, 12H), 6.9-6.84 (br, 12H), 5.56 (s, 2H).  $^{13}\text{C}$  NMR ( $\text{CDCl}_3$ ):  $\delta$  144.5, 130.6, 129.3, 120.2, 116.6, 113.9. HRMS:  $[\text{M}]^+$  calcd for  $\text{C}_{30}\text{H}_{25}\text{N}_4$ , 441.2074; Found: 441.2074.

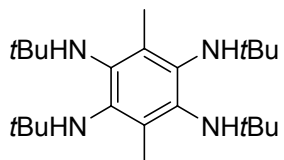


**1,2,4,5-Tetrakis(2,4,6-trimethylphenylamino)benzene (3.8).** The aryl amination was performed in a manner analogous to the synthesis of **3.4** using 1,2,4,5-tetrabromobenzene (2.00 g, 5.1 mmol) and mesityl amine (7 mL, 51 mmol). Upon completion, the cooled reaction mixture was filtered in a drybox to afford a beige solid. The solids were rinsed with toluene and extracted with degassed  $\text{CHCl}_3$ . The extract was then concentrated under reduced pressure to afford 2.71 g (94%) of the desired product as a white powder.  $^1\text{H}$  NMR ( $\text{CDCl}_3$ ):  $\delta$  6.75 (s, 8H), 5.40 (s, 2H), 4.86 (br s, 4H), 2.22 (s, 12H), 2.05 (s, 24 H).  $^{13}\text{C}$  NMR ( $\text{CDCl}_3$ ):  $\delta$  137.9, 132.6, 132.1, 129.4, 129.0, 105.3, 20.6, 18.2. HRMS:  $[\text{M}]^+$  calcd for  $\text{C}_{42}\text{H}_{49}\text{N}_4$ , 609.3978; Found: 609.3952.



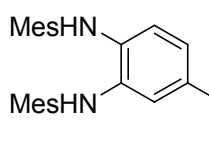
**Mesityl-derived azophenine (3.9).** The tetraamine **3.8** (0.1 g, 0.164 mmol) was stirred in aerated  $\text{CHCl}_3$  (3 mL) for 2 h. The mixture was concentrated to give an orange-red solid (0.1 g) in quantitative yield.  $^1\text{H}$  NMR ( $\text{CDCl}_3$ ):  $\delta$  6.79 (s, 4H), 6.75 (s, 4H), 5.40 (s, 2H), 4.61 (s, 2H), 2.23 (s, 12H), 2.07 (s, 12H), 2.05 (s, 12H).  $^{13}\text{C}$  NMR ( $\text{CDCl}_3$ ):  $\delta$  137.9, 132.6, 132.1, 129.4, 129.0, 128.6, 88.9, 20.8, 20.6, 18.2, 18.0. HRMS:  $[\text{M}]^+$  calcd for  $\text{C}_{42}\text{H}_{49}\text{N}_4$ , 609.3956; Found: 609.3952.

**1,2,4,5-Tetrakis(2-methoxyphenylamino)benzene (3.10).** The aryl amination was performed in a manner analogous to the synthesis of **3.4** using 1,2,4,5-tetrabromobenzene (4.00 g, 10.2 mmol) and *o*-anisidine (11.5 mL, 100.6 mmol). Upon completion, the cooled reaction mixture was filtered in a drybox to afford a beige solid. The solids were rinsed with toluene and extracted with degassed CHCl<sub>3</sub> and the extract was concentrated under reduced pressure to afford 6.92 g (96%) of the desired product as an off-white powder. Alternatively, the cooled reaction mixture was opened under a cone of nitrogen and HCl (2 mL) in MeOH (10 mL) was added quickly to produce a deep purple slurry. The mixture was poured into H<sub>2</sub>O (25 mL) and the solids were collected via vacuum filtration, rinsed with H<sub>2</sub>O and Et<sub>2</sub>O, and dried under vacuum to provide the tetrahydrochloride salt as a light purple solid in nearly quantitative yield. <sup>1</sup>H NMR of free base (CDCl<sub>3</sub>): δ 7.33 (s, 2H), 7.06-7.04 (m, 4H), 6.86-6.76 (m, 12H), 6.02 (br s, 4H), 3.82 (s, 12 H). <sup>13</sup>C NMR (CDCl<sub>3</sub>): δ 148.2, 134.4, 130.5, 121.0, 119.1, 114.4, 110.3, 114.2, 55.5. HRMS: [M]<sup>+</sup> calcd for C<sub>34</sub>H<sub>35</sub>N<sub>4</sub>O<sub>4</sub>, 563.2606; Found 563.2653.



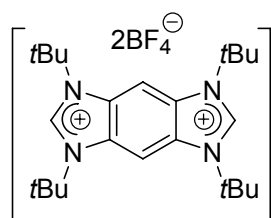
**1,2,4,5-Tetrakis(*tert*-butylamino)-*para*-xylene (3.11).** The aryl amination was performed in a manner analogous to the synthesis of **3.4** using 2,3,5,6-tetrabromoxylene (3.0 g, 7.11 mol) and *tert*-butyl amine (2.13 g, 29.2 mmol). Upon completion, the cool reaction mixture was filtered over Celite under a cone of nitrogen with the aid of degassed toluene. The filtrate was concentrated under reduced pressure to afford 2.7g (99%) of the desired product as a brown solid. It should be noted that the product is bench stable in aerated solutions for >months. <sup>1</sup>H NMR (CDCl<sub>3</sub>): δ 3.39 (br, 4H), 2.28 (s,

6H), 1.06 (s, 36H).  $^{13}\text{C}$  NMR ( $\text{CDCl}_3$ ):  $\delta$  138.1, 128.2, 55.3, 30.7, 18.6. HRMS:  $[\text{M}]^+$  calcd for  $\text{C}_{24}\text{H}_{46}\text{N}_4$ , 390.3722; Found, 390.3719.



### 3,3',4,4'-Tetrakis(2,4,6-

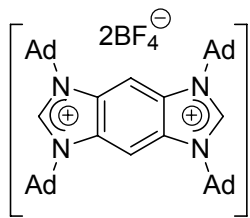
**trimethylphenylamino)biphenyl (3.13).** A catalyst for mediating aryl-amination coupling reactions was prepared by charging a 10 mL vial with 1,3-bis(2,6-diisopropylphenyl)imidazolium chloride (86 mg, 0.02 mmol),  $\text{NaOtBu}$  (3 mg, 0.03 mmol),  $\text{Pd}(\text{OAc})_2$  (30 mg, 0.01 mmol), toluene (3 mL), and a stir bar followed by stirring this mixture at 23 °C for 10 minutes. 2-Bromomesitylene (410 mg, 2.05 mmol) was added to the catalyst solution. 3,3'-diaminobenzidine (110 mg, 0.5 mmol) and  $\text{NaOtBu}$  (0.20 g, 2.05 mmol) were then added and the resulting mixture was sealed and stirred at 110 °C overnight. After cooling to ambient temperature, precipitated solids (NaBr) were removed by filtration under a cone of nitrogen. Solvent was removed under reduced pressure. Analysis of the crude product indicated that the reaction was >98% complete. The crude product was triturated with hexanes and then dried under reduced pressure to afford 160 mg (47 % yield) of the desired product as a grey solid.  $^1\text{H}$  NMR ( $\text{CDCl}_3$ ):  $\delta$  6.94 (s, 8H), 6.68-6.66 (m, 2H), 6.27-6.24 (m, 4H), 5.18 (br, 2H), 4.99 (br, 2H), 2.36 (br, 6H), 2.31 (s, 6H), 2.17 (s, 12H), 2.13 (s, 12H).  $^{13}\text{C}$  NMR ( $\text{CDCl}_3$ ):  $\delta$  137.11, 137.06, 136.7, 135.7, 135.6, 134.0, 133.9, 133.54, 133.48, 133.3, 133.2, 133.1, 129.30, 129.26, 117.8, 114.7, 112.4, 20.9, 20.8, 18.1, 18.0. HRMS:  $[\text{M}]^+$  calcd for  $\text{C}_{48}\text{H}_{55}\text{N}_4$ , 687.4427; Found: 687.4423.



### Tetrakis(tert-butyl) benzobis(imidazolium) tetrafluoroborate (3.14).

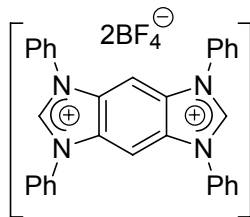
A 10 mL flask was charged with triethylorthoformate (5

mL), compound **3.4** (590 mg, 1.63 mmol), and HBF<sub>4</sub> (1 mL, 48% aq.). The reaction mixture was heated to 65 °C for 24 h. Upon completion, the product was collected by filtration, washed with hot acetonitrile (3 x 15 mL) to obtain 700 mg (77%) of the desired product as a light yellow powder. <sup>1</sup>H NMR (DMSO-*d*<sub>6</sub>): δ 9.06 (s, 2H), 8.62 (s, 2H), 1.91 (s, 36H). <sup>13</sup>C NMR (DMSO-*d*<sub>6</sub>): δ 142.9, 128.9, 102.7, 62.0, 28.0, 9.1.



**Tetraadamantyl benzobis(imidazolium) tetrafluoroborate (3.15).**

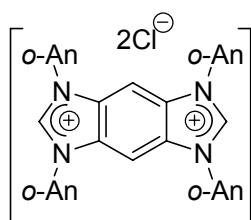
In a manner analogous to **3.14** using tetraamine **3.6** (3.3 g, 4.89 mmol), the product was obtained in 70% yield as a light yellow powder. <sup>1</sup>H NMR (C<sub>6</sub>D<sub>6</sub>): δ 9.13 (s, 2H), 8.54 (s, 2H), 2.39 (s, 12H), 1.88-1.76 (br, 24H). <sup>13</sup>C NMR (C<sub>6</sub>D<sub>6</sub>): δ 142.9, 127.9, 103.3, 62.7, 40.4, 35.4, 29.1.



**Tetraphenyl benzobis(imidazolium) tetrafluoroborate (3.16).**

In a manner analogous to **3.14** using tetraamine **7** (0.3 g, 0.68 mmol), with a reaction temperature of 140 °C and time of 24 h 162 mg (51%) of the desired product was obtained as a light yellow powder (purification required rinsing with copious amounts of MeOH). <sup>1</sup>H NMR (DMSO-*d*<sub>6</sub>) δ 10.8 (s, 2H), 8.15(s, 2H) 7.9-7.8 (br, 20H). <sup>13</sup>C NMR (DMSO-*d*<sub>6</sub>) δ 147.3, 132.9, 131.0, 130.6, 125.6, 99.2. HRMS: [M]<sup>2+</sup> calcd for C<sub>32</sub>H<sub>24</sub>N<sub>4</sub>, 232.1000; Found: 232.1002. Alternatively, a one-pot, two-step synthesis of **3.16** may be accomplished in 84% overall yield by eliminating the workup of the tetrakis(phenylamino)benzene. Aryl amination reaction of 1,2,4,5-tetrabromobenzene (6 g, 15.2 mmol) was carried out as described above. After cooling the reaction vessel, the reaction mixture was acidified with HBF<sub>4</sub> (5

mL, 48% aq.) and  $\text{HC(OEt)}_3$  (200 mL) was added. The vessel was then heated to 140 °C for 16 h, then cooled to 23 °C. Additional  $\text{HBF}_4$  (3 mL) was added and the solution was re-heated to 140 °C for 6 h. After cooling to room temperature, the resulting precipitate was collected by filtration and then washed with water (3 x 50 mL), methanol (1 x 50 mL), and ether (2 x 30 mL) to obtain 8.2 g (84% yield) of analytically pure product as a brown solid.



**Tetrakis(2-methoxyphenyl) benzobis(imidazolium) chloride (3.17).** The tetrahydrochloride of tetraamine **3.10** (5.0 g, 7.06 mmol) was dissolved in  $\text{HC(OEt)}_3$  (60 mL) and conc. HCl (0.2 mL). The deep purple solution was stirred at 120 °C for 2 h during which time the homogenous reaction mixture became a light red slurry. The reaction mixture was allowed to cool and  $\text{Et}_2\text{O}$  (30 mL) was added to facilitate precipitation of the product. The solids were collected, rinsed with  $\text{Et}_2\text{O}$  and recrystallized from hot MeOH/ $\text{Et}_2\text{O}$  to give 4.26 g (92%) of the bis(azolium) as a pink-brown solid.  $^1\text{H}$  NMR (DMSO- $d_6$ ):  $\delta$  10.79 (s, 2H), 8.00 (dd,  $J = 7.8, 1.4$  Hz, 2H), 7.98 (s, 2H), 7.73 (t,  $J = 8.0$  Hz, 4H), 7.48 (d,  $J = 6.8$  Hz, 4H), 7.28 (t,  $J = 7.2$  Hz, 4H), 3.87 (s, 12H).  $^{13}\text{C}$  NMR (DMSO- $d_6$ ):  $\delta$  153.7, 148.5, 133.0, 130.8, 128.4, 121.3, 120.6, 113.7, 100.4, 56.4. HRMS:  $[\text{M}]^+$  calcd for  $\text{C}_{36}\text{H}_{32}\text{N}_4\text{O}_4$ , 584.2462; Found: 584.2418.

## REFERENCES

- † Portions of this chapter have been previously reported, see: Khramov, D. M.; Boydston, A. J.; Bielawski, C. W. *Org Lett.* **2006**, 8, 1831.
- 1 (a) Boydston, A. J.; Williams, K. A.; Bielawski, C. W. *J. Am. Chem. Soc.* **2005**, 127, 12496. (b) Kamplain, J. W.; Bielawski, C. W. *Chem. Commun.* **2006**, DOI:10.1039/b518246h.

- 2 (a) Nietzki, R.; Hagenbach, E. *Ber. Dtsch. Chem. Ges.* **1887**, *20*, 328. (b) Nietzki, R. *Ber. Dtsch. Chem. Ges.* **1887**, *20*, 2114.
- 3 Azophenines generally refer to N,N',N'',N'''-tetrakis(phenyl) 1,4-diamino-2,5-benzoquinonediimine and their respective derivatives, see: (a) Fischer, O.; Hepp, E. *Ber. Dtsch. Chem. Ges.* **1888**, *21*, 676. (b) Kimich, C. *Ber. Dtsch. Chem. Ges.* **1875**, *8*, 1026.
- 4 (a) Shimakoshi, H.; Hirose, S.; Ohba, M.; Shiga, T.; Okawa, H.; Hisaeda, Y. *Bull. Chem. Soc. Jpn.* **2005**, *78*, 1040. (b) Frantz, S.; Rall, J.; Hartenback, I.; Scheid, T.; Zalis, S.; Kaim, W. *Chem. Eur. J.* **2004**, *10*, 149. (c) Groselj, U.; Bevk, D.; Jakse, R.; Meden, A.; Pirc, S.; Recnik, S.; Stanovnik, B.; Svetec, J. *Tetrahedron: Asymmetry* **2004**, *15*, 2367. (d) Groselj, U.; Bevk, D.; Jakse, R.; Meden, A.; Pirc, S.; Recnik, S.; Stanovnik, B.; Svetec, J. *Tetrahedron: Asymmetry* **2004**, *15*, 2367. (e) Beckmann, U.; Bill, E.; Weyhermueller, T.; Wieghardt, K. *Inorg. Chem.* **2003**, *42*, 1045. (f) Gordon-Wylie, S. W.; Blanton, W. B.; Claus, B. L.; Horwitz, C. P.; Collins, T. J.; Boskovic, C.; Christou, G. *Inorg. Synth.* **2002**, *33*, 1. (g) Chichak, K.; Jacquemard, U.; Branda, N. R. *Eur. J. Inorg. Chem.* **2002**, *2*, 357. (h) Siri, O.; Braunstein, P. *Chem. Comm.* **2000**, *22*, 2223. (i) Masui, H.; Freda, A. L.; Zerner, M. C.; Lever, A. B. P. *Inorg. Chem.* **2000**, *39*, 141. (j) Aukauloo, A.; Ottenwaelder, X.; Ruiz, R.; Poussereau, S.; Pei, Y.; Journaux, Y.; Fleurat, P.; Volatron, F.; Cervera, B.; Munoz, M. C. *Eur. J. Inorg. Chem.* **1999**, *7*, 1067. (k) Gordon-Wylie, S. W.; Claus, B. L.; Horwitz, C. P.; Leychakis, Y.; Workman, J.; Marzec, A. J.; Clark, G. R.; Rickard, C. E. F.; Conklin, B. J.; Sellers, S.; Yee, G. T. Collins, T. J. *Chem. Eur. J.* **1998**, *4*, 2173. (l) Rall, J.; Stange, A. F.; Hubler, K.; Kaim, W. *Angew. Chem. Int. Ed.* **1998**, *37*, 2681. (m) Espenson, J. H.; Kirker, G. W. *Inorg. Chim. Acta* **1980**, *40*, 105. (n) Merrell, P. H.; Maheu, L. J. *Inorg. Chim. Acta* **1978**, *28*, 47. (o) Hasty, E. F.; Colburn, T. J.; Hendrickson, D. N. *Inorg. Chem.* **1973**, *12*, 2414.
- 5 (a) Elhabiri, M.; Siri, O.; Sornosa-tent, A.; Albrecht-Gary, A.-M.; Braunstein, P. *Chem. Eur. J.* **2004**, *10*, 134. (b) Siri, O.; Braunstein, P.; Rohmer, M.-M.; Benard, M.; Welter, R. *J. Am. Chem. Soc.* **2003**, *125*, 13793.
- 6 Archer, R. D.; Illingsworth, M. L.; Rau, D. N.; Hardiman, C. J. *Macromolecules* **1985**, *18*, 1371.
- 7 Kleij, A. W.; Kuil, M.; Tooke, D. M.; Lutz, M.; Spek, A. L.; Reek, J. N. H. *Chem. Eur. J.* **2005**, *11*, 4743.
- 8 Staab, H. E.; Elbl-Weiser, K.; Krieger, C. *Eur. J. Org. Chem.* **2000**, *2*, 327.
- 9 Ruggli, P.; Fischer, R. *Helv. Chim. Acta* **1945**, *28*, 1270.

- 10 Wenderski, T.; Light, K. M.; Ogrin, D.; Bott, S. G.; Harlan, C. J. *Tetrahedron Lett.* **2004**, *45*, 6851.
- 11 (a) Prim, D.; Campagne, J.-M.; Joseph, D.; Andrioletti, B. *Tetrahedron* **2002**, *58*, 2041. (b) Wolfe, J. P.; Wagaw, S.; Marcox, J.-F.; Buchwald, S. L. *Acc. Chem. Res.* **1998**, *31*, 805. (c) Hartwig, J. F. *Angew. Chem., Int. Ed.* **1998**, *37*, 2046. (d) Louie, J.; Hartwig, J. F. *Tetrahedron Lett.* **1995**, *36*, 3609.
- 12 In a related example, Pd-catalyzed aryl amination was used to synthesize 1,2,4,5-tetra(morpholino)benzene in 76% yield via coupling of 1,2,4,5-tetrabromobenzene with morpholine, see: Witulski, B.; Senft, S.; Thum, A. *Synlett* **1998**, 504.
- 13 (a) Hillier, A. C.; Grasa, G. A.; Viciu, M. S.; Lee, H. M.; Yang, C.; Nolan, S. P. *J. Organomet. Chem.*, **2002**, *653*, 69. (b) The use of 1,3-bis(2,6-diisopropylphenyl)imidazolylidene-HCl ( $H_2\text{IPr}\cdot\text{HCl}$ ) in lieu of  $\text{IPr}\cdot\text{HCl}$  afforded comparable results.
- 14  $\text{PdCl}_2$  was found to be equally effective as  $\text{Pd}(\text{OAc})_2$ .
- 15 Aside from  $\text{IPr}$  and  $\text{H}_2\text{IPr}$ , a variety of other ligands for Pd including bulky phosphines ( $\text{PCy}_3$ , rac-BINAP,  $\text{PtBu}_3$ ) and imidazolylidenes (1,3-bis(2,6-di-*tert*-butyl)imidazolylidene, 1,3-bis(2,6-dimesityl)imidazolylidene) were screened, but did not afford appreciable yields of product.
- 16 Residual inorganic salts were removed by filtering chloroform solutions of the tetraaminobenzenes followed by evaporation.
- 17 Use of an oxygen atmosphere effects azophenine formation more rapidly than use of aerated solvents.
- 18 Selected bond lengths (Å) and degrees (°): For **3.4**: N1-C1, 1.429(2); N2-C2, 1.441(2); C1-C2, 1.411(2); C2-C3, 1.394(2); C1-C3A, 1.394(2); C2-C1-N1, 121.1(1); C1-C2-N2, 119.6(1); C2-C1-N1-C4, 109.8(1); C1-C2-N2-C8, 99.8(2). For **5**: N1-C1, 1.349(1); N2-C2, 1.294(1); C1-C2, 1.513(1); C1-C3A, 1.367(1); C2-C3, 1.437(1); N1-C1-C2, 113.0(1); N2-C2-C1, 113.9(1); C4-N1-C1-C2, 175.1(1); C1-C2-N2-C8, 179.3(1).
- 19 A solution to the crystal structure of 1,2,4,5-tetrakis(mesitylamino)benzene (**3.8**) was also determined; key bond distances (Å) and angles (°): N1-C1, 1.413(2); N2-C3, 1.424(2); C1-C2, 1.391(2); C2-C3, 1.398(2); C1-C3A, 1.404(2); C3A-C1-N1, 118.9(1); C1A-C3-N2, 118.5(1); C4-N1-C1-C3A, 173.9(2); C1A-C3-N2-C13, 172.9(2). Using the procedure described in the text, the corresponding azophenine (**3.9**) was synthesized and a solution to its corresponding crystal

- structure was determined; key bond lengths ( $\text{\AA}$ ) and angles ( $^{\circ}$ ): N1-C1, 1.293(2); N2-C3, 1.357(2); C1-C2, 1.440(2); C2-C3, 1.356(2); C1-C3A, 1.494(2); N1-C1-C3A, 115.6(1); N2-C3-C1A, 114.2(1); C3A-C1-N1-C4, 176.9(1); C1A-C3-N2-C13, 171.3(1).
- 20 Efforts toward optimizing these reactions are underway.
- 21 Oxidative susceptibilities of the 1,2,4,5-tetraminobenzenes can be greatly reduced through protonation with HCl prior to isolation.
- 22 For discussions comparing relative stabilities of electron deficient arylamines, see: (a) Li, Z.; Cheng, J.-P. *J. Org. Chem.* **2002**, *68*, 7350. (b) Kemnitz, C. R.; Karney, W. L.; Borden, W. T. *J. Am. Chem. Soc.* **1998**, *120*, 3499. (c) Miura, Y.; Kitagishi, Y.; Ueno, S. *Bull. Chem. Soc. Jap.* **1994**, *67*, 3282.
- 23 The mechanistic implications of these findings are currently under investigation in our laboratories.
- 24 Lehmler, H.-J.; Robertson, L. W.; Kania-Korwel, I. *Chemosphere*, **2004**, *56*, 735.
- 25 The aryl amination reaction was determined to be quantitative by  $^1\text{H}$  NMR spectroscopy; however, the isolation of **13** was made challenging by its high solubility in common solvents.
- 26 A similar approach utilizing aryl amination of 1,2-dibromobenzene followed by cyclization has been reported: Rivas, R. M.; Riaz, U.; Giessart, A.; Smulik, J. A.; Diver, S. T. *Org. Lett.* **2001**, *3*, 2673. For syntheses of related benzimidazolium and benzimidazolylidene compounds, see: (a) Huynh, H. V.; Holtgrewe, C.; Pape, T.; Koh, L. L.; Hahn, F. E. *Organometallics* **2006**, *25*, 245. (b) Hahn, F. E.; Jahnke, M. C.; Gomez-Benitez, V.; Morales-Morales, D.; Pape, T. *Organometallics* **2005**, *24*, 6458. (c) Hahn, F. E.; Wittenbecher, L.; Le Van, D.; Frohlich, R. *Angew. Chem., Int. Ed.* **2000**, *39*, 541.
- 27 Shorter reaction times were observed with  $\text{HBF}_4$  which may be related to the higher solubilities of bis(benzobisimidazolium) tetrafluoroborate salts as compared to their analogous chloride salts.
- 28 The overall yield of **3.16** from 1,2,4,5-tetrabromobenzene was improved to 84% using a one-pot, two-step procedure.
- 29 Khramov, D. M.; Boydston, A. J.; Bielawski, C W. Manuscript in preparation.

## **Chapter 4: An alternative synthesis of benzobis(imidazolium) salts via a “one-pot” cyclization/oxidation reaction sequence<sup>†</sup>**

### **ABSTRACT**

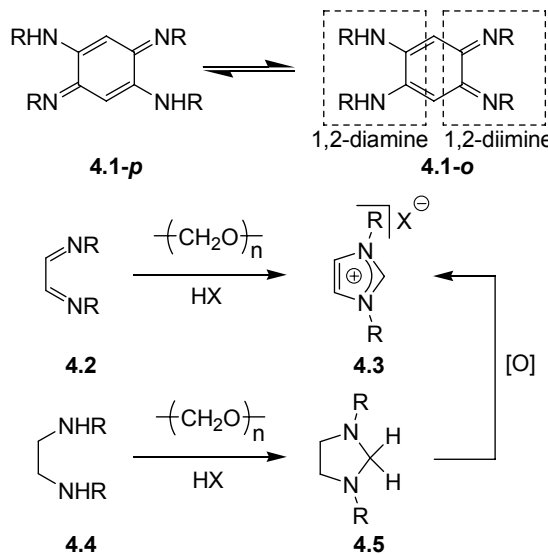
Cyclization of *N*-aryl and *N*-alkyl 2,5-diamino-1,4-benzoquinonediimines using paraformaldehyde under acidic conditions followed by oxidation with catalytic amounts of Pd(OAc)<sub>2</sub> afforded their respective benzobis(imidazolium) salts in yields of 48 – 98%. A comparative solid-state study between a 2,5-diamino-1,4-benzoquinonediimine and its corresponding benzobis(imidazolium) dichloride was also performed.

### **INTRODUCTION**

We have recently reported a concise synthesis of a series of 1,2,4,5-tetrakis(*N*-alkyl and *N*-aryl amino)benzenes<sup>1</sup> and demonstrated that they undergo formylative cyclization with triethylorthoformate to afford their respective benzobis(imidazolium) salts.<sup>2</sup> The electron-rich tetraaminobenzene intermediates were found to oxidize under aerobic conditions which necessitated the use of inert atmosphere or drybox techniques for their isolation and storage. In contrast, their oxidized products, namely azophenines<sup>3</sup> and related 2,5-diamino-1,4-benzoquinonediimines,<sup>4</sup> are robust and accessible *via* numerous synthetic protocols.<sup>3-5</sup> These quinone derivatives have found tremendous utility in coordination chemistry,<sup>6</sup> as pH-dependent chromophores,<sup>7</sup> and in theoretical studies.<sup>8</sup> In an effort to build upon our previous work and encompass new methodologies for preparing benzobis(imidazolium) salts using simple, bench-top procedures, we envisioned that azophenines and 2,5-diamino-1,4-benzoquinonediimines could function as a highly versatile class of appropriate starting materials.

As shown in Scheme 4.1, the *ortho*-quinoid tautomer<sup>9</sup> (**4.1-o**) of 2,5-diamino-1,4-benzoquinonediimine **4.1** displays 1,2-diamino and 1,2-diimino moieties which are

independently known for undergoing dehydrative cyclizations. For example, treatment of 1,2-diimine **4.2** with formaldehyde affords imidazolium salt **4.3**<sup>10</sup> whereas the corresponding vicinal diamine **4.4** affords the cyclic *N,N'*-acetal **4.5**.<sup>11</sup> With these considerations in mind, we suspected analogous cyclization reactions with **4.1** should afford an annulated benzimidazolium/*N,N'*-acetal hybrid.<sup>12</sup> Oxidation of this intermediate using Thorn's recently reported<sup>13</sup> Pd-mediated process for efficiently generating hydrogen gas from phenylene diamine-derived *N,N'*-acetals should then afford the respective benzobis(imidazolium) salts. Furthermore, the apparent compatibility of the cyclization and oxidation reaction conditions suggested they could be performed successively in a single reaction vessel.

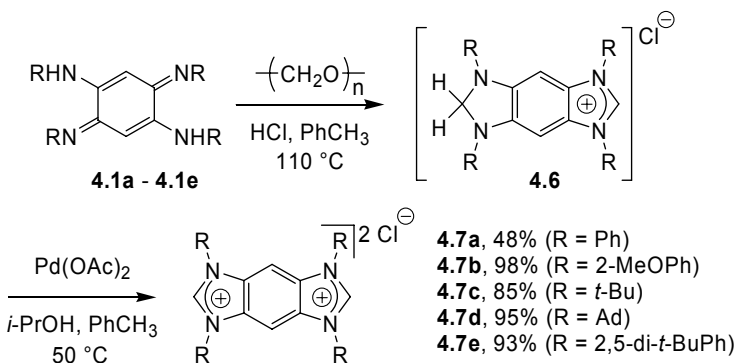


**Scheme 4.1** (TOP) The *o*-tautomer of 2,5-diamino-1,4-benzoquinonediimine (**4.1-*o***) exhibits 1,2-diamino and 1,2-diimino fragments which are (BOTTOM) independently known for undergoing dehydrative cyclizations with paraformaldehyde.

## RESULTS

To test this hypothesis, azophenine **4.1a** was obtained *via* condensation of aniline with *o*-benzoquinone dioxime according to literature protocol.<sup>5a</sup> Related 2,5-diamino-1,4-quinonediimines **4.1b** – **4.1e** were prepared *via* Pd-catalyzed aryl amination<sup>14</sup> of 1,2,4,5-tetrabromobenzene followed by an aerobic workup,<sup>15</sup> in analogy with our previously reported procedure. Confirmation of the 2,5-diamino-1,4-quinonediimine structure was determined through identification of the diagnostic chemical shift of the vinylic proton of the quinoid ring ( $\delta = 5.5$  ppm in  $\text{CDCl}_3$ ) and single crystal X-ray analysis for **4.1b**.<sup>16</sup> As shown in Scheme 2, compounds **4.1** were each reacted with paraformaldehyde in  $\text{PhCH}_3$  under acidic conditions at  $110^\circ\text{C}$ .<sup>17</sup> Within 2 – 6 h, the intense colors associated with these quinone derivatives had dissipated and the reaction mixtures developed yellow-brown solids suggesting hybrid intermediate **4.6** had formed.<sup>18</sup> The reaction temperature

was then reduced to 50 °C and, to facilitate dissolution of solids, *i*-PrOH (10% by volume) was added. Upon the addition of catalytic amounts of Pd(OAc)<sub>2</sub> (1 mol %), slow and persistent generation of gas was observed. Analysis of the crude reaction mixtures by <sup>1</sup>H NMR spectroscopy indicated the 2,5-diamino-1,4-benzoquinonediimines were cleanly converted to the desired benzobis(imidazolium) products (diagnostic signal: C-H, δ = 10 - 11 ppm in DMSO-*d*<sub>6</sub>) **4.7** in good to excellent yields (48 – 98%).<sup>19</sup>



Scheme 4.2 Conversion of 2,5-diamino-1,4-quinonediimines to their respective benzobis(imidazolium) salts using a “one-pot” cyclization/ oxidation reaction sequence.

Although <sup>1</sup>H NMR analyses of the products obtained above were strongly indicative of the desired benzobis(imidazolium) structure, they were further characterized using X-ray analysis after quality crystals of benzobis(imidazolium) dichloride **4.7b** were obtained by slow cooling of a hot, saturated, DMSO solution.<sup>16</sup> As shown in Figure 1, the N1-C2-N2 bond angle (110.2°) was typical of annulated imidazolium compounds as were the imidazole bond lengths.<sup>20</sup> Furthermore, C-C bond lengths typical of arene rings were observed (1.38 to 1.41 Å) in the tetraaminoarene fragment, which indicated the parent quinone core was successfully reduced. The *N*-anisidyl rings were rotated out-of-plane with respect to the benzobis(imidazolium) core (dihedral angles ranged between 35 and

60°) suggesting there was relatively minimal electronic overlap between the two moieties.

## CONCLUSION

In summary, we have developed an alternative, “one-pot” protocol for synthesizing a variety of benzobis(imidazolium) salts from readily available 2,5-diamino-1,4-benzoquinonediimines. This procedure builds upon our recent contributions in preparing bis(azolium) compounds by eliminating the need for inert atmosphere or drybox techniques. In particular, the *o*-quinoid tautomers of 2,5-diamino-1,4-benzoquinonediimines were cyclized using paraformaldehyde to obtain benzimidazolium/*N,N'*-acetal hybrid intermediates which were subsequently oxidized to afford their respective bis(azolium) salts.

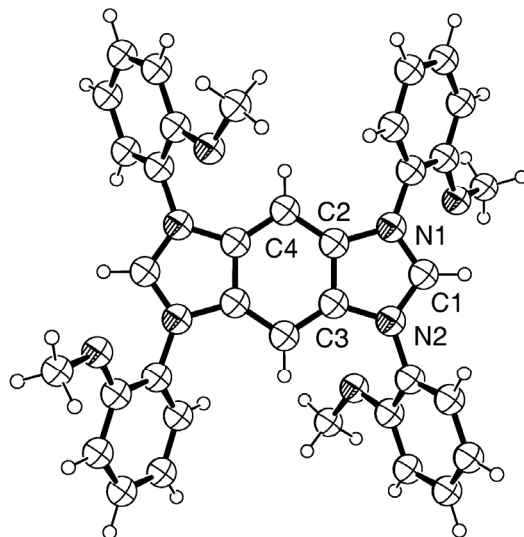


Figure 4.1 ORTEP drawing of **4.7b** (counterions have been removed for clarity). Selected bond lengths (Å) and angles (°): N1-C1, 1.3352(19); N2-C1, 1.3398(19); N1-C2, 1.4007(18); N2-C3, 1.3986(18); C2-C3, 1.4062(19); C2-C4, 1.384(2); N1-C1-N2, 110.21(13); C1-N1-C2, 108.55(11); N1-C2-C3, 106.37(12); C4-C2-N1, 130.60(13); C6-C5-N1-C2, 126.27(15); C3-N2-C12-C13, 59.12(19).

## REFERENCES

- † Portions of this chapter have been previously reported, see: Boydston, A. J.; Khramov, D. M.; Bielawski, C. W. *Tetrahedron Lett.* **2006**, *47*, 5123.
1. Khramov, D. M.; Boydston, A. J.; Bielawski, C. W. *Org. Lett.* **2006**, *8*, 1831.
  2. (a) Boydston, A. J.; Williams, K. A.; Bielawski, C. W. *J. Am. Chem. Soc.* **2005**, *127*, 12496. (b) Kamplain, J. W.; Bielawski, C. W. *Chem. Commun.* **2006**, 1727.
  3. Azophenine generally refers to N,N',N'',N'''-tetraphenyl-2,5-diamino-1,4-benzoquinonediimine; see: (a) Fischer, O.; Hepp, E. *Ber. Dtsch. Chem. Ges.* **1888**, *21*, 676. (b) Kimich, C. *Ber. Dtsch. Chem. Ges.* **1875**, *8*, 1026.
  4. (a) Siri, O.; Braunstein, P. *Chem. Commun.* **2000**, 2223. (b) Masui, H.; Freda, A. L.; Zerner, M. C.; Lever, A. B. P. *Inorg. Chem.* **2000**, *39*, 141.
  5. (a) Paetzold, F.; Niclas, H. J.; Foerster, H. J. *J. Prakt. Chem.* **1986**, *328*, 5. (b) Adams, R.; Schowalter, K. A. *J. Am. Chem. Soc.* **1952**, *74*, 2597. (c) Ruggli, P.; Buchmeier, F. *Helv. Chim. Acta* **1945**, *28*, 850.
  6. (a) Frantz, S.; Rall, J.; Hartenback, I.; Scheid, T.; Záliš, S.; Kaim, W. *Chem. Eur. J.* **2004**, *10*, 149. (b) Siri, O.; Braunstein, P. *Chem. Commun.* **2002**, 208. (c) Rall, J.; Stange, A. F.; Hübner, K.; Kaim, W. *Angew. Chem. Int. Ed.* **1998**, *37*, 2681.
  7. (a) Elhabiri, M.; Siri, O.; Sornosa-Tent, A.; Albrecht-Gary, A.-M.; Braunstein, P. *Chem. Eur. J.* **2004**, *10*, 134. (b) Siri, O.; Braunstein, P.; Rohmer, M.-M.; Bénard, M.; Welter, R. *J. Am. Chem. Soc.* **2003**, *125*, 13793. (c) Rumpel, H.; Limbach, H.-H. *J. Am. Chem. Soc.* **1989**, *111*, 5429.
  8. Haas, Y.; Zilberg, S. *J. Am. Chem. Soc.* **2004**, *126*, 8991.
  9. The equilibrium between the ortho- and para-quinoid tautomers has been previously shown to favor the latter.<sup>6</sup>
  10. (a) Yamashita, M.; Goto, K.; Kawashima, T. *J. Am. Chem. Soc.* **2005**, *127*, 7294. (b) Böhler, C.; Stein, D.; Donati, N.; Grützmacher, H. *New J. Chem.* **2002**, *26*, 1291. (c) Niehus, M.; Erker, G.; Kehr, G.; Schwab, P.; Fröhlich; Blacque, O.; Berke, H. *Organometallics* **2002**, *21*, 2905. (d) Jafarpour, L.; Stevens, E. D.; Nolan, S. P. *J. Organomet. Chem.* **2000**, *606*, 49.
  11. (a) Donia, R. A.; Shotton, J. A.; Bentz, L. O.; Smith, G. E. P. *J. Org. Chem.* **1949**, *14*, 952. (b) Bildstein, B.; Malaun, M.; Kopacka, H.; Wurst, K.; Mitterbock, M.; Ongania, K.-H.; Opronolla, G.; Zanello, P. *Organometallics* **1999**, *18*, 4325.

12. Attempts at direct conversion of 2,5-diamino-1,4-benzoquinonediimines to their respective benzobis(imidazolium) salts using mixtures of electrophiles (e.g., equimolar amounts of HC(OEt)<sub>3</sub> and paraformaldehyde under equilibrating conditions) were met with limited success.
13. Schwarz, D. E.; Cameron, T. M.; Hay, P. J.; Scott, B. L.; Tumas, W.; Thorn, D. L. *Chem. Commun.* **2005**, 5919. For a related example, see: Montgrain, F.; Ramos, S. M.; Wuest, J. D. *J. Org. Chem.* **1988**, 53, 1489.
14. (a) Wenderski, T.; Light, K. M.; Ogrin, D.; Bott, S. G.; Harlan, C. J. *Tetrahedron Lett.* **2004**, 45, 6851. (b) Hillier, A. C.; Grasa, G. A.; Viciu, M. S.; Lee, H. M.; Yang, C.; Nolan, S. P. *J. Organomet. Chem.* **2002**, 653, 69. (c) Prim, D.; Campagne, J.-M.; Joseph, D.; Andrioletti, B. *Tetrahedron* **2002**, 58, 2041. (d) Hartwig, J. F. *Angew. Chem. Int. Ed.* **1998**, 37, 2046. (e) Wolfe, J. P.; Wagaw, S.; Marcox, J.-F.; Buchwald, S. L. *Acc. Chem. Res.* **1998**, 31, 805.
15. General procedure for preparing compounds 4.1b – 4.1e: A 20 mL vial charged with 1,3-bis(2,6-diisopropylphenyl)imidazolium chloride (0.02 mmol), NaOt-Bu (0.02 mmol), Pd(OAc)<sub>2</sub> (0.01 mmol), and PhCH<sub>3</sub> (5 mL). After stirring the resulting mixture for 10 min, 1,2,4,5-tetrabromobenzene (1.00 mmol), amine (4.10 mmol), NaOtBu (4.20 mmol) and PhCH<sub>3</sub> (5 mL) were added. The resulting mixture was sealed under an atmosphere of nitrogen and stirred at 110 °C for 8 h. After cooling to ambient temperature, the resulting mixture was diluted with hexanes and precipitated solids were collected by filtration. Residual inorganic salts were removed by filtering CHCl<sub>3</sub> solutions of the products. Characterization data for new compounds: Azophenine 1b: <sup>1</sup>H NMR (CDCl<sub>3</sub>): δ 8.55 (s, 2H), 7.05 – 6.91 (m, 16H), 6.16 (s, 2H) 3.83 (s, 12H); <sup>13</sup>C NMR (CDCl<sub>3</sub>) δ 150.4, 148.2, 134.4, 130.5, 121.0, 120.6, 119.1, 114.4, 111.3, 110.3, 93.1, 55.7, 55.5; HRMS: [M]<sup>+</sup> calcd for C<sub>34</sub>H<sub>32</sub>N<sub>4</sub>O<sub>4</sub>, 560.2424; Found: 560.2428; Spectral data of 1c was consistent with its previously reported<sup>1</sup> value; Compound 1d: <sup>1</sup>H NMR (CDCl<sub>3</sub>): δ 6.69 (br, 2H), 5.77 (s, 2H), 2.10 (br, 12H), 1.97 (br, 24H), 1.68 (br, 24H); <sup>13</sup>C NMR (CDCl<sub>3</sub>): δ (ca 138), 92.2, 52.7, 42.6, 36.9, 29.8; HRMS: [M]<sup>+</sup> calcd for C<sub>46</sub>H<sub>64</sub>N<sub>4</sub>, 672.5131; Found: 672.5134; Azophenine 1e: <sup>1</sup>H NMR (CDCl<sub>3</sub>): δ 8.13 (s, 2H), 7.03 (s, 2H), 6.78 (br, 8H), 6.31 (s, 2H), 1.17 (s, 72H); <sup>13</sup>C NMR (CDCl<sub>3</sub>): δ 151.4, 117.6, 90.7, 34.8, 31.4; HRMS: [M+1]<sup>+</sup> calcd for C<sub>62</sub>H<sub>88</sub>N<sub>4</sub>, 889.7009; Found, 889.7089.
16. Crystal data for 4.1b: C<sub>34</sub>H<sub>32</sub>N<sub>4</sub>O<sub>4</sub> - 2 C<sub>4</sub>H<sub>8</sub>O, M = 704.84, triclinic, P1, a = 12.5090(8), b = 13.3300(9), c = 14.2730(11) Å, α = 64.179(3), β = 89.750(4), γ = 64.058(5)°, V = 1874.8(2) Å<sup>3</sup>, Z = 2, D<sub>c</sub> = 1.249 g cm<sup>-3</sup>, μ = 0.084 mm<sup>-1</sup>, F(000) = 752, λ (Mo Kα) = 0.71073 Å, large red prisms, crystal size 0.33 × 0.30 × 0.25 mm, 10820 reflections measured (R<sub>int</sub> = 0.0499), 6570 unique, R<sub>1</sub> = 0.1268 for I > 2σ(I) and 0.2564 for all data. There were two molecules of

THF in the asymmetric unit, one of which was found to be disordered and could not be adequately modeled. Key bond lengths ( $\text{\AA}$ ) and angles ( $^\circ$ ): N1-C1, 1.301(5); N2-C2, 1.376(5); C1-C2, 1.493(6); C1-C3, 1.431(6); C2-C3, 1.340(6); C4-N1-C1-C2, 176.1(4). Crystal data for 7b: (C<sub>36</sub>H<sub>32</sub>N<sub>4</sub>O<sub>4</sub>) 2Cl - 4C<sub>2</sub>H<sub>6</sub>SO, M = 968.07, triclinic, P1, a = 8.2689(2), b = 11.4843(2), c = 13.3347(3)  $\text{\AA}$ ,  $\alpha$  = 112.090(1),  $\beta$  = 96.690(1),  $\gamma$  = 90.029(1) $^\circ$ , V = 1164.00(4)  $\text{\AA}^3$ , Z = 1, D<sub>c</sub> = 1.381 g cm<sup>-3</sup>,  $\mu$  = 0.375 mm<sup>-1</sup>, F(000) = 510,  $\lambda$  (Mo K $\alpha$ ) = 0.71073  $\text{\AA}$ , colorless prisms, crystal size 0.49 x 0.31 x 0.20 mm, 7435 reflections measured (R<sub>int</sub> = 0.0162), 5229 unique, R<sub>1</sub> = 0.0363 for I > 2 $\sigma$ (I) and 0.0460 for all data. The data were collected at 153(2) K using an Oxford Cryostream low temperature device. The structures were solved by direct methods and refined by full-matrix least-squares on F<sub>2</sub> with anisotropic displacement parameters for the non-H atoms using SHELXL-97 (Sheldrick, G. M. University of Gottingen, Germany, 1994). Data for these structures have been deposited with the Cambridge Crystallographic Data Centre (12 Union Road, Cambridge CB2 1EZ, UK) as CCDC 603509 (1b) and 603510 (7b).

17. General procedure for preparing compounds 4.7: A 50 mL flask was charged 1 (0.5 mmol), PhCH<sub>3</sub> (20 mL), paraformaldehyde (1.2 mmol), and conc. HCl (1 drop). After stirring the mixture at 110 °C for 2 – 6 h, the temperature was reduced to 50 °C and i-PrOH (2 mL) was added to facilitate partial dissolution of solids. Pd(OAc)<sub>2</sub> (5  $\mu$ mol) was then added and slow gas evolution followed. The mixture was stirred for an additional 2 – 4 h and then concentrated to afford crude product. Note: this protocol was found to work equally well in other solvents (e.g., CH<sub>3</sub>CN, DMF, DMSO, and EtOH). Spectral data of 7a – 7d were in accord with their previously reported values.<sup>1</sup> Characterization data for 7e: <sup>1</sup>H NMR (CDCl<sub>3</sub>):  $\delta$  9.98 (br, 2H), 7.97 (br, 8H), 7.82 (br, 2H), 7.62 (s, 4H), 1.32 (s, 72H); <sup>13</sup>C NMR (CDCl<sub>3</sub>):  $\delta$  154.0, 144.7, 132.1, 125.5, 120.7, 114.9, 99.6, 35.5, 31.4; HRMS: [M]<sup>+</sup> calcd for C<sub>64</sub>H<sub>88</sub>N<sub>4</sub>, 912.7009; Found, 912.6983.
18. Subjecting N,N',N'',N'''-tetra(p-chlorophenyl)-2,5-diamino-1,4-benzoquinonediimine 5a to the cyclization-oxidation reaction sequence outlined in Scheme 4.2 afforded 1,3-di(p-chlorophenyl)-5,6-di(p-chlorophenyl-amino)benzimidazolium chloride (95% yield): <sup>1</sup>H NMR (CDCl<sub>3</sub>):  $\delta$  10.14 (s, 1H), 7.97 (d, J = 9.2 Hz, 4H), 7.84 (d, J = 9.2 Hz, 4H), 7.49 (s, 8H), 7.13 (s, 2H), 5.95 (s, 2H).
19. It was also found that benzobis(imidazolium) salts 4.7 could be prepared via a one-pot, reduction-cyclization reaction sequence: Subjecting 1a – 1d independently to standard hydrogenative conditions (10% Pd/C, 400 PSI H<sub>2</sub>) in HC(OEt)<sub>3</sub> for 16 – 24 h followed by addition of acid (HCl or HBF<sub>4</sub>) at 60 – 110 °C for 2 – 24 h afforded the respective benzobis(imidazolium) salts 7a – 7d in high purity and in good to excellent yields (51 – 92%).

20. (a) Saravanakumar, S.; Oprea, A. I.; Kindermann, M. K.; Jones, P. G.; Heinicke, J. *Chem. Eur. J.* **2006**, *12*, 3143. (b) Hahn, F. E; Jahnke, M. C.; Gomez-Benitez, V.; Morales-Morales, D.; Pape, T. *Organometallics* **2005**, *24*, 6458.

## **Chapter 5: Synthesis and Study of Janus Bis(carbene)s and Their Transition Metal Complexes<sup>†</sup>**

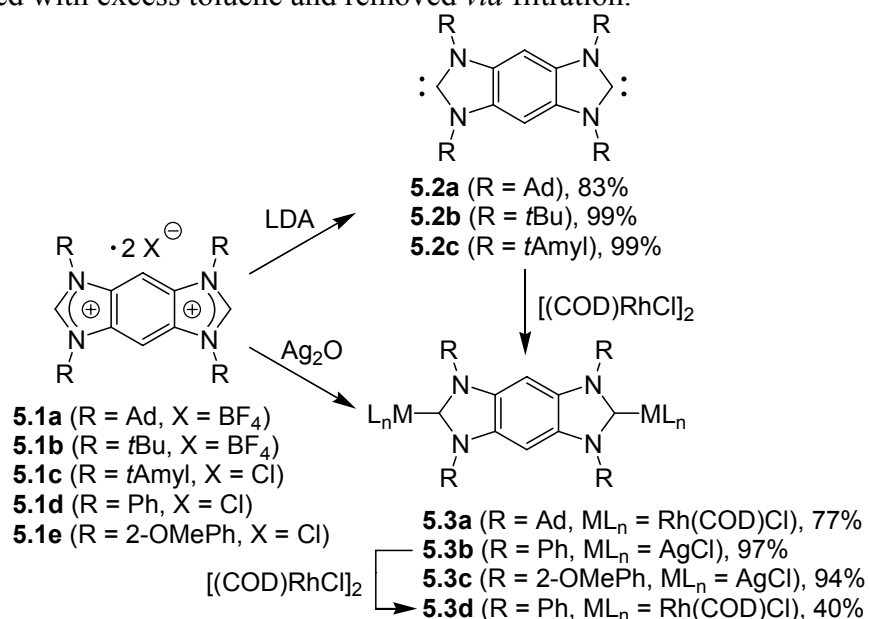
### **INTRODUCTION**

The construction of new organic-inorganic hybrid materials with interesting structural features and technologically-useful functions is a vibrant area of research with considerable potential.<sup>1</sup> The key to growth in this field is the development of new, tunable molecular scaffolds for bridging transition metals. Ideal linkers should be readily accessible, exhibit high affinities toward a broad range of transition metals, and possess modular features amenable for precisely manipulating their inherent physical and electronic characteristics. Stable N-heterocyclic carbenes (NHCs),<sup>2</sup> particularly imidazolylidenes,<sup>3</sup> fall in this category. They have been found to form robust complexes with nearly every transition metal<sup>2,4</sup> and the basic *N*-heterocyclic nucleus as well as its *N*-substituents can be acutely modified.<sup>5</sup> As such, an impressive amount of attention has been devoted toward optimizing and understanding the interaction of carbenes with various transition metals to form monometallic complexes.<sup>2-6</sup> However, comparatively less attention has been directed toward the development of discrete, multifunctional carbenes that are poised to bind multiple transition metals.<sup>7,8</sup> Herein, we report the synthesis and characterization of benzobis(imidazolylidene)s, a new class of Janus<sup>9</sup> bis(carbene)s comprised of two linearly opposed imidazolylidenes annulated to a common arene backbone, and demonstrate their utility in preparing new organometallic materials.

### **RESULTS**

Requisite benzobis(imidazolium) salts possessing a range of *N*-substituents (**5.1**) were synthesized *via* Pd-catalyzed aryl amination of 1,2,4,5-tetrabromobenzene followed

by formylative cyclization or *via* reductive cyclization of their respective 2,5-diamino-1,4-benzoquinonediimines according to our previously reported procedures.<sup>10</sup> Independent treatment of **5.1a-c** with 2.2 equiv of lithium diisopropylamide (LDA) in THF at RT caused precipitation of products **5.2a** and **5.2b** which were subsequently isolated *via* filtration in yields of 83 and 99%, respectively. While **5.2a** and **5.2b** were only slightly soluble in common organic solvents (THF, toluene, benzene, etc.), a highly soluble derivative featuring *N*-*t*-amyl groups (**5.2c**) was obtained in 99% yield after LiCl was precipitated with excess toluene and removed *via* filtration.<sup>11</sup>



Scheme 5.1      Synthesis of benzobis(imidazolylidene)s and their related transition metal complexes.

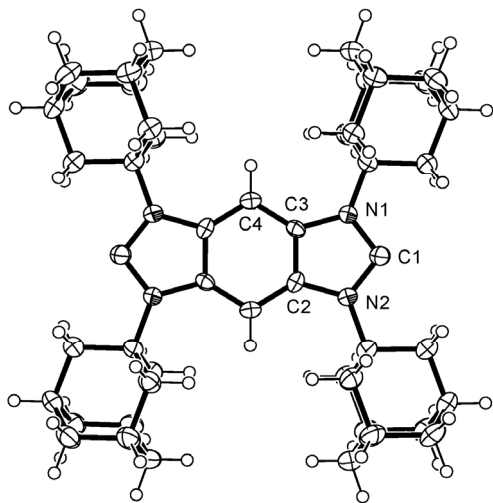


Figure 5.1 ORTEP view of **5.2a**. Selected bond lengths ( $\text{\AA}$ ) and angles ( $^{\circ}$ ): C1-N1, 1.369(3); C1-N2, 1.368(3); N1-C3, 1.411(3); N2-C2, 1.408(3); C2-C3, 1.402(3); C3-C4, 1.388(3); N1-C1-N2, 104.8(2).

The  $^{13}\text{C}$  NMR spectra of products **5.2a – 5.2c** in  $\text{C}_6\text{D}_6$  each exhibited a single, diagnostic signal between  $\delta = 227 - 231$  ppm which was indicative of the highly symmetric structures shown in Scheme 1 and consistent with other known annulated imidazolylidenes.<sup>12</sup> To confirm, a crystal of **5.2a** was obtained by vapor diffusion of pentane into a saturated toluene/THF solution (1:1 v/v) and analyzed using X-ray diffraction analysis.<sup>13</sup> An ORTEP view of the molecular structure is shown in Figure 4.1 with selected bond lengths and angles in the caption. Notably, the N-C-N bond angle was found to be  $104.8(2)^{\circ}$ <sup>14</sup> which was similar to saturated imidazolylidenes<sup>15</sup> and benzimidazolylidenes.<sup>12a</sup> This promising result strongly suggested that each carbene “face” of these Janus ligands should display similar chemistries and affinities toward transition metals as their monofunctional analogues.

Addition of an equimolar amount of  $[(\text{COD})\text{RhCl}]_2$  (COD = cis,cis-1,5-cyclooctadiene) to a THF solution of **5.2a** at RT resulted in the precipitation of Rh complex **5.3a** as a yellow solid, which was isolated in 77% yield. Analysis of this

complex by NMR spectroscopy confirmed the stoichiometry between the Rh centers and bis(carbene) nucleus was 2:1. A single  $^{13}\text{C}$  resonance appeared at  $\delta = 198$  ppm and two distinct sets of olefinic 1H signals were observed at 3.0 (cis to the carbene) and 5.0 ppm (trans), which was suggestive of a square planar geometry for each of the metal centers.<sup>16</sup> The structure of **5.3a** was confirmed by X-ray diffraction analysis after a suitable crystal was obtained by slow cooling of a hot  $\text{CHCl}_3$  solution (see Figure 5.2). Although key bond lengths were in accord with known NHC-Rh complexes,<sup>16</sup> a notable exception was the positions of Rh atoms which were displaced perpendicularly from the plane of the benzobis(imidazolylidene) by 0.75 Å. This unusual structural feature was attributed to the substantial steric bulk of the N-adamantyl groups balanced by the high affinity of imidazolylidenes for Rh(I) (vide infra).<sup>17</sup>

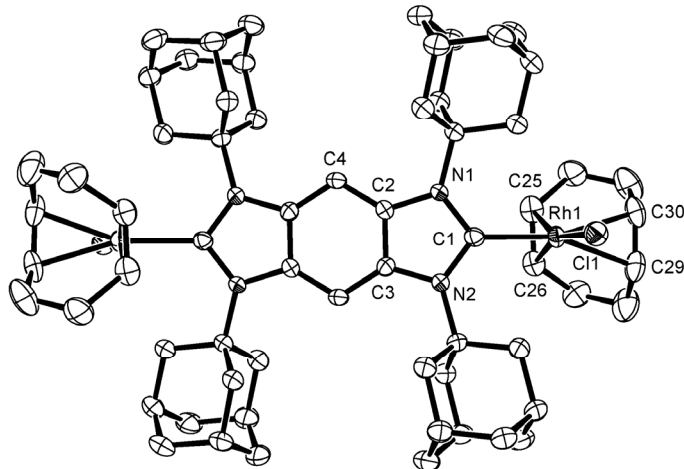


Figure 5.2 ORTEP view of **5.3a**. Selected bond lengths (Å) and angles (°): Rh1-C1, 2.073(3); Rh1-C25, 2.125(3); Rh1-C26, 2.131(3); Rh1-C29, 2.184(3); Rh1-C30, 2.197(3); C1-N1, 1.387(4); C1-N2, 1.406(4); N1-C2, 1.406(4); N2-C3, 1.395(4); C2-C3, 1.401(4); C2-C4, 1.397(4); N1-C1-N2, 105.7(2). Hydrogen atoms have been removed for clarity.

In cases where the free bis(carbene)s were not isolable (**5.1d-e**),<sup>18</sup> an alternative method of forming metal complexes was desired. Direction shifted toward Lin's<sup>19</sup>

versatile Ag-mediated carbene transfer protocol for accessing organometallic complexes.<sup>[20]</sup> As shown in Scheme 5.1, bis(azolium) salts **5.1d** and **5.1e** were respectively treated with Ag<sub>2</sub>O (1.0 equiv) in CH<sub>2</sub>Cl<sub>2</sub> (23 °C) or CH<sub>3</sub>CN (40 °C). Following filtration of inorganic salts which precipitated during the reaction, concentration of the resulting solutions afforded products **5.3b** and **5.3c** in excellent yields (97 and 94%, respectively). Crystals of **5.3c** were obtained from slow diffusion of hexanes into a saturated CH<sub>2</sub>Cl<sub>2</sub> solution and analyzed using X-ray diffraction analysis. As shown in Figure 5.3, the structure was essentially linear along its main axis with a C1-Ag1-C11 bond angle of 176° and its *N*-aryl substituents were rotated out of the plane of the benzobis(imidazolylidene) with an average dihedral angle = 69°. Interestingly, in the solid-state the complexes arranged in infinite rows governed by intermolecular argentophilic interactions.<sup>20</sup>

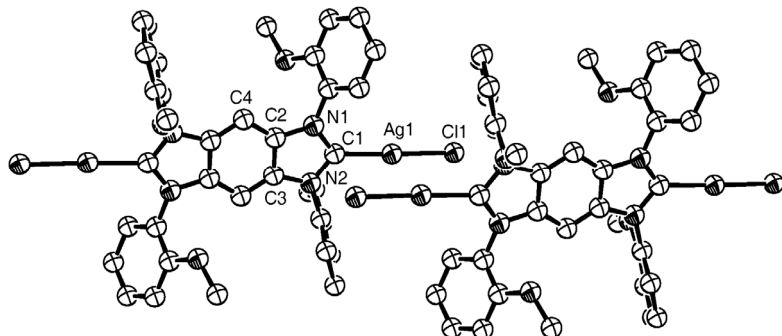
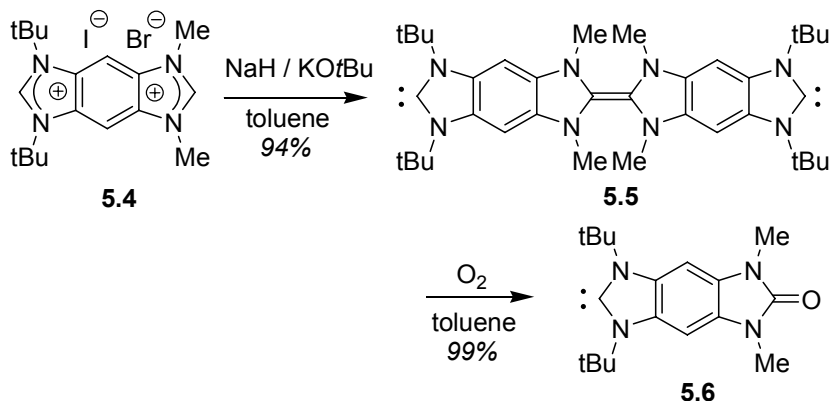


Figure 5.3 ORTEP view of **5.3c**. Selected bond lengths (Å) and angles (°): Ag1-C1, 2.072(11); Ag1-Cl1, 2.236(3); C1-N1, 1.352(12); C1-N2, 1.360(11); N1-C2, 1.409(11); N2-C3, 1.409(12); C2-C3, 1.411(12); C2-C4, 1.353(13); N1-C1-N2, 106.4(9). Ag-Ag, 3.3054(15). Hydrogen atoms have been removed for clarity.

Treatment of complex **5.3b** with an equimolar amount of [(COD)RhCl]<sub>2</sub> in CH<sub>2</sub>Cl<sub>2</sub> at 50 °C for 24 h afforded bimetallic Rh complex **5.3d** as an orange-brown powder in 40% yield.<sup>21</sup> Although solution and solid-state<sup>22</sup> structural analyses indicated

**5.3d** was superficially similar to **5.3a**, a key difference was the Rh atoms were now coplanar with the benzobis(imidazolylidene). Considering the N-phenyl groups were rotated by an average of 63° relative to this same plane (minimizing any electronic contributions) and both complexes showed a similar trans effect (average Rh-olefin bond distances: **5.3a**: 2.20 Å vs. **5.3d**: 2.19 Å), the size of the N-substituents appeared to dominate structural features about the metals centers.

Finally, we focused on the synthesis of bis(azolium) **5.4**, a desymmetrized precursor that was envisioned to provide a Janus bis(carbene) with differential characteristics at each carbene “face.” The dissimilar environments of the 1,3-dimethyl- and 1,3-di-t-butylimidazolium fragments were manifested in the <sup>1</sup>H NMR spectrum (DMSO-*d*6) of **5.4** which exhibited signals at δ = 9.9 and 9.0 ppm, respectively. Deprotonation of **5.4** using 2.1 equiv of NaH (and catalytic KOtBu) in toluene at 120 °C resulted in selective dimerization to afford enetetraamine **5.5** which was subsequently isolated in 94% yield. Crystals suitable for X-ray analysis were obtained by slow cooling of a saturated toluene solution of **5.5** and an ORTEP view of the structure of this compound is shown in Figure 5.4. Key bond lengths and angles of the benzimidazolylidene fragments were in accord with **5.2b**,<sup>13</sup> and the torsion angle about the enetetraamine was found to be 15.2°, consistent with the dimer of 1,3-dimethylbenzimidazolylidene.<sup>16a</sup> The solution structure of **5.5** was confirmed by treatment with O<sub>2</sub> which rapidly and selectively oxidized the enetetramine moiety to afford urea **5.6**.<sup>23</sup>



Scheme 5.2      Selective dimerization and oxidation of a desymmetrized Janus bis(carbene) precursor.

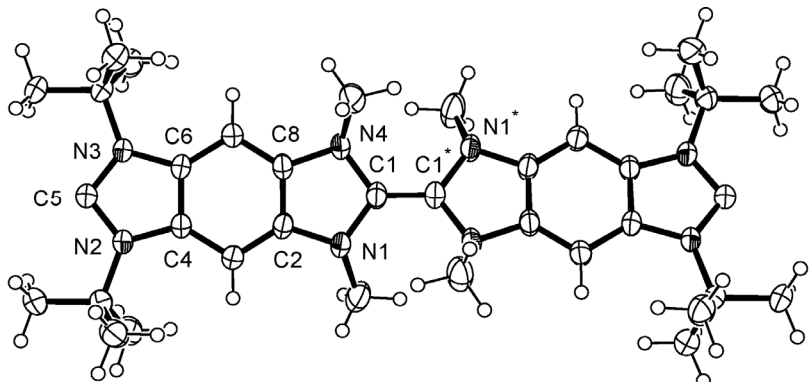


Figure 5.4    ORTEP view of **5.5**. Selected bond lengths ( $\text{\AA}$ ) and angles ( $^\circ$ ): C5-N3, 1.366(3); C5-N2, 1.371(3); N3-C6, 1.406(2); N2-C4, 1.404(3); C4-C6, 1.397(3); C1-N1, 1.426(3); C1-N4, 1.424(3); N4-C8, 1.416(3); N1-C2, 1.408(2); C2-C8, 1.399(3); C1-C1\*, 1.349(4); C1-N4-C18, 117.79(18); N2-C5-N3, 104.00(17); N1-C1-N4, 108.48(16).

## CONCLUSION

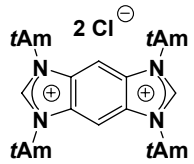
In summary, we report the first Janus bis(carbene)s with facially opposed imidazolylidenes annulated to a common arene core. Synthetic routes employed to obtain these compounds were modular, high yielding, and permitted access to derivatives with *N*-alkyl or *N*-aryl substituents as well as a desymmetrized variant. Their promise as

ligands was borne out through synthesis of a variety of new homobimetallic complexes; efforts toward heterobimetallic complexes are currently underway.

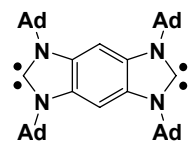
## EXPERIMENTAL

Compounds **5.1a-e** were prepared according to our previously reported procedures.<sup>24</sup> All reactions were conducted under an atmosphere of dry nitrogen using standard Schlenk techniques or in a nitrogen filled glove-box. CH<sub>2</sub>Cl<sub>2</sub> was distilled from CaH<sub>2</sub> under nitrogen and degassed by three freeze-pump-thaw cycles. THF and toluene were distilled from Na/benzophenone under nitrogen and degassed by three freeze-pump-thaw cycles. [(COD)RhCl]<sub>2</sub> and 1,3-bis(2,6-diisopropylphenyl)imidazolium chloride were purchased from Strem and used without further purification. All other reagents were purchased from Aldrich or Acros and were used without further purification. <sup>1</sup>H NMR spectra were recorded using a Varian Gemini (300 MHz or 400 MHz) spectrometer. Chemical shifts are reported in delta ( $\delta$ ) units, expressed in parts per million (ppm) downfield from tetramethylsilane using the residual protonated solvent as an internal standard (CDCl<sub>3</sub>, 7.24 ppm; C<sub>6</sub>D<sub>6</sub>, 7.15 ppm, DMSO-d<sub>6</sub>, 2.49 ppm). <sup>13</sup>C NMR spectra were recorded using a Varian Gemini (75 MHz or 100 MHz) spectrometer and were routinely run with broadband decoupling. Chemical shifts are reported in delta ( $\delta$ ) units, expressed in parts per million (ppm) downfield from tetramethylsilane using the residual protio solvent as an internal standard (CDCl<sub>3</sub>, 77.0 ppm; C<sub>6</sub>D<sub>6</sub>, 128.0 ppm, DMSO-d<sub>6</sub>, 39.5 ppm). High-resolution mass spectra (HRMS) were obtained with a VG analytical ZAB2-E or a Karatos MS9 instrument and are reported as m/z (relative intensity). X-ray crystal structure data was collected for compounds 1a (CCDC 605308), 2a (CCDC 605309), 2b (CCDC 605310), 3a (CCDC 605311), 3c (CCDC 605312), 3d (CCDC 605313), 5 (CCDC 605314), and (COD)RhCl(1,3-diadamantylbenzimidazolylidene) (CCDC 605315) and deposited with the Cambridge Crystallographic Data Centre, 12

Union Road, Cambridge CB2 1EZ, UK. A separate Crystallographic Information File (CIF) for each of these structures has also been included.

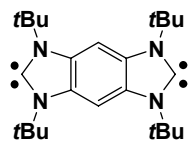


**Tetrakis-*N*-*t*-amylbenzobis(imidazolium) dichloride (5.1c).** 1,2,4,5-Tetrakis-*N*-*t*-amylaminobenzene was first prepared according to literature procedure<sup>24a</sup> using 1,2,4,5-tetrabromobenzene and *t*-amylamine. <sup>1</sup>H NMR (C<sub>6</sub>D<sub>6</sub>): δ 6.65 (s, 2H), 3.57 (br, 4H), 1.62 (q, *J* = 7.6 Hz, 8H), 1.22, (s, 24H) 0.95 (t, *J* = 7.6 Hz, 12H); <sup>13</sup>C NMR (C<sub>6</sub>D<sub>6</sub>): δ 132.0, 114.8, 54.3, 35.4, 27.5, 8.9. A 25 mL flask was charged with triethylorthoformate (10 mL), 1,2,4,5-tetrakis-*N*-*t*-amylaminobenzene (610 mg, 1.46 mmol), conc. HCl (1 mL), and a stir bar. The mixture was stirred vigorously at RT until complete dissolution of all solids was observed. The reaction was then heated at 60 °C for 10 h. Ethanol was partially removed from the solution by evaporation under reduced pressure. Precipitated solids were collected by filtration and dried under vacuum to afford 484 mg (65%) of the desired product as a white powder. <sup>1</sup>H NMR (DMSO-*d*<sub>6</sub>): δ 9.23 (s, 2H), 8.55 (s, 2H), 2.28 (q, *J* = 7.2, 8H), 1.93 (s, 24H), 0.73 (t, *J* = 7.2 Hz, 12H); <sup>13</sup>C NMR (DMSO-*d*<sub>6</sub>): δ 144.3, 128.9, 102.5, 65.6, 31.9, 25.9, 8.2.

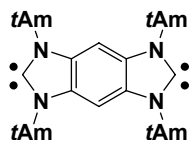


**Tetrakis-*N*-adamantylbenzobis(imidazolylidene) (5.2a).** In a nitrogen-filled drybox, a 20 mL flask was charged with bis(azolium) salt **5.1a** (680 mg, 0.78 mmol), THF (10 mL), LDA (1.83 M in THF/hexanes, 0.93 mL, 1.70 mmol), and a stir bar. The flask was sealed and the resulting slurry was stirred for 10 h at RT. Precipitated solids were collected by filtration, washed with THF (5 mL) and dried under reduced pressure to afford 450 mg (83%) of the desired product as a white solid. Crystals suitable for X-ray analysis were obtained by solvent diffusion of pentane into a saturated solution of **5.2a** in toluene/THF (1:1 v/v) (CCDC 605309). <sup>1</sup>H NMR

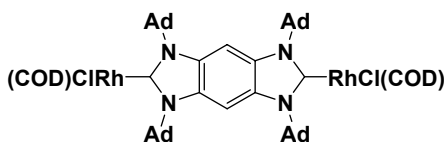
(C<sub>6</sub>D<sub>6</sub>): δ 8.37 (s, 2H), 2.81 (s, 24H), 2.15 (s, 12H), 1.81-1.67 (br, 24H); <sup>13</sup>C NMR (C<sub>6</sub>D<sub>6</sub>): δ 227.6, 130.5, 98.5, 58.3, 43.6, 37.2, 30.5.



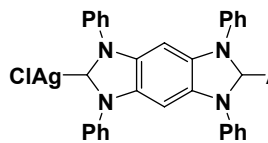
**Tetrakis-N-t-butylbenzobis(imidazolylidene) (5.2b).** In a nitrogen-filled drybox, a 20 mL flask was charged with bis(azolium) salt **5.1b** (1.27 g, 2.3 mmol), THF (10 mL), LDA (1.80 M in THF/hexanes, 2.8 mL, 5.05 mmol), and a stir bar. The flask was sealed and the resulting slurry was stirred for 10 h at RT. Precipitated solids were collected by filtration, washed with THF (5 mL) and dried under vacuum to afford 870 mg (99%) of the desired product as a light gray solid. Crystals suitable for X-ray analysis were obtained by slow cooling of a hot, saturated toluene solution (CCDC 605310). <sup>1</sup>H NMR (C<sub>6</sub>D<sub>6</sub>): δ 7.79 (s, 2H), 1.78 (s, 36H); <sup>13</sup>C NMR (C<sub>6</sub>D<sub>6</sub>): δ 228.3, 130.9, 97.5, 57.2, 30.5; HRMS calcd. for C<sub>24</sub>H<sub>34</sub>N<sub>4</sub> [M+H<sup>+</sup>]: 383.3175, found: 383.3177.



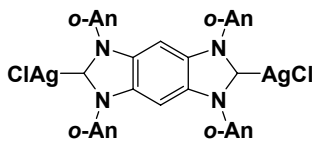
**Tetrakis-N-t-amylbenzobis(imidazolylidene) (5.2c).** In a nitrogen-filled drybox, a 10 mL flask was charged with bis(azolium) salt **5.1c** (50 mg, 0.098 mmol), LDA (0.41 M in THF/hexanes, 0.48 mL, 0.195 mmol), and a stir bar. The resulting slurry was stirred for 15 minutes at RT, then toluene (1 mL) was added. The reaction mixture was filtered through Celite and the solvent was removed under reduced pressure to afford 22 mg (99%) of the desired product as a white solid. <sup>1</sup>H NMR (C<sub>6</sub>D<sub>6</sub>): δ 7.89 (s, 2H), 2.14 (q, J = 7.2 Hz, 8H), 1.85 (s, 24H), 0.76 (t, J = 7.2 Hz, 12H); <sup>13</sup>C NMR (C<sub>6</sub>D<sub>6</sub>): δ 230.2, 131.1, 96.9, 60.1, 33.7, 29.0, 8.5; HRMS calcd. for C<sub>26</sub>H<sub>46</sub>N<sub>4</sub> [M+H<sup>+</sup>]: 438.3722, found: 438.3722.



**Bimetallic Rhodium Complex 5.3a.** In a nitrogen-filled drybox, a 10 mL flask was charged with bis(carbene) **5.2a** (70 mg, 0.1 mmol),  $[(\text{COD})\text{RhCl}]_2$  (50 mg, 0.1 mmol), THF (2 mL), and a stir bar. The resulting slurry became homogeneous after stirring for 5 min at RT. Product precipitation began within 30 min and the reaction was stirred for an additional 2 h. Precipitated solids were collected by filtration, washed with THF (3 mL), and dried under vacuum to afford 100 mg (77%) of the desired product as a yellow powder. Crystals suitable for X-ray analysis were obtained by slow evaporation of a saturated  $\text{CHCl}_3$  solution (CCDC 605311).  $^1\text{H}$  NMR ( $\text{CDCl}_3$ ):  $\delta$  8.20 (s, 2H), 4.98 (s, 2H), 3.50-3.47 (m, 12H), 3.00-2.97 (m, 16H), 2.47-2.41 (m, 22H), 1.67-1.61 (m, 36H);  $^{13}\text{C}$  NMR ( $\text{CDCl}_3$ ):  $\delta$  198 (d), 129.5, 109.7, 99.9, 92.5 (d,  $J = 6.9$  Hz), 67.7 (d,  $J = 14.8$  Hz), 62.2, 43.2, 36.6, 32.3, 30.4, 28.8.



**Diargento Complex 5.3b.** Bis(azolium) salt **5.1d** (535 mg, 1.0 mmol) was dissolved in  $\text{CH}_3\text{CN}$  (10 mL) and  $\text{Ag}_2\text{O}$  (243 mg, 1.05 mmol) was added. The resulting suspension was stirred at 40 °C for 2 h. The cooled reaction mixture was filtered through Celite and concentrated to give 726 mg (97%) of **5.3b** as a brown powder.  $^1\text{H}$  and  $^{13}\text{C}$  NMR analysis revealed broad peaks indicative of aggregation/oligomerization.  $^1\text{H}$  NMR ( $\text{DMSO}-d_6$ )  $\delta$  7.82-7.78 (m, 8H), 7.73-7.60 (m, 12H), 7.45 (s, 2H).



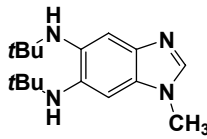
**Diargento Complex 5.3c.** Bis(azolium) salt **5.1e** (1.20 g, 1.82 mmol) was suspended in  $\text{CH}_2\text{Cl}_2$  (100 mL). To the mixture was added  $\text{Ag}_2\text{O}$  (423 mg, 1.82 mmol) and the flask was protected from light using Al foil. After stirring for 2 h at room RT, a brown suspension formed

which was filtered over Celite and concentrated to a brown glassy solid (1.49 g, 94%). <sup>1</sup>H and <sup>13</sup>C NMR analysis revealed broad peaks indicative of aggregation/oligomerization. Crystals suitable for X-ray analysis were obtained by diffusion of hexanes into a solution of **5.3c** in CH<sub>2</sub>Cl<sub>2</sub> (CCDC 605312).

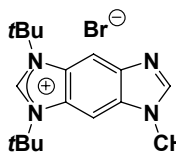
**Bimetallic Rhodium Complex **5.3d**.** From bis(azolium) salt **5.1d·BF<sub>4</sub>**: The bis(azolium) salt (100 mg, 0.157 mmol) was added to THF (3 mL) followed by NaHMDS (0.16 mL, 0.32 mmol, 2.0 M in THF). The slurry was stirred for 1 h, then [(COD)RhCl]<sub>2</sub> (77 mg, 0.157 mmol) was added and the solution was heated to 50 °C in a sealed vial for 10 h. The cooled reaction mixture was diluted with hexanes (6 mL) and solids were collected by filtration, washed with toluene (5 mL) and hexanes (5 mL). Solvent was removed under reduced pressure. Residual inorganic salts were removed by treating the crude solid with chloroform and filtering through a 0.45 µm PTFE filter, followed by removal of solvent under reduced pressure to obtain the product as a tan solid (51 mg, 34%).

From diargento complex **5.3b**: The diargento complex **5.3b** (373 mg, 0.50 mmol) and [(COD)RhCl]<sub>2</sub> (258 mg, 0.52 mmol) were partially dissolved in CH<sub>2</sub>Cl<sub>2</sub> (12 mL) in a screw-cap vial under an atmosphere of dry nitrogen. The vial was sealed with a Teflon-coated cap and stirred at 50 °C for 20 h protected from light with Al foil. The cooled reaction mixture was then filtered through Celite and concentrated to give 191 mg (40%) of the desired product. Crystals suitable for X-ray analysis were obtained by slow diffusion of hexanes into a saturated CH<sub>2</sub>Cl<sub>2</sub> solution (CCDC 605313). <sup>1</sup>H NMR (CDCl<sub>3</sub>): δ 8.13 (br, 8H), 7.64-7.52 (br, 12H), 7.13 (s, 2H), 4.89 (br, 4H), 2.73 (br, 4H), 1.8-1.46 (br, 16H); <sup>13</sup>C NMR (CDCl<sub>3</sub>): δ

137.7, 132.7, 129.3, 128.9, 127.8, 127.4, 109.7, 99.3, 91.9, 68.5 (d,  $J = 13.9$  Hz), 32.0, 28.2.

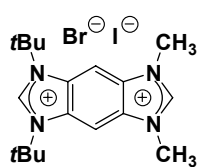


**5,6-Bis(*t*-butylamino)-1-methylbenzimidazole.** Under an atmosphere of nitrogen, a 10 mL vial was charged with 1,3-bis(2,6-diisopropylphenyl)imidazolium chloride (17 mg, 0.04 mmol), NaOtBu (2 mg, 0.02 mmol), Pd(OAc)<sub>2</sub> (5 mg, 0.02 mmol), toluene (5 mL), and a stir bar. The resulting mixture was stirred at 80 °C for 5 minutes. Then, 5,6-dichloro-1-methylbenzimidazole<sup>[25]</sup> (101 mg, 0.50 mmol) was added, followed by *t*-butyl amine (146 mg, 2.0 mmol) and NaOtBu (101 mg, 1.05 mmol). The resulting mixture was sealed and stirred at 150 °C for 24 h. After cooling to RT, precipitated solids were removed by filtration and solvent was removed to obtain a brown solid which was used in the next step without additional purification. <sup>1</sup>H NMR (CDCl<sub>3</sub>): δ 7.57 (s, 1H), 7.32 (s, 1H), 6.70 (s, 1H), 3.70 (s, 3H), 1.34 (s, 9H), 1.21 (s, 9H); <sup>13</sup>C NMR (CDCl<sub>3</sub>): δ 141.2, 140.0, 136.1, 131.9, 131.4, 115.6, 95.6, 52.8, 51.3, 38.5, 29.8, 29.7.

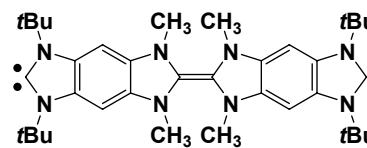


**Desymmetrized Benzimidazolium Salt.** Crude 5,6-bis(*t*-butylamino)-1-methylbenzimidazole was partially dissolved in HC(OEt)<sub>3</sub> and HBr (48%). The resulting slurry was stirred for 3 h at 65 °C. After cooling to RT, the solids were collected by vacuum filtration. The crude product was then dissolved in *i*PrOH and stirred with excess Na<sub>2</sub>CO<sub>3</sub> for 2 h. Filtration through Celite followed by removal of solvent under reduced pressure provided the desired product as a golden solid in 65% yield from 5,6-dichloro-1-methylbenzimidazole. <sup>1</sup>H NMR (DMSO-*d*<sub>6</sub>): δ 8.83 (s, 1H), 8.53 (s, 1H), 8.5 (s, 1H), 8.39 (s, 1H), 4.0 (s, 3H), 1.88 (s, 9H), 1.85 (s, 9H); <sup>13</sup>C NMR (DMSO-*d*<sub>6</sub>): δ 141.2, 140.0, 136.1, 131.9, 131.4, 115.6, 95.6, 52.8, 51.3, 38.5, 29.8, 29.7.

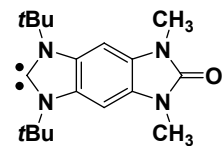
NMR (DMSO-*d*<sub>6</sub>): δ 148.8, 141.8, 139.1, 133.5, 127.5, 127.0, 105.4, 96.9, 60.72, 60.68, 31.4, 27.9, 27.8; HRMS calcd for C<sub>17</sub>H<sub>25</sub>N<sub>4</sub>: 285.2079, found: 285.2079.



**Desymmetrized Benzobis(imidazolium) Salt 5.4.** The desymmetrized benzimidazolium salt (3.00 g, 8.21 mmol) was dissolved in CH<sub>3</sub>CN (100 mL) and MeI (5 mL, 78.0 mmol) was added. The solution was stirred in a sealed vessel at 60 °C for 3 h. The cooled reaction mixture was then concentrated under vacuum to obtain 4.17 g (99%) of **5.4** as a brown powder. <sup>1</sup>H NMR (DMSO-*d*<sub>6</sub>): δ 9.96 (s, 2H), 9.05 (s, 2H), 8.85 (s, 2H), 4.24 (s, 6H), 1.93 (s, 18H); <sup>13</sup>C NMR (DMSO-*d*<sub>6</sub>): δ 147.0, 142.4, 130.0, 129.4, 100.9, 61.8, 34.1, 27.7.

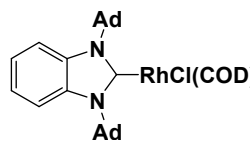


**Enetetraamine 5.5.** A 10 mL vial was charged with desymmetrized salt **5.4** (100 mg 0.197 mmol), NaH (12 mg 0.48 mmol), a catalytic amount of KO*t*Bu (ca. 1 mg) and toluene (2 mL). The vial was then sealed and the reaction mixture was heated to 120 °C for 2 h. The cooled solution was then filtered through a 0.2 μm PTFE filter and solvent was removed under vacuum to obtain 55 mg (94%) of the desired product as a dark red powder. Crystals suitable for X-ray analysis were obtained by slowly cooling of a saturated toluene solution (CCDC 605314). <sup>1</sup>H NMR (C<sub>6</sub>D<sub>6</sub>): δ 6.84 (s, 2H), 2.84 (s, 6H), 1.82 (s, 18H); <sup>13</sup>C NMR (C<sub>6</sub>D<sub>6</sub>): 221.2, 138.7, 130.8, 125.9, 94.7, 57.0, 36.9, 30.7.



**Urea 5.6.** Enetetraamine **5.5** (0.05 g, 0.168 mmol) was dissolved in benzene and exposed to an atmosphere of oxygen for < 1 minute. After the color of the solution changed from red to brown, the solvent was

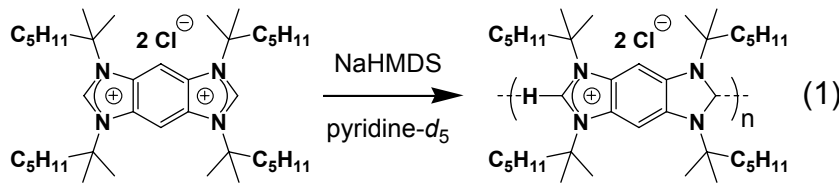
removed under vacuum to obtain 51 mg (99%) of product as a brown powder.  $^1\text{H}$  NMR ( $\text{C}_6\text{D}_6$ ):  $\delta$  6.83 (s, 2H), 2.91 (s, 6H), 1.79 (s, 18H);  $^{13}\text{C}$  NMR ( $\text{C}_6\text{D}_6$ ):  $\delta$  223.0, 155.0, 130.6, 125.8, 92.7, 57.2, 20.5, 26.5; HRMS calcd. for  $\text{C}_{18}\text{H}_{28}\text{N}_4\text{O} [\text{M}+\text{H}^+]$ : 315.2185; found, 315.2185.



**(COD)RhCl(1,3-diadamantylbenzimidazolylidene).** 1,3-Diadamantylbenzimidazolylidene was first prepared by deprotonating the corresponding salt<sup>[26]</sup> using standard methods.  $^1\text{H}$  NMR ( $\text{C}_6\text{D}_6$ ):  $\delta$  7.68-7.64 (m, 2H), 7.07-7.04 (m, 2H), 2.56 (s, 12H), 2.07 (s, 6H), 1.69-1.60 (m, 12H);  $^{13}\text{C}$  NMR ( $\text{C}_6\text{D}_6$ ):  $\delta$  224.0, 135.6, 120.0, 114.5, 58.3, 43.4, 36.9, 30.4. In a nitrogen-filled drybox, a 10 mL flask was charged with 1,3-diadamantylbenzimidazolylidene (120 mg, 0.31 mmol),  $[(\text{COD})\text{RhCl}]_2$  (76 mg, 0.15 mmol), THF (4 mL), and a stir bar. After stirring solution at 60 °C, product began to precipitate within 30 min. After an additional 1 h, the solution was cooled to 23 °C and hexanes (2 mL) were added. Precipitated solids were collected by filtration and dried under vacuum to afford 135 mg (69%) of the desired product as a yellow powder. Crystals suitable for X-ray analysis were obtained by slow evaporation of a saturated  $\text{CH}_2\text{Cl}_2/\text{CH}_3\text{OH}$  solution (2:1 v/v) (CCDC 605315).  $^1\text{H}$  NMR ( $\text{CDCl}_3$ ):  $\delta$  7.81-7.78 (m, 2H), 7.08-7.06 (m, 2H), 4.95 (s, 2H), 3.47-3.44 (m, 6H), 2.99 (m, 8H), 2.41 (s, 10H), 1.94-1.68 (m, 16H);  $^{13}\text{C}$  NMR ( $\text{CDCl}_3$ ):  $\delta$  194.1 (d,  $J = 49.1$  Hz), 135.0, 120.3, 115.3, 92.0 (d,  $J = 8.5$  Hz), 67.2 (d,  $J = 15.3$  Hz), 62.0, 42.9, 36.4, 32.3, 30.3, 28.7.

**Footnote 11: Addition of 1.0 equiv of base to benzobis(imidazolium) salts 5.1 afforded polymeric materials.** The feasibility of selectively monodeprotonating the bis(azolium) salts described above was studied using  $^1\text{H}$  NMR spectroscopy. Addition of

1.0 equiv of NaHMDS to a suspension of bis(azolium) salts **5.1c** in common solvents ( $C_6D_6$ , toluene- $d_8$ ,  $CD_2Cl_2$ , pyridine- $d_5$ , THF- $d_8$ ) resulted in formation of the respective bis(carbene) leaving an equivalent amount of bis(azolium) salt; mono(azolium) species were not detected. We believed this process was driven by the high solubility of the bis(carbene)s facilitated by the insolubility of the bis(azolium) salts in these solvents. To overcome this limitation, a highly soluble variant featuring *N*-(1,1-dimethylhexyl) groups was synthesized as described below. Addition of 1.0 equiv of NaHMDS to a pyridine- $d_5$  solution of this compound revealed signals indicative of coordination-type polymers in the  $^1H$  NMR spectrum (see Eq. 1). Similar coordination phenomena with mixtures of imidazolylidenes and their respective imidazolium salts has been reported.<sup>27</sup>



**Tetrakis[*N*-(1,1-dimethylhexyl)]benzobis(imidazolium) dichloride.** The tetrakis[*N*-(1,1-dimethylhexyl)]benzobis(imidazolium) dichloride salt was prepared according to our previously reported procedure using 1,1-dimethylhexylamine.<sup>[24a]</sup>  $^1H$  NMR ( $DMSO-d_6$ ):  $\delta$  9.15 (s, 2H), 8.60 (s, 2H), 2.24 (br, 8H), 1.94 (s, 24H), 1.12-1.03 (br, 24H), 0.68 (br, 12H);  $^{13}C$  NMR ( $DMSO-d_6$ ):  $\delta$  128.8, 102.5, 65.3, 31.1, 26.4, 22.7, 21.7, 13.6.

**Monodeprotonation Experiment.** In a drybox, tetrakis[*N*-(1,1-dimethylhexyl)]benzobis(imidazolium) dichloride (72 mg, 0.11 mmol) was dissolved in pyridine- $d_5$  (1.0 mL). To the solution was added NaHMDS in THF (2.0 M, 55  $\mu$ L, 0.11 mmol). The mixture was stirred for 1 h then filtered through 0.2  $\mu$ m PTFE filter.  $^1H$

NMR analysis revealed significantly broadened signals indicative of polymer formation. Notably, the resonances for imidazolium ( $\text{NCHN}$ ) and arene ( $\text{C}_6\text{H}_2$ ) protons were shifted upfield ( $\delta = 10.88$  and  $8.42$  ppm, respectively) relative to the bis(azolium) salt (corresponding signals at  $\delta = 10.95$  and  $8.95$ ; solvent = pyridine- $d_5$ ).

## REFERENCES

- † Portions of this chapter have been previously reported, see: Khramov, D. M.; Boydston, A. J.; Bielawski, C. W. *Angew. Chem. Int. Ed.* **2006**, *45*, 6186.
- 1 a) P. Baxter, J.-M. Lehn, A. DeCian, J. Fischer, *Angew. Chem.* **1993**, *105*, 92; *Angew. Chem. Int. Ed.* **1993**, *32*, 69; b) S. Leininger, B. Olenyuk, P. J. Stang, *Chem. Rev.* **2000**, *100*, 853; c) F. A. Cotton, C. Lin, C. A. Murillo, *Acc. Chem. Res.* **2001**, *34*, 759; d) M. F. Lappert, *J. Organomet. Chem.* **2005**, *690*, 5467.
- 2 For excellent reviews, see: a) W. A. Herrmann, K. Köcher, *Angew. Chem.* **1997**, *109*, 2362; *Angew. Chem. Int. Ed.* **1997**, *36*, 2162; b) A. J. Arduengo, III, *Acc. Chem. Res.* **1999**, *32*, 913; c) D. Bourissou, O. Guerret, F. P. Gabbaï, G. Bertrand, *Chem. Rev.* **2000**, *100*, 39.
- 3 a) A. J. Arduengo, III, R. L. Harlow, M. Kline, *J. Am. Chem. Soc.* **1991**, *113*, 361; b) A. J. Arduengo, III, F. Davidson, H. V. R. Dias, J. R. Goerlich, D. Khasnis, W. J. Marshall, T. K. Prakasha, *J. Am. Chem. Soc.* **1997**, *119*, 12742.
- 4 a) M. F. Lappert, *J. Organomet. Chem.* **1988**, *358*, 185; b) W. A. Herrmann, *Angew. Chem.* **2002**, *114*, 1342; *Angew. Chem. Int. Ed.* **2002**, *41*, 1290; c) E. Peris, R. H. Crabtree, *Coord. Chem. Rev.* **2004**, *248*, 2239; d) F. E. Hahn, *Angew. Chem.* **2006**, *118*, 1374; *Angew. Chem. Int. Ed.* **2006**, *45*, 1348.
- 5 a) D. Enders, K. Breuer, G. Raabe, J. Runsink, J. H. Teles, J.-P. Melder, K. Ebel, S. Brode, *Angew. Chem.* **1995**, *107*, 1119; *Angew. Chem. Int. Ed.* **1995**, *34*, 1021; b) R. W. Alder, P. R. Allen, M. Murray, A. G. Orpen, *Angew. Chem.* **1996**, *108*, 1211; *Angew. Chem. Int. Ed.* **1996**, *35*, 1121; c) A. J. Arduengo, III, J. R. Goerlich, W. J. Marshall, *Lieb. Ann./Recueil.* **1997**, 365; d) R. Weiss, S. Reichel, M. Handke, F. Hampel, *Angew. Chem.* **1998**, *110*, 352; *Angew. Chem. Int. Ed.* **1998**, *37*, 344; e) C. Burstein, C. W. Lehmann, F. Glorius, *Tetrahedron* **2005**, *61*, 6207; f) C. Prässang, B. Donnadieu, G. Bertrand, *J. Am. Chem. Soc.* **2005**, *127*, 10182; g) A. J. Arduengo, III, D. Tapu, W. J. Marshall, *J. Am. Chem. Soc.* **2005**, *127*, 16400.

- 6 For theoretical treatments of NHC-metal interactions, see: a) C. Boehme, G. Frenking, *Organometallics* **1998**, *17*, 5801; b) D. S. McGuinness, N. Saendig, B. F. Yates, K. J. Cavell, *J. Am. Chem. Soc.* **2001**, *123*, 4029; c) D. V. Deubel, *Organometallics* **2002**, *21*, 4303; d) C. D. Abernethy, G. M. Codd, M. D. Spicer, M. K. Taylor, *J. Am. Chem. Soc.* **2003**, *125*, 1128; e) A. T. Termaten, M. Schakel, A. W. Ehlers, M. Lutz, A. L. Spek, K. Lammertsma, *Chem. Eur. J.* **2003**, *9*, 3577; f) X. Hu, I. Castro-Rodriguez, K. Olsen, K. Meyer, *Organometallics* **2004**, *23*, 755.
- 7 For selected examples of bimetallic complexes formed between transition metals and (non-rigid) bis(carbene)s connected *via* saturated linkers, see: a) W. A. Herrmann, M. Elison, J. Fischer, C. Köcher, G. R. J. Artus, *Chem. Eur. J.* **1996**, *2*, 772; b) R. S. Simons, P. Custer, C. A. Tessier, W. J. Youngs, *Organometallics* **2003**, *22*, 1979; c) F. E. Hahn, M. C. Jahnke, V. Gomez-Benitez, D. Morales-Morales, T. Pape, *Organometallics* **2005**, *24*, 6458.
- 8 a) O. Guerret, S. Solé, H. Gornitzka, M. Teichert, G. Trinquier, G. Bertrand, *J. Am. Chem. Soc.* **1997**, *119*, 6668; b) W. Li, PhD thesis, University of Alabama, Tuscaloosa (USA), **2004**; c) B. Gehrhus, P. B. Hitchcock, M. F. Lappert, *Z. Anorg. Allg. Chem.* **2005**, *631*, 1383; d) A. J. Boydston, K. A. Williams, C. W. Bielawski, *J. Am. Chem. Soc.* **2005**, *127*, 12496.
- 9 Janus ligands are named after the Roman god *Janus Geminus*, represented in Roman art as two-faced, featuring one face looking forward fused to another looking backward. For examples, see: a) S. J. Cristol, D. C. Lewis, *J. Am. Chem. Soc.* **1967**, *89*, 1476; b) A. Marsh, E. G. Nolen, K. M. Gardinier, J.-M. Lehn, *Tetrahedron Lett.* **1994**, *35*, 397.
- 10 a) D. M. Khramov, A. J. Boydston, C. W. Bielawski, *Org. Lett.* **2006**, *8*, 1831. b) A. J. Boydston, D. M. Khramov, C. W. Bielawski, *Tetrahedron Lett.* **2006**, *47*, 5123.
- 11 Addition of 1.0 equiv of base to benzobis(imidazolium) salts **1** afforded polymeric materials,<sup>24</sup> see: A. J. Arduengo, III, S. F. Gamper, M. Tamm, J. C. Calabrese, F. Davidson, H. A. Craig, *J. Am. Chem. Soc.* **1995**, *117*, 572.
- 12 a) F. E. Hahn, L. Wittenbecher, R. Boose, D. Bläser, *Chem. Eur. J.* **1999**, *5*, 1931; b) F. M. Rivas, U. Riaz, A. Giessert, J. A. Smulik, S. T. Diver, *Org. Lett.* **2001**, *3*, 2673; c) S. Saravanakumar, A. I. Oprea, M. K. Kindermann, J. Heinicke, *Chem. Eur. J.* **2006**, *12*, 3143; F. E. Hahn, L. Wittenbecher, D. L. Van, R. Fröhlich, *Angew. Chem.* **2000**, *112*, 551; *Angew. Chem. Int. Ed.* **2000**, *39*, 541.
- 13 The crystal structure of **5.2b** was found to be similar to **5.2a**.<sup>24</sup>

- 14 For comparison, X-ray structures were determined for bis(azolium) salts **5.1a**<sup>[24]</sup> and **5.1e**.<sup>10b</sup>
- 15 a) A. J. Arduengo III, J. R. Goerlick, W. J. Marshall, *J. Am. Chem. Soc.* **1995**, *117*, 11027; b) M. K. Denk, A. Thadani, K. Hatano, A. J. Lough, *Angew. Chem. 1997*, *109*, 2719; *Angew. Chem. Int. Ed.* **1997**, *36*, 2067; c) F. E. Hahn, M. Paas, D. L. Van, T. Lügger, *Angew. Chem.* **2003**, *115*, 5402; *Angew. Chem. Int. Ed.* **2003**, *42*, 5243.
- 16 a) E. Çetinkaya, P. B. Hitchcock, H. Küçükbay, M. F. Lappert, S. J. Al-Juaid, *Organomet. Chem.* **1994**, *481*, 89; b) F. E. Hahn, T. von Fehren, W. Lars, R. Froehlich, *Z.fuer Naturforsch.* **2004**, *59*, 544.
- 17 These structural characteristics were consistent with (COD)RhCl(1,3-diadamantylbenzimidazolylidene).<sup>24</sup>
- 18 Attempts to deprotonate **5.1d** and **5.1e** resulted in dark red colored solutions of polymeric materials, see: J. W. Kamplain, C. W. Bielawski, *Chem. Commun.* **2006**, 1727.
- 19 H. M. J. Wang, I. J. B. Lin, *Organometallics* **1998**, *17*, 972.
- 20 For an excellent review of Ag-NHC complexes, see: J. C. Garrison, W. J. Youngs, *Chem. Rev.* **2005**, *105*, 3978.
- 21 Deprotonation of **5.1d** followed by addition of [(COD)RhCl]2 also afforded complex **5.3d**, although in lower yields (34%).
- 22 Crystals suitable for X-ray analysis were obtained by slow diffusion of hexanes into a saturated CH<sub>2</sub>Cl<sub>2</sub> solution of **5.3d**.<sup>24</sup>
- 23 For other examples of oxidizing NHC dimers with O<sub>2</sub>, see: a) H. E. Winberg, J. R. Downing, D. D. Coffman, *J. Am. Chem. Soc.* **1965**, *87*, 2054; b) Z. Shi, R. P. Thummel, *J. Org. Chem.* **1995**, *60*, 5935.
- 24 a) D. M. Khramov, A. J. Boydston, C. W. Bielawski, *Org. Lett.* **2006**, *8*, 1831. b) A. J. Boydston, D. M. Khramov, C. W. Bielawski, *Tetrahedron Lett.* **2006**, *47*, 5123.
- 25 B. N. Feitelson, P. Mamalis, R. J. Moualim, V. Petrow, O. Stephenson, B. Sturgeon, *J. Chem. Soc.* **1952**, 2389.
- 26 N. Hadei, E. A. B. Kantchev, C. J. O'Brien, M. G. Organ, *Org. Lett.* **2005**, *7*, 1991.

- 27 A. J. Arduengo, III, S. F. Gamper, M. Tamm, J. C. Calabrese, F. Davidson, H. A. Craig, *J. Am. Chem. Soc.* **1995**, *117*, 572.

## **Chapter 6: Donor-Acceptor Triazenes: Synthesis, Characterization, and Study of Their Electronic and Thermal Properties<sup>†</sup>**

### **ABSTRACT**

A new class of 1,3-disubstituted-triazenes were synthesized by coupling functionalized benzimidazol-2-ylidenes, as their free N-heterocyclic carbenes or generated in situ from their respective benzimidazolium precursors, to various aryl azides in modest to excellent isolated yields (36 – 99%). Electron delocalization between the two coupled components was studied using UV-Vis spectroscopy, NMR spectroscopy, and X-ray crystallography. Depending on the complementarity of the functional groups on the N-heterocyclic carbenes and the organic azides, the respective triazenes were found to exhibit  $\lambda_{\max}$  values ranging between 364 and 450 nm. X-ray crystallography revealed bond alteration patterns in a series of triazenes characteristic of donor-acceptor compounds. Triazene thermal stabilities were studied using thermogravimetric analysis and found to be strongly dependent on the sterics of the benzimidazol-2-ylidene component and the electronics of the azide component. Triazenes possessing bulky N-substituents (e.g., *neo*-pentyl, *tert*-butyl, etc.) were stable in the solid-state to temperatures exceeding 150 °C, whereas analogues with small N-substituents (e.g., methyl) were found to slowly decompose at room temperature. Triazenes featuring electron-rich phenyl azide components decomposed at higher temperatures than their electron-deficient analogues. Products of the thermally-induced triazene decomposition reaction were found to be molecular nitrogen and the respective guanidine. Using an isotopically-labeled triazene, the mechanism of the decomposition reaction was determined to be consistent with the Staudinger reaction.

## INTRODUCTION

Triazenes are a unique class of polyazo compounds containing three consecutive nitrogen atoms in an acyclic arrangement.<sup>1</sup> Historically, they have found use as DNA alkylating agents in tumor therapy,<sup>2</sup> iodo-masking groups in the synthesis of small<sup>3</sup> and macromolecules,<sup>4</sup> protecting groups for amines and diazonium salts,<sup>5</sup> photoactive substrates,<sup>6</sup> and precursors to various types of compounds of medicinal importance.<sup>7</sup> More recently, triazenes have been used to facilitate coupling of functionalized arenes to passivated Si surfaces for applications in semiconductors and nanoelectronics.<sup>8</sup>

The two most widely-utilized methods of synthesizing triazenes<sup>1</sup> are coupling of aryl diazonium salts to amines<sup>9</sup> and addition of organometallic reagents (RMgX, RLi, etc.) to alkyl azides.<sup>10</sup> However, the reagents used in these reactions are extremely reactive, and often flammable, which necessitates the use of relatively sophisticated equipment and techniques for safety and success. As a result, the scope of compatible substrates and the range of associated applications for preparing triazenes are restrictive. These limitations warrant the development of new methods for accessing this important class of compound.

Recently, we discovered a new, practical method for preparing triazenes. In our initial communication,<sup>11</sup> we reported that addition of a N-heterocyclic carbene<sup>12</sup> (NHC) to an organic azide afforded a 1,3-disubstituted triazene in excellent yield (see Figure 6.1).<sup>13</sup> The coupling reaction was found to proceed rapidly at room temperature ( $\tau_{1/2} \sim$  minutes) and showed good tolerance toward a broad array of functional groups and structural variations. For example, alkyl, aryl, acyl, and tosylated azides were coupled to imidazol-2-ylidene with N-substituents ranging in size from relatively small methyl groups to bulky mesityl (1,3,5-trimethylbenzene) groups in 54 – 94% isolated yields. Since imidazol-2-ylidene are typically prepared via deprotonation of their more stable

and readily-accessible imidazolium precursors,<sup>14</sup> we also demonstrated that N-heterocyclic carbenes (NHCs) can be generated *in situ* from their respective precursors prior to azide coupling.

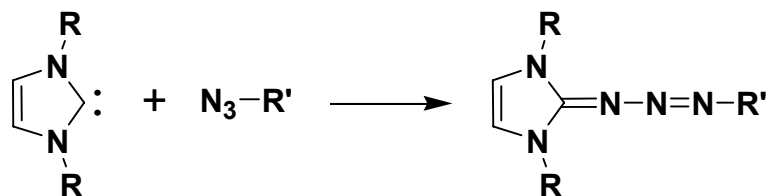


Figure 6.1 Triazene formation via coupling of a N-heterocyclic carbene with an azide.

In many ways, the aforementioned NHC/azide coupling reaction is similar to the Cu-catalyzed [3+2] Huisgen<sup>15</sup> cycloaddition reaction between alkynes and azides, now commonly categorized under “click chemistry.”<sup>16</sup> Both reactions: 1.) provide products in excellent yields, 2.) are atom-economical, 3.) proceed with relatively high rates, 4.) exhibit good functional group tolerance, and 5.) utilize a relatively broad range of substrates. Over a short time span, click chemistry has found utility in a multitude of synthetic, biological, and materials applications.<sup>17</sup> Likewise, in an effort to expand this repertoire, we demonstrated that the NHC/azide coupling reaction was useful for the postpolymerization modification of polyolefins containing pendant azido groups.<sup>18</sup>

We have recently launched a program that utilizes NHCs as building blocks for polymer synthesis, with an emphasis on preparing functional materials suitable for use in electronic applications.<sup>19</sup> In addition to the practical advantages discussed above, the NHC/azide coupling reaction has two unique features for this purpose: 1.) chemical unsaturation is conserved as reactants are converted to products and 2.) the triazeno bridge formed formally conjugates the two organic components to each other (i.e., the imidazole ring and the organic fragment stemming from the azide).

The primary purpose of this study was to explore the feasibility of preparing triazenes that exhibit extensively delocalized structures and examine their potential in preparing robust materials with useful electronic properties. In particular, we describe the synthesis of a variety of “donor-acceptor” triazenes where various benzimidazol-2-ylidene<sup>20</sup> were coupled to aryl azides possessing complementary functional groups. The extent of electron delocalization was studied using UV-Vis spectroscopy, NMR spectroscopy, and X-ray crystallography. The thermal stabilities of the triazene products formed from the NHC/azide coupling reaction were also evaluated and included efforts toward deconvoluting how various steric and electronic features influence this important physical characteristic. Previously, we discovered that at elevated temperatures triazenes obtained from coupling NHCs to organic azides lose molecular nitrogen and afford the respective guanidines.<sup>11</sup> In the well-known Staudinger reaction,<sup>21</sup> the intermediate phosphatriazene formed upon combination of a phosphine with an azide also extrudes molecular nitrogen to form a phosphazene; hence, we also tested whether triazene decomposition proceeded via an analogous mechanism.

A secondary objective of this study was fundamental. The triazeno linkage ( $\text{C}=\text{N}-\text{N}=\text{N}$ ) formed in the NHC/azide reaction bears structural similarities to azine ( $\text{C}=\text{N}-\text{N}=\text{C}$ ) and 1,3-diene ( $\text{C}=\text{C}-\text{C}=\text{C}$ ) linkages, which prompted us to study the electronic properties of four-electron, conjugated  $\pi$ -systems containing three consecutive nitrogen atoms. Previously, Glaser, Euler, and others prepared and studied the electronic and structural properties in donor-acceptor azines by NMR spectroscopy,<sup>22</sup> cyclic voltammetry,<sup>23</sup> and X-ray crystallography for select crystalline materials.<sup>24</sup> It was concluded that electronic communication across the N-N bond was minimal. Hence, while 1,3-dienes are known to exhibit extensively delocalized structures, azines were called effective “conjugation stoppers.”<sup>25</sup> However, Clyburne and co-workers

demonstrated that azines prepared via coupling of an imidazol-2-ylidene to 9-diazofluorene were extensively delocalized, and under certain conditions exhibited non-linear optical (NLO) responses.<sup>26</sup>

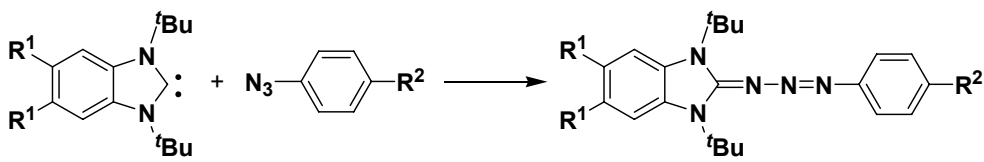
## RESULTS

As shown in Table 1, a range of functionalized benzimidazol-2-ylidenes and aryl azides were chosen as coupling partners. Our hypothesis was that if the triazo linkage enabled electronic communication, then bathochromic shifts should be observed by UV-Vis spectroscopy as the pendant electron-donating and electron-withdrawing substituents in the resulting triazenes became more complementary. Similarly, successive downfield shifts were also expected in the NMR spectra for the same series of compounds. If quality crystals suitable for X-ray diffraction could be obtained, then distinct changes in the triazo bond length patterns should be observed as a function of the electronic character of the peripheral groups in the solid-state as well.

**Triazene Nomenclature.** In order to simplify the identification of the triazene's discussed in this study, the following convention was applied: Following the triazene numeric label, which refers to class of benzimidazol-2-ylidene used (with attention directed toward changes in the N-substituents), the first suffix identifies the pendant functional group on the NHC moiety and the second suffix identifies the pendant functional group on the aryl azide. For example, 1-(1,3-di-*tert*-butyl-benzimidazol-2-ylidene)-3-phenyltriazene was identified as **6.1-H-H** (see Table 1). Likewise, 1-(1,3-di-methyl-5,6-dimethoxybenzimidazol-2-ylidene)-3-(para-nitrophenyl)triazene was identified as **6.3-OCH<sub>3</sub>-NO<sub>2</sub>** (see Table 3).

**Synthesis of Triazenes 6.1.** In general, triazenes **6.1** were prepared by coupling 1,3-di-*tert*-butyl-benzimidazol-2-ylidene (generated through deprotonation of its corresponding benzimidazolium salt<sup>27</sup> using potassium *tert*-butoxide, then isolated and

used as its free NHC) with a molar equivalent of aryl azide.<sup>28</sup> The reactions were conducted at ambient temperature using tetrahydrofuran (THF) as solvent at 0.1 M substrate concentrations. Depending on the electronics of the azide component, reaction times ranged from minutes (electron-poor azides) to hours (electron-rich azides), as monitored by <sup>1</sup>H NMR spectroscopy. To obtain more quantitative information on reaction progress versus time, the bimolecular rate constants of reactions involving 1,3-di-*tert*-butyl-benzimidazol-2-ylidene and a select range of azides with various electronic properties were measured by <sup>1</sup>H NMR spectroscopy (THF-*d*<sub>8</sub>, 23 °C). The coupling reaction between the free NHC and an electron-poor azide, 1-azido-4-nitrobenzene, was extremely fast and measured to be 0.215 L·mol<sup>-1</sup>·s<sup>-1</sup>. In contrast, the rate constants for coupling the same NHC to relatively more electron-rich azides, phenylazide and 1-azido-4-methoxybenzene, were relatively slow and found to be 0.003 L·mol<sup>-1</sup>·s<sup>-1</sup> and 0.001 L·mol<sup>-1</sup>·s<sup>-1</sup>, respectively. Collectively, these observations were consistent with a coupling mechanism that involves nucleophilic attack of a NHC at the terminal nitrogen of an aryl azide. Purification of the products generated from this reaction was straight-forward, requiring only filtration of the reaction media through a PTFE filter followed by evaporation of solvent. Using this methodology, triazene products were consistently obtained in excellent (> 99%) yields and in high purities. The molecular structures of triazenes **6.1** shown in Table 1 were confirmed by NMR spectroscopy, UV-Vis spectroscopy, and for select crystalline compounds, X-ray crystallography (see below). Mass spectrometry and elemental analyses provided additional support for their structure and purity.



Entry	Product	R <sup>1</sup>	R <sup>2</sup>	6.1 Yield (%) <sup>b</sup>
1	<b>6.1-H-H</b>	H	H	99
2	<b>6.1-H-OCH<sub>3</sub></b>	H	OCH <sub>3</sub>	99
3	<b>6.1-H-NO<sub>2</sub></b>	H	NO <sub>2</sub>	99
4	<b>6.1-OCH<sub>3</sub>-H</b>	OCH <sub>3</sub>	H	99
5	<b>6.1-OCH<sub>3</sub>-OCH<sub>3</sub></b>	OCH <sub>3</sub>	OCH <sub>3</sub>	99
6	<b>6.1-OCH<sub>3</sub>-NO<sub>2</sub></b>	OCH <sub>3</sub>	NO <sub>2</sub>	99
7	<b>6.1-F-H</b>	F	H	99
8	<b>6.1-F-OCH<sub>3</sub></b>	F	OCH <sub>3</sub>	99
9	<b>6.1-F-NO<sub>2</sub></b>	F	NO <sub>2</sub>	99

Table 6.1 Synthesis of donor-acceptor triazenes bearing bulky N-*tert*-butyl groups. General reaction conditions: 1,3-di-*tert*-butylbenzimidazol-2-ylidene (1.0 equiv) and an organic azide (1.0 equiv), concentration of substrates = 0.1 M, solvent = THF, 23 °C. <sup>b</sup> Isolated yields.

**Characterization of 6.1: UV-Vis Absorption Spectroscopy.** After the donor-acceptor triazenes shown in Table 1 were synthesized, UV-Vis absorption spectroscopy was used to measure the electronic properties of these compounds. As shown in the UV-

Vis absorption spectra included in Figure 6.2 and summarized in Table 6.2, a gradual bathochromic shift in the  $\lambda_{\max}$  of the triazene chromophore was observed as the electron-donating / electron-withdrawing character of its peripheral functional groups became more complementary. Close analysis of the data suggested that while electronic communication between the terminal functional group on the benzimidazol-2-ylidene and the azide was observed, the interaction was relatively minor. For example, only 4 – 8 nm bathochromic shifts were observed in the  $\lambda_{\max}$  upon replacing two hydrogens in the benzimidazol-2-ylidene to either methoxy or fluoro groups (i.e., **6.1-H-H** → **6.1-OCH<sub>3</sub>-H** or **6.1-F-H**; entries 1 – 3). These observations were in accord with the high degree of bond polarization previously observed in complexes formed between imidazol-2-ylidenes and main group elements,<sup>26b,29</sup> and may be rationalized by the strong electron-donating character of the nitrogen atoms present in the imidazole moiety. In contrast, significant effects on  $\lambda_{\max}$  were observed when the terminal functional group on the azide coupling partner was varied. For example, replacing a methoxy group with a nitro group resulted in a 60 nm bathochromic shift in the  $\lambda_{\max}$  (i.e., **6.1-H-OCH<sub>3</sub>** → **6.1-H-NO<sub>2</sub>**; entries 4 – 5). Similar spectroscopic changes were observed with triazenes containing electron-poor (i.e., **6.1-F-OCH<sub>3</sub>** → **6.1-F-NO<sub>2</sub>**,  $\Delta\lambda_{\max} = 55$  nm; entries 6 – 7) and electron-rich (i.e., **6.1-OCH<sub>3</sub>-OCH<sub>3</sub>** → **6.1-OCH<sub>3</sub>-NO<sub>2</sub>**,  $\Delta\lambda_{\max} = 48$  nm; entries 8 – 9) benzimidazol-2-ylidene components. As expected, triazene **6.1-OCH<sub>3</sub>-NO<sub>2</sub>**, prepared by coupling a highly electron-rich benzimidazol-2-ylidene with a highly electron-deficient azide, exhibited the longest  $\lambda_{\max}$  at 450 nm for any of the triazenes studied (Entry 9). Collectively, these results suggested that the triazeno linkages (C=N-N=N) were effective in delocalizing electronic charge between complementary NHC and organic azide components.

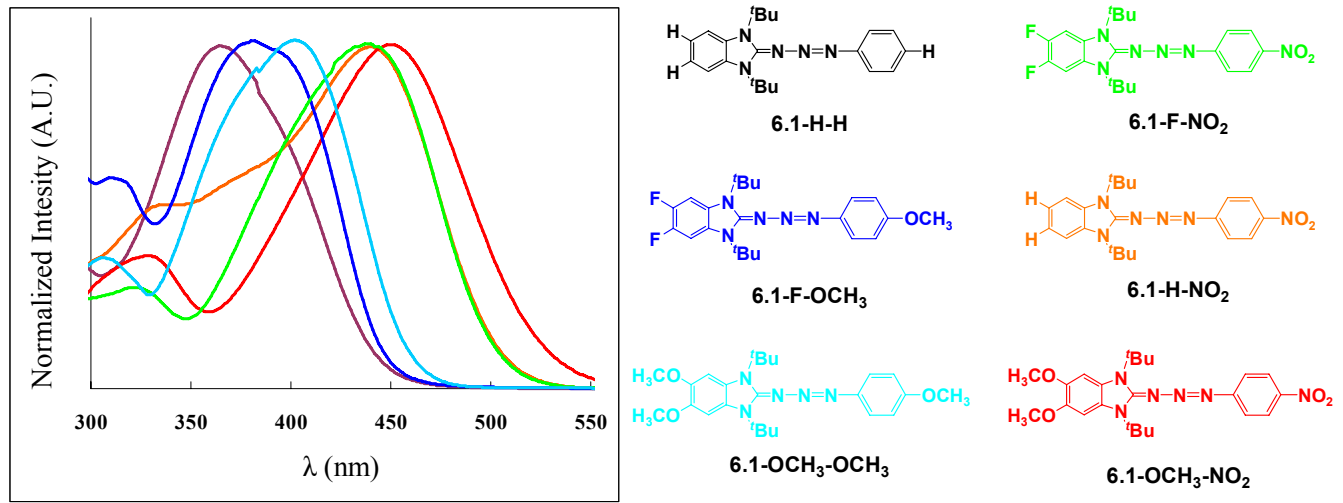
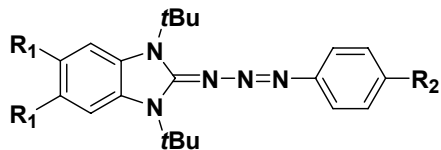


Figure 6.2 UV-Vis absorbance spectra (left) color coded with their respective compound (right). Spectra were acquired in CH<sub>2</sub>Cl<sub>2</sub> at ambient temperature. For  $\lambda_{\text{max}}$  (nm) values, see Table 6.2.



Entry	Compound	R <sub>1</sub>	R <sub>2</sub>	λ <sub>max</sub> (nm)	Log (ε) <sup>b</sup>
1	<b>6.1-H-H</b>	H	H	364	4.20
2	<b>6.1-OCH<sub>3</sub>-H</b>	OCH <sub>3</sub>	H	372	4.17
3	<b>6.1-F-H</b>	F	H	368	4.16
4	<b>6.1-H-OCH<sub>3</sub></b>	H	OCH <sub>3</sub>	380	4.12
5	<b>6.1-H-NO<sub>2</sub></b>	H	NO <sub>2</sub>	440	4.35
6	<b>6.1-F-OCH<sub>3</sub></b>	F	OCH <sub>3</sub>	383	4.28
7	<b>6.1-F-NO<sub>2</sub></b>	F	NO <sub>2</sub>	438	4.52
8	<b>6.1-OCH<sub>3</sub>-OCH<sub>3</sub></b>	OCH <sub>3</sub>	OCH <sub>3</sub>	402	4.41
9	<b>6.1- OCH<sub>3</sub>-NO<sub>2</sub></b>	OCH <sub>3</sub>	NO <sub>2</sub>	450	4.49

Table 6.2 Summary of key UV-Vis absorbance data for triazenes **6.1**. UV-Vis spectra were acquired in CH<sub>2</sub>Cl<sub>2</sub> at ambient temperature. <sup>b</sup> ε is the molar absorptivity with units of L mol<sup>-1</sup> cm<sup>-1</sup>.

**Characterization of 6.1: NMR Spectroscopy.** Next, we turned our attention toward studying the donor-acceptor triazenes (**6.1**) via <sup>1</sup>H and <sup>13</sup>C NMR spectroscopy. In general, signals attributed to the arene protons on the azide-containing moieties shifted upfield whereas the benzimidazol-2-ylidene protons shifted downfield upon coupling. This result was consistent with charge transfer from the electron-rich component to the relatively electron-poor component. The magnitude of these shifts were strongly dependent on the nature of the functional group on the azide with a smaller dependency on the pendant functional group on the benzimidazol-2-ylidene, although overall changes were small for all compounds studied (<sup>1</sup>H NMR: < 0.1 ppm; <sup>13</sup>C NMR: < 1.0 ppm). The

most pronounced shifts were observed in the series ( $^1\text{H}$  NMR, solvent =  $\text{CDCl}_3$ ): **6.1-OCH}\_3-\text{NO}\_2** ( $\delta$  = 8.11 ppm, Ar-H ortho to  $\text{NO}_2$ ; 7.50 ppm Ar-H meta to  $\text{NO}_2$ ), **6.1-H-NO}\_2** ( $\delta$  = 8.14 ppm; 7.54 ppm), and **6.1-F-NO}\_2** ( $\delta$  = 8.18 ppm; 7.58 ppm).

**X-ray Crystallography Studies of Triazenes.** To obtain additional support for the existence of conjugation through the triazeno linkage and to help quantify the extent to which a dipolar triazene can effectively distribute charge, single-crystal X-ray crystallography was used to study the donor-acceptor triazenes described above. Shown in Figure 3 (top) are two bona fide resonance structures (**A** and **B**) for triazenes flanked by donor (D) and acceptor (A) groups. In our initial investigation, X-ray crystallography revealed that 1-(1,3-dimesityl-imidazol-2-ylidene)-3-benzyl-triazene (**6.2**), prepared via coupling of 1,3-dimesityl-imidazol-2-ylidene with benzyl azide, exhibited alternating bond lengths consistent with the structure **A** (see Figure 5.3, bottom).<sup>11</sup> However, we anticipated that the donor-acceptor triazenes (**6.1**) discussed above would adopt resonance structure **B** as the pendant electron-withdrawing group on one component was matched with an electron-donating group on the other. More specifically, the single N-N bonds should shorten and the double N=N bonds should elongate as the complementarity of the donor-acceptor groups on the triazenes increased.

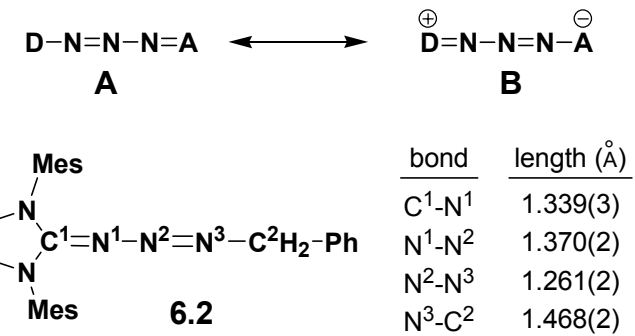


Figure 6.3 (top) Illustration of two resonance structures for triazenes containing donor (D) and acceptor (A) groups. (bottom) Key bond lengths for 1-(1,3-dimesityl-imidazol-2-ylidene)-3-benzyl-triazene (**6.2**).<sup>11</sup>

**Synthesis and Characterization of Triazenes **6.3**.** While we were unable to obtain quality crystals suitable for X-ray analysis of the donor-acceptor triazenes **6.1**, a related series of crystalline analogues (**6.3**) were obtained by effectively replacing the bulky N-*tert*-butyl substituents on the benzimidazol-2-ylidene moieties with smaller N-methyl groups. Since benzimidazol-2-ylidenes with N-methyl groups are known to dimerize to their respective enetetraamines, which oxidize rapidly in the presence of air,<sup>30</sup> NHCs were generated *in situ* under basic conditions from their known<sup>30</sup> benzimidazolium precursors in the presence of an organic azide. Using this approach, a range of donor-acceptor triazenes **6.3** were prepared in moderate to good yields (36 – 74%, see Table 3.3).<sup>31,32</sup> As shown in the UV-Vis absorption spectra (see Figure 4) and summarized in Table 3.3, the  $\lambda_{\text{max}}$  of triazenes **6.3** in CH<sub>2</sub>Cl<sub>2</sub> were found to be nearly identical to their di-*tert*-butyl analogues (**6.1**), which indicated that the main chromophore was only minimally affected by the differences in steric bulk between these two series of compounds. Notably, the dipole moments ( $\mu$ ) of these compounds, as calculated using density functional theory, correlated with the donor-acceptor groups on their periphery (see Table 6.3).<sup>33</sup> For example, replacement of the para hydrogen atom on the azide

component with a nitro group resulted in a large increase in the calculated dipole, compare: **6.3-H-H**, 4.29 D vs. **6.3-H-NO<sub>2</sub>**, 10.6 D (entries 1 and 2). In contrast, incorporation of electron-donating methoxy groups into the benzimidazol-2-ylidene fragment (i.e., **6.3-OCH<sub>3</sub>-H**) resulted in only a modest increase in the calculated dipole (5.39 D) relative to **6.3-H-H**. This result was in accord with the aforementioned UV-Vis spectroscopy data and consistent with the benzimidazol-2-ylidene component showing high polarization. As expected, **6.3-OCH<sub>3</sub>-NO<sub>2</sub>** exhibited the calculated largest dipole of 11.2 D.

Entry	Compound	R <sup>1</sup>	R <sup>2</sup>	Yield (%) <sup>b</sup>	$\lambda_{\max}$ (nm) <sup>c</sup>	Log ( $\epsilon$ ) <sup>c</sup>	$\mu_{\text{calc}}$ (D) <sup>d</sup>
1	<b>6.3-H-H</b>	H	H	36	372	4.40	4.29
2	<b>6.3-H-NO<sub>2</sub></b>	H	NO <sub>2</sub>	56	444	4.38	10.6
3	<b>6.3-OCH<sub>3</sub>-H</b>	OCH <sub>3</sub>	H	69	400	4.39	5.39
4	<b>6.3-OCH<sub>3</sub>-NO<sub>2</sub></b>	OCH <sub>3</sub>	NO <sub>2</sub>	74	467	4.22	11.2

Table 6.3 Synthesis and UV-Vis data of crystalline triazenes bearing N-methyl groups. General conditions: 1,3-Di-methyl-benzimidazol-2-ylidene (1.00 equiv) was generated in situ in THF (0.2 M) at -30 °C from its respective benzimidazolium salt using potassium *tert*-butoxide (1.05 equiv). The noted organic azide (1.00 equiv) was then added to the resulting reaction mixture.

<sup>b</sup> Isolated yield. <sup>c</sup> UV-Vis spectra were acquired in CH<sub>2</sub>Cl<sub>2</sub> at ambient temperature.  $\epsilon$  is the molar absorptivity with units of L mol<sup>-1</sup> cm<sup>-1</sup>.

<sup>d</sup> Calculated using density functional theory; see: ref. 33.

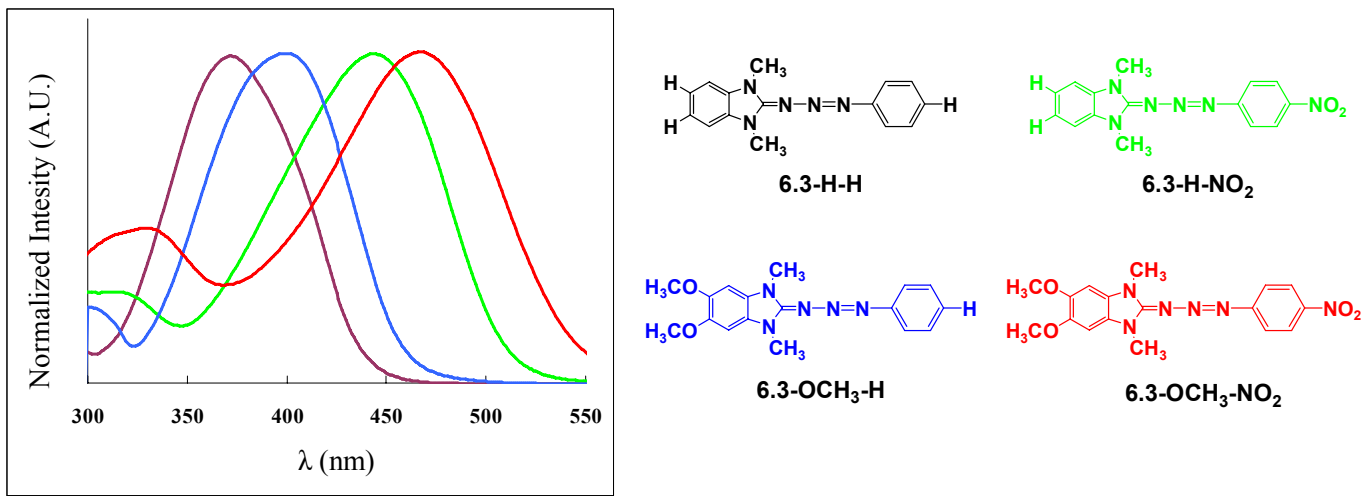


Figure 6.4 UV-Vis absorbance spectra (left) color coded with their respective compound (right). Spectra were acquired in  $\text{CH}_2\text{Cl}_2$  at ambient temperature. For  $\lambda_{\text{max}}$  (nm) values, see Table 6.3.

Crystals suitable for X-ray analysis were obtained by slow evaporation of saturated chloroform solutions of triazenes **6.3**. ORTEP diagrams for these structures are shown in Figure 6.5 with key crystallographic information summarized in Tables 6.4 (selected bond lengths and angles) and **6.5** (selected crystal data). Analysis of the data sets revealed that as the complementarity of the pendant electron-donating and electron-withdrawing groups on the periphery of the triazenes improved (i.e., **6.3-H-H** vs. **6.3-OCH<sub>3</sub>-NO<sub>2</sub>**): the C2-N2 and N3-N4 bonds elongated ( $1.329(4) \rightarrow 1.354(4)$  Å and  $1.281(4) \rightarrow 1.287(3)$  Å, respectively), while the N2-N3 bond shortened ( $1.358(3) \rightarrow 1.328(4)$  Å). Further support for electron delocalization was apparent from the angles between the planes of the two azide and NHC components, as defined in Table 4. Triazenes **6.3-H-NO<sub>2</sub>** and **6.3-OCH<sub>3</sub>-NO<sub>2</sub>** revealed near perfect planarity between the two components (angles = 0.7 and 1.3°, respectively), a manifestation of good orbital overlap between terminal electron-poor and electron-rich groups. In contrast, triazenes **6.3-H-H** and **6.3-H-OCH<sub>3</sub>** which possessed relatively mis-matched functional groups

exhibited angles up to  $26.5^\circ$ . Collectively, these results were consistent with the UV-Vis and NMR spectroscopic data discussed above and supported the notion that triazenes **3** possessing complementary functional groups exhibited extensively electron delocalized structures. In concert, the solid-state data suggested structure **B** (see Figure 3, top) was a major resonance contributor in electronically-matched, donor-acceptor triazenes.

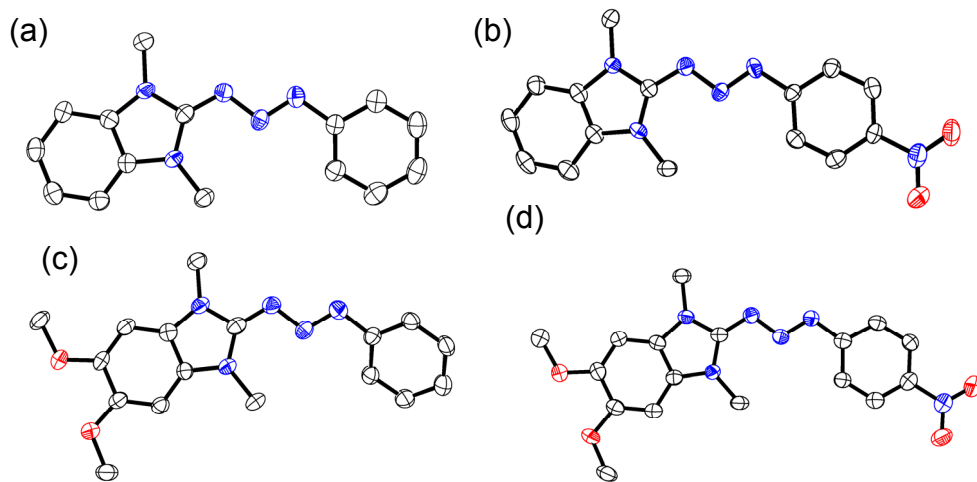
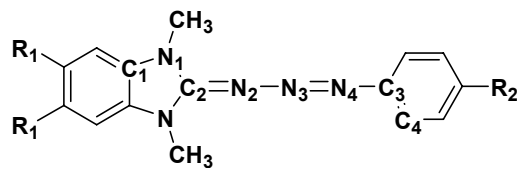


Figure 6.5 ORTEP diagrams for (a) **6.3-H-H**, (b) **6.3-H-NO<sub>2</sub>**, (c) **6.3-OCH<sub>3</sub>-H**, (d) **6.3-OCH<sub>3</sub>-NO<sub>2</sub>**. Selected bond lengths ( $\text{\AA}$ ) and angles ( $^\circ$ ) are summarized in Table 6.4. Solvent molecules have been removed for clarity.



Entry	Compound	C <sub>1</sub> -N <sub>1</sub> (Å)	N <sub>1</sub> -C <sub>2</sub> (Å)	C <sub>2</sub> -N <sub>2</sub> (Å)	N <sub>2</sub> -N <sub>3</sub> (Å)	N <sub>3</sub> -N <sub>4</sub> (Å)	N <sub>4</sub> -C <sub>3</sub> (Å)	<N <sub>1</sub> C <sub>2</sub> N <sub>2</sub> -N <sub>4</sub> C <sub>3</sub> C <sub>4</sub> (°) <sup>b</sup>
1	<b>6.3-H-H</b>	1.375(4)	1.365(4)	1.329(4)	1.358(3)	1.281(4)	1.423(4)	7.56
2	<b>6.3-H-NO<sub>2</sub></b>	1.390(5)	1.360(5)	1.343(5)	1.346(5)	1.285(4)	1.403(5)	0.69
3	<b>6.3-OCH<sub>3</sub>-H</b>	1.387(4)	1.370(4)	1.339(4)	1.367(4)	1.279(3)	1.430(4)	26.48
4	<b>6.3-OCH<sub>3</sub>-NO<sub>2</sub></b>	1.397(4)	1.360(4)	1.354(4)	1.328(4)	1.287(3)	1.410(4)	1.34

Table 6.4 Selected bond lengths (Å) and angles (°) for triazenes **6.3**. All crystals analyzed were obtained by slow evaporation of concentrated chloroform solutions. <sup>b</sup> Absolute angles between planes defined by N<sub>1</sub>-C<sub>2</sub>-N<sub>2</sub> and N<sub>4</sub>-C<sub>3</sub>-C<sub>4</sub>.

	<b>6.3-H-H</b>	<b>6.3-H-NO<sub>2</sub></b>	<b>6.3-OCH<sub>3</sub>-H</b>	<b>6.3-OCH<sub>3</sub>-NO<sub>2</sub></b>
CCDC No.	643401	643400 C16 H15 Cl3 N6	643398	643399
empirical formula	C15 H17 N5 O	O2	C17 H21 N5 O3	C17 H18 N6 O4
formula weight	283.34	429.69	343.39	370.37
cryst syst	Tetragonal	Triclinic	Triclinic	Monoclinic
space group	I-4	P-1	P-1	P21/c
<i>a</i> , Å	22.4468(7)	6.7593(3)	7.1500(2)	8.9005(4)
<i>b</i> , Å	22.4468(7)	11.8068(5)	13.9550(3)	7.5544(3)
<i>c</i> , Å	22.4468(7)	12.3651(5)	17.4200(5)	25.4468(12)
$\alpha$ , deg	90°	95.814(3)°	105.406(1)°	90°
$\beta$ , deg	90°	102.092(2)°	90.710(1)°	90.197(2)°
$\gamma$ , deg	90°	100.095(2)°	93.4630(13)°	90°
<i>V</i> , Å <sup>3</sup>	2893.5(2)	940.16(7)	1671.89(8)	1710.98(13)
<i>T</i> , K	153(2)	153(2)	153(2)	153(2)
<i>Z</i>	8	2	4	4
<i>D</i> <sub>calc</sub> , Mg/m <sup>3</sup>	1.301	1.518	1.364	1.438
cryst size (mm) reflections	0.40 x 0.15 x 0.13	0.40 x 0.10 x 0.08	0.30 x 0.20 x 0.14	0.36 x 0.24 x 0.15
collected independent reflections	2665	6116	10827	5428
<i>R</i> <sub>1</sub> , w <i>R</i> <sub>2</sub> { <i>I</i> > $2\sigma(I)$ }	0.0493, 0.1060	0.0671, 0.1274	0.0563, 0.0922	0.0527, 0.0831
goodness of fit	1.164	1.121	1.059	1.063

Table 6.5 Selected bond crystal data for triazenes **6.3**.

**Evaluation of the Thermal Stabilities of Triazenes: Introduction.** During our spectroscopic and crystallographic studies, qualitative observations suggested that triazenes with small N-substituents were relatively unstable in solution and in the solid-state. In contrast, triazenes with large N-substituents were found to be exceptionally stable, even at elevated temperatures (> 150 °C) for extended periods of time. In our initial communication, we found that the major product of **6.2** decomposition was guanidine **6.4** (R = Mes, R' = Bn), which formed *via* extrusion of molecular nitrogen at

elevated temperatures ( $> 120$  °C) (see Figure 6.6a).<sup>11</sup> To determine if the triazenes synthesized in this study were also susceptible to a similar decomposition process, **6.3-H-H** was heated to 150 °C in toluene in a pressure vessel. Under these conditions, the respective guanidine (**6.5**) was observed by  $^1\text{H}$  NMR spectroscopy, and subsequently isolated in 95% yield (see Figure 6.6b).<sup>34</sup> Supplementary support for the decomposition reaction was obtained from mass spectrometry and elemental analysis. When compared to the triazene starting material (**6.3-H-H**), the decomposition product (**6.5**) was 28 Da lower in molecular weight and exhibited a compositional difference consistent with the loss of molecular nitrogen. However, the mechanism for the decomposition reaction was unknown and we were interested in deconvoluting the key steric and electronic factors governing triazene stability.

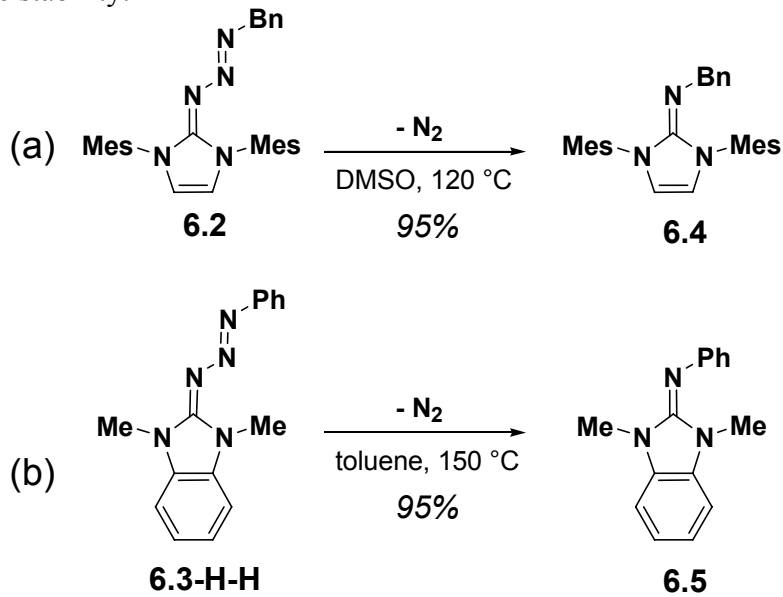
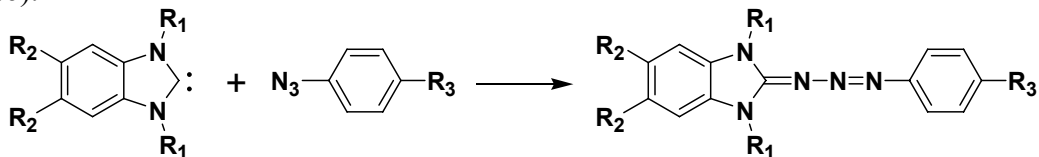


Figure 6.6 Guanidine formation from triazene *via* loss of nitrogen. Bn = benzyl, Mes = 1,3,5-trimethylphenyl, Ph = phenyl. (a) This reaction was reported in ref. 11. (b) This work.

## Evaluation of the Thermal Stabilities of Triazenes: Thermogravimetric Analysis.

In addition to the aforementioned solution-mediated decomposition reactions, triazene stability was also studied in the solid-state. Particular attention was directed toward proving thermal stabilities as a function of triazene size and electronic characteristics. Initial efforts focused on studying how the size of the N-substituent as well as electronics of the benzimidazol-2-ylidene component affects triazene stability. A range of benzimidazol-2-ylidenes with N-substituents ranging in size from methyl to bulky *neo*-pentyl groups were synthesized using known methods<sup>27,35</sup> and coupled to phenyl azide under basic conditions using the in situ methodology described above (see Table 6.6).<sup>36</sup>



Entry	Compound	R <sub>1</sub>	R <sub>2</sub>	R <sub>3</sub>	M <sub>p</sub> (°C) <sup>a</sup>	T <sub>d</sub> (°C) <sup>b</sup>
1	<b>6.3-H-H</b>	Me	H	H	c	93
2	<b>6.6-H-H</b>	<i>i</i> Bu	H	H	c	118
3	<b>6.1-H-H</b>	<i>t</i> Bu	H	H	100-105	148
4	<b>6.7-H-H</b>	<i>n</i> Pn	H	H	126-131	156
5	<b>6.1-OCH<sub>3</sub>-H</b>	<i>t</i> Bu	OCH <sub>3</sub>	H	140-142	154
6	<b>6.6-H-NO<sub>2</sub></b>	<i>i</i> Bu	H	NO <sub>2</sub>	128-131	174
7	<b>6.6-H-OCH<sub>3</sub></b>	<i>i</i> Bu	H	OCH <sub>3</sub>	c	139

Table 6.6 Steric and electronic effects on triazene stability. Melting points (M<sub>p</sub>) are uncorrected and were determined under an atmosphere of air.<sup>b</sup> Decomposition temperatures (T<sub>d</sub>) determined using thermogravimetric analysis under an atmosphere of nitrogen and defined as the temperature at which 5% mass loss occurred. <sup>c</sup> Melting point was below ambient temperature.

After synthesis and characterization, the thermal stabilities of various triazenes were evaluated in the solid-state using thermogravimetric analysis (TGA); results are summarized in Table 6.6. To ensure that each triazene studied was decomposing in the same phase, melting points were also determined and found to be below the

decomposition temperature ( $T_d$ ) for all compounds studied. In accord with the qualitative assessment noted above, increasing the size of the N-substituent positively influenced triazene stability. For example, while triazenes containing N-methyl groups exhibited a  $T_d = 93$  °C (Entry 1), they were found to slowly decompose at ambient temperature over time. Comparatively, analogous triazenes with N-isobutyl (**6.6-H-H**), N-*tert*-butyl (**6.1-H-H**), or N-*neo*-pentyl (**6.7**) substituents exhibited  $T_{dS}$  of 118, 148, and 156 °C, respectively (Entries 2 – 4).<sup>34</sup> In contrast, the role of benzimidazol-2-ylidene electronics in influencing triazene thermal stability was found to be relatively minor. For example, **6.1-H-H** and **6.1-OCH<sub>3</sub>-H** were found to exhibit decomposition temperatures ( $T_{dS}$ ) of 148 and 154 °C, respectively (Entries 3 and 5), which was consistent with the aforementioned UV-Vis, NMR, and X-ray spectroscopic data, indicating that donor groups in these positions have only moderate influences on triazene electronics.

Next, attention was focused on studying the role of azide electronics. Variation of azide electronics appeared to significantly influence triazene stability. The  $T_d$  of **6.6-H-NO<sub>2</sub>** which possessed an electron-deficient para-nitro substituent was 35 °C higher than an analogue containing a para-methoxy substituent (**6.6-H-OCH<sub>3</sub>**) ( $T_{dS} = 174$  and 139 °C, respectively; Entries 6 and 7). Collectively, these results suggested that coupling benzimidazol-2-ylidenes possessing bulky N-substituents with electron deficient azides affords triazenes with the highest thermal stabilities.

**Mechanistic Investigation of the Triazene Decomposition Reaction.** It is well-established that NHCs often function as phosphine analogues.<sup>12,37</sup> Indeed, the NHC/azide coupling reaction to form triazenes and its thermal decomposition products share many similarities with the Staudinger reaction. In the Staudinger reaction, addition of a phosphine to an azide results in formation of a phosphatriazene (see Figure 6.7).<sup>21</sup> This compound subsequently undergoes intramolecular cyclization to form an unstable four-

membered intermediate that rapidly decomposes to a phosphazene, extruding molecular nitrogen in the process. As with the triazenes discussed above, the thermal stabilities of the triazenophosphoranes have been improved through the incorporation of bulky groups.<sup>38</sup>

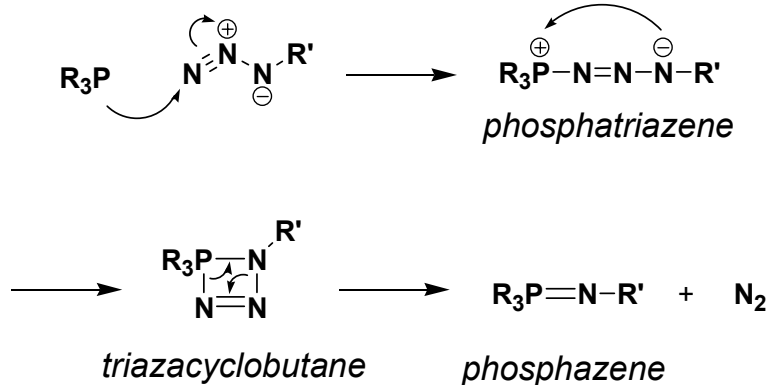


Figure 6.7 Illustration of the Staudinger reaction. Nucleophilic addition of the phosphine on the terminal atom of the organic azides affords an intermediate phosphatriazene. Subsequent intramolecular cyclization leads to an unstable triazacyclobutadiene intermediate that decomposes to a phosphazene and molecular nitrogen.

To confirm that the decomposition mechanism of the triazenes was similar to the Staudinger reaction, a decomposition reaction involving an  $^{15}\text{N}$ -labeled triazene was performed. Phenyl azide containing an isotopically-enriched nitrogen atom bonded to the phenyl ring was synthesized using literature protocols from  $^{15}\text{N}$ -labeled aniline.<sup>39</sup> After coupling the  $^{15}\text{N}$ -labeled azide with 1,3-di-*iso*-butyl-benzimidazol-2-ylidene, the resulting triazene **6.8** was heated to 170 °C (closed vessel) in toluene at 0.1 M. Guanidine **6.9** was found as the major product (> 95% conversion)<sup>34</sup> by  $^1\text{H}$  NMR spectroscopy and exhibited a isotopic mass distribution consistent with  $^{15}\text{N}$ -labeled azide starting material by mass spectrometry. Based on these results, we believe the mechanism to proceed as shown in Figure 6.8. The nitrogen atom bonded to the phenyl ring attacks the benzimidazol-2-ylidene carbon to form a four-membered intermediate

(6.10). Subsequent fragmentation expelled molecular nitrogen to afford the observed guanidine **6.9**. This mechanism also provides an explanation for increased stability observed with triazenes possessing bulky N-substituents and electron-deficient azide components. The former groups would sterically prevent nucleophilic attack at the electrophilic benzylidene carbon atom while the latter groups would be expected to diminish nucleophilicity of aryl nitrogen atom through resonance.

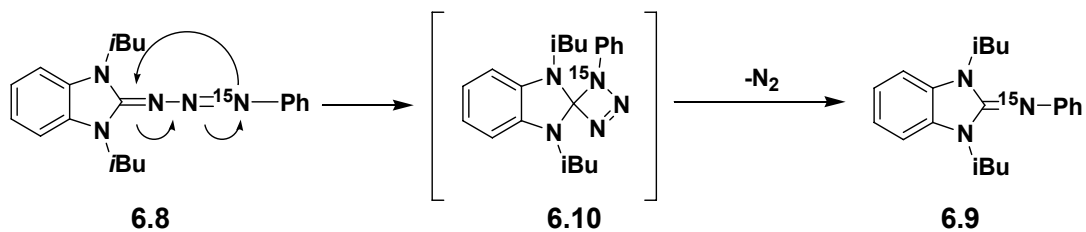


Figure 6.8 Proposed mechanism of thermally-induced triazene decomposition based on a  $^{15}\text{N}$ -labeling experiment.

## CONCLUSION

In summary, we have prepared a novel series of 1,3-disubstituted-triazenes by coupling N-heterocyclic carbenes (NHCs) with various aryl azides. The coupling reactions were accomplished using free NHCs or NHCs generated *in situ* under basic conditions from their azolium precursors. Modest to excellent isolated yields (36 – 99%) of triazene product were obtained from these coupling reactions, with typical yields exceeding 95%. The triazenes prepared from this reaction were examined using UV-Vis spectroscopy, X-ray crystallography, NMR spectroscopy and thermogravimetric analysis. Results obtained from the UV-Vis spectroscopy experiments suggested that the triazenes exhibited electronically-delocalized structures with  $\lambda_{\text{max}}$  values ranging between 364 and 450 nm and dependent on the complementarities of the coupled N-heterocyclic carbene

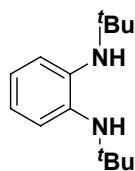
and azide components. The electronic properties were dominated by the azide, with minor contributions stemming from the benzimidazol-2-ylidene moiety. Additional support for electronic communication was obtained by X-ray crystallography which revealed bond alteration patterns in the triazeno (-C=N-N=N-) linkages characteristic of donor-acceptor compounds. Triazene stability was found to be governed by the N-substituents of the benzimidazol-2-ylidene and the electronic nature of the azide component. Notably, a triazene comprised of a benzimidazol-2-ylidene with bulky N-isobutyl groups and a para-nitrophenylazide was stable up to 174 °C in the solid-state. The mechanism of decomposition was elucidated using an isotopically-labeled azide and found to afford molecular nitrogen and the respective guanidine, in analogy with the Staudinger reaction.

Taken together, these results suggest that the azide-NHC coupling reaction holds tremendous potential for creating materials with high nitrogen contents, delocalized electronic structures, and high thermal stabilities. Recently, we reported<sup>19,35c-d,40</sup> a novel class of bis(NHC)s which feature two diametrically-opposed imidazol-2-ylidenes connected to a common arene linker. Combination of this monomer with ditopic bis(azide)s (e.g., 1,4-diazidobenzene) may lead to a novel class of conjugated polymeric materials. Furthermore, compounds exhibiting extensively delocalized structures often leads to molecular polarization, which is a key requirement for creating highly ordered materials. By judiciously combining functionalized azides and NHCs, highly polarized triazenes may find new applications in non-linear optics. Efforts toward accomplishing these goals as well as exploring the utility of triazenes obtained from the NHC/azide coupling reaction in electronic materials will be reported in due course.

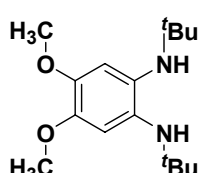
## EXPERIMENTAL

**General Considerations.** All reactions were conducted under an atmosphere of nitrogen using standard Schlenk techniques or in a nitrogen filled glove-box. CH<sub>2</sub>Cl<sub>2</sub> was distilled from CaH<sub>2</sub> and degassed by two freeze-pump-thaw cycles. THF and toluene were distilled from Na/benzophenone and degassed by two freeze-pump-thaw cycles. 1,3-Bis(2,6-di-isopropylphenyl)imidazolium chloride was purchased from Strem Chemicals and used without further purification. 1,2-Di-*iso*-butylaminobenzene,<sup>41</sup> 1,2-di-*neo*-pentylaminobenzene,<sup>42</sup> and 1,3-di-methyl-benzimidazolium iodide<sup>43</sup> were prepared as previously described. All other reagents were used without further purification, unless otherwise noted. <sup>1</sup>H NMR spectra were recorded using a 300 MHz or 400 MHz spectrometer. Chemical shifts are reported in delta ( $\delta$ ) units, expressed in parts per million (ppm) downfield from tetramethylsilane using residual protonated solvent as an internal standard (CDCl<sub>3</sub>, 7.24 ppm; C<sub>6</sub>D<sub>6</sub>, 7.15 ppm; CD<sub>2</sub>Cl<sub>2</sub>, 5.32 ppm; DMSO-*d*<sub>6</sub>, 2.49 ppm). <sup>13</sup>C NMR spectra were recorded using a 75 MHz or 100 MHz spectrometer. Chemical shifts are reported in delta ( $\delta$ ) units, expressed in parts per million (ppm) downfield from tetramethylsilane using the solvent as an internal standard (CDCl<sub>3</sub>, 77.0 ppm; C<sub>6</sub>D<sub>6</sub>, 128.0 ppm; CD<sub>2</sub>Cl<sub>2</sub>, 53.8 ppm; DMSO-*d*<sub>6</sub>, 39.5 ppm). <sup>13</sup>C NMR spectra were routinely run with broadband decoupling. High-resolution mass spectra (HRMS) are reported as m/z (relative intensity). Melting points were determined under ambient atmosphere and are uncorrected. Decomposition temperatures (T<sub>d</sub>s) were determined under nitrogen atmosphere and were reported as the temperature at which 5% weight loss occurred using a proprietary high resolution dynamic heating method. X-ray crystal structure data was collected for compounds **6.3-H-H** (CCDC 643401), **6.3-H-NO<sub>2</sub>** (CCDC 643400), **6.3-OCH<sub>3</sub>-H** (CCDC 643398) and **6.3-OCH<sub>3</sub>-NO<sub>2</sub>** (CCDC 643399),

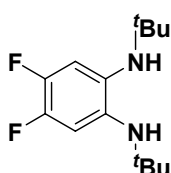
and deposited with the Cambridge Crystallographic Data Centre, 12 Union Road, Cambridge CB2 1EZ, UK.



**1,2-Di-*tert*-butylaminobenzene (A).** Following a previously reported procedure,<sup>44</sup> 1,2-dibromobenzene (1.12 g, 4.75 mmol) was coupled to *tert*-butylamine (0.73 g, 10 mmol) to afford 1.04 g (99% yield) of the titled compound as a brown oil. <sup>1</sup>H NMR (CDCl<sub>3</sub>): δ 6.82 (dd, J = 3.6, 11.6 Hz, 2H), 6.75 (dd, J = 3.6, 11.6 Hz, 2H), 3.7 (br, 2H), 1.28 (s, 18H). <sup>13</sup>C NMR (CDCl<sub>3</sub>): δ 138.5, 120.5, 120.1, 51.9, 29.9. HRMS: [M+H]<sup>+</sup> calcd for C<sub>14</sub>H<sub>25</sub>N<sub>2</sub>: 221.2018; found, 221.2014.

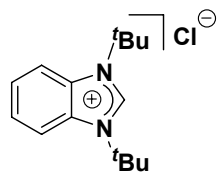


**1,2-Di-*tert*-butylamino-4,5-dimethoxybenzene (B).** Following a previously reported procedure,<sup>44</sup> 4,5-dibromoveratrole (1.48 g, 5.0 mmol) was coupled to *tert*-butylamine (0.80 g, 11 mmol) to afford 1.4 g (99% yield) of the titled compound as a brown oil. <sup>1</sup>H NMR (CDCl<sub>3</sub>): δ 6.55 (s, 2H), 3.78 (s, 6H), 3.41 (br, 2H), 1.20 (s, 18H). <sup>13</sup>C NMR (CDCl<sub>3</sub>): δ 143.4, 132.6, 108.0, 56.3, 52.4, 30.1. HRMS: [M+H]<sup>+</sup> calcd for C<sub>16</sub>H<sub>29</sub>N<sub>2</sub>O<sub>2</sub>: 281.2229; found, 281.2229.

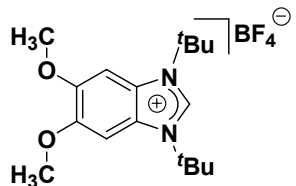


**1,2-Di-*tert*-butylamino-4,5-difluorobenzene (C).** Following a previously reported procedure,<sup>44</sup> 1,2-difluoro-4,5-dibromobenzene (1.36 g, 5.0 mmol) was coupled to *tert*-butylamine (0.80 g, 11 mmol) to afford 1.4 g (99% yield) of the titled compound as a brown oil, which was used without additional purification. <sup>1</sup>H NMR (CDCl<sub>3</sub>): δ 6.67 (t, J<sub>F-H</sub> = 10.4 Hz, 2H), 3.55 (br, 2H), 1.23 (s, 18H). <sup>13</sup>C NMR (CDCl<sub>3</sub>): δ 144.1 (dd, J<sub>C-F</sub> = 14.6, 240 Hz), 134.6 (m),

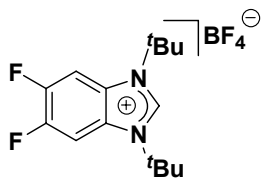
108.9 (m), 52.0, 29.7. HRMS:  $[M+H]^+$  calcd for  $C_{14}H_{23}F_2N_2$ : 257.1829; found, 257.1826.



**1,3-Di-*tert*-butyl-benzimidazolium chloride (D).** Crude 1,2-di-*tert*-butylaminobenzene (**A**) (1.10 g, 5 mmol) was treated with aq. HCl (5.1 mmol, 0.47 mL) in 20 mL of  $HC(OEt)_3$ . The resulting reaction mixture was stirred for 10 h at 50 °C and then concentrated to one-half of its original volume, which caused solids to precipitate. These solids were then collected by filtration and washed with diethyl ether (20 mL) to afford 1.2 g of the titled compound as a tan powder (90% yield).  $^1H$  NMR (DMSO-*d*6):  $\delta$  8.93 (s, 1H), 8.32 (dd,  $J$  = 3.2, 6.2 Hz, 2H), 7.63 (dd,  $J$  = 3.2, 6.2 Hz, 2H), 1.82 (s, 18H).  $^{13}C$  NMR (DMSO-*d*6):  $\delta$  139.1, 130.4, 125.7, 116.6, 60.9, 28.0. HRMS:  $[M]^+$  calcd for  $C_{15}H_{23}N_2$ : 231.1861; found, 231.1860.

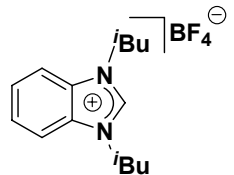


**1,3-Di-*tert*-butyl-4,5-dimethoxy-benzimidazolium tetrafluoroborate (E).** Crude 1,2-di-*tert*-butylamino-4,5-dimethoxybenzene (**B**) (1.40 g, 5 mmol) was treated with aq.  $HBF_4$  (5.1 mmol, 0.65 mL) in 20 mL of  $HC(OEt)_3$ . The resulting reaction mixture was stirred for 10 h at 50 °C and then concentrated to one-half of its original volume, which caused solids to precipitate. These solids were then collected by filtration and washed with diethyl ether (20 mL) to afford 1.8 g of the titled compound as a white powder (94% yield).  $^1H$  NMR (DMSO-*d*6):  $\delta$  8.66 (s, 1H), 7.48 (s, 2H), 3.96 (s, 6H), 1.81 (s, 18H).  $^{13}C$  NMR (DMSO-*d*6):  $\delta$  148.6, 136.1, 124.9, 98.0, 60.6, 56.6, 28.1. HRMS:  $[M]^+$  calcd for  $C_{17}H_{27}N_2O_2$ : 291.2067; found, 291.2073.

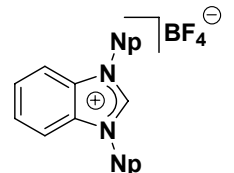


**1,3-Di-*tert*-butyl-4,5-difluoro-benzimidazolium**

**tetrafluoroborate (F).** Crude 1,2-di-*tert*-butylamino-4,5-difluorobenzene (C) (1.3 g, 5 mmol) was treated with a 6.8 M diethyl ether solution of HBF<sub>4</sub> (5.1 mmol, 0.75 mL) in 20 mL of HC(OEt)<sub>3</sub>. The resulting reaction mixture was stirred for 10 h at 50 °C and then concentrated to one-half of its original volume, which caused solids to precipitate. These solids were then collected by filtration and washed with diethyl ether (20 mL) to afford 1.56 g of the titled compound as a grey powder (87% yield). <sup>1</sup>H NMR (DMSO-*d*<sub>6</sub>): δ 8.87 (s, 1H), 8.62 (t, J<sub>H-F</sub> = 9.2 Hz, 2H), 1.79 (s, 18H). <sup>13</sup>C NMR (DMSO-*d*<sub>6</sub>): δ 148.3 (d, J<sub>C-F</sub> = 249 Hz), 140.6, 126.8 (t, J<sub>C-F</sub> = 6.1 Hz), 105.3 (m), 61.6, 27.8. HRMS: [M]<sup>+</sup> calcd for C<sub>15</sub>H<sub>21</sub>F<sub>2</sub>N<sub>2</sub>: 267.1673; found, 267.1676.

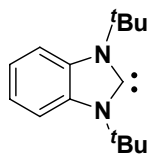


**1,3-Di-*iso*-butyl-benzimidazolium tetrafluoroborate (G).** 1,2-Di-*iso*-butylaminobenzene<sup>41</sup> (5.14 g, 23.4 mmol) was treated with aq. HBF<sub>4</sub> (25 mmol, 3.2 mL) in 50 mL HC(OEt)<sub>3</sub>. The resulting reaction mixture was stirred at 60 °C for 10 h and then concentrated to one-half of its original volume, which caused solids to precipitate. After washing the solids with diethyl ether (30 mL), these solids were dried under high vacuum to give 3.13 g of the titled compound as a light pink solid (42% yield). Spectral data were in accord with literature reports.<sup>45</sup>

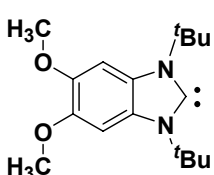


**1,3-Di-*neo*-pentyl-benzimidazolium tetrafluoroborate (H).** 1,2-Di-*neo*-pentylaminobenzene<sup>42</sup> (3.5 g, 14.1 mmol) was treated with aq. HBF<sub>4</sub> (16 mmol, 2.1 mL) in 30 mL HC(OEt)<sub>3</sub>. The resulting reaction mixture was stirred at 60 °C for 10 h and then concentrated

to one-half of its original volume, which caused solids to precipitate. After washing the solids with diethyl ether (50 mL), they were dried under high vacuum to give 4.3 g of the titled compound as a white solid (88% yield).  $^1\text{H}$  NMR (DMSO- $d_6$ ):  $\delta$  9.68 (s, 1H), 8.16 (dd,  $J$  = 3.0, 6.4, Hz, 2H), 7.68 (dd,  $J$  = 3.0, 6.4 Hz, 2H), 4.39 (s, 4H), 0.99 (s, 18H).  $^{13}\text{C}$  NMR (DMSO- $d_6$ ):  $\delta$  143.6, 132.0, 126.4, 114.2, 56.8, 33.1, 27.0. HRMS:  $[\text{M}]^+$  calcd for  $\text{C}_{17}\text{H}_{27}\text{N}_2$ : 259.2174; found, 259.2142.

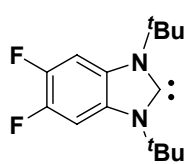


**1,3-Di-*tert*-butyl-benzimidazol-2-ylidene (**I**).** A mixture of 1,3-di-*tert*-butyl-benzimidazolium chloride (**D**) (1.55 g, 5.8 mmol), potassium *tert*-butoxide (0.65 g, 5.8 mmol), and 15 mL THF were stirred at ambient temperature for 2 h. After removing inorganic salts which precipitated from the reaction mixture by filtration, the resulting solution was concentrated to afford 1.3 g of the titled compound as a brown powder (97% yield).  $^1\text{H}$  NMR ( $\text{C}_6\text{D}_6$ ):  $\delta$  7.41 (dd,  $J$  = 3.6, 6.2 Hz, 2H), 7.00 (dd,  $J$  = 3.6, 6.2 Hz, 2H), 1.69 (s, 18H).  $^{13}\text{C}$  NMR ( $\text{C}_6\text{D}_6$ ):  $\delta$  224.7, 135.6, 120.2, 113.9, 57.3, 30.5. HRMS:  $[\text{M}+\text{H}]^+$  calcd for  $\text{C}_{15}\text{H}_{23}\text{N}_2$ : 231.1861; found, 231.1865.

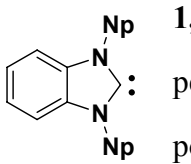


**1,3-Di-*tert*-butyl-4,5-dimethoxy-benzimidazol-2-ylidene (**J**).** A mixture of 1,3-di-*tert*-butyl-4,5-dimethoxy-benzimidazolium tetrafluoroborate (**E**) (1.13 g, 3 mmol), potassium *tert*-butoxide (0.34 g, 3 mmol), and 17 mL THF were stirred at ambient temperature for 2 h. After removing inorganic salts which precipitated from the reaction mixture by filtration, the resulting solution was concentrated to afford 0.83 g of the titled compound as a white powder (95% yield).  $^1\text{H}$  NMR ( $\text{C}_6\text{D}_6$ ):  $\delta$  7.12 (s, 2H), 3.52 (s, 6H), 1.74 (s,

18H).  $^{13}\text{C}$  NMR ( $\text{C}_6\text{D}_6$ ):  $\delta$  223.1, 145.7, 129.8, 99.8, 57.0, 56.8, 30.6. HRMS:  $[\text{M}+\text{H}]^+$  calcd for  $\text{C}_{17}\text{H}_{27}\text{N}_2\text{O}_2$ : 291.2067; found, 291.2073.



**1,3-Di-*tert*-butyl-4,5-difluoro-benzimidazol-2-ylidene (K).** A mixture of 1,3-di-*tert*-butyl-4,5-difluoro-benzimidazolium tetrafluoroborate (**F**) (1.0 g, 2.83 mmol), potassium *tert*-butoxide (0.32 g, 2.83 mmol), and 10 mL THF were stirred at ambient temperature for 2 h. After removing inorganic salts which precipitated from the reaction mixture by filtration, the resulting solution was concentrated to afford 0.72 g of the titled compound as a brown powder (96% yield).  $^1\text{H}$  NMR ( $\text{C}_6\text{D}_6$ ):  $\delta$  7.16 (t,  $J_{\text{F}-\text{C}} = 8.8$  Hz, 2H), 1.51 (s, 18H).  $^{13}\text{C}$  NMR ( $\text{C}_6\text{D}_6$ ):  $\delta$  228.5, 145.8 (dd,  $J_{\text{F}-\text{C}} = 17, 234$  Hz), 130.6 (t,  $J_{\text{F}-\text{C}} = 4.1$  Hz), 50.8 (dd,  $J_{\text{F}-\text{C}} = 8.8, 14.3$  Hz), 57.5, 30.3. HRMS:  $[\text{M}+\text{H}]^+$  calcd for  $\text{C}_{15}\text{H}_{21}\text{F}_2\text{N}_2$ : 267.1673; found, 267.1677.



**1,3-Di-*neo*-pentyl-benzimidazol-2-ylidene (L).** A mixture of 1,3-di-*neo*-pentyl-benzimidazolium tetrafluoroborate (**H**) (1.0 g, 2.89 mmol), potassium *tert*-butoxide (0.32 g, 2.89 mmol), and 10 mL THF were stirred at ambient temperature for 30 min. After removing inorganic salts which precipitated from the reaction mixture by filtration, the resulting solution was concentrated to afford 0.64 g of the titled compound (96% yield) as a light brown solid. Spectral data were in accord with literature reports.<sup>46</sup>

**NMR Kinetics of N-Heterocyclic Carbene – Azide Coupling Reactions.** Three separate kinetics experiments were performed by independently studying the rate of reaction between a free N-heterocyclic carbene (NHC), 1,3-di-*tert*-butyl-benzimidazol-2-ylidene, and three different azides: phenyl azide, para-methoxyphenyl azide, and para-

nitrophenyl azide. In these experiments, stock solutions of the NHC and various azides were first prepared and utilized. A vial containing 1,3-di-*tert*-butyl-benzimidazol-2-ylidene (115 mg, 0.50 mmol) was dissolved in 2.5 mL of THF-*d*<sub>8</sub> to create a 0.2 M stock solution of this compound. Three separate vials were then independently charged with phenyl azide (30 mg, 0.25 mmol), para-methoxyphenyl azide (38 mg, 0.25 mmol), and para-nitrophenyl azide (41 mg, 0.25 mmol), respectively. To each vial containing an azide, 1.25 mL of THF-*d*<sub>8</sub> was added to create 0.2 M stock solutions of these compounds. Three separate NMR tubes were then independently charged with 1 mL of THF-*d*<sub>8</sub> and 0.3 mL (0.06 mmol) of the NHC stock solution. After recording an initial spectrum, 0.3 mL (0.06 mmol) of an organic azide stock solution was added to generate solutions with initial substrate concentrations of 37.5 mM ( $[NHC]_0 = [azide]_0 = [substrate]_0$ ). Using <sup>1</sup>H NMR spectroscopy, the coupling reactions were monitored over time by integrating peak areas of diagnostic signals attributed to starting materials relative to analogous signals attributed to their respective triazene products. To determine rate constants (*k*), the data was fitted to Eq. 1, the integrated rate law of the bimolecular reaction:  $2 \cdot [substrate] \rightarrow [product]$ .<sup>47</sup>

$$1/[substrate] = kt + 1/[substrate]_0 \quad (1)$$

The observed rate constants are summarized in Table 6.S1; experimental data (with a linear fit corresponding to Eq. 1) are shown in Figures 6.S1 – 6.S3.

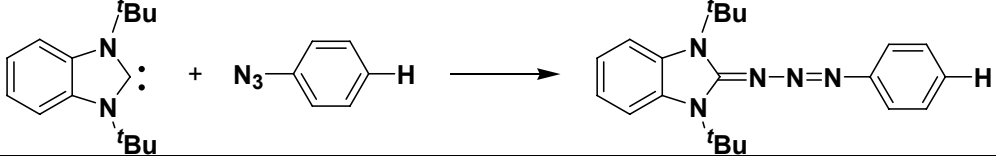
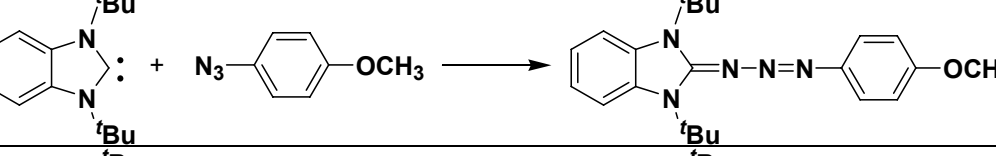
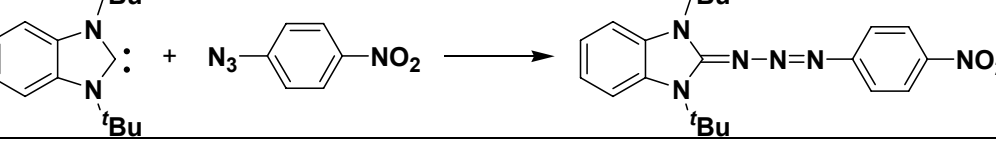
Entry	Reaction <sup>a</sup>	$k$ (L·mol <sup>-1</sup> ·s <sup>-1</sup> ) <sup>b</sup>
1		0.003
2		0.001
3		0.215

Table 6.S1 Rate constants for a variety of triazene forming reactions.<sup>a</sup> General reaction conditions:  $[NHC]_0 = [azide]_0 = 37.5$  mM, solvent = THF- $d_8$ , temperature = 23 °C. <sup>b</sup> Rate constants ( $k$ ) were determined by fitting the concentrations of the substrates, as determined by integrating the areas of diagnostic  $^1H$  NMR signals, to Eq. 1 as a function of time (see Figures 6.S1 –6.S3 for experimental data).

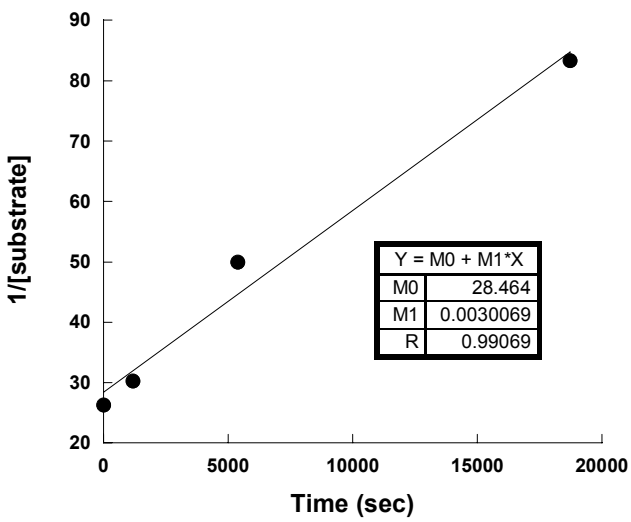


Figure 6.S1 Plot of  $1/[\text{substrate}]$  versus time for the reaction of 1,3-di-*tert*-butylbenzimidazol-2-ylidene with phenylazide (Table 6.S1, Entry 1).

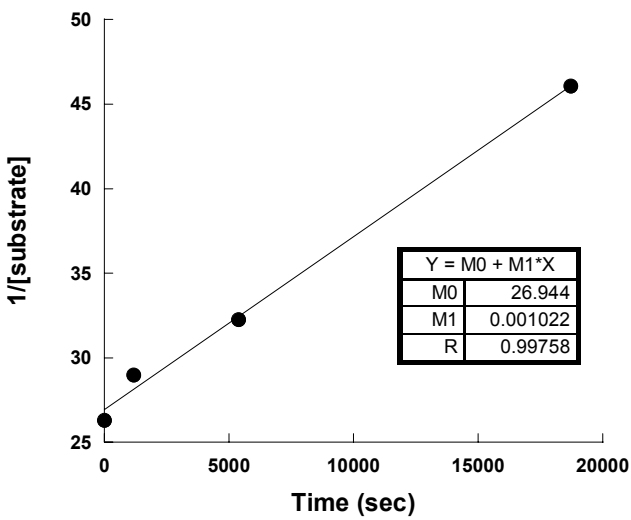


Figure 6.S2 Plot of  $1/[\text{substrate}]$  versus time for the reaction of 1,3-di-*tert*-butylbenzimidazol-2-ylidene with para-methoxyphenyl azide (Table 6.S1, Entry 2).

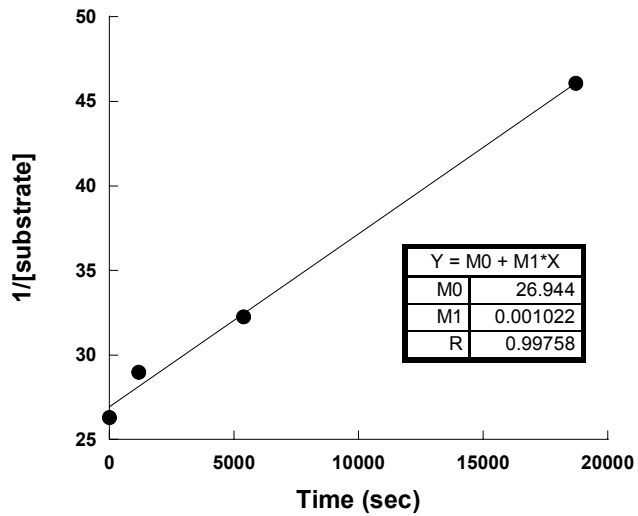


Figure 6.S3 Plot of  $1/\text{[substrate]}$  versus time for the reaction of 1,3-di-*tert*-butylbenzimidazol-2-ylidene with para-nitrophenyl azide (Table 6.S1, Entry 3).

Table 6.S2 Absolute energy, calculated dipole moment, and coordinates for triazene **6.3-H-H** (*cf.* Table 3, Entry 1) at B3LYP/6-31G\*-level of theory.<sup>48</sup>

$E(HF) = -854.3416596$  a.u.

$\mu_{\text{calc}} = 4.29$  debye

Atom	Cartesian Coordinates (Angstroms)		
	X	Y	Z
1 H H1	-3.0465456	-2.9404470	-0.2692333
2 C C1	-3.4724851	-1.9477675	-0.1663443
3 C C4	-4.6045964	0.6537080	0.1295950
4 C C2	-2.6708728	-0.8142976	-0.1058249
5 C C6	-4.8584759	-1.7634029	-0.0793414
6 C C5	-5.4133526	-0.4876467	0.0661895
7 C C3	-3.2294208	0.4673606	0.0423476
8 H H6	-5.5108982	-2.6303626	-0.1219772
9 H H5	-6.4915337	-0.3767028	0.1338991
10 H H4	-5.0361664	1.6429421	0.2436069
11 N N1	-1.2848699	-0.6596482	-0.1701331
12 N N2	-2.1729539	1.3636700	0.0766593
13 C C7	-0.9709028	0.6846481	-0.0388151
14 C C8	-0.3764244	-1.7765217	-0.3951806
15 H H7	0.5719631	-1.4001808	-0.7680560
16 H H9	-0.8303430	-2.4537118	-1.1257523
17 H H10	-0.1931244	-2.3246233	0.5364511
18 C C9	-2.2815587	2.8022014	0.2385198
19 H H8	-2.8725008	3.2312743	-0.5782399
20 H H11	-1.2722016	3.2125142	0.2177885
21 H H12	-2.7607001	3.0432228	1.1941295
22 N N3	0.1531270	1.3666611	-0.0292620
23 N N4	1.2867787	0.6174254	0.0206787
24 N N5	2.3183361	1.3421372	-0.1102023
25 C C10	3.5329709	0.6242634	0.0019240
26 C C11	6.0611299	-0.5891295	0.1451657
27 C C12	3.6752438	-0.6560523	0.5675016
28 C C13	4.6740482	1.2926145	-0.4667984
29 C C14	5.9272246	0.6875849	-0.4040743

30	C	C15	4.9307927	-1.2527717	0.6336077
31	H	H3	2.7996926	-1.1597746	0.9623837
32	H	H13	4.5465914	2.2873408	-0.8833272
33	H	H14	6.8005938	1.2147842	-0.7790816
34	H	H15	5.0330820	-2.2403341	1.0774803
35	H	H16	7.0383524	-1.0609778	0.2037158

Table 6.S3 Absolute energy, calculated dipole moment, and coordinates for triazene **6.3-H-NO<sub>2</sub>** (*cf.* Table 5.3, Entry 2) at B3LYP/6-31G\*-level of theory.<sup>48</sup>

E (HF) = -1058.8466354 a.u.

$\mu_{\text{calc}}$  = 10.6 debye

Atom	Cartesian Coordinates (Angstroms)		
	X	Y	Z
1 H H1	3.3576505	-2.9681504	0.3566272
2 C C1	3.8194678	-1.9961930	0.2180702
3 C C4	5.0501493	0.5478461	-0.1769766
4 C C2	3.0628207	-0.8320947	0.1400132
5 C C6	5.2079987	-1.8704973	0.0992529
6 C C5	5.8117092	-0.6223068	-0.0947716
7 C C3	3.6700845	0.4199226	-0.0571073
8 H H6	5.8258159	-2.7615511	0.1544141
9 H H5	6.8917587	-0.5584512	-0.1864959
10 H H4	5.5196357	1.5141417	-0.3303039
11 N N1	1.6852464	-0.6154401	0.2258488
12 N N2	2.6502934	1.3588060	-0.0984335
13 C C7	1.4309680	0.7327189	0.0584990
14 C C8	0.7244098	-1.6748971	0.5096735
15 H H7	-0.1304543	-1.2624601	1.0398844
16 H H9	1.2185701	-2.4275596	1.1301309
17 H H10	0.3689193	-2.1436795	-0.4139135
18 C C9	2.8157866	2.7869949	-0.3099235
19 H H8	3.4521162	3.2111585	0.4739553
20 H H11	1.8278892	3.2450037	-0.2701510
21 H H12	3.2725744	2.9752596	-1.2876380
22 N N3	0.3268278	1.4588110	0.0545665

23	N	N4	-0.8189302	0.7500744	0.0102758
24	N	N5	-1.8348544	1.5072856	0.1409192
25	C	C10	-3.0582624	0.8213245	0.0244505
26	C	C11	-5.5919938	-0.3202520	-0.1344839
27	C	C12	-3.2268220	-0.4664593	-0.5266534
28	C	C13	-4.1912632	1.5262426	0.4700790
29	C	C14	-5.4568012	0.9612615	0.4017416
30	C	C15	-4.4879218	-1.0372947	-0.6038026
31	H	H3	-2.3604568	-0.9992376	-0.9003602
32	H	H13	-4.0453015	2.5224813	0.8746031
33	H	H14	-6.3353941	1.4901031	0.7498849
34	H	H15	-4.6390668	-2.0235124	-1.0261124
35	N	N6	-6.9217006	-0.9241048	-0.2172362
36	O	O1	-7.8789720	-0.2701569	0.2033139
37	O	O2	-7.0124970	-2.0551378	-0.7018405

Table 6.S4 Absolute energy, calculated dipole moment, and coordinates for triazene **6.3-OCH<sub>3</sub>-H** (*cf.* Table 5.3, Entry 3) at B3LYP/6-31G\*-level of theory.<sup>48</sup>

E (HF) = -1083.3757044 a.u.

$\mu_{\text{calc}}$  = 5.39 debye

Atom	Cartesian Coordinates (Angstroms)		
	X	Y	Z
1 H H1	-2.1465577	-2.1946880	-0.0566186
2 C C1	-2.4460652	-1.1609012	0.0592547
3 C C4	-3.1998519	1.5647907	0.3856499
4 C C2	-1.4971556	-0.1427751	0.1120741
5 C C6	-3.7956292	-0.7999637	0.1773617
6 C C5	-4.1667882	0.5590017	0.3332742
7 C C3	-1.8623696	1.1968204	0.2788491
8 H H4	-3.5197792	2.5923431	0.5186357
9 N N1	-0.1055093	-0.1903019	0.0204193
10 N N2	-0.6880086	1.9366034	0.2920635
11 C C7	0.4007362	1.0965888	0.1379039
12 C C8	0.6200538	-1.4316768	-0.2135050
13 H H7	1.6564824	-1.1989855	-0.4409156
14 H H9	0.1550450	-1.9664853	-1.0494209

15	H	H10	0.5845797	-2.0668189	0.6798204
16	C	C9	-0.5901157	3.3753956	0.4549671
17	H	H8	-1.1673104	3.8835129	-0.3255320
18	H	H11	0.4624826	3.6447574	0.3697803
19	H	H12	-0.9708684	3.6772110	1.4373254
20	N	N3	1.6096600	1.6187761	0.1040505
21	N	N4	2.6339587	0.7290054	0.0829285
22	N	N5	3.7454316	1.3140578	-0.0962637
23	C	C10	4.8563701	0.4391941	-0.0598916
24	C	C11	7.1975203	-1.1124791	-0.0788944
25	C	C12	4.8714481	-0.8325893	0.5413382
26	C	C13	6.0342662	0.9299219	-0.6437258
27	C	C14	7.1923182	0.1563776	-0.6622506
28	C	C15	6.0342407	-1.5978270	0.5269559
29	H	H3	3.9733698	-1.1967709	1.0286633
30	H	H13	6.0098879	1.9215929	-1.0855445
31	H	H14	8.0940586	0.5466016	-1.1271699
32	H	H15	6.0381976	-2.5768820	1.0003959
33	O	O1	-4.8290648	-1.6950299	0.1632236
34	O	O2	-5.4831912	0.9123942	0.5077418
35	C	C16	-4.5185220	-3.0750427	0.0659987
36	H	H5	-4.0085841	-3.3112569	-0.8781274
37	H	H17	-5.4753605	-3.5991416	0.0986394
38	H	H18	-3.8942046	-3.4073013	0.9062777
39	C	C17	-6.3077205	0.8054621	-0.6555766
40	H	H2	-5.9197960	1.4346240	-1.4683406
41	H	H19	-7.2952874	1.1666705	-0.3590284
42	H	H20	-6.3850041	-0.2309504	-0.9990283
43	H	H21	8.1026367	-1.7138355	-0.0837591

Table 6.S5 Absolute energy, calculated dipole moment, and coordinates for triazene **6.3-OCH<sub>3</sub>-NO<sub>2</sub>** (*cf.* Table 3, Entry 4) at B3LYP/6-31G\*-level of theory.<sup>48</sup>

E(HF) = -1287.8812702 a.u.

$\mu_{\text{calc}}$  = 12.2 debye

Atom	Cartesian Coordinates (Angstroms)		
	X	Y	Z
1 H H1	-2.3732828	-2.2561783	-0.2404470

2	C	C1	-2.7468512	-1.2576665	-0.0537524
3	C	C4	-3.6997837	1.3743054	0.4781917
4	C	C2	-1.8774353	-0.1728978	0.0475372
5	C	C6	-4.1149261	-1.0113250	0.1185581
6	C	C5	-4.5864689	0.3033934	0.3758962
7	C	C3	-2.3409556	1.1181698	0.3175217
8	H	H4	-4.0923980	2.3624502	0.6904770
9	N	N1	-0.4879950	-0.0993453	-0.0763258
10	N	N2	-1.2276392	1.9463152	0.3655086
11	C	C7	-0.0876021	1.2071755	0.1364731
12	C	C8	0.3400396	-1.2460719	-0.4282964
13	H	H7	1.2786287	-0.8991728	-0.8513934
14	H	H9	-0.2014114	-1.8537807	-1.1599374
15	H	H10	0.5589741	-1.8556631	0.4557998
16	C	C9	-1.2373494	3.3721033	0.6458085
17	H	H8	-1.8593058	3.8944203	-0.0889806
18	H	H11	-0.2095957	3.7275105	0.5799297
19	H	H12	-1.6322460	3.5583655	1.6504862
20	N	N3	1.0859817	1.8206389	0.1279319
21	N	N4	2.1574400	1.0094426	0.0881346
22	N	N5	3.2378287	1.6749798	-0.0440801
23	C	C10	4.3910262	0.8713498	-0.0156682
24	C	C11	6.8047153	-0.5171764	-0.0325400
25	C	C12	4.4571414	-0.4512565	0.4724960
26	C	C13	5.5680027	1.4836175	-0.4856825
27	C	C14	6.7728042	0.7962839	-0.5047839
28	C	C15	5.6574430	-1.1446522	0.4612787
29	H	H3	3.5607149	-0.9137900	0.8683571
30	H	H13	5.5028593	2.5071972	-0.8399699
31	H	H14	7.6829739	1.2534695	-0.8726820
32	H	H15	5.7294714	-2.1596100	0.8333397
33	O	O1	-5.0774944	-1.9771945	0.0720376
34	O	O2	-5.9185220	0.5383259	0.6050899
35	C	C16	-4.6715191	-3.3253669	-0.1052727
36	H	H5	-4.1718464	-3.4749436	-1.0721497
37	H	H17	-5.5876862	-3.9175689	-0.0779890
38	H	H18	-4.0036939	-3.6523360	0.7027542
39	C	C17	-6.7713458	0.4372344	-0.5397999
40	H	H2	-6.4641186	1.1489944	-1.3179476
41	H	H19	-7.7738592	0.6936965	-0.1902350
42	H	H20	-6.7742186	-0.5775576	-0.9493582
43	N	N6	8.0686496	-1.2514720	-0.0448529
44	O	O3	9.0669070	-0.6750564	-0.4839777
45	O	O4	8.0679489	-2.4093575	0.3825148

## REFERENCES

- † Portions of this chapter have been previously reported, see: Khramov, D. M.; Bielawski, C. W. *Org. Lett.* **2006**, 72, 4907.
- 1 (a) Zollinger, H.; *Diazo Chemistry*, Vol. 1, VCH, Weinheim, 1994. (b) Smith, P. A. S.; *Open Chain Chain Nitrogen Compounds*, Vol. 2. W. A. Benjamin, New York, 1966. (c) Kimball, D. B.; Haley, M. M. *Angew. Chem. Int. Ed.* **2002**, 41, 3338. (c) Ang, H. G.; Koh, L. L.; Yang, G. Y. *J. Chem. Soc., Dalton Trans.* **1996**, 1573. (d) Saunders, K. H.; *The Aromatic Diazo Compounds*, 2<sup>nd</sup> Ed., Longmans, Green and Co., New York, 1949.
  - 2 Rouzer, C. A.; Sabourin, M.; Skinner, T. L.; Thompson, E. J.; Wood, T. O.; Chmurny, G. N.; Klose, J. R.; Roman, J. M.; Smith Jr, R. H.; Michejda, C. J. *Chem. Res. Toxicol.* **1996**, 9, 172.
  - 3 (a) Moore, J. S.; Weinstein, E. J.; Wu, Z. *Tetrahedron Lett.* **1991**, 32, 2465. (b) Nicolau, K. C.; Boddy, C. N. C.; Li, H.; Koumbis, A. E.; Hughes, R.; Natarajan, S.; Jain, N. F.; Ramanjulu, J. M.; Bräse, S.; Soloman, M. *Chem. Eur. J.* **1999**, 5, 2602. (c) Wirschun, W.; Winkler, M.; Lutz, K.; Jochims, J. C. *J. Chem. Soc., Perkin Trans. 1* **1998**, 1755. (d) Wirschun, W.; Jochims, J. C. *Synthesis* **1997**, 233. (e) Wirschun, W.; Maier, G.-M.; Jochims, J. C. *Tetrahedron* **1997**, 53, 5755.
  - 4 (a) Jones II, L.; Schumm, J. S.; Tour, J. M. *J. Org. Chem.* **1997**, 62, 1388. (b) Moore, J. S. *Acc. Chem. Res.* **1997**, 30, 402.
  - 5 (a) Gross, M. L.; Blank, D. H.; Welch, W. M. *J. Org. Chem.* **1993**, 58, 2104. (b) Jian, H.; Tour, J. M. *J. Org. Chem.* **2005**, 70, 3396. (c) Merkushev, E. B. *Synthesis* **1985**, 1104. (d) Lunn, G.; Sansone, E. B. *Synthesis* **1988**, 923.
  - 6 Lippert, T.; Nuyken, O. *Makromol. Chem., Rapid Commun.* **1993**, 13, 365.
  - 7 (a) Wanner, M. J.; Koch, M.; Koomen, G. J. *J. Med. Chem.* **2004**, 47, 6875. (b) Hooper, D. L.; Pottie, I. R.; Vacheresse, M.; Baughan, K. *Can. J. Chem.* **1998**, 76, 125. (c) Bräse, S.; Dahmen, S.; Pfefferkorn, M. *J. Comb. Chem.* **2000**, 2, 710. (d) Wirschun, W.; Winkler, M.; Lutz, K.; Jochims, J. C. *J. Chem. Soc., Perkin Trans. 2* **1998**, 1755.
  - 8 Chen, B.; Flatt, A. K.; Jian, H.; Hudson, J. L.; Tour, J. M. *Chem. Mater.* **2005**, 17, 4832.
  - 9 Sadtchikova, E. V.; Morkushin, V. S. *Mendeleev Commun.* **2002**, 2, 70.

- 10 Kirk, K. L. *J. Org. Chem.* **1978**, *43*, 4381.
- 11 Khramov, D. M.; Bielawski, C. W. *Chem. Commun.* **2005**, 4958.
- 12 For excellent reviews on N-heterocyclic carbenes, see: (a) Canal, John P.; Ramnial, Taramatee; Dickie, Diane A.; Clyburne, Jason A. C. *Chem. Commun.* **2006**, 1809. (b) Hahn, F. E. *Angew. Chem. Int. Ed.* **2006**, *45*, 1348. (c) Crabtree, R. H. *J. Organomet. Chem.* **2005**, *690*, 5451. (d) Herrmann, W. A.; Köcher, C. *Angew. Chem., Int. Ed. Engl.* **1997**, *36*, 2162. (e) Arduengo, A. J. III *Acc. Chem. Res.* **1999**, *32*, 913. (f) Bourissou, D.; Guerret, O.; Gabbaï, F. P.; Bertrand, G. *Chem. Rev.* **2000**, *100*, 39. (g) Nair, V.; Bindu, S.; Sreekumar, V. *Angew. Chem., Int. Ed.* **2005**, *44*, 1907.
- 13 Previously, Winberg and Coffman reported that peraminoethylenes react with azides to afford triazenes similar in structure to the compounds reported herein, see: Winberg, H. E.; Coffman, D. D. *J. Am. Chem. Soc.* **1965**, *87*, 2776.
- 14 (a) Arduengo, A. J., III; Harlow, R. L.; Kline, M. *J. Am. Chem. Soc.* **1991**, *113*, 361. (b) Herrmann, W. A. *Angew. Chem. Int. Ed.* **2002**, *41*, 1291. (c) Hahn, F. E.; Wittenbecher, L.; Boese, R.; Bläser, D. *Chem. Eur. J.* **1999**, *5*, 1931.
- 15 (a) Huisgen, R.; Blaschke, H. *Tetrahedron Lett.* **1964**, *5*, 1409. (b) Tornøe, C. W.; Christensen, C.; Meldal, M. *J. Org. Chem.* **2002**, *67*, 3057. (c) For a recent review, see: Bock, V. D.; Hiemstra, H.; van Maarseveen, J. H. *Eur. J. Org. Chem.* **2006**, *51*.
- 16 (a) Kolb, H. C; Finn, M. G.; Sharpless, K. B. *Angew. Chem., Int. Ed.* **2001**, *40*, 2004. (b) Rostovtsev, V. V.; Green, L. G.; Fokin, V. V.; Sharpless, K. B. *Angew. Chem. Int. Ed.* **2002**, *41*, 2596.
- 17 For representative examples, see: (a) Diaz, D. D.; Punna, S.; Holzer, P.; McPherson, A. K.; Sharpless, K. B.; Fokin, B. B.; Finn, M. G. *J. Polym. Sci., Part A: Polym. Chem.* **2004**, *42*, 4392. (b) Wu, P.; Feldman, A. K.; Nugent, A. K.; Hawker, C. J.; Scheel, A.; Voit, B.; Pyun, J.; Fréchet, J. M. J.; Sharpless, K. B.; Fokin, V. V. *Angew. Chem., Int. Ed.* **2004**, *43*, 3928. (c) Joralemon, M. J.; O'Reilly, R. K.; Hawker, C. J.; Wooley, K. L. *J. Am. Chem. Soc.* **2005**, *127*, 16892. (d) Lutz, J. F.; Borner, H. G.; Weichenhan, K. *Macromol. Rapid Commun.* **2005**, *38*, 3558. (e) Opsteen, J. A.; van Hest, J. C. M. *Chem. Commun.* **2005**, 57. (f) Sumerlin, B. S.; Tsarevsky, N. V.; Louche, G.; Lee, R. Y.; Matyjaszewski, K. *Macromolecules* **2005**, *38*, 7540. (g) Parrish, B.; Breitenkamp, R. B.; Emrick, T. *J. Am. Chem. Soc.* **2005**, *127*, 7404. (h) Ladmiral, V.; Mantovani, G.; Clarkson, G. J.; Cauet, S.; Irwin, J. L.; Haddleton, D. M. *J. Am. Chem. Soc.* **2006**, *128*, 4823. (i) Thibault, R.J.; Takizawa, K.; Lowenheilm, P.; Helms, B.; Mynar, J. L.;

- Frechet, J. M. J.; Hawker, C. J. *J. Am. Chem. Soc.* **2006**, *128*, 12084. (j) Tejler, J.; Tullberg, E.; Frejd, T.; Leffler, H.; Nilsson, U. J. *Carbohydr. Res.* **2006**, *341*, 1353. (k) Fernandez-Megia, E.; Correa, J.; Rodriguez-Meizoso, I.; Riguera, R. *Macromolecules* **2006**, *39*, 2113. (l) Feldman, A. K.; Colasson, B.; Sharpless, K. B.; Fokin, V. V. *J. Am. Chem. Soc.* **2005**, *127*, 13444. (m) Hawker, C. J.; Wooley, K. L. *Science* **2005**, *309*, 1200. (n) Laurent, B. A.; Grayson, S. M. *J. Am. Chem. Soc.* **2006**, *128*, 4238. (o) Vogt, A. P.; Sumerlin, B. S. *Macromolecules* **2006**, *39*, 5286. (p) Thibault, R. J.; Takizawa, K.; Lowenheilm, P.; Helms, B.; Mynar, J. L.; Frechet, J. M. J.; Hawker, C. J. *J. Am. Chem. Soc.* **2006**, *128*, 12084.
- 18 Coady, D. J.; Bielawski, C. W. *Macromolecules* **2006**, *39*, 8895.
- 19 (a) Boydston, A. J.; Williams, K. A.; Bielawski, C. W. *J. Am. Chem. Soc.* **2005**, *127*, 12496. (b) Kamplain, J. W.; Bielawski, C. W. *Chem. Commun.* **2006**, 1727. (c) Boydston, A. J.; Rice, J. D.; Sanderson, M. D.; Dykhno, O. L.; Bielawski, C. W. *Organometallics* **2006**, *25*, 6087.
- 20 (a) Hahn, F.E.; von Fehrena, T.; Froelich, R. Z. *Naturforsch.* **2004**, *59*, 348. (b) Boesveld, W. Marco; Gehrhus, B; Hitchcock, P. B.; Lappert, M. F.; Schleyer, P. *Chem. Commun.* **1999**, *8*, 755.
- 21 Staudinger, H.; Meyer, J. *Helv. Chim. Acta* **1919**, *2*, 635.
- 22 (a) Lewis, M. Glaser, R. *J. Org. Chem.* **2002**, *67*, 1441. (b) Glaser, R.; Chen, G. S.; Anthamatten, M.; Barnes, C. L. *J. Chem. Soc., Perkin Trans. 2* **1995**, 1449. (c) Chen, G. S.; Wilbur, J. K.; Barnes, C. L.; Glaser, R. *J. Chem. Soc., Perkin Trans. 2* **1995**, 2311.
- 23 Sauro, V. A.; Workentin, M. S. *J. Org. Chem.* **2001**, *66*, 831.
- 24 Chen G. S.; Anthamatten, M.; Barnes, C. L.; Glaser, R. *Angew. Chem., Int. Ed. Engl.* **1994**, *33*, 1081. (b) Kesslen, E. C.; Euler, W. B.; *Tetrahedron Lett.* **1995**, *36*, 4725. (c) Kesslen, E. C.; Euler, W. B.; Foxman, B. M. *Chem. Mater.* **1999**, *11*, 336. (d) Euler, W. B.; Cheng, M.; Zhao, C. *Chem. Mater.* **1999**, *11*, 3702.
- 25 Chen, G. S.; Anthamatten, M.; Barnes, C. L.; Glaser, R. *J. Org. Chem.* **1994**, *59*, 4336
- 26 (a) Choytun, D. D.; Langlois, L. D.; Johansson, T. P.; Macdonald, C. L. B.; Leach, G. W.; Weinberg, N.; Clyburne, J. A. C. *Chem. Commun.* **2004**, *16*, 1842. (b) Hopkins, J. M.; Bowdridge, M.; Robertson, K. N.; Cameron, T. S.; Jenkins, H. A.; Clyburne, J. A. C. *J. Org. Chem.* **2001**, *66*, 5713.

- 27 Hadei, N.; Kantchev, E. A. B.; O'Brien, C. J.; Organ, M. G. *Org. Lett.* **2005**, 7, 1991.
- 28 Alternatively, many of the triazenes shown in Table 1 may be prepared by generating the free NHC in situ (from its benzimidazolium salt) in the presence of an equimolar amount of organic azide. However, this approach appears to be limited to substrates which are stable to base. For example, 1-azido-4-nitrobenzene was found to rapidly decompose under strongly basic conditions. Hence, the use of free NHCs (e.g., 1,3-di-*tert*-butyl-benzimidazol-2-ylidene-4,5-dimethoxy-1,3-di-*tert*-butyl-benzimidazol-2-ylidene, and 1,3-di-*tert*-butyl-4,5-difluoro-benzimidazol-2-ylidene) were necessary to form triazenes containing aryl azide moieties (e.g., Table 6.1: **6.1-H-NO<sub>2</sub>**, **6.1-OCH<sub>3</sub>-NO<sub>2</sub>**, and **6.1-F-NO<sub>2</sub>**).
- 29 Arduengo, A. J.; Calabrese, J. C.; Cowley, A. H.; Dias, H. V. R.; Goerlich, J. R.; Marshall, W. J.; Riegel, B. *Inorg. Chem.* **1997**, 36, 2151.
- 30 (a) Wanzlick, H. W.; Buchler, J. W. *Chem. Ber.* **1964**, 97, 2447. (b) Arduengo III, A. J.; Goerlich, J. R.; Marshall, W. J. *Leibigs Ann.* **1997**, 265. (c) Liu, Y.; Lindner, P. E.; Lemal, D. M. *J. Amer. Chem. Soc.* **1999**, 121, 10626.
- 31 Since benzimidazol-2-ylidene with small N-substituents are prone to exist as equilibrium between free NHC and its oxygen-sensitive dimer,<sup>30</sup> these reactions must be conducted with the rigorous exclusion of oxygen.
- 32 Unlike their N-*tert*-butyl analogues, triazenes **6.3** were found to exhibit low solubilities in common organic solvents (i.e., THF, toluene, DMF, DMSO, CH<sub>3</sub>CN, etc.) and decomposed slowly over several days in solution or in the solid-state (see main text for a more detailed discussion of this phenomenon). These characteristics are partially responsible for the relatively low yields of the reactions summarized in Table 6.3.
- 33 Dipole moments were calculated at the B3LYP (6-31G\*) level of density functional theory, as implemented in the Spartan 2004 software package (Wavefunction, Irvine, CA 92612).
- 34 Similarly, heating toluene solutions of triazenes **6.6-H-H** and **6.6-H-NO<sub>2</sub>** (see Table 6.6) to > 150 °C afforded their respective guanidines (**6.11** and **6.12**, not shown) in ≥ 95% yields. This process was conveniently monitored using <sup>1</sup>H NMR spectroscopy. For example, the methylene groups (N-CH<sub>2</sub>-) in triazenes **6.6** exhibit diagnostic chemical shifts at 4.0-4.5 ppm in their <sup>1</sup>H NMR spectra; chemical shifts corresponding to same group in their respective guanidine products were found at 3.5-3.8 ppm. Note that while the thermally-induced triazene decomposition reactions generally afforded high yields (> 95%) of

- guanidine products, a side-reaction was evident. The residual mass was comprised of a mixture of products that eluded NMR spectroscopic identification and could not be purified via column chromatography.
- 35 (a) Quast, H.; Schmitt, E. *Chem. Ber.* **1968**, *101*, 4012. (b) Huynh, H. V.; Han, Y.; Ho, J. H. H.; Tan, G. K. *Organometallics* **2006**, *25*, 3267. (c) Khramov, D. M.; Boydston, A. J.; Bielawski, C. W. *Org. Lett.* **2006**, *8*, 1831. (d) Khramov D. M.; Boydston, A. J.; Bielawski, C. W. *Angew. Chem. Int. Ed.* **2006**, *45*, 6186. (e) Gehrhus, B.; Hitchcock, P. B.; Pongtavornpinyo, R.; Zhang, L. *Dalton Trans.* **2006**, 1847. (f) Daniele, S.; Drost, C.; Gehrhus, B.; Hawkins, S. M.; Hitchcock, P. B.; Lappert, M. F.; Merle, P. G.; Bott, S. G. *J. Chem. Soc., Dalton Trans.* **2001**, *21*, 3179. (g) Myes, T. L.; Diver, S. T.; Richard, J. P.; Rivas, F. M.; Toth, K. *J. Am. Chem. Soc.* **2004**, *126*, 4366.
- 36 Although the spectroscopic signatures of the resulting triazenes were in accord with the aforementioned triazenes, one notable exception was found. Signals attributable to the methylene groups of the N-isobutyl substituents ( $N-CH_2-$ ) in triazene **6.6-H-H** appeared as two doublets at 3.97 ppm and 4.16 ppm in its  $^1H$  NMR spectrum (solvent =  $CDCl_3$ ), and were tentatively assigned to cis and trans diazo ( $-N=N-$ ) isomers, respectively. While geometric isomers often absorb radiation to differing degrees (see: Hartley, G. S. *J. Chem. Soc.* **1938**, 633 and El Halabieh, R. H.; Mermut, O.; Barrett, C. J. *Pure Appl. Chem.* **2004**, *76*, 1445), triazene **6.6-H-H** exhibited a single signal at  $\lambda_{max} = 367$  nm that was similar in shape to the triazenes discussed above (i.e., **6.1**). This result suggested that the absorption of radiation was concomitant with geometric isomerization (i.e., cis  $\rightarrow$  trans). A similar observation was observed in benzothiazole-based triazenes analogous to **6.6-H-H** where it was determined that cis  $\rightarrow$  trans isomerization was facilitated with  $\lambda = 405$  nm radiation (see: Dorsch, H.-T.; Hoffman, H.; Hänsel, R.; Rasch, G.; Fanghänel, E. *J. fuer Pract. Chemie* **1976**, *318*, 671 and Fanghänel, E; Hänsel, R.; Hohlfeld, J. *J. fuer Pract. Chemie* **1977**, *319*, 485). Notably, of all the triazenes reported herein, only **6.6-H-H** and **6.6-H-Me** exhibited isomers that were clearly resolved at room temperature by  $^1H$  NMR spectroscopy. Considering density functional theory calculations at the B3LYP (6-31G\*\*) level of theory suggested that trans **6.6-H-H** was more stable than its cis isomer by 5.1 kcal/mol, the trans isomer was assumed to dominate in all of the triazenes prepared in this study (DFT calculations were performed using Spartan 2004, Wavefunction, Irvine, CA 92612).
- 37 For a direct comparision of N-heterocyclic carbenes with phosphines in various applications, see: (a) Rogers, M. M.; Stahl, S. S. *Top. Organomet. Chem.* **2007**, *21*, 21. (b) Shaughnessy, K. H. *Eur. J. Org. Chem.* **2006**, *71*, 1827. (c) Zuo, G.; Louie, J. *Angew. Chem. Int. Ed.* **2004**, *43*, 2277.

- 38 (a) Shalimov, A.A; Malenko, D.M.; Repina, L.A.; Sinitsa, A.D. Russ. J. Org. Chem. **2005**, 75, 1376. (b) LePichon, L.; Stephan, D.W. Inorg. Chem. **2001**, 40, 3827. (c) Blum, J.; Yona, I.; Tsaroorom, S.; Sasson, Y. J. Org. Chem. **1979**, 44, 4178.
- 39 For additional examples of synthesizing <sup>15</sup>N-labeled azides see: Leseticky, L.; Barth, R.; Nemec, I.; Sticha, M.; Tislerova, I. Cz. J. Phys. **2003**, 53, A777.
- 40 Boydston, A. J.; Bielawski, C. W. Dalton Trans. **2006**, 4073.
- 41 Gehrhus, B.; Hitchcock, P. B.; Pongtavornpinyo, R.; Zhang, L. Dalton Trans. **2006**, 1847.
- 42 Daniele, S.; Drost, C.; Gehrhus, B.; Hawkins, S. M.; Hitchcock, P. B.; Lappert, M. F.; Merle, P. G.; Bott, S. G. J. Chem. Soc., Dalton Trans. **2001**, 21, 3179.
- 43 Myes, T. L.; Diver, S. T.; Richard, J. P.; Rivas, F. M.; Toth, K. J. Am. Chem. Soc. **2004**, 126, 4366.
- 44 Hadei, N.; Kantchev, E. A. B.; O'Brien, C. J.; Organ, M. G. Org. Lett. **2005**, 7, 1991.
- 45 Starikova, O. V.; Dolgushin, G. V.; Larina, L. I.; Ushakov, P. E.; Komarova, T. N.; Lopyrev, V. A. Russ. J. Org. Chem. **2003**, 39, 1467.
- 46 Gehrhus, B.; Hitchcock, P. B.; Lappert, M. F. J. Chem. Soc., Dalton Trans. **2000**, 3094.
- 47 Anslyn, E. V.; Dougherty, D. A. *Modern Physical Organic Chemistry*; University Science Books: Sausalito, CA, 2006; pp 382-390.
- 48 Calculations were performed at the B3LYP/6-31G\* level of density functional theory, as implemented in the Spartan 2004 software package (Wavefunction, Irvine, CA 92612).

## Chapter 7: N-Heterocyclic Carbene – Transition Metal Complexes: Spectroscopic and Crystallographic Analyses of $\pi$ -Backbonding Interactions<sup>†</sup>

### ABSTRACT

The ability of N-heterocyclic carbenes (NHCs) to participate in  $\pi$ -backbonding interactions was evaluated in a range of transition metal complexes. Rh chloride complexes containing a systematic series of various 1,3-dimethyl-4,5-disubstituted-imidazol-2-ylidenes and either 1,5-cyclooctadiene (cod) or two carbon monoxide ligands were synthesized (i.e., (NHC)RhCl(cod) and (NHC)RhCl(CO)<sub>2</sub>, respectively) and studied using <sup>1</sup>H NMR and IR spectroscopies. In the former series, the <sup>1</sup>H NMR chemical shifts of the signals attributable to the olefin *trans* to the NHC ligand were found to shift downfield by up to 0.17 ppm as the  $\pi$ - acidity of the substituents on the 4,5-positions increased (i.e., H → Cl → CN). Similarly, in the latter series, the IR stretching frequencies of the carbonyl groups *trans* to the NHC ligands were found to increase by 11 ± 0.5 cm<sup>-1</sup> as  $\pi$ - acidity increased over the same series. Using the nitrile group as a diagnostic handle, the CN stretching frequency of (1,3-dimethyl-4,5-dicyano-imidazol-2-ylidene)(cod)RhCl was found to be 4 ± 0.5 cm<sup>-1</sup> higher than 1,3-dimethyl-4,5-dicyano-imidazol-2-ylidene)(CO)<sub>2</sub>RhCl, a more  $\pi$ -acidic analogue. X-ray analysis of the aforementioned series of (NHC)(cod)RhCl complexes indicated changes in N-C<sub>carbene</sub> bond lengths that were consistent with greater  $\pi$ -donation from complexes containing 4,5-dihydro-imidazol-2-ylidene relative to their 4,5-dicyano analogues. Collectively, these results suggest that imidazol-2-ylidenes are not only capable of  $\pi$ -backbonding, but that this interaction may be tuned by changing the  $\pi$ - acidity of the substituents on the imidazole ring.

## INTRODUCTION

Since the discovery of transition metal complexes containing N-heterocyclic carbene (NHC) ligands by Wanzlick,<sup>1</sup> Öfele,<sup>2</sup> and Lappert,<sup>3</sup> an impressive number of new catalysts for facilitating synthetically-useful transformations have been developed.<sup>4</sup> Continued interest in these ligands has been extraordinary and driven by their abilities to often significantly enhance the catalytic activities of a broad range of transition metals upon complexation.<sup>4,5</sup> To understand and ultimately control these unique features, the nature of the metal-NHC interaction has been intensely investigated by a number of research groups.<sup>6</sup> A general consensus is that N-heterocyclic carbenes (NHCs) are strong, two electron  $\sigma$ -donors that coordinate to transition metals in a fashion analogous to, and in some cases better than, trialkylphosphines.<sup>7</sup> For example, *trans* carbonyl stretching frequencies are generally lower in metal complexes containing NHC ligands than analogous complexes containing trialkylphosphines.<sup>8,9</sup>

Although there are many distinguishing features between NHCs and phosphines, the former possess an empty p-orbital at the carbene atom poised to accept  $\pi$ -electron density from a complexed transition metal (i.e.,  $\pi$ -backbonding). However, due to competing  $\pi$ -overlap of electron-rich nitrogen atoms adjacent to the carbene atom, the extent to which NHCs are capable of participating in this type of bonding interaction has been under debate. Using photoelectron spectroscopy, Green found<sup>10</sup> that the  $\pi$ -systems of free NHCs were similar to their transition metal complexes. Combined with the results in the aforementioned studies involving NHC versus phosphine metal carbonyl complexes, Herrmann concluded that  $\pi$ -backbonding in NHC – transition metal complexes was “negligible”,<sup>7a,11</sup>; a conclusion supported theoretically by a number of groups.<sup>12</sup>

A general consensus of negligible  $\pi$ -backbonding in NHC-metal complexes is challenged by numerous anomalies reported in the literature.<sup>13</sup> In 1975, Clarke and Taube reported spectroscopic evidence for  $\pi$ -interactions in carbon-bound xanthine Ru complexes.<sup>14</sup> Arduengo found increased  $\pi$ -electron density on the NHC moieties in a series of (1,3-dimesityl-imidazol-2-ylidene)<sub>2</sub>M (M = Ni, Pt) complexes (**7.1**), and attributed this phenomena to a greater degree of  $\pi$ -backbonding relative to analogous cationic group 11 complexes.<sup>15</sup> By corroborating DFT calculations with X-ray crystal structure data obtained from a range of NHC-metal complexes, Meyer determined that  $\pi$ -backbonding accounted for up to 30% of the metal-ligand interaction.<sup>16</sup> Using well-designed annulated NHCs (e.g., **7.2**), Heinicke found<sup>17</sup> that  $\pi$ -backbonding interactions could be effectively increased by extending the  $\pi$ -system of the NHC ligand. Likewise, Albrecht<sup>18</sup> designed an elegant series of half metallocene NHC-complexes (**3**) and then utilized a combination of cyclic voltammetry, NMR spectroscopy, and DFT calculations to experimentally show that NHCs exhibit  $\pi$ -backbonding capabilities on the same order as pyridine, a well-known  $\pi$ -acidic ligand.<sup>19</sup> At the extreme, Nolan found<sup>20</sup>  $\pi$ -donation from a NHC was responsible for the high stability of a low-valent, 14-electron Ir complex (**7.4**). Theoretical support for  $\pi$ -backbonding and  $\pi$ -donation in a variety of other NHC-metal complexes was subsequently reported.<sup>21</sup> Manifesting these fundamental studies, Organ reported<sup>22</sup> strong correlation between  $\pi$ -electronics and catalytic activities in a range of NHC-metal complexes.

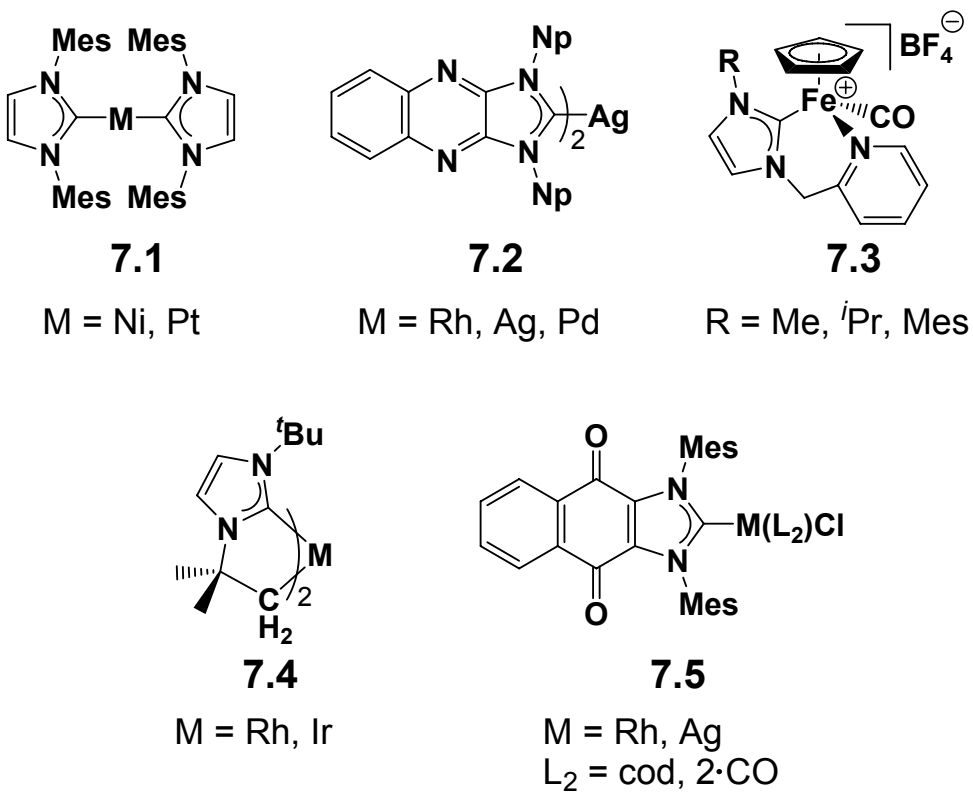


Figure 7.1 Examples of metal complexes used to study  $\pi$ -backbonding in NHCs. Np = *neo*-pentyl, Me = methyl, *i*Pr = *iso*-propyl, Mes = 1,3,5-trimethylbenzene, *t*Bu = *tert*-butyl, cod = 1,5-cyclooctadiene.

Our interest in understanding the nature of the NHC-metal interaction, and in particular the existence and potential tunability of  $\pi$ -backbonding, stems from a different perspective. We have recently launched a program that utilizes the affinities of NHCs for transition metals to create unique classes of main chain organometallic polymers.<sup>23</sup> With applications in electronics and catalysis in mind, understanding role of  $\pi$ -backbonding is essential for enhancing conductivities, thermal stabilities, catalytic functions, and other physical properties of these materials. For example, we found that copolymerization of a bis(NHC) with various group 10 metals (i.e., Pd, Pt, Ni) resulted in polymeric materials that exhibited modest bathochromic shifts relative to small molecule models.<sup>24</sup> Gaining

insights into key factors that govern NHC-metal  $\pi$ -backbonding interactions, including developing parameters for fine tuning, should help guide future efforts for optimizing electronic characteristics and other physical properties of such organometallic polymers.

Many of the aforementioned experimental approaches for studying NHC-metal interactions involve coordinating a NHC to a transition metal complex followed by monitoring spectroscopic changes in ancillary ligands (e.g., recording changes in *trans* carbonyl stretching frequencies upon ligation). Individual  $\sigma$ - versus  $\pi$ -contributions in the NHC-metal interaction are then deconvoluted through comparison with other types of ligands. We recently introduced a new approach for studying NHC-metal interactions by examining spectroscopic changes that occur *at the NHC ligand* upon coordination of ancillary ligands with varying degrees of  $\pi$ -backbonding capabilities. In particular, various naphthoquinone-annulated NHC (NqMes) transition metal complexes (**7.5**) were synthesized and characterized.<sup>25</sup> The quinone group, which contains two equivalent carbonyl moieties formally conjugated to the carbene atom, provided a distinct spectroscopic handle for studying  $\pi$ -interactions using IR spectroscopy. Furthermore, the redox-active character of quinodal moieties provided an independent means to measure ligand electronics using cyclic voltammetry. Using these spectroscopic techniques, (NqMes)RhCl(cod) (cod = 1,5-cyclooctadiene) was found to exhibit lower quinone carbonyl stretching frequencies and higher reduction potentials than (NqMes)RhCl(CO)<sub>2</sub>. These results, supported by a comprehensive X-ray crystallographic analysis, suggested that the  $\pi$ -backbonding capability of NqMes lies in between an olefin and a carbon monoxide, two ligands with well-established  $\pi$ -backbonding capabilities.<sup>19</sup>

In this contribution, we supplement this approach by evaluating a series of NHC-metal complexes with differing degrees of  $\pi$ -backbonding capabilities using a variety of spectroscopic techniques. As illustrated in Figure 7.2, the basic design utilizes IR and

NMR active functional groups on both the NHC and other ancillary ligands complexed to a transition metal. Corroborating changes in  $\pi$ -acidity of one ligand with spectroscopic changes at the other should not only establish the existence of  $\pi$ -backbonding but also demonstrate that this interaction is tunable. In particular, the synthesis of 4,5-dicyano-imidazol-2-ylidene metal complexes which feature two nitrile groups formally conjugated to the carbene atom are described. Similar to the aforementioned quinone carbonyl groups in NqMes, these IR-sensitive groups were envisioned to function as probes for evaluating the  $\pi$ -electronics of its respective metal complexes. For example, observation of an increased nitrile IR stretching frequency upon replacement of an ancillary olefinic ligand (i.e., 1,5-cyclooctadiene) with carbon monoxide would suggest that  $\pi$ -backbonding is operative in this NHC architecture. If this could be established, then systematic replacement of the nitrile groups with functional groups of varying  $\pi$ -acidities should cause corresponding spectroscopic changes in the ancillary olefin and/or carbon monoxide ligands using NMR spectroscopy and IR spectroscopy, respectively. Additional evidence for the existence and tunability of  $\pi$ -backbonding interactions may be obtained through the observation of distinctive bond length changes using X-ray crystallography.

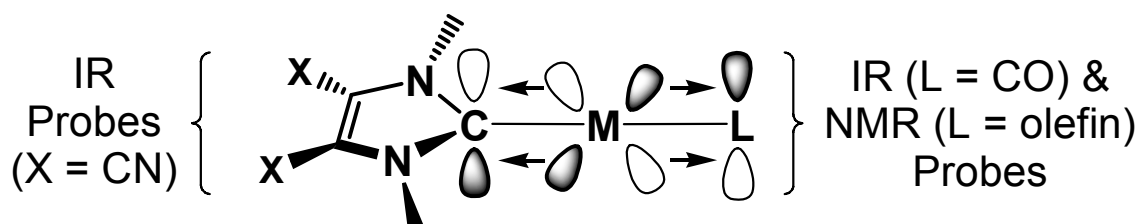


Figure 7.2 Basic design for evaluating  $\pi$ -backbonding in a range of NHC metal complexes using IR and NMR spectroscopies.

With the goals of evaluating and tuning  $\pi$ -backbonding characteristics of NHCs in mind, we targeted a series of transition metal complexes fulfilling two key requirements: 1.) The transition metals must be capable of coordinating to NHCs with a range of  $\pi$ -backbonding capabilities. As such, 1,3-dimethyl-imidazol-2-ylidene derivatives possessing nitro and cyano groups in 4- and/or 5-positions should show differing degrees of  $\pi$ -backbonding in their respective metal complexes and may be conveniently compared against its parent (4,5-dihydro) NHC. To deconvolute inductive  $\sigma$ -effects due to the installation of electronegative atoms, the plan also included synthesis and study of a 4,5-dichloro derivative. 2.) Ancillary ligands coordinated to the NHC-transition metal complex must be readily exchanged without perturbing other physical characteristics of that same complex (oxidation state, geometry, coordination number, etc.) Ligand exchange should also influence the  $\pi$ -system of the respective complexes, manifesting in distinct spectroscopic and/or structural changes. In particular, a system was required such that an ancillary ligand with modest  $\pi$ -backbonding capability (e.g., an olefin) could be readily substituted with a ligand that is highly capable (e.g., carbon monoxide). Building upon our experiences with using Rh complexes for the purposes of studying NHC  $\pi$ -backbonding, Rh complexes of the general type (NHC)RhCl(cod) were targeted as the cod ligand is known to rapidly exchange with two units of carbon monoxide, with essentially no other change in the metal environment.<sup>26,27</sup>

## RESULTS

The synthetic outline of various complexes meeting the aforementioned requirements is summarized in Figure 7.3. Independent treatment of commercially-available 1-methyl-4,5-disubstituted-imidazoles (**7.6**) with excess methyl iodide in CH<sub>3</sub>CN at 50 °C (sealed tube) resulted in the respective imidazolium salts **7.7** in yields

ranging from 70 – 97%.<sup>28</sup> Although organometallic complexes containing NHCs are commonly prepared through direct treatment of the desired neutral ligand, this approach can be problematic as it requires isolation of the free NHC or the use of strong bases to generate in the NHC in situ. To circumvent the need for free NHCs, Lin developed a practical and operationally-straightforward protocol that involves NHC-Ag complexes capable of transmetalation.<sup>29</sup> Following this procedure, Ag complexes **7.8** were prepared in 88 – 95% yields through treatment of the respective imidazolium salts with Ag<sub>2</sub>O. Subsequent transmetalation to [Rh(cod)Cl<sub>2</sub>]<sub>2</sub> afforded Rh complexes **7.9** in 74 – 99% yields. Finally, bubbling carbon monoxide through solutions of Rh(cod) complexes **7.9** produced the respective Rh carbonyl complexes **7.10** in excellent yields ( $\geq 99\%$ ).<sup>26,30</sup>

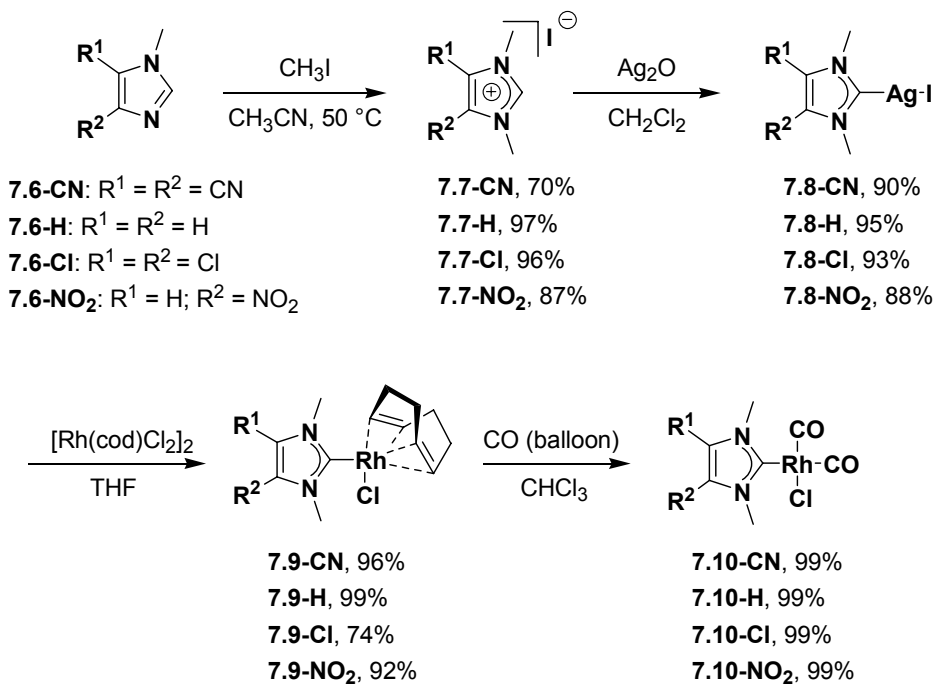


Figure 7.3 Synthesis of various metal complexes containing 4,5-disubstituted-imidazol-2-ylidenes.

Once compounds **7.7 – 7.10** were synthesized, they were studied using a variety of spectroscopic techniques. Initial attention was directed toward using solid-state (KBr) IR spectroscopy to examine the nitrile-substituted compounds **7.7-CN – 7.10-CN**; selected data is summarized in Table 1. As expected, imidazolium salt **7.7-CN** exhibited a relative high nitrile stretching frequency ( $\nu_{\text{CN}}$ ) of  $2250 \text{ cm}^{-1}$ .<sup>31</sup> Since the imidazolium proton has no  $\pi$ -backbonding capability, this compound served as a comparative model. Reflecting relative charge densities and M→C electron-donating abilities, complexes **7.8-CN**, **7.9-CN** and **7.10-CN** exhibited lower nitrile stretching frequencies to differing degrees. For example, the bis(NHC) cationic Ag complex (1,3-dimethyl-4,5-dicyano-imidazolylidene)<sub>2</sub>Ag•BF<sub>4</sub> (**7.11**)<sup>32</sup> exhibited a  $\nu_{\text{CN}} = 2247 \text{ cm}^{-1}$  whereas Ag complex **7.8-CN** registered a  $\nu_{\text{CN}} = 2239 \text{ cm}^{-1}$ .

Compound	$\nu_{\text{CN}} (\text{cm}^{-1})$
<b>7.7-CN</b>	2250
<b>7.11</b>	2247
<b>7.8-CN</b>	2239
<b>7.9-CN</b>	2238
<b>7.10-CN</b>	2242

Table 7.1 Selected IR stretching frequencies of CN groups in a variety of NHC-metal complexes. Carbonyl stretching frequencies were determined for compounds in the solid-state using IR spectroscopy (KBr). Reported values are  $\pm 0.5 \text{ cm}^{-1}$ . Compound 11 = (1,3-dimethyl-4,5-dicyano-imidazolylidene)<sub>2</sub>Ag•BF<sub>4</sub>.<sup>32</sup>

While study of the aforementioned azolium and Ag complexes highlighted the sensitivity of IR spectroscopy for studying  $\pi$ -electronics, Rh complexes **7.9-CN** and **7.10-CN** were studied to probe for the existence of  $\pi$ -backbonding in NHC – metal complexes. Since  $\pi$ -withdrawing effects from the cod and Cl ligands are relatively weak, complex **7.9-CN** was poised for NHC  $\pi$ -backbonding. In contrast, the two carbon monoxide ligands in complex **7.10-CN** should greatly diminish the ability of the Rh to  $\pi$ -backbond to the NHC. Dominant resonance contributors describing these two limiting cases are illustrated in Figure 7.4 and were supported by observed nitrile stretching frequencies of 2242 and 2238  $\text{cm}^{-1}$  for complexes **7.9-CN** and **7.10-CN**, respectively. Interestingly, the  $\nu_{\text{CN}}$  of Rh complex **7.9-CN** was comparable to Ag complex **7.8-CN**, which suggests that these two metal complexes may participate in  $\pi$ -backbonding with NHCs to similar degrees.

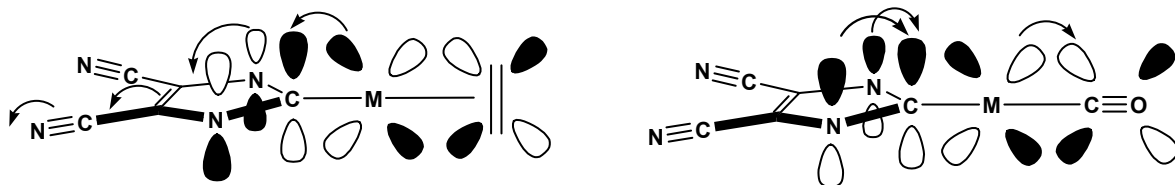


Figure 7.4 Dominant resonance contributors for complexes 9-CN (left) and 10-CN (right).

Subsequent attention was directed toward using other spectroscopic tools to evaluate relative  $\pi$ -backbonding abilities in a related series of NHC-transition metal complexes. Crabtree and Quirk demonstrated that NMR spectroscopy is a powerful technique for measuring electron densities in Ir-olefin complexes.<sup>33</sup> In relatively electron deficient systems, coordinated olefins act as conventional two-electron donors and maintain a significant degree of  $\text{C}=\text{C}$  double bond character. As electron density on the

metal increases, the olefin adopts metallocyclopropane character due to M→olefin  $\pi$ -backbonding. By monitoring chemical shifts of the protons on the olefin, relative contributions from these two extreme states can be measured using  $^1\text{H}$  NMR spectroscopy. We envisioned that evaluation of Rh complexes **7.9** and **7.10** using NMR spectroscopy should provide a relative scale for measuring  $\pi$ -backbonding in NHC – transition metal complexes.

The  $^1\text{H}$  NMR chemical shift of the olefin *trans* to the NHC ligand in complexes **7.9** were recorded and summarized in Table 7.2. Relative to **7.9-H**, downfield shifts were observed for each of the 4,5-disubstituted derivatives studied. In particular, electron deficient complex **7.9-Cl**, which contains two electronegative chlorine atoms in the 4- and 5-positions of the imidazol-2-ylidene, was found to exhibit a chemical shift nearly identical to **7.9-H** (5.03 versus 5.00 ppm, respectively). In contrast, relatively significant downfield shifts were observed for compounds **7.9-NO<sub>2</sub>** and **7.9-CN** (5.12 versus 5.17 ppm, respectively) which contain  $\pi$ -acidic nitro and cyano groups with group electronegativities similar to Cl.<sup>34</sup> In other words, the Rh centers in metal complexes **7.9-CN** and **7.9-NO<sub>2</sub>** were apparently more electron deficient than not only its parent complex **9-H**, but also dichloro derivative **7.9-Cl**.

To help deconvolute  $\pi$ -withdrawing from  $\sigma$ -inductive effects in **7.9**, Hammett  $\sigma_{\text{meta}}$  parameters were calculated from experimentally-derived acidity constants for 3-nitrobenzoic acid ( $\text{pK}_\text{a} = 3.46$ ), 3,5-dichlorobenzoic acid ( $\text{pK}_\text{a} = 3.54$ ), and benzoic acid ( $\text{pK}_\text{a} = 4.19$ ).<sup>35</sup> Specifically, the inductive effect of one NO<sub>2</sub> group ( $\sigma_{\text{meta}} = 0.73$ ) is approximately the same as two Cl groups (additive  $\sigma_{\text{meta}} = 0.65$ ). Consequently, if the relative metal electron deficiencies in the series of NHC complexes studied was due solely to diminished  $\sigma$ -donation, and not  $\pi$ -backbonding, one would expect the *trans* olefins in **7.9-Cl** and **7.9-NO<sub>2</sub>** to show similar  $^1\text{H}$  NMR chemical shifts. As shown in

Table 7.2, a significant difference was observed between these two complexes, whereas only a small difference was observed between **7.9-H** and **7.9-Cl**. Since these results could not be readily rationalized in terms of  $\sigma$ -induction, we propose the observed trend in spectroscopic data is due to the relative  $\pi$ -withdrawing effects of the NHC ligands.

Complex	$\delta(=CH)$ (ppm) <sup>a</sup>
<b>7.9-H</b>	5.00
<b>7.9-Cl</b>	5.03
<b>7.9-NO<sub>2</sub></b>	5.12
<b>7.9-CN</b>	5.17

Table 7.2  $^1\text{H}$  NMR chemical shifts of the protons on the olefin *trans* to the NHC ligand. Chemical shifts were determined using  $^1\text{H}$  NMR spectroscopy (solvent =  $\text{CDCl}_3$ ), reported downfield to tetramethylsilane, and referenced to residual protio solvent.

Having evaluated relative  $\pi$ -backbonding contributions in a series ( $\text{NHC}\text{Rh}(\text{cod})\text{Cl}$ ) complexes using  $^1\text{H}$  NMR spectroscopy, attention turned toward using IR spectroscopy to study analogous interactions in a related series of ( $\text{NHC}\text{Rh}(\text{CO})_2\text{Cl}$ ) complexes. As summarized in Table 7.3, *trans* carbonyl stretching frequencies ( $\nu_{\text{COS}}$ ) were recorded for complexes **7.10**. For each complex analyzed, two unique CO stretching frequencies were observed, corresponding to in-plane and out-of-plane stretching CO vibrational modes. In accord with the aforementioned NMR data,  $\nu_{\text{COS}}$  correlated with the  $\pi$ -acidities of the NHC ligands. For example, complexes **7.10-H** and **7.10-Cl**, which contained imidazol-2-ylidenes with hydro and chloro substituents in the 4,5-positions, respectively, exhibited almost identical  $\nu_{\text{COS}}$ . In contrast, complexes **7.10-CN** and **7.10-NO<sub>2</sub>**, which contained  $\pi$ -acidic cyano and nitro groups, respectively,

exhibited significantly higher values. Since it is well-known that the interaction between a transition metal and carbon monoxide involves a considerable degree of M $\rightarrow$ CO  $\pi$ -donation, the higher  $\nu_{\text{CO}}$  observed for Rh complexes containing  $\pi$ -acidic NHCs were suggestive of competitive  $\pi$ -backbonding interactions.

Complex	$\nu_{\text{CO}} (\text{cm}^{-1})^{\text{b}}$
<b>7.10-H</b>	2087, 2004
<b>7.10-Cl</b>	2091, 2010
<b>7.10-NO<sub>2</sub></b>	2094, 2012
<b>7.10-CN</b>	2099, 2017

Table 7.3 Selected carbonyl stretching frequencies for a series of (NHC)Rh(CO)<sub>2</sub>Cl complexes. Carbonyl stretching frequencies were determined using IR spectroscopy for compounds in solution (CDCl<sub>3</sub>). Values reported are  $\pm 0.5 \text{ cm}^{-1}$ . The two frequencies correspond to in-plane and out-of-plane vibrational modes.<sup>b</sup> The carbonyl stretching frequencies of the carbon monoxide ligand *trans* to the NHC ligand is reported.

To obtain additional support for  $\pi$ -backbonding in NHC-transition metal complexes, attention was directed toward studying the solid-state structures of Rh complexes **7.9**. In general, three distinct structural changes were expected as the relative  $\pi$ -backbonding ability of the NHC ligand increased: 1.) the average C<sub>carbene</sub>-N bond length should elongate due to population of the carbene p-orbital with electrons, 2.) the Rh-C<sub>carbene</sub> bond length should contract due to a stronger interaction being formed between these two atoms, and 3.) the length of the bond formed between the Rh atom and the olefin *trans* to the NHC ligand should elongate due to decreased electron density at the Rh center. All other bond lengths and angles in the respective metal complexes should remain relatively constant. For clarity, expected changes are summarized in Figure 7.5A.

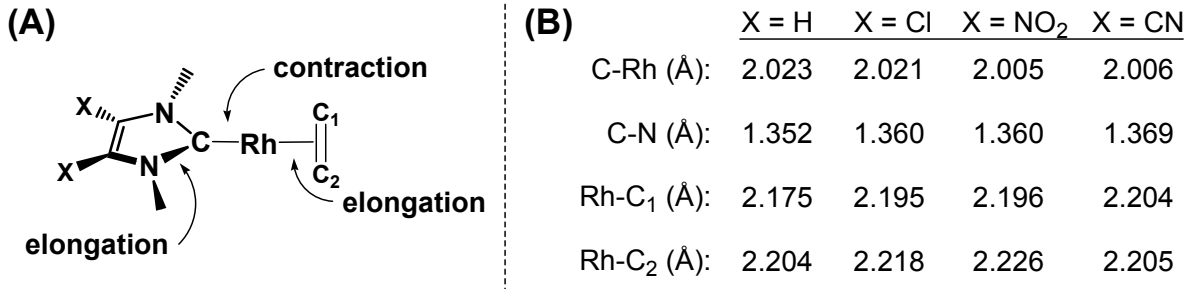


Figure 7.5 (a) Expected changes in key bond lengths as the  $\pi$ -backbonding ability of the NHC ligand increases. (b) Summary of key bond lengths observed for a series of (NHC)Rh(cod)Cl complexes with NHC ligands of varying degrees of  $\pi$ -acidity; the data reported was taken from Table 5. Note: average C-N bond lengths are reported.

Quality crystals of **7.9-Cl**, **7.9-CN**, and **7.9-NO<sub>2</sub>** suitable for X-ray diffraction analysis were independently obtained. Selected crystallographic data as well as bond lengths and angles are summarized in Tables 7.4 and 7.5, respectively. For comparison, key data for known<sup>30</sup> **7.9-H** has been included. As shown in Figure 6, the ORTEP diagrams for each of these complexes are remarkably similar. In general, increased  $\pi$ -acidities of the NHC ligand resulted in elongated C<sub>carbene</sub>-N and Rh-olefin bond lengths with concomitant contractions in the Rh-C<sub>carbene</sub> bond length (summarized in Figure 5B). Other bond lengths and angles remained relatively constant within this same series. Furthermore, complexes **7.9-H** and **7.9-Cl** exhibited comparable C<sub>carbene</sub>-Rh bond lengths (2.023(2) and 2.021(2) Å, respectively), whereas analogous bond lengths in complexes **7.9-NO<sub>2</sub>** and **7.9-CN** were relatively short (2.005(3) and 2.006(6) Å, respectively). Combined with the IR and NMR spectroscopic data described above, these results suggested that NHCs are not only capable of  $\pi$ -backbonding but the extent of this interaction is dependent on its  $\pi$ -acidity.

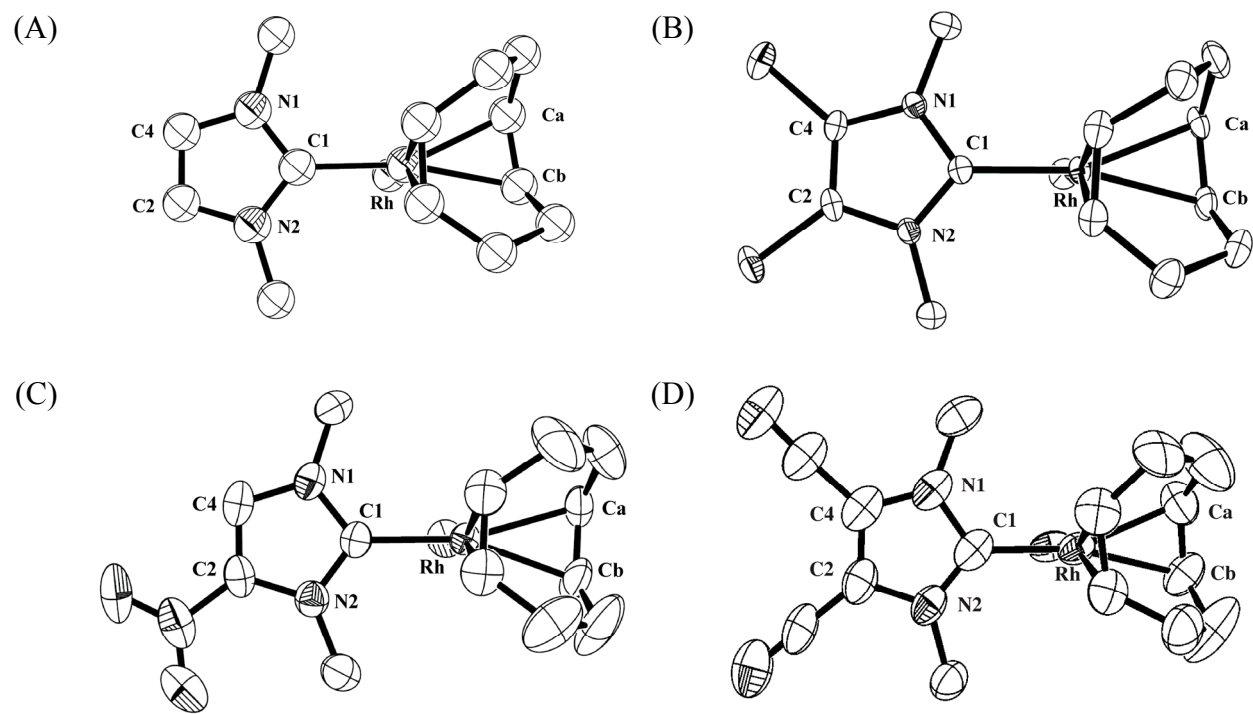


Figure 7.6 ORTEP diagrams of (A) 7.9-H, (B) 7.9-Cl, (C) 7.9-NO<sub>2</sub> and (D) 7.9-CN. Ellipsoids were drawn at the 50% probability level. Hydrogen atoms have been omitted for clarity. Data for 7.9-H was reproduced from ref. 30.

	<b>7.9-H<sup>a</sup></b>	<b>7.9-Cl</b>	<b>7.9-NO<sub>2</sub></b>	<b>7.9-CN</b>
CCDC No.	109494	650155	650157	650156
empirical formula	C <sub>13</sub> H <sub>2</sub> ClN <sub>2</sub> Rh	C <sub>13</sub> H <sub>18</sub> Cl <sub>3</sub> N <sub>2</sub> Rh	C <sub>13</sub> H <sub>19</sub> ClN <sub>3</sub> O <sub>2</sub> Rh	C <sub>15</sub> H <sub>18</sub> ClN <sub>4</sub> Rh
formula weight	342.67	411.55	387.67	392.69
cryst syst	Monoclinic	Monoclinic	Monoclinic	Monoclinic
space group	P 21/n	C2/c	P21/c	P21/n
<i>a</i> , Å	10.162(2)	18.6430(3)	14.3364(9)	14.4910(8)
<i>b</i> , Å	11.137(1)	12.0050(2)	8.0561(5)	11.0430(5)
<i>c</i> , Å	13.223(2)	14.9100(2)	14.0038(10)	20.0880(10)
<i>α</i> , deg	90°	90°	90°	90°
<i>β</i> , deg	112.400(10) °	113.8410(9)°	109.016(2)°	96.598(3)°
<i>γ</i> , deg	90°	90°	90°	90°
<i>V</i> , Å <sup>3</sup>	1383.6(4)	3052.25(8)	1529.12(17)	3193.3(3)
<i>T</i> , K	223(3)	153(2)	233(2)	153(2)
<i>Z</i>	4	8	4	8
<i>D</i> <sub>calc</sub> , Mg/m <sup>3</sup>	1.6450(5)	1.791	1.684	1.634
cryst size (mm)	0.23 x 0.209 x 0.356	0.19 x 0.18 x 0.11	0.25 x 0.09 x 0.07	0.37 x 0.26 x 0.14
reflections collected	4131	20443	5470	11522
independent reflections	2583	3464	3448	7227
<i>R</i> <sub>1</sub> , w <i>R</i> <sub>2</sub> { <i>I</i> > 2σ( <i>I</i> )}	0.021, 0.017	0.0249, 0.0552	0.0340, 0.0773	0.0536, 0.1157
goodness of fit	NA	1.090	1.014	1.028

Table 7.4 Selected crystal data for Rh complexes **7.9**. Data for **7.9-H** was reproduced from ref. 30. NA = Information not available.

Bond	<b>7.9-H</b> <sup>b</sup>	<b>7.9-Cl</b>	<b>7.9-NO<sub>2</sub></b>	<b>7.9-CN</b>
C1-Rh	2.023(2)	2.021(2)	2.005(3)	2.006(6)
Rh-Ca	2.175(3)	2.195(2)	2.196(4)	2.205(6)
Rh-Cb	2.204(3)	2.218(2)	2.226(3)	2.204(6)
N2-C1	1.349(2)	1.363(3)	1.366(4)	1.366(9)
N1-C1	1.356(3)	1.358(3)	1.354(4)	1.372(7)
N1-C4	1.385(4)	1.383(3)	1.367(5)	1.371(7)
N2-C2	1.387(3)	1.384(3)	1.387(5)	1.391(7)
C2-C4	1.333(4)	1.340(3)	1.334(5)	1.344(8)
N1-C1-N2	104.06(16)	104.55(18)	105.1(3)	104.4(7)

Table 7.5 Selected bond lengths ( $\text{\AA}$ ) and angles ( $^\circ$ ) for Rh complexes **7.9**. ORTEP diagrams are shown in Figure 6. <sup>b</sup> Data for **7.9-H** was reproduced from ref. 30.

## CONCLUSION

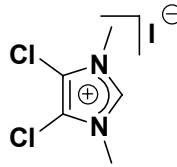
A range of new Rh and Ag complexes containing 1,3-dimethyl-imidazol-2-ylidene with varying degrees of  $\pi$ -acidity were synthesized and then studied using NMR spectroscopy, IR spectroscopy, and X-ray crystallography. A new NHC ligand featuring

two nitrile groups formally conjugated to the carbene atom, 1,3-dimethyl-4,5-dicyano-imidazol-2-ylidene, was found to be useful for studying  $\pi$ -backbonding using FT-IR spectroscopy. In particular, the  $\nu_{\text{CN}}$  of (1,3-dimethyl-4,5-dicyano-imidazol-2-ylidene)Rh(cod)Cl was found to be  $4 \pm 0.5 \text{ cm}^{-1}$  higher than its respective Rh(CO)<sub>2</sub>Cl complex, suggesting that this NHC was a stronger  $\pi$ -acid than an olefin but weaker than carbon monoxide. Using the 4,5-dicyano derivative as a reference, NMR and IR spectroscopies were employed to study a range of Ag and Rh containing various imidazol-2-ylidenes. In general, chemical shifts of the coordinated olefin and the stretching frequencies of the carbonyl group *trans* to the NHC ligand correlated with the  $\pi$ -acidity of the NHC. Furthermore,  $\sigma$ -inductive effects were found to be relatively minimal, as determined by comparison to complexes containing 4,5-dichloro-imidazol-2-ylidenes. Finally, structural analysis of a series (NHC)Rh(cod)Cl complexes possessing NHCs with varying degrees of  $\pi$ -acidities supported the NMR and IR spectroscopic data. In particular, the average N-C<sub>carbene</sub> and Rh-(olefin) bond lengths elongated while the Rh-C<sub>carbene</sub> bond length contracted as the  $\pi$ -acidity of the NHC ligand increased. Collectively, these results suggest that  $\pi$ -backbonding in NHC-metal complexes is not only non-negligible, but tunable. This information should help guide efforts toward fine tuning transition metal-based catalysts for facilitating synthetically-useful transformations and/or optimizing the electronic properties of organometallic polymers containing NHCs.

## EXPERIMENTAL

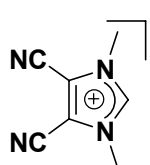
**Materials and Methods:** All reactions were performed under an atmosphere of nitrogen using standard Schlenk techniques or in a nitrogen filled glove-box. Dichloromethane was distilled from calcium hydride and degassed by two freeze-pump-thaw cycles.

Tetrahydrofuran and toluene were distilled from Na/benzophenone and degassed by two freeze-pump-thaw cycles. [(cod)RhCl]2 and 1,3-bis(2,6-diisopropylphenyl)imidazolium chloride were purchased from Strem Chemicals and used without further purification. 1,3-Dimethyl-imidazolium iodide (1-H) was prepared according to literature procedures.<sup>36</sup> All other reagents were purchased from Aldrich or Acros and were used without further purification. <sup>1</sup>H NMR spectra were recorded using a Varian Gemini (300 MHz or 400 MHz) spectrometer. Chemical shifts are reported in delta ( $\delta$ ) units, expressed in parts per million (ppm) downfield from tetramethylsilane using residual protio solvent as an internal standard (CDCl<sub>3</sub>, 7.24 ppm; C<sub>6</sub>D<sub>6</sub>, 7.15 ppm; CD<sub>2</sub>Cl<sub>2</sub>, 5.32 ppm; DMSO-*d*6, 2.49 ppm). <sup>13</sup>C NMR spectra were recorded using a Varian Gemini (100 MHz) spectrometer. Chemical shifts are reported in delta ( $\delta$ ) units, expressed in parts per million (ppm) downfield from tetramethylsilane using the solvent as an internal standard (CDCl<sub>3</sub>, 77.0 ppm; C<sub>6</sub>D<sub>6</sub>, 128.0 ppm; CD<sub>2</sub>Cl<sub>2</sub>, 53.8 ppm, DMSO-*d*6, 39.5 ppm). <sup>13</sup>C NMR spectra were routinely run with broadband decoupling. Coupling constants are expressed in hertz (Hz). IR spectra were record using Perkin-Elmer Spectrum BX FT-IR system. High-resolution mass spectra (HRMS) were obtained with a VG analytical ZAB2-E or a Karatos MS9 instrument and are reported as m/z (relative intensity). X-ray crystal structure data for compounds 9-Cl (CCDC 650155), 9-NO<sub>2</sub> (CCDC 650157), and 9-CN (CCDC 650156) were deposited with the Cambridge Crystallographic Data Centre, 12 Union Road, Cambridge CB2 1EZ, UK.



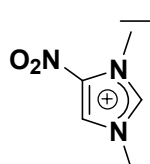
**1,3-Dimethyl-4,5-dichloro-imidazolium iodide (7.7-Cl).** A 30 mL pressure vessel was charged with 4,5-dichloro-1-methyl-imidazole (7.5 g,

49.7 mmol), CH<sub>3</sub>I (5.0 mL, 80.2 mmol), CH<sub>3</sub>CN (60 mL), and a stir bar. After sealing the vessel, the reaction mixture was stirred at 60 °C for 12 h. Subsequent cooling to 0 °C caused solids to precipitate which were collected by filtration and washed with Et<sub>2</sub>O (30 mL). Removal of residual solvent under reduced pressure afforded the desired product (14.0 g, 96% yield) as a white crystalline solid. <sup>1</sup>H NMR (DMSO-*d*<sub>6</sub>): δ 9.39 (s, 1H), 3.82 (s, 6H). <sup>13</sup>C NMR (DMSO-*d*<sub>6</sub>): δ 136.6, 118.9, 34.9. HRMS: [M]<sup>+</sup> calcd for C<sub>5</sub>H<sub>7</sub>Cl<sub>2</sub>N<sub>2</sub>: 164.9981; found, 164.9981.



**1,3-Dimethyl-4,5-dicyano-imidazolium iodide (7.7-CN).** A 30 mL pressure vessel was charged with 4,5-dicyano-1-methyl-imidazole (1.0 g, 7.57 mmol), CH<sub>3</sub>I (2 mL, 32.1 mmol), CH<sub>3</sub>CN (15 mL), and a stir bar.

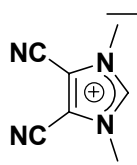
After sealing the vessel, the reaction mixture was stirred at 80 °C for 24 h. The mixture was then cooled to ambient temperature and poured into Et<sub>2</sub>O (50 mL). The precipitated solids were collected by filtration and dried under reduced pressure to afford the desired product as yellow crystals (1.45 g, 70% yield). IR (KBr): 2250 cm<sup>-1</sup>. <sup>1</sup>H NMR (DMSO-*d*<sub>6</sub>): δ 9.76 (s, 1H), 4.05 (s, 6H). <sup>13</sup>C NMR (DMSO-*d*<sub>6</sub>): δ 142.5, 115.6, 106.1, 37.2. HRMS: [M]<sup>+</sup> calcd for C<sub>7</sub>H<sub>7</sub>N<sub>4</sub>: 147.0665; found, 147.0672.



**1,3-Dimethyl-4-nitro-imidazolium iodide (7.7-NO<sub>2</sub>).** A 30 mL pressure vessel was charged with 1-methyl-4-nitro-imidazole (3.6 g, 28.3 mmol), CH<sub>3</sub>I (5.0 mL, 80.2 mmol), CH<sub>3</sub>CN (25 mL), and a stir bar.

After sealing the vessel, the reaction mixture was stirred at 50 °C for 12 h. Subsequent cooling to 0 °C caused solids to precipitate which were collected by filtration and washed with Et<sub>2</sub>O (30 mL). Removal of residual solvent under reduced pressure afforded the

desired product as an orange crystalline solid (6.61 g, 87% yield). Spectroscopic data were in accord with literature values.<sup>37</sup>



**1,3-Dimethyl-4,5-dicyano-imidazolium tetrafluoroborate.** A vial was charged with Me<sub>3</sub>O·BF<sub>4</sub> (0.62 g, 4.2 mmol), CH<sub>3</sub>CN (4 mL), and 4,5-dicyano-1-methyl-imidazole (0.50 g, 3.79 mmol), and a stir bar.<sup>38</sup> After stirring for 1 h at ambient temperature, solid white flakes precipitated from the reaction mixture. The solids were then collected by filtration and dried under reduced pressure to afford the desired product as white crystals (0.89 g, 70% yield). IR (KBr): 2264 cm<sup>-1</sup>. <sup>1</sup>H NMR (DMSO-*d*<sub>6</sub>): δ 9.66 (s, 1H), 4.05 (s, 6H). <sup>13</sup>C NMR (DMSO-*d*<sub>6</sub>): δ 142.6, 115.6, 106.1, 37.0. HRMS: [M]<sup>+</sup> calcd for C<sub>7</sub>H<sub>7</sub>N<sub>4</sub>: 147.0665; found, 147.0672.

**Ag Complex 7.8-H.** A 30 mL pressure vessel was charged with 1,3-dimethyl-imidazolium iodide (**1-H**)<sup>36</sup> (2.14 g, 9.8 mmol), Ag<sub>2</sub>O (1.13 g, 4.9 mmol), CH<sub>2</sub>Cl<sub>2</sub> (10 mL), and a stir bar. After sealing the vessel, the reaction mixture was stirred at 50 °C for 10 h. Subsequent cooling to ambient temperature caused solids to precipitate which were collected by filtration. Removal of residual solvent under reduced pressure afforded the desired product as a gray powder (3.0 g, 95% yield). Spectroscopic data were in accord with literature values.<sup>39</sup>

**Ag Complex 7.8-Cl.** A 30 mL pressure vessel was charged with 1,3-dimethyl-4,5-dichloro-imidazolium iodide (**7.7-Cl**) (1.05 g, 3.57 mmol), Ag<sub>2</sub>O (0.41 g, 1.78 mmol), CH<sub>2</sub>Cl<sub>2</sub> (15 mL), and a stir bar. After sealing the vessel, the reaction mixture was stirred at 50 °C for 2 h. Subsequent cooling to ambient temperature caused solids to precipitate which were collected by filtration. Removal of residual solvent under reduced pressure

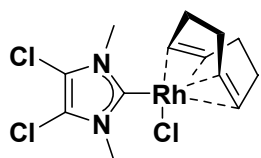
afforded the desired product as a gray powder (1.33 g, 93% yield). HRMS:  $[M]^+$  calcd for  $C_5H_6Cl_2N_2AgI$ : 397.8004; found, 397.8000. This complex exhibited extremely poor solubilities in common organic solvents and therefore was used directly without further purification or characterization.

**Ag Complex 7.8-CN.** A 30 mL pressure vessel was charged with 1,3-dimethyl-4,5-dicyano-imidazolium iodide (**7.7-CN**) (0.19 g, 0.68 mmol),  $Ag_2O$  (78 mg, 0.34 mmol),  $CH_2Cl_2$  (5 mL), and a stir bar. After sealing the vessel, the reaction mixture was stirred at 50 °C for 4 h. Subsequent cooling to ambient temperature caused solids to precipitate which were collected by filtration. Removal of residual solvent under reduced pressure afforded the desired product as a gray powder (0.24 g, 90% yield). IR (KBr): 2239, 1449, 1384, 885, 490  $cm^{-1}$ .  $^1H$  NMR ( $DMSO-d_6$ ):  $\delta$  4.04.  $^{13}C$  NMR ( $DMSO-d_6$ ):  $\delta$  192.7, 115.5, 107.7, 39.0.

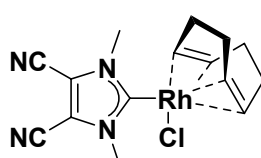
**Ag Complex 7.8-NO<sub>2</sub>.** A 30 mL pressure vessel was charged with 1,3-dimethyl-4-nitro-imidazolium iodide (**7.7-NO<sub>2</sub>**) (0.67 g, 2.47 mmol),  $Ag_2O$  (0.29 g, 1.24 mmol),  $CH_2Cl_2$  (7 mL), and a stir bar. After sealing the vessel, the reaction mixture was stirred at 50 °C for 3 h. Subsequent cooling to ambient temperature caused solids to precipitate which were collected by filtration. Removal of residual solvent under reduced pressure afforded the desired product as a green-yellow powder (0.82 g, 87% yield).  $^1H$  NMR ( $DMSO-d_6$ ):  $\delta$  8.79 (s, 1H), 4.12 (s, 3H), 3.91 (s, 3H).  $^{13}C$  NMR ( $DMSO-d_6$ ):  $\delta$  188.2, 139.1, 126.8, 39.4.

**Ag Complex 7.11.** A 30 mL pressure vessel was charged with 1,3-dimethyl-4,5-dicyano-imidazolium tetrafluoroborate (0.12 g, 0.5 mmol),  $Ag_2O$  (60 mg, 0.25 mmol),  $CH_3CN$  (5

mL), and a stir bar. The vessel was then sealed and the reaction mixture was stirred at 80 °C for 16 h. After cooling to ambient temperature, the reaction mixture was filtered through 0.2 µm PTFE filter. Residual solvent was then removed under reduced pressure to afford the desired product as a white foam (0.24 g, 98% yield). Note: the product is extremely hydrophilic and rapidly turns into an oil upon exposure to air. IR (KBr): 2247, 1457, 1260, 890 cm<sup>-1</sup>. <sup>1</sup>H NMR (DMSO-d<sub>6</sub>): δ 3.97. <sup>13</sup>C NMR (DMSO-d<sub>6</sub>): δ 190.3, 115.6, 107.7, 38.7. HRMS: [M]<sup>+</sup> calcd for C<sub>14</sub>H<sub>12</sub>AgN<sub>8</sub>: 399.0230; found, 399.02304.

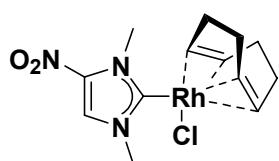


**Rh Complex 7.9-Cl.** A 20 mL flask was charged with Ag complex **7.8-Cl** (0.29 g, 0.72 mmol), [Rh(cod)Cl]<sub>2</sub> (0.16 g, 0.33 mmol), THF (10 mL), and a stir bar. The resulting reaction mixture was then stirred at 60 °C for 3 h. Afterward, the reaction mixture was cooled to ambient temperature and then filtered through 0.2 µm PTFE filter. Removal of residual solvent under reduced pressure afforded desired product as yellow solid (0.2 g, 74% yield). <sup>1</sup>H NMR (CDCl<sub>3</sub>): δ 5.03 (br, 2H), 4.04 (s, 6H), 3.26 (br, 2H), 2.40-2.37 (br, 4H), 1.97-1.93 (br, 4H). <sup>13</sup>C NMR (CDCl<sub>3</sub>): δ 188.2 (d, *J*<sub>Rh-C</sub> = 52.3 Hz), 116.3 (d, *J*<sub>Rh-C</sub> = 1.4 Hz), 99.5 (d, *J*<sub>Rh-C</sub> = 6.7 Hz), 68.4 (d, *J*<sub>Rh-C</sub> = 15.0 Hz), 36.4, 32.8, 28.8. HRMS: [M]<sup>+</sup> calcd for C<sub>13</sub>H<sub>18</sub>Cl<sub>3</sub>N<sub>2</sub>Rh: 409.9591; found, 409.9596.



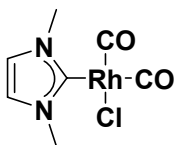
**Rh Complex 7.9-CN.** A 20 mL flask was charged with Ag complex **7.8-CN** (0.1 g, 0.26 mmol), [Rh(cod)Cl]<sub>2</sub> (60 mg, 0.12 mol), THF (5 mL), and a stir bar. The resulting reaction mixture was stirred at 50 °C for 6 h and then filtered hot through a 0.2 µm PTFE filter. Removal of residual solvent under reduced pressure afforded desired product as an orange powder (98 mg, 95% yield). IR (KBr): 2238 cm<sup>-1</sup>. <sup>1</sup>H NMR

(CDCl<sub>3</sub>): δ 5.17 (br, 2H), 4.26 (s, 6H), 3.29 (br, 2H), 2.42-2.40 (br, 4H), 2.03-2.01 (br, 4H). <sup>13</sup>C NMR (CDCl<sub>3</sub>): δ 196.6 (d, *J*<sub>Rh-C</sub> = 53.0 Hz), 115.4, 106.8, 102.4 (d, *J*<sub>Rh-C</sub> = 6.7 Hz), 68.5 (d, *J*<sub>Rh-C</sub> = 14.2 Hz), 38.3, 33.0, 29.0. HRMS: [M]<sup>+</sup> calcd for C<sub>15</sub>H<sub>18</sub>ClN<sub>4</sub>Rh: 392.0275; found, 392.0272.

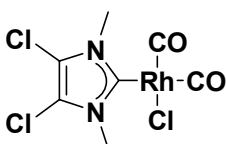


**Rh Complex 7.9-NO<sub>2</sub>.** A 20 mL flask was charged with Ag complex 7.8-NO<sub>2</sub> (0.3 g, 0.8 mmol), [Rh(cod)Cl]<sub>2</sub> (0.16 g, 0.33 mmol), THF (5 mL), and a stir bar. The resulting reaction mixture was then stirred at 60 °C for 1 h. Afterward, the reaction mixture was cooled to ambient temperature and then filtered through a 0.2 μm PTFE filter. Removal of residual solvent under reduced pressure afforded desired product as a yellow solid (0.29 g, 92% yield). <sup>1</sup>H NMR (CDCl<sub>3</sub>): δ 7.82 (s, 1H), 5.12 (br, 2H), 4.48 (s, 3H), 4.19 (s, 3H), 3.33 (br, 2H), 2.45-2.39 (br, 4H), 2.01-1.98 (br, 4H). <sup>13</sup>C NMR (CDCl<sub>3</sub>): δ 192.8 (d, *J*<sub>Rh-C</sub> = 53.0 Hz), 125.1, 101.28 (d, *J*<sub>Rh-C</sub> = 6.6 Hz), 101.25 (d, *J*<sub>Rh-C</sub> = 6.8 Hz), 69.2 (d, *J*<sub>Rh-C</sub> = 14.2 Hz), 69.0 (d, *J*<sub>Rh-C</sub> = 14.2 Hz), 39.6, 39.0, 33.1, 33.0, 29.05, 28.98. HRMS: [M]<sup>+</sup> calcd for C<sub>13</sub>H<sub>19</sub>ClN<sub>3</sub>O<sub>2</sub>Rh: 387.0221; found, 387.0224.

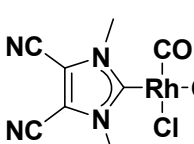
**General Procedures for the Synthesis of Rh Carbonyl Complexes 7.10.** Rh complex 7.9 was dissolved in CDCl<sub>3</sub> (approx. conc. = 0.07 M) and then placed under an atmosphere of carbon monoxide (balloon). Ligand exchange was monitored using <sup>1</sup>H NMR spectroscopy and accompanied with a gradual loss in color. In general, reactions were complete in less than 10 min. Concentration of the reaction solutions resulted in decomposition of the desired product.<sup>25</sup>



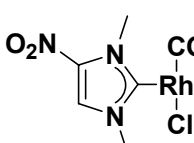
**Rh Complex 7.10-H.** IR ( $\text{CDCl}_3$ ): 2087, 2004  $\text{cm}^{-1}$ . NMR data were in accord with literature values.<sup>30</sup>



**Rh Complex 7.10-Cl.** IR ( $\text{CDCl}_3$ ): 2091, 2010  $\text{cm}^{-1}$ .  $^1\text{H}$  NMR ( $\text{CDCl}_3$ ):  $\delta$  3.89 (s, 6H).  $^{13}\text{C}$  NMR ( $\text{CDCl}_3$ ): 184.7 (d,  $J_{\text{Rh-C}} = 54.6$  Hz), 182.2, 174.7 (d,  $J_{\text{Rh-C}} = 44.6$  Hz), 117.9, 37.1.



**Rh Complex 7.10-CN.** IR (KBr): 2242, 2085, 2007  $\text{cm}^{-1}$ . IR ( $\text{CDCl}_3$ ): 2252, 2099, 2017  $\text{cm}^{-1}$ .  $^1\text{H}$  NMR ( $\text{CDCl}_3$ ):  $\delta$  4.13 (s, 6H).  $^{13}\text{C}$  NMR ( $\text{CDCl}_3$ ):  $\delta$  186.9 (d,  $J_{\text{Rh-C}} = 45.2$  Hz), 183.8 (d,  $J_{\text{Rh-C}} = 55.8$  Hz), 181.2 (d,  $J_{\text{Rh-C}} = 72.0$  Hz), 115.8, 105.9, 38.9. HRMS:  $[\text{M}]^+$  calcd for  $\text{C}_9\text{H}_6\text{ClN}_4\text{O}_2\text{Rh}$ : 339.9234; found, 339.9229.



**Rh Complex 7.10-NO<sub>2</sub>.** IR ( $\text{CDCl}_3$ ): 2094, 2012  $\text{cm}^{-1}$ .  $^1\text{H}$  NMR ( $\text{CDCl}_3$ ):  $\delta$  7.96 (s, 1H), 4.31 (s, 3H), 4.03 (s, 3H).  $^{13}\text{C}$  NMR ( $\text{CDCl}_3$ ):  $\delta$  184.4 (d,  $J_{\text{Rh-C}} = 54.6$  Hz), 182.8 (d,  $J_{\text{Rh-C}} = 45.6$  Hz), 181.6 (d,  $J_{\text{Rh-C}} = 73.0$  Hz), 139.6, 125.1, 40.1, 39.4. HRMS:  $[\text{M}]^+$  calcd for  $\text{C}_7\text{H}_7\text{ClN}_3\text{O}_4\text{Rh}$ : 334.9180; found, 394.9181.

## REFERENCES

- † Portions of this chapter have been previously reported, see: Khramov, D. M.; Lynch, V. M.; Bielawski, C. W. *Organometallics*. **2006**, *26*, 6042.
- 1 Wanzlick, H. W.; Schönherr, H. J. *Angew. Chem. Int. Ed.* **1968**, *7*, 141.
- 2 Öfele, K. *J. Organomet. Chem.* **1968**, *12*, P42.

- 3 Cardin, D. J.; Çetinkaya, B.; Çetinkaya, E.; Lappert, M. F. *J. Chem. Soc., Dalton Trans.* **1973**, 514.
- 4 For recent reviews of catalytically-active transition metal complexes containing N-heterocyclic carbenes, see: (a) Peris, E.; Crabtree, R. H. *Coord. Chem. Rev.* **2004**, 248, 2239. (b) Cavell, K. J.; McGuiness, D. S. *Coord. Chem. Rev.* **2004**, 248, 671. (c) Herrmann, W. A. *Angew. Chem., Int. Ed.* **2002**, 41, 1290. (d) Hillier, A. C.; Gasa, G. A.; Viciu, M. S.; Lee, H. M.; Yang, C. L.; Nolan, S. P. *J. Organomet. Chem.* **2002**, 653, 69.
- 5 For representative examples, see: (a) Marion, N.; Navarro, O.; Mei, J.; Stevens, E. D.; Scott, N. M.; Nolan, S. P. *J. Am. Chem. Soc.* **2006**, 128, 4101. (b) Navarro, O.; Marion, N.; Oonishi, Y.; Kelly, R. A., III; Nolan, S. P. *J. Org. Chem.* **2006**, 71, 685. (c) Louie, J.; Gibby, J. E.; Farnworth, M. V.; Tekavec, T. N. *J. Am. Chem. Soc.* **2002**, 124, 15188. (d) Jørgensen, M.; Lee, S.; Liu, X.; Wolkowski, J. P.; Hartwig, J. F. *J. Am. Chem. Soc.* **2002**, 124, 12557. (e) Trnka, T. M.; Grubbs, R. H. *Acc. Chem. Res.* **2001**, 34, 18. (f) Herrmann, W. A.; Elison, M.; Fischer, J.; Köcher, C.; Artus, G. R. *J. Angew. Chem., Int. Ed. Engl.* **1995**, 34, 2371.
- 6 For representative examples, see: (a) Hahn, F. E.; Jahnke, M. C.; Pape, T. *Organometallics* **2007**, 26, 150. (b) Arnold, P. L.; Liddle, S. T. *Chem. Commun.* **2006**, 3959. (c) Kuhn, N.; Al-Sheikh, A. *Coord. Chem. Rev.* **2005**, 249, 829. (d) Garrison, J. C.; Youngs, W. J. *Chem. Rev.* **2005**, 105, 3978. (e) Lappert, Michael F. *J. Organomet. Chem.* **2005**, 690, 5467. (f) Oldham, W. J.; Oldham, S. M.; Scott, B. L.; Abney, K. D.; Smith, W. H.; Costa, D. A. *Chem. Commun.* **2001**, 1348. (g) Abernethy, C. D.; Clyburne, J. A. C.; Cowley, A. H.; Jones, R. A. *J. Am. Chem. Soc.* **1999**, 121, 2329. (h) Herrmann, W. A.; Köcher, C.; Gooßen, L. J.; Artus, G. R. *J. Chem. Eur. J.* **1996**, 2, 1627. (i) Enders D.; Breuer, K.; Raabe, G.; Rulsink, J.; Teles, J. H.; Melder, J. P.; Ebel, K. Brode, S. *Angew. Chem., Int. Ed. Engl.* **1995**, 34, 1021. (j) Arduengo, A. J., III; Dias, H. V. R.; Calabrese, J. C.; Davidson, F. *Organometallics* **1993**, 12, 3405. (k) Regitz, M. *Angew. Chem., Int. Ed. Engl.* **1996**, 35, 725.
- 7 (a) Herrmann, W. A.; Kocher, C. *Angew. Chem., Int. Ed.* **1997**, 36, 2163. (b) Frölich, N.; Pidun, U.; Stahl, M.; Frenking, G. *Organometallics* **1997**, 16, 442. (c) Herrmann, W. A.; Runte, O.; Artus, G. *J. Organomet. Chem.* **1995**, 501, C1. (d) Herrmann, W. A.; Öfele, K.; Elison, M.; Kühn, F. E.; Roesky, P. W. *J. Organomet. Chem.* **1994**, 480, C7.
- 8 (a) Perrin, L.; Clot, E.; Eisenstein, O.; Loch, J.; Crabtree, R. H. *Inorg. Chem.* **2001**, 40, 5806. (b) Chianese, A. R.; Li, X.; Janzen, M. C.; Faller, J. W.; Crabtree, R. H. *Organometallics* **2003**, 22, 1663. (c) Denk, K.; Sirsch, P.; Herrmann, W. A. *J. Organomet. Chem.* **2002**, 649, 219. (d) Köcher, C.; Herrmann, W.

- A. *J. Organomet. Chem.* **1997**, *532*, 261. (e) Öfele, K.; Herrmann, W. A.; Mihalios, D.; Elison, M.; Herdtweck, E.; Priermeier, T.; Kiprof, P. *J. Organomet. Chem.* **1995**, *498*, 1. (f) Öfele, K.; Herrmann, W. A.; Mihalios, D.; Elison, M.; Herdtweck, E.; Scherer, W.; Mink, J. *J. Organomet. Chem.* **1993**, *459*, 177.
- 9 For related studies which compare NHC-metal bond dissociation energies to phosphine analogues, see: (a) Dorta, R.; Stevens, D.; Scott, N. M.; Costabile, C.; Cavallo, L.; Hoff, C. D.; Nolan, S. P. *J. Am. Chem. Soc.* **2005**, *127*, 2485. (b) Hillier, A. C.; Sommer, W. J.; Yong, B. S.; Petersen, J. L.; Cavallo, L.; Nolan, S. P. *Organometallics* **2003**, *22*, 4322. (c) Huang, J.; Jafarpour, L.; Hillier, A. C.; Stevens, E. D.; Nolan, S. P. *Organometallics* **2001**, *20*, 2878. (d) Huang, J.; Schanz, H.-J.; Stevens, E. D.; Nolan, S. P. *Organometallics* **1999**, *18*, 2370.
- 10 (a) Green, J. C.; Herbert, B. J. *Dalton Trans.* **2005**, *7*, 1214. (b) Green, J. C.; Scurr, R. G.; Arnold, P. L.; Cloke, F. G. N. *Chem. Commun.* **1997**, 1963.
- 11 (a) Öfele, K.; Herberhold, M. *Z. Naturforsch.* **1973**, *28b*, 306. (b) Öfele, K.; Kreiter, C. G. *Chem. Ber.* **1972**, *105*, 529.
- 12 (a) Lee, M.; Hu, C. *Organometallics* **2004**, *23*, 976. (b) Niehues, M.; Erker, G.; Kehr, G.; Schwab, P.; Fröhlich, R.; Blacque, O.; Berke, H. *Organometallics* **2002**, *21*, 2905. (c) Boehme, C.; Frenking, G. *Organometallics* **1998**, *17*, 5801. (d) Fröhlich, N.; Pidun, U.; Stahl, M.; Frenking, G. *Organometallics* **1997**, *16*, 442.
- 13 For a recent and excellent review of the nature of the bond formed between N-heterocyclics and transition metals, see: Díez-González, S.; Nolan, S. P. *Coord. Chem. Rev.* **2007**, *251*, 874.
- 14 Clarke, M. J.; Taube, H. *J. Am. Chem. Soc.* **1975**, *97*, 1397.
- 15 Arduengo, A. J., III; Gamper, S. F.; Calabrese, J. C.; Davidson, F. *J. Am. Chem. Soc.* **1994**, *116*, 4391.
- 16 (a) Hu, X.; Castro-Rodriguez I.; Olsen, K.; Meyer, K. *Organometallics* **2004**, *23*, 755. (b) Hu, X.; Tang, Y.; Gantzel, P.; Meyer, K. *Organometallics* **2003**, *22*, 612.
- 17 (a) Saravanakumar, S.; Kindermann, K. M.; Heinicke, J.; Kockerling, M. *Chem. Commun.* **2006**, 640. (b) Saravankumar, S.; Oprea, A. I.; Kindermann, M. K.; Jones, P. G.; Heinicke, J. *Chem.-Eur. J.* **2006**, *12*, 3143.
- 18 Mercs, L.; Labat, G.; Neels A.; Ehlers, A.; Albrecht, M. *Organometallics* **2006**, *25*, 5648. For an earlier study which supports  $\pi$ -interactions in pyridine-N-functionalized NHC complexes, see: Tulloch, A. D. D.; Danopoulos, A. B.;

- Kleinhenz, S.; Light, M. E.; Hursthouse, M. B.; Eastham, G. *Organometallics* **2001**, *20*, 2027.
- 19 Cotton, F. A.; Wilkinson, G. *Advanced Inorganic Chemistry*, 5th ed.; Wiley-Interscience: New York, 1988.
- 20 Scott, N. M.; Dorta, R.; Stevens, E. D.; Correa, A.; Cavallo, L.; Nolan, S. P. *J. Am. Chem. Soc.* **2005**, *127*, 3516.
- 21 (a) Jacobsen, H.; Correa, A.; Costabile, C.; Cavallo, L. *J. Organomet. Chem.* **2006**, *691*, 4350. (b) Cavallo, L.; Correa, A.; Costabile, C.; Jacobsen, H. *J. Organomet. Chem.* **2005**, *690*, 5407. (c) Nemcsok, D.; Wichmann, K.; Frenking, G. *Organometallics* **2004**, *23*, 3640. (d) McGuinness, D. S.; Saendig, N.; Yates, B. F.; Cavell, K. *J. J. Am. Chem. Soc.* **2001**, *123*, 4029.
- 22 Hadei, N.; Assen, B.; Kantchev, B.; O'Brien, C. J.; Organ, M. G. *Org. Lett.* **2005**, *7*, 1991.
- 23 (a) Boydston, A. J.; Bielawski, C. W. *Dalton Trans.* **2006**, 4073. (b) Boydston, A. J.; Williams, K. A.; Bielawski, C. W. *J. Am. Chem. Soc.* **2005**, *127*, 12496.
- 24 Boydston, A. J.; Rice, J. D.; Sanderson, M. D.; Dykhno, O. L.; Bielawski, C. W. *Organometallics* **2006**, *25*, 6087.
- 25 Sanderson, M. D.; Kamplain, J. W.; Bielawski, C. W. *J. Am. Chem. Soc.* **2006**, *128*, 16514.
- 26 Herrmann, W. A.; Schütz, J.; Frey, G. D.; Herdtweck, E. *Organometallics* **2006**, *25*, 2437.
- 27 Transition metals in higher oxidation states may induce more positive charge buildup at the carbene atom, which may be a decisive factor for NHCs to undergo  $\pi$ -backbonding, see: (a) Shukla, P.; Johnson, J. A.; Vidovic, D.; Cowley, A. H.; Abernethy, C. D. *Chem. Commun.* **2004**, 360. (b) Abernethy, C. D.; Codd, G. M.; Spicer, M. D.; Taylor, M. K. *J. Am. Chem. Soc.* **2003**, *125*, 1128.
- 28 All attempts at synthesizing 1,3-dimethyl-4,5-dinitroimidazolium *via* methylation of 1-methyl-4,5-dinitroimidazole were unsuccessful. Similar results were observed by Katritzky, see: Katritzky, A. R.; Yang, H.; Zhang, D.; Kirichenko, K.; Smiglak, M.; Holbrey, J. D.; Reichert, W. M.; Rogers, R. D. *New J. Chem.* **2006**, *30*, 349.
- 29 (a) Lin, I. J. B.; Vasam, C. S. *Coord. Chem. Rev.* **2007**, *251*, 642. (b) Wang, H. M. J.; Lin, I. J. B. *Organometallics* **1998**, *17*, 972.

- 30 Herrmann, W. A.; Elison, M.; Fischer, J.; Köcher, C.; Artus, G. R. *J. Chem. Eur. J.* **1996**, 2, 772.
- 31 1,3-Dimethyl-4,5-dicyano-imidazolium tetrafluoroborate exhibited a  $\nu_{\text{CN}} = 2264 \text{ cm}^{-1}$  (KBr).
- 32 Complex **7..11** was prepared by treating 1,3-dimethyl-4,5-dicyano-imidazolium tetrafluoroborate with  $\text{Ag}_2\text{O}$ .
- 33 Crabtree, R. H.; Quirk, J. M. *J. Organomet. Chem.* **1980**, 199, 99.
- 34 Group electronegativities: H, 2.1; Cl, 3.0; CN, 3.3;  $\text{NO}_2$ , 3.4, see: (a) Wells, P. R. *Prog. Phys. Org. Chem.* **1968**, 6, 111. (b) Anslyn, E. V.; Dougherty, D. A. *Modern Physical Organic Chemistry*; University Science Books: Sausalito, CA, 2006; pp 16.
- 35 Tehana, B. G.; Lloyda, E. J.; Wong, M. G.; Pitt, W. R.; Montana, J. G.; Manallack, D. T.; Gancia, E. *Quant. Struct.-Act. Relat.* **2002**, 21, 457. For an extended compilation of pKa values for substituted benzoic acids, see: Kalfus, K.; Kroupa, J.; Vecera, M.; Exner, O. *Collect. Czech. Chem. Commun.* **1975**, 40, 3009.
- 36 (a) Benac, B. L.; Burgess, E. M.; Arduengo, A. J., III. *Org. Synth.* **1986**, 64, 92.  
(b) Herrmann, W. A.; Elison, M.; Fischer, J.; Köcher, C.; Artus, G. R. *J. Chem. Eur. J.* **1996**, 2, 772.
- 37 Xue, H.; Gao, Y.; Twamley, B.; Shreeve, J. *Chem. Mater.* **2005**, 17, 191.
- 38 For additional examples of facilitating anion metathesis reactions with oxonium salts, see: Vu, P. D.; Boydston, A. J.; Bielawski, C. W. *Green Chem.* **2007**, in press (DOI: 10.1039/b705745h).
- 39 Chen, W.; Liu, F. *J. Organomet. Chem.* **2003**, 673, 5.

## Chapter 8: Diaminocarbene[3]ferrocenophanes and Their Transition Metal Complexes<sup>†</sup>

### INTRODUCTION

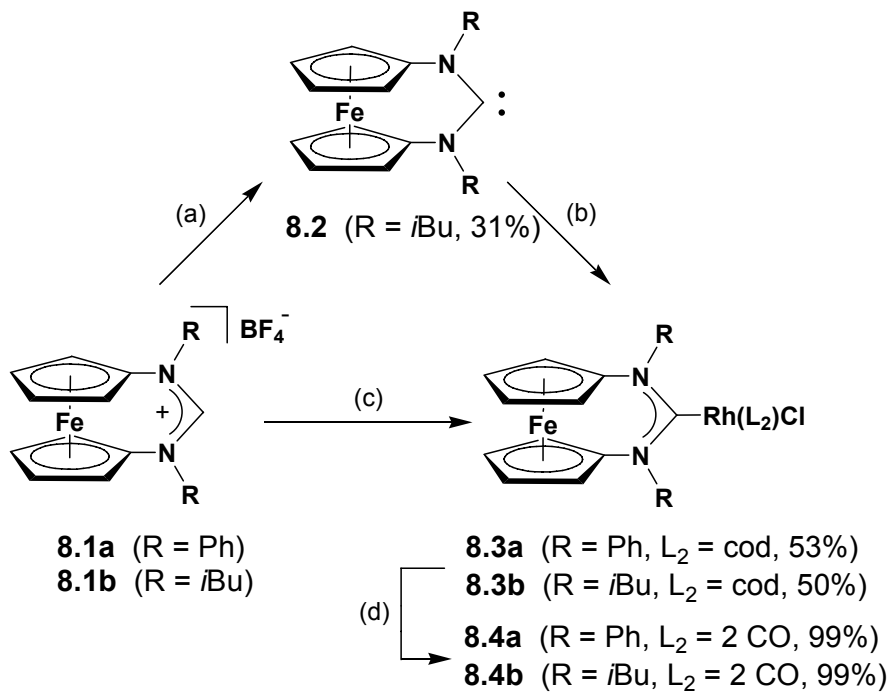
*N*-heterocyclic carbenes<sup>1</sup> (NHCs) form robust complexes with nearly every transition metal, often resulting in catalysts with superior activities and selectivities.<sup>2</sup> The broad utilities and applications of NHCs can be traced to synthetic advances enabling access to derivatives possessing novel *N*-substituents and architectures.<sup>3</sup> By linking diaminocarbenes to 1,1'-disubstituted-metallocenes,<sup>4</sup> we envisioned a new class of carbene-based ligands with relatively wide N-C-N angles and redox-switchable functions.<sup>5</sup> Considering the affinities of carbenes for transition metals, such ligands may lead to new redox-active complexes with tunable electronic properties. Herein, we report a novel carbene architecture that comprises a 1,1'-disubstituted-ferrocene moiety and demonstrate its ability to engage in unique electronic interactions with coordinated transition metals.<sup>6</sup>

### RESULTS

Formamidinium salts **8.1a** and **8.1b** were synthesized *via* formylative cyclization of their respective 1,1'-dianilino-<sup>7</sup> and 1,1'-dialkylamino-ferrocene precursors using trimethylorthoformate and HBF<sub>4</sub> in yields of up to 95%.<sup>8</sup> Diagnostic formamidinium signals were found at 9.3 and 8.8 ppm (DMSO-*d*<sub>6</sub>), respectively, in the <sup>1</sup>H NMR spectra of these compounds. As shown in Figure 1, the solid-state structure of **8.1a** revealed eclipsing cyclopentadienyl (Cp) ligands that were tilted toward each other ( $\phi = 15.7^\circ$ ) due to the tethering effect of the diaminocarbene fragment. This strain manifested in a relatively large N-C-N angle of 129.6(3) $^\circ$ , a value commonly seen in tetrasubstituted formamidinium ions ( $\sim 130^\circ$ ).<sup>9</sup>

Attempts at generating a free carbene *in situ* via deprotonation of **8.1a** using various bases and solvents resulted in rapid decomposition. However, treatment of **8.1b**, which possessed *N*-*iso*-butyl groups,<sup>10</sup> with sodium hexamethyldisilazide (NaHMDS) in C<sub>6</sub>D<sub>6</sub> resulted in a solution of diaminocarbene[3]ferrocenophane **8.2** that was sufficiently stable to be analyzed by NMR spectroscopy. The <sup>13</sup>C NMR spectrum of **8.2** revealed a signal at 260 ppm, which is slightly downfield of known acyclic diaminocarbenes (237 – 256 ppm).<sup>9</sup> Unfortunately, **8.2** decomposed upon concentration which precluded its isolation.<sup>11</sup>

Having demonstrated that free carbenes can be generated *in situ*, subsequent efforts were focused on coordinating these ligands to transition metals and probing for electronic interactions between the two moieties. Previously, it has been shown that Rh-olefin complexes ligated to NHCs are excellent systems for such purposes.<sup>12</sup> In particular, the olefin can be replaced with carbon monoxide without disrupting other physical characteristics of the complex. For the systems reported herein, this exchange should result in detectable changes of the ferrocene's oxidation potentials and support communication between the Rh and Fe centers.



**Scheme 8.1** Synthesis of diaminocarbene[3]ferrocenophanes and related bimetallic complexes. Conditions: (a) NaHMDS, benzene; yield determined by  $^1\text{H}$  NMR spectroscopy. (b)  $[(\text{cod})\text{RhCl}]_2$ , benzene. (c) From 1a: KOTBu,  $[(\text{cod})\text{RhCl}]_2$ , THF. From 1b: NaHMDS,  $[(\text{cod})\text{RhCl}]_2$ , benzene. (d) CO (1 atm),  $\text{CH}_2\text{Cl}_2$ . Reported yields for 8.3 were based on 8.1.

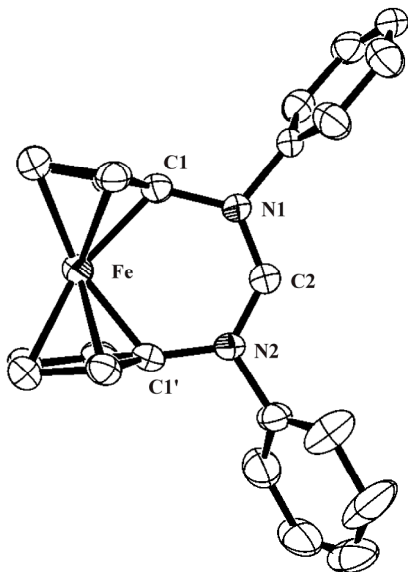


Figure 8.1 ORTEP view of **8.1a**. Ellipsoids are drawn at the 50% probability level. Hydrogen atoms and counterions have been omitted for clarity. Selected bond lengths (Å) and angles (°): C1-N1, 1.437(4); C1'-N2, 1.442(6); C2-N1, 1.327(4); C2-N2, 1.311(4); N1-C2-N2, 129.6(3). The Fe-C2 distance is 3.284(3) Å.

Rh complex **8.3a** was prepared in 53% yield by in situ deprotonation of **8.1a** in the presence of  $[(\text{cod})\text{RhCl}]_2$ . Alternatively, addition of  $[(\text{cod})\text{RhCl}]_2$  to a benzene solution of **2** at ambient temperature resulted in the formation of Rh complex **8.3b** as a yellow solid, which was subsequently isolated in 50% yield. Bubbling carbon monoxide through  $\text{CH}_2\text{Cl}_2$  solutions of **8.3a** or **8.3b** afforded the respective complexes **8.4a** and **8.4b** in excellent yields (> 99%). The carbonyl stretching frequencies ( $\nu_{\text{CO}}$ ) for complexes **8.4a** and **8.4b** were 2074, 1994  $\text{cm}^{-1}$  and 2075, 1995  $\text{cm}^{-1}$  ( $\text{CH}_2\text{Cl}_2$ ), respectively,<sup>13</sup> which are in accord with known  $(\text{NHC})(\text{CO})_2\text{RhCl}$  complexes.<sup>12</sup>

The solid-state structures of **8.3a** and **8.4a** were evaluated using X-ray crystallography (see Figures 8.2 and 8.3, respectively).<sup>14</sup> As expected, the N-C-N angles in these complexes were relatively wide (**8.3a**: 120.7(4)°; **8.4a**: 120.4(3)°) and in accord

with (bis(di-*iso*-propylamino)carbene)RhCl(CO)<sub>2</sub><sup>[15]</sup> (118°). Furthermore, these complexes exhibited relatively long C-N bond lengths (avg. for **8.3a**: 1.36 Å; **8.4a**: 1.35 Å) when compared to **8.1a** (1.32 Å), which may be attributed to the relief of ring strain, Rh-carbene π-backbonding (see below),<sup>12, 16</sup> or a combination thereof.

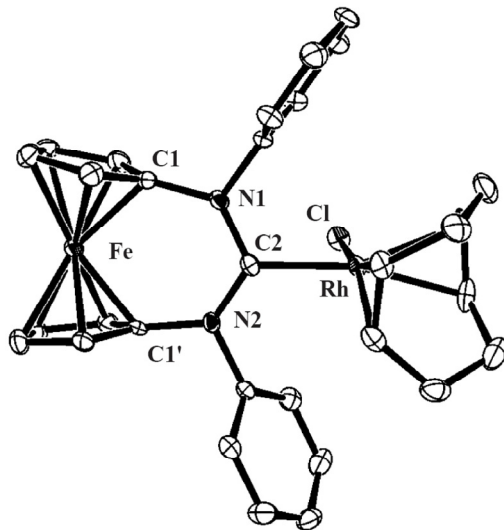


Figure 8.2 ORTEP view of **8.3a**. Ellipsoids are drawn at the 50% probability level. Hydrogen atoms have been omitted for clarity. Selected bond lengths (Å) and angles (°): C1-N1, 1.443(5); C1'-N2, 1.433(5); C2-N1, 1.359(5); C2-N2, 1.349(5); Rh-C2, 2.044(4); N1-C2-N2, 120.7(3). The Fe-C2 distance is 3.438(5) Å.

After **8.3** and **8.4** were synthesized and characterized, the effect of ancillary ligand exchange (i.e., olefin → carbonyl) on the electronic properties of these complexes was studied using cyclic voltammetry.<sup>17</sup> Complex **8.3a** revealed two reversible redox processes at  $E_{1/2} = +1.00$  V and +0.54 V, which were attributed to Rh<sup>I</sup>/Rh<sup>II</sup> and Fe<sup>II</sup>/Fe<sup>III</sup> couples, respectively.<sup>[18]</sup> As expected, the analogous redox couples exhibited by **8.4a**, which bears two carbonyl ligands, were found at relatively high potentials:  $E_{1/2}$  (Rh<sup>I</sup>/Rh<sup>II</sup>) = +1.07 V and  $E_{1/2}$  (Fe<sup>II</sup>/Fe<sup>III</sup>) = +0.91 V. While σ-inductive effects are possible,<sup>[19]</sup> the large difference in  $E_{1/2}$  observed for the Fe<sup>II</sup>/Fe<sup>III</sup> couples in **8.3a** and **8.4a** may be

rationalized in part by unique through-space interactions<sup>20</sup> between the Fe centers and the diaminocarbene moieties. Close analysis of the crystal structures of these two complexes supports this view. The Fe–C<sub>carbene</sub> distances observed in **8.3a** (3.438(5) Å) and **8.4a** (3.406(4) Å) are within their van-der-Waals radii and their respective Rh–C<sub>carbene</sub> bond lengths (**8.3a**: 2.044(4) Å; **8.4a**: 2.081(3) Å) coincide with established  $\pi$ -backbonding capabilities of (NHC)RhCl olefin and carbonyl complexes.<sup>12, 21</sup>

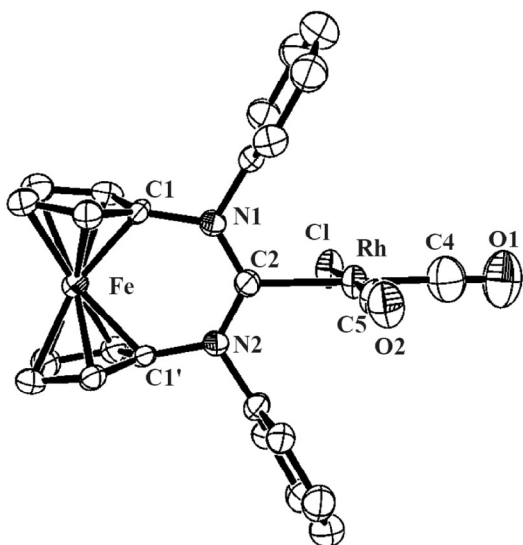


Figure 8.3 ORTEP view of **8.4a**. Ellipsoids are drawn at the 50% probability level. Selected bond lengths (Å) and angles (°): C1-N1, 1.446(4); C1'-N2, 1.441(4); C2-N1, 1.348(4); C2-N2, 1.345(4); Rh-C2, 2.081(3); Rh-C4, 1.900(4); Rh-C5, 1.827(4); N1-C2-N2, 120.4(3). The Fe-C2 distance is 3.406(4) Å.

Additional support for the existence of through-space vis-à-vis  $\pi$ -backbonding interactions in the aforementioned complexes was obtained from the cyclic voltammogram of **8.3b**, which revealed two redox processes at  $E_{1/2}$  (Rh<sup>I</sup>/Rh<sup>II</sup>) = +0.98 V and  $E_{1/2}$  (Fe<sup>II</sup>/Fe<sup>III</sup>) = +0.69 V.<sup>17</sup> Compared to its *N*-aryl analogue **8.3a**, the Fe<sup>II</sup>/Fe<sup>III</sup> couple in **8.3b** occurred at a significantly higher potential. The difference was attributed to diminished Rh→C<sub>carbene</sub>  $\pi$ -donation due to the increased steric bulk of the *N*-*iso*-butyl

substituents, as evidenced by the relatively long Rh-C<sub>carbene</sub> bond observed in the solid-state structure<sup>14</sup> of **8.3b** (2.059(4) Å) (see Figure 8.4).<sup>22, 23</sup>

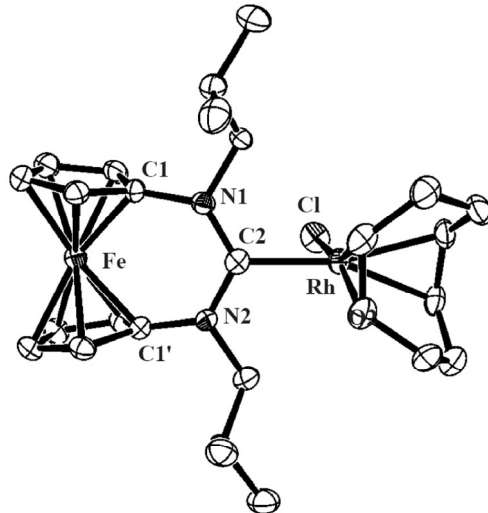


Figure 8.4 ORTEP view of **8.3b**. Ellipsoids are drawn at the 50% probability level. Hydrogen atoms have been omitted for clarity. Selected bond lengths (Å) and angles (°): C1-N1, 1.441(5); C1'-N2, 1.434(5); C2-N1, 1.358(4); C2-N2, 1.356(4); Rh-C2, 2.059(4); N1-C1-N2, 121.2(3). The Fe-C2 distance is 3.434(4) Å.

Finally, the ability of these redox-active diaminocarbenes to electronically modulate ligated transition metals was evaluated by examining the  $\nu_{\text{CO}}$  of **8.4** as a function of the Fe's oxidation state.<sup>24</sup> Because the addition of strong oxidants to **8.4** resulted in decomposition,<sup>25</sup> a spectroelectrochemical experiment that combined bulk electrolysis with time resolved FT-IR spectroscopy was devised.<sup>26</sup> A thin-layer cell was assembled and a solution of complex **8.4a** was recorded as the background.<sup>27</sup> To selectively oxidize the Fe center, a potential of +0.9 V was applied while FT-IR spectra were recorded over time. As shown in Figure 5, signals attributable to **8.4a** disappeared as a new material (assigned to **8.4a<sup>+</sup>**) exhibiting  $\nu_{\text{CO}} = 2088$  and 2015 cm<sup>-1</sup> formed over the same time period.<sup>28</sup> These changes may be explained by the formation of stronger CO bonds and are consistent with diminished electron density at the Rh center induced by

the development of positive charge at the Fe center (i.e.,  $\text{Fe}^{\text{II}} \rightarrow \text{Fe}^{\text{III}}$ ). To place this result into context, the  $\nu_{\text{CO}}$  exhibited by the **8.4a**/**8.4a**<sup>+</sup> couple encompassed a broad range of known Rh carbonyl complexes bearing electron rich and deficient NHCs.<sup>12</sup>

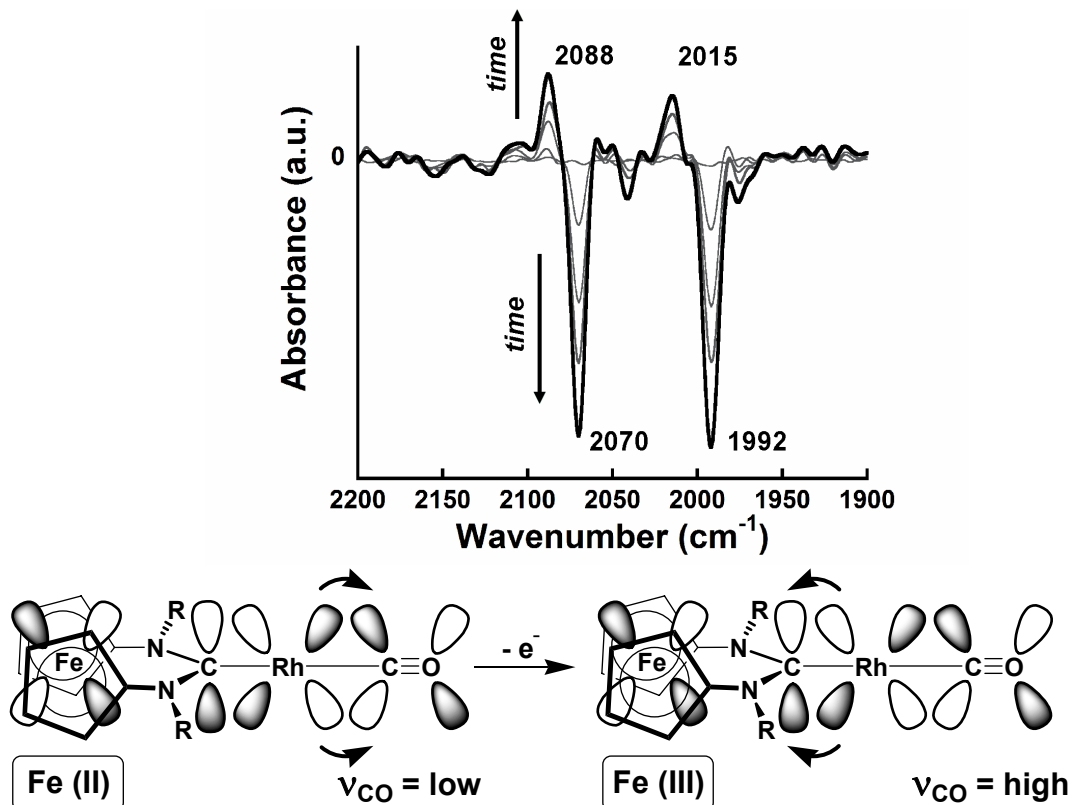


Figure 8.5 (top) Superimposed difference FT-IR spectra showing (bottom) the disappearance of **8.4a** ( $\nu_{\text{CO}} = 2070, 1992 \text{ cm}^{-1}$ ) with concomitant formation of **8.4a**<sup>+</sup> ( $\nu_{\text{CO}} = 2088, 2015 \text{ cm}^{-1}$ ) upon oxidation ( $E = +0.9 \text{ V}$ ) over the duration of 200 s.<sup>27</sup> The Rh center has been truncated for clarity; R = Ph.

## CONCLUSION

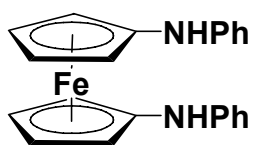
In conclusion, novel *N*-aryl and *N*-alkyl diaminocarbenes that comprise 1,1'-disubstituted-ferrocenes in their backbones and their transition metal complexes have been synthesized. The well-known electrochemistry of ferrocene was utilized to confirm

long range, but significant, electronic communication between the Fe centers in these redox-active carbenes and coordinated transition metals.

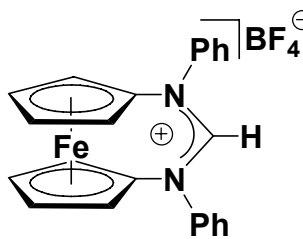
## EXPERIMENTAL

**General Considerations.** All reactions were performed under an atmosphere of nitrogen using standard Schlenk techniques or in a nitrogen filled glove-box. Dichloromethane was distilled from calcium hydride and degassed by two freeze-pump-thaw cycles. Tetrahydrofuran and toluene were distilled from Na/benzophenone and degassed by two freeze-pump-thaw cycles.  $[\text{Rh}(\text{cod})\text{Cl}]_2$  and 1,1'-diphenylphosphinoferrocene (DPPF) were purchased from Strem Chemicals and used without further purification. All other reagents were purchased from Aldrich or Acros and were used without further purification.  $^1\text{H}$  NMR spectra were recorded using a Varian Gemini (300 MHz or 400 MHz) spectrometer. Chemical shifts are reported in delta ( $\delta$ ) units and expressed in parts per million (ppm) downfield from tetramethylsilane using the residual protio solvent as an internal standard ( $\text{CDCl}_3$ , 7.24 ppm;  $\text{C}_6\text{D}_6$ , 7.15 ppm;  $\text{CD}_2\text{Cl}_2$ , 5.32 ppm;  $\text{DMSO}-d_6$ , 2.49 ppm). Coupling constants ( $J$ ) are expressed in Hertz (Hz). Where appropriate, descriptions of signals include singlet (s), doublet (d), triplet (t), multiplet (m), and broad (br).  $^{13}\text{C}$  NMR spectra were recorded using a Varian Gemini (75 MHz or 100 MHz) spectrometer. Chemical shifts are reported in delta ( $\delta$ ) units and expressed in parts per million (ppm) downfield from tetramethylsilane using the solvent as an internal standard ( $\text{CDCl}_3$ , 77.0 ppm;  $\text{C}_6\text{D}_6$ , 128.0 ppm;  $\text{CD}_2\text{Cl}_2$ , 53.8 ppm,  $\text{DMSO}-d_6$ , 39.5 ppm).  $^{13}\text{C}$  NMR spectra were routinely run with broadband decoupling. IR spectra were recorded using a Perkin-Elmer Spectrum BX FT-IR system. High-resolution mass spectra (HRMS) were obtained with a VG analytical ZAB2-E or a Karatos MS9 instrument and are reported as m/z (relative intensity). X-ray crystal structure data was collected for **8.1a** (CCDC 660615), **8.3a** (CCDC 660617), **8.4a**

(CCDC 660616), and **8.4b** (CCDC 666986) and deposited with the Cambridge Crystallographic Data Centre, 12 Union Road, Cambridge CB2 1EZ, UK.

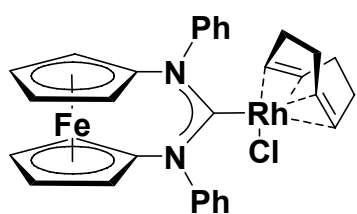


**1,1'-Dianilinoferrocene.** Using a modified literature procedure,<sup>29</sup> a 25 mL flask was charged with DPPF (0.06 g, 0.11 mmol), Pd<sub>2</sub>dba<sub>3</sub> (0.05 g, 0.05 mmol), toluene (15 mL), and a stir bar. The reaction was stirred for 10 minutes to form a coupling catalyst *in situ* as monitored by a color change from deep purple to orange. Following the color change, iodobenzene (1.52 g, 7.46 mmol), 1,1'-diaminoferrocene<sup>30</sup> (0.80 g, 3.73 mmol), and NaOtBu (0.73 g, 7.65 mmol) were added to the reaction mixture in that order. After heating the reaction vessel at 90 °C for 16 h, then mixture was filtered hot and the mother liquor was subsequently concentrated under reduced pressure to obtain the desired product as brown solid (1.35 g, 98% yield). The product was sufficiently pure to be used in the next step without additional purification. Spectroscopic data matched literature reports.<sup>1</sup>

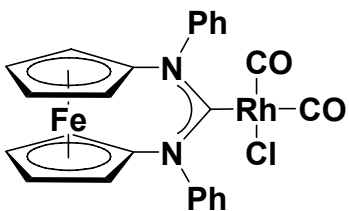


**(8.1a).** A 100 mL flask was charged with 1,1'-dianilinoferrocene (2.21 g, 6.0 mmol), degassed HC(OCH<sub>3</sub>)<sub>3</sub> (50 mL), ethereal HBF<sub>4</sub> (50-54% w/v; 1 mL, 7 mmol), and a stir bar. After stirring the reaction mixture at ambient temperature for 60 min, solvent volume was reduced by 70% and Et<sub>2</sub>O was added until the total volume was 100 mL. During this process, precipitate formed which was collected *via* filtration and washed with 2 x 25 mL portions of diethyl ether. The precipitate was then dried under reduced pressure for 96 h to obtain the desired compound as a brown powder (2.7 g, 95% yield). A crystal suitable for X-ray analysis

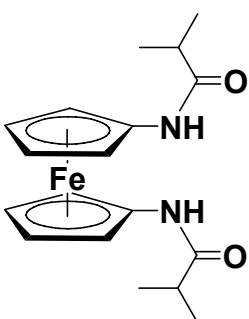
was obtained by slow diffusion of toluene/Et<sub>2</sub>O into a DMSO solution of **8.1a**. <sup>1</sup>H NMR (DMSO-*d*<sub>6</sub>): δ 9.32 (s, 1H), 7.66 (d, *J* = 8 Hz, 4H), 7.54-7.43 (m, 6H), 4.97 (br, 4H), 4.60 (br, 4H). <sup>13</sup>C NMR (DMSO-*d*<sub>6</sub>): δ 160.3, 142.2, 129.1, 128.4, 123.4, 93.7, 72.2, 67.9. HRMS: [M]<sup>+</sup> calcd for C<sub>23</sub>H<sub>19</sub>N<sub>2</sub>Fe: 379.0905; found, 379.0892.



**Complex 3a.** A 10 mL flask was charged with *N,N'*-diphenylformamidinium[3]ferrocenophane•BF<sub>4</sub> (**8.1a**) (0.14 g, 0.30 mmol), KO*t*Bu (34 mg, 0.30 mmol), [Rh(cod)Cl]<sub>2</sub> (75 mg, 0.15 mmol), THF (5 mL), and a stir bar. After sealing the flask, the reaction mixture was stirred at ambient temperature for 16 h. During this time, precipitate formed which was collected by filtration. To remove inorganic salts, the collected precipitate was re-dissolved in CH<sub>2</sub>Cl<sub>2</sub> and filtered. Solvent was then removed under reduced pressure leaving crude product that was triturated with Et<sub>2</sub>O (5 mL) to remove unreacted [Rh(cod)Cl]<sub>2</sub>. The product was dried under reduced pressure to obtain the desired compound as a light yellow, crystalline solid (0.10 g, 53% yield). A crystal suitable for X-ray analysis was obtained by slow evaporation of a CH<sub>2</sub>Cl<sub>2</sub> solution saturated with **8.3a**. <sup>1</sup>H NMR (CD<sub>2</sub>Cl<sub>2</sub>): δ 8.04 (d, *J* = 7.6 Hz, 4H), 7.43 (t, *J* = 8 Hz, 4H), 7.34 (m, 2H), 4.39 (s, 6H), 4.26 (s, 4H), 2.88 (br, 2H), 1.48 (br, 2H), 1.33-1.25 (br, 6H). <sup>13</sup>C NMR (CD<sub>2</sub>Cl<sub>2</sub>): δ 224.5, (d, *J*<sub>Rh-C</sub> = 45.6 Hz), 147.4, 129.9, 128.6, 127.5, 100.33, 100.31, 95.6 (d, *J*<sub>Rh-C</sub> = 7.0 Hz), 71.9, 71.3, 68.6 (d, *J*<sub>Rh-C</sub> = 14.9 Hz), 67.6, 67.2, 31.6, 27.7. HRMS: [M-Cl]<sup>+</sup> calcd for C<sub>31</sub>H<sub>30</sub>N<sub>2</sub>FeRh: 589.0800; found, 589.0808.



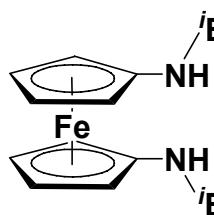
**Complex 8.4a.** After charging a 10 mL flask with **8.3a** (50 g, 0.08 mmol),  $\text{CD}_2\text{Cl}_2$  (3 mL), and a stir bar, the resulting solution was placed under slight CO pressure (balloon). After stirring the solution for 2 h at ambient temperature, quantitative formation of the desired product was observed *via* NMR spectroscopy. The solvent was removed under reduced pressure and the crude product was triturated with pentane. The product was then dried under reduced pressure to obtain the desired compound as a pale yellow, crystalline solid (46 mg, 99% yield). A crystal suitable for X-ray analysis was obtained by slow evaporation of  $\text{CH}_2\text{Cl}_2$  solution saturated with **8.3a**.  
 $^1\text{H}$  NMR ( $\text{CD}_2\text{Cl}_2$ ):  $\delta$  7.56-7.54 (m, 4H), 7.43-7.39 (m, 4H), 7.36-7.32 (m, 2H), 4.58 (m, 2H), 4.50 (m, 2H), 4.37-4.33 (m, 4H).  $^{13}\text{C}$  NMR ( $\text{CD}_2\text{Cl}_2$ ):  $\delta$  214.1 (d,  $J_{\text{Rh-C}} = 39.4$  Hz), 187.0 (d,  $J_{\text{Rh-C}} = 55.2$  Hz), 183.3 (d,  $J_{\text{Rh-C}} = 77.9$  Hz), 146.5, 129.0, 128.99, 128.1, 99.08, 99.07, 72.0, 71.6, 67.3, 67.1. HRMS:  $[\text{M}-\text{Cl}]^+$  calcd for  $\text{C}_{25}\text{H}_{18}\text{FeN}_2\text{O}_2\text{Rh}$ : 536.9773; found, 536.9767.



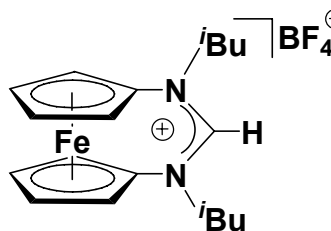
***N,N'*-Di-iso-butylamidoferrocene.** A 100 mL flask was charged with 1,1'-diaminoferrocene<sup>2</sup> (0.99 g, 4.6 mmol),  $\text{CH}_2\text{Cl}_2$  (50 mL), and a stir bar. The flask was then placed in an ice bath and stirred for 5 min. Triethylamine (2.5 mL, 18 mmol) was then added, followed by *iso*-butyryl chloride (1.0 mL, 9.5 mmol). The ice bath was removed and the reaction mixture was stirred for an additional 30 min. The reaction mixture was then washed with a saturated  $\text{NaHCO}_3$  solution (3 x 100 mL) and dried with  $\text{Na}_2\text{SO}_4$ . Subsequent concentration of the organic phase under reduced pressure afforded the desired product as a brown-orange solid (1.6 g, 98% yield).

$^1\text{H}$  NMR ( $\text{DMSO}-d_6$ ):  $\delta$  9.07 (s, 2H), 4.47 (t, 4H,  $J = 2.8$  Hz), 3.84 (t, 4H,  $J = 2.8$  Hz),

2.45-2.40 (m, 2H), 1.05 (d, 12H,  $J$  = 6.9 Hz).  $^{13}\text{C}$  NMR (DMSO- $d_6$ ):  $\delta$  175.47, 96.43, 65.66, 62.45, 35.22, 20.23. HRMS: [M] $^+$  calcd for  $\text{C}_{18}\text{H}_{25}\text{N}_2\text{O}_2\text{Fe}$ : 357.1265; found 357.1264.

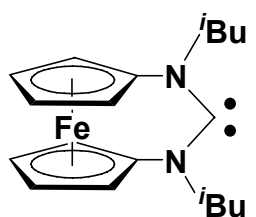


***N,N'-Di-iso-butylaminoferrocene.*** A 250 mL flask fitted with a reflux condenser and a  $\text{N}_2$  balloon was charged with *N,N'-di-iso-butylamidoferrocene* (1.6 g, 4.5 mmol), THF (50 mL), and lithium aluminum hydride (0.70 g, 18 mmol). The reaction mixture was heated to 85 °C and stirred for 10 h. After cooling the flask with an ice bath, degassed ethyl acetate (90 mL) followed by a degassed aqueous solution of Rochelle's Salt (7 g, 25 mmol, 0.25 M) were carefully added *via* syringe while stirring the reaction mixture. The ice bath was removed and the solution was allowed to stir for an additional 1 h. After allowing the resulting biphasic solution to settle, the organic phase was extracted *via* syringe and concentrated under reduced pressure to afford the desired product as a brown oil (1.2 g, 82% yield).  $^1\text{H}$  NMR ( $\text{C}_6\text{D}_6$ ):  $\delta$  3.90 (s, 4H), 3.80 (s, 4H), 2.65 (d, 4H,  $J$  = 6.7 Hz), 1.67-1.58 (m, 2H), 0.88 (d, 12H,  $J$  = 6.7 Hz).  $^{13}\text{C}$  NMR ( $\text{C}_6\text{D}_6$ ):  $\delta$  63.45, 56.22, 55.69, 29.02, 20.76. HRMS: [M] $^+$  calcd for  $\text{C}_{18}\text{H}_{29}\text{N}_2\text{Fe}$ : 329.1680; found 329.1678.



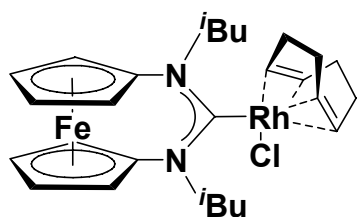
***N,N'-Di-iso-butylformamidinium[3]ferrocenophane•BF<sub>4</sub>***  
**(8.1b).** A 50 mL flask was charged with *N,N'-di-iso-butylaminoferrocene* (1.0 g, 3.2 mmol), degassed  $\text{HC}(\text{OCH}_3)_3$  (10 mL), aqueous  $\text{HBF}_4$  (50% w/v, 0.3 mL, 4.71 mmol), and a stir bar. After the solution was stirred at ambient temperature for 90 min, it was concentrated under reduced pressure. The resulting brown solid was dissolved in  $\text{CH}_2\text{Cl}_2$  and then poured into  $\text{Et}_2\text{O}$  which caused

solids to precipitate. The solids were collected by filtration and dried under vacuum to afford the desired product as a golden brown powder (600 mg, 44 % yield).  $^1\text{H}$  NMR (DMSO- $d_6$ ):  $\delta$  8.80 (s, 1H), 4.73 (s, 4H), 4.50 (s, 4H), 3.59 (d, 4H,  $J$  = 7.9 Hz), 1.92 (m, 2H), 0.93 (d, 12H,  $J$  = 6.5 Hz).  $^{13}\text{C}$  NMR (DMSO- $d_6$ ):  $\delta$  162.76, 92.79, 72.96, 68.51, 65.70, 26.65, 19.70. HRMS: [M] $^+$  calcd for  $\text{C}_{19}\text{H}_{27}\text{N}_2\text{Fe}$ : 339.1524; found 339.1527.



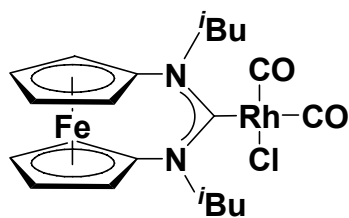
***N,N'*-Di-*iso*-butyldiaminocarbene[3]ferrocenophane (8.2).** A 10 mL flask was charged with *N,N'*-di-*iso*-butylformamidinium[3]ferrocenophane•BF<sub>4</sub> (**8.1b**) (71 mg, 0.17 mmol), NaHMDS (41 mg, 0.22 mmol), C<sub>6</sub>D<sub>6</sub> (3 mL), and a stir bar.

The flask was then sealed and stirred at room temperature for 1 h. The solution was then filtered through a 0.2  $\mu\text{m}$  PTFE membrane under an atmosphere of nitrogen to afford the free carbene as a brown solution. The yield of free carbene was determined to be 31% from the known concentration of the residual protio solvent (C<sub>6</sub>D<sub>5</sub>H), calculated by spiking the sample with 0.04 mL of ethyl acetate in 0.9 mL C<sub>6</sub>D<sub>6</sub>.  $^1\text{H}$  NMR (C<sub>6</sub>D<sub>6</sub>): 3.96 (t, 4H,  $J$  = 2.0 Hz), 3.86 (t, 4H,  $J$  = 2.0 Hz), 3.83 (d, 4H,  $J$  = 7.6 Hz), 2.10 (m, 2H), 0.97 (d, 12H,  $J$  = 6.6 Hz).  $^{13}\text{C}$  NMR (C<sub>6</sub>D<sub>6</sub>):  $\delta$  259.55, 101.29, 70.00, 69.02, 67.22, 27.70, 20.09.



**Complex 8.3b.** A 10 mL flask was charged with *N,N'*-di-*iso*-butylformamidinium[3]ferrocenophane•BF<sub>4</sub> (**8.1b**) (71 mg, 0.17 mmol), NaHMDS (30 mg, 0.17 mmol), benzene (6 mL), and a stir bar. The flask was then sealed and stirred at ambient temperature for 1 h. The solution was then filtered through a 0.2  $\mu\text{m}$  PTFE filter under an atmosphere of nitrogen. [Rh(cod)Cl]<sub>2</sub> (27 mg, 0.055 mmol) was added and the

reaction mixture was stirred at ambient temperature for an additional 18 h. Removal of the solvent under reduced pressure afforded a brown solid which was then purified by column chromatography (media: silica gel; eluent: CH<sub>2</sub>Cl<sub>2</sub>) to obtain the desired product as a bright yellow solid (49 mg, 50% yield). <sup>1</sup>H NMR (C<sub>6</sub>D<sub>6</sub>): δ 5.36 (br, 2H), 5.29-5.15 (m, 4H), 4.03 (s, 2H), 3.89 (d, 4H, *J* = 7.5 Hz), 3.56 (s, 2H), 3.41 (br, 2H), 2.33 (br, 4H), 1.98-1.94 (m, 2H), 1.81-1.75 (br m, 4H), 1.13 (d, 6H, *J* = 6.8 Hz), 0.97 (d, 6H, *J* = 6.8 Hz). <sup>13</sup>C NMR (C<sub>6</sub>D<sub>6</sub>): δ 225.81 (d, *J*<sub>Rh-C</sub> = 47.0 Hz), 98.02, 94.95 (d, *J*<sub>Rh-C</sub> = 7.4 Hz), 71.0, 70.85, 68.73 (d, *J*<sub>Rh-C</sub> = 14.4 Hz), 68.07, 67.20, 66.23, 32.84, 29.34, 27.07, 20.80, 20.41. HRMS: [M]<sup>+</sup> calcd for C<sub>27</sub>H<sub>38</sub>N<sub>2</sub>ClFeRh: 584.1128, found 584.1129.



**Complex 8.4b.** After charging a 10 mL flask with **8.3b** (25 mg, 0.043 mmol), C<sub>6</sub>D<sub>6</sub> (2 mL), and a stir bar, the resulting solution was placed under a slight pressure (balloon) of carbon monoxide. After stirring the solution for 2 h at ambient temperature, quantitative formation of the desired product was observed *via* NMR spectroscopy. Concentration of the solution under reduced pressure afforded the desired product as a yellow solid (23 mg, 99% yield). <sup>1</sup>H NMR (C<sub>6</sub>D<sub>6</sub>): δ 5.62-5.56 (m, 2H), 4.00 (s, 2H), 3.86 (s, 4H), 3.66-3.62 (m, 4H), 1.90-1.86 (m, 2H), 1.00 (d, 6H, *J* = 4.5 Hz), 0.73 (d, 6H, 6.84). <sup>13</sup>C NMR (C<sub>6</sub>D<sub>6</sub>): δ 212.76 (d, *J*<sub>Rh-C</sub> = 40.4 Hz), 187.76 (d, *J*<sub>Rh-C</sub> = 54.5 Hz), 184.92 (d, *J*<sub>Rh-C</sub> = 75.8 Hz), 128.76, 128.63, 97.43, 97.41, 71.60, 71.13, 69.07, 66.87, 66.53, 27.04, 20.08, 19.75. IR (CH<sub>2</sub>Cl<sub>2</sub>): 2075, 1995 cm<sup>-1</sup>. IR (KBr): 2072, 1994 cm<sup>-1</sup>. HRMS: [M]<sup>+</sup> calcd for C<sub>21</sub>H<sub>26</sub>N<sub>2</sub>O<sub>2</sub>ClFeRh: 532.0087, found 532.0084.

**Electrochemical Analyses.** Cyclic voltammetry experiments were conducted using a CH Instruments Electrochemical Workstation (series 700B). The electrochemical cell contained platinum working and counter electrodes and a silver wire as a quasi reference electrode.  $\text{Fe}(\text{Cp}^*)_2$  was added as an internal standard to each sample. Conditions:  $\text{CH}_2\text{Cl}_2$ , 1 mM analyte, 0.1 M  $(\text{Bu}_4\text{N})(\text{PF}_6)$  as electrolyte, referenced to  $\text{Fe}(\text{Cp}^*)_2/\text{Fe}(\text{Cp}^*)_2^+$  at -0.13 V vs SCE, scan rate =  $0.1 \text{ V s}^{-1}$ . Cyclic voltammograms for **8.1**, **8.3**, and **8.4** are shown in Figures 8.6 – 8.8.

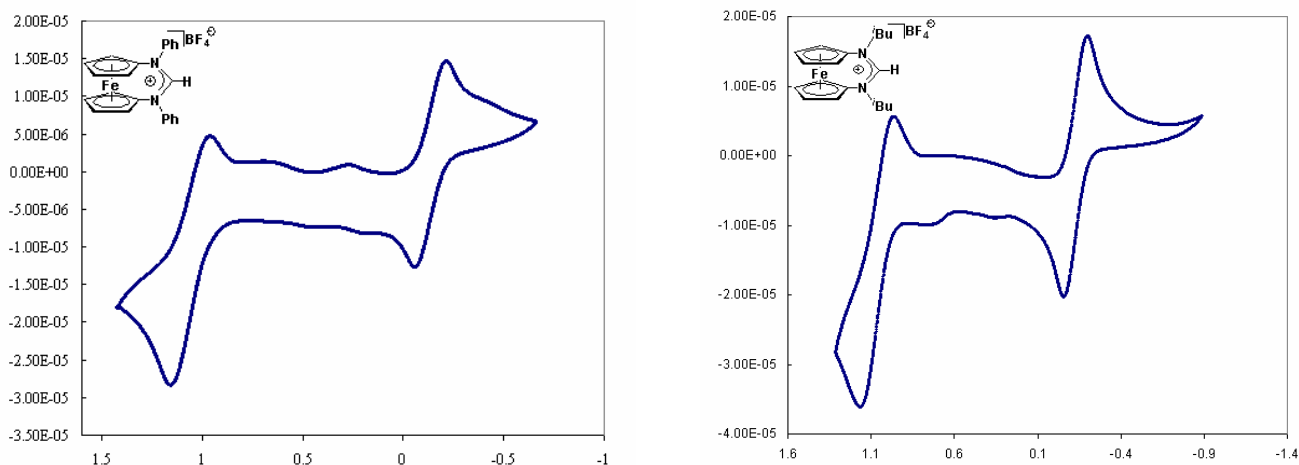


Figure 8.6 Cyclic voltammograms for **8.1a** (left) and **8.1b** (right).

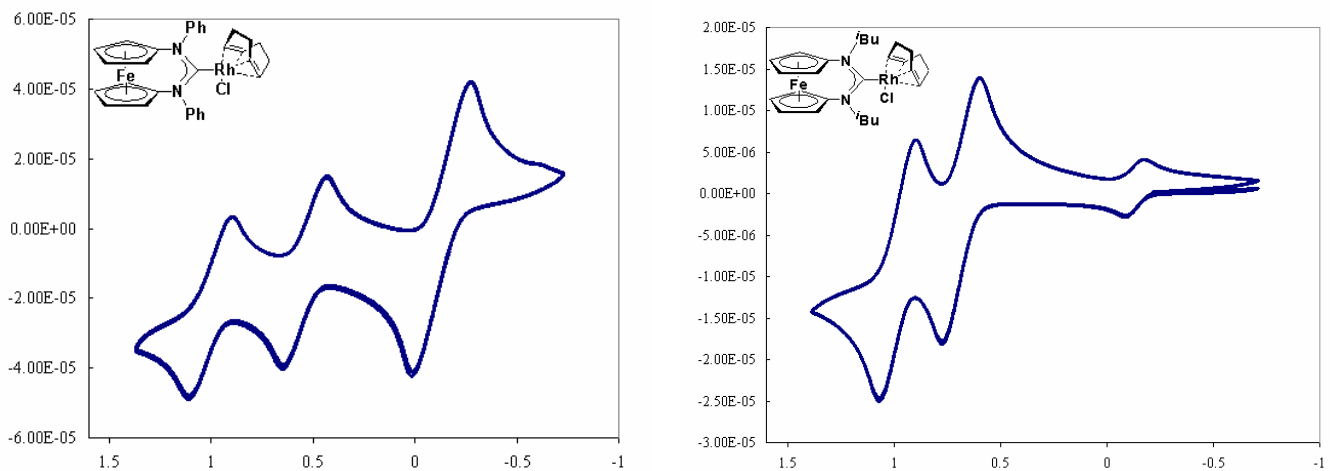


Figure 8.7 Cyclic voltammograms for **8.3a** (left) and **8.3b** (right).

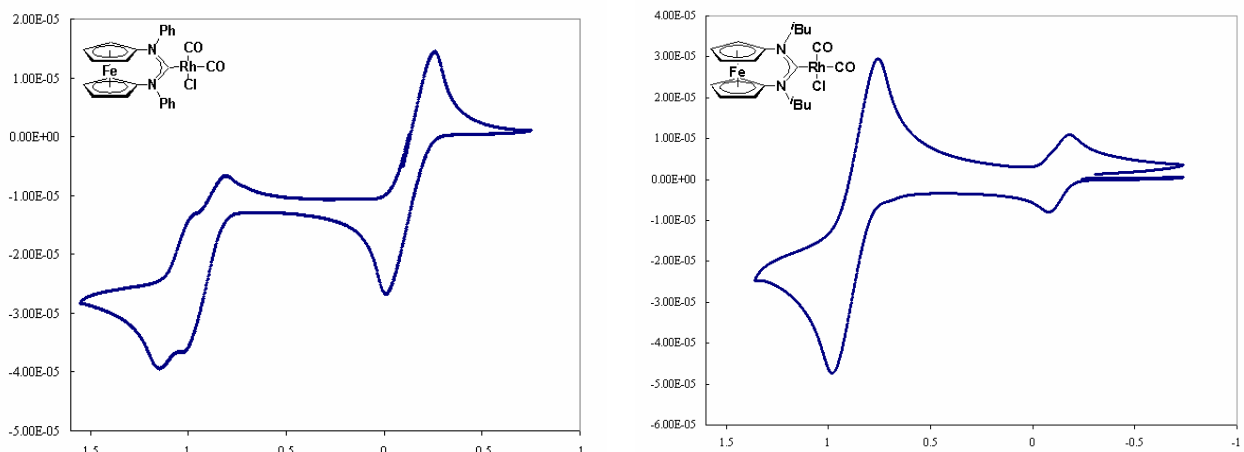


Figure 8.8 Cyclic voltammograms for **8.4a** (left) and **8.4b** (right).

**Spectroelectrochemical Experiment.** A thin layer spectroelectrochemical cell was assembled using a modified International Crystal Labs demountable cell. The body of the cell was machined from Derlin® to eliminate potential current leakage through the cell body. The path length was determined by the thickness of the platinum mesh electrode and was set at 0.06 mm. The counter electrode was platinum/gold mesh with

platinum wire connectors. Silver wire was used as the reference electrode. A rubber O-ring was used to form an leak-proof seal between the body of the cell and the crystal. Similarly, a rubber seal was used as a cushion for the NaBr crystals. Pictures of the cell in pieces and assembled are shown in Figure 8.9.



Figure 8.9 Spectroelectrochemical cell in pieces (left) and assembled (right).

## REFERENCES

- † Portions of this chapter have been previously reported, see: Khramov, D. M.; Rosen E. L.; Lynch, V. M.; Bielawski, C. W. *Angew. Chem. Int. Ed.* **2008**, DOI: 10.1002/anie.200704978.
- 1 a) D. Bourissou, O. Guerret, F. P. Gabbaï, G. Bertrand, *Chem. Rev.* **2000**, *100*, 39; b) A. J. Arduengo, III, *Acc. Chem. Res.* **1999**, *32*, 913; c) W. A. Herrmann, C. Köcher, *Angew. Chem.* **1997**, *109*, 2256; *Angew. Chem. Int. Ed. Engl.* **1997**, *36*, 2162.
- 2 a) E. Peris, R. H. Crabtree, *Coord. Chem. Rev.* **2004**, *248*, 2239; b) A. C. Hillier, G. A. Gasa, M. S. Viciul, H. M. Lee, C. L. Yang, S. P. Nolan, *J. Organomet. Chem.* **2002**, *653*, 69; c) W. A. Herrmann, *Angew. Chem.* **2002**, *114*, 1342; *Angew. Chem. Int. Ed.* **2002**, *41*, 1290.
- 3 For selected examples, see: a) S. Richeter, A. Hadj-Aïssa, C. Taffin, A. van der Lee, D. Leclercq, *Chem. Commun.* **2007**, 2148; b) R. S. Bon, F. J. J. de Kanter, M. Lutz, A. L. Spek, M. C. Jahnke, F. E. Hahn, M. B. Groen, R. V. A. Orru, *Organometallics* **2007**, *26*, 3639; c) A. Fürstner, M. Alcarazo, H. Krause, C. W. Lehmann, *J. Am. Chem. Soc.* **2007**, *129*, 12676; d) F. E. Hahn, *Angew. Chem.* **2006**, *118*, 1374; *Angew. Chem. Int. Ed.* **2006**, *45*, 1348; e) K. E. Krahulic, G. D. Enright, M. Parvez, R. Roesler, *J. Am. Chem. Soc.* **2005**, *127*, 4142; f) F. E. Hahn, M. Paas, D. L. Van, R. Fröhlich, *Chem. Eur. J.* **2005**, *11*, 5080; g) F. E. Hahn, M. Paas, D. L. Van, T. Lügger, *Angew. Chem.* **2003**, *115*, 5402; *Angew. Chem. Int. Ed.* **2003**, *42*, 5243;
- 4 Siemeling, U.; Auch, T.-C. *Chem. Soc. Rev.* **2005**, *34*, 584.
- 5 A. M. Allgeier, C. A. Mirkin, *Angew. Chem.* **1998**, *110*, 936; *Angew. Chem. Int. Ed.* **1998**, *37*, 894.
- 6 For an example of a bimetallic complex containing a NHC annulated to the cyclopentadienyl ligand of a ruthenocene, see: a) A. J. Arduengo, III, D. Tapu, W. J. Marshall, *J. Am. Chem. Soc.* **2005**, *127*, 16400; b) A. J. Arduengo, III, D. Tapu, W. J. Marshall, *Angew. Chem.* **2005**, *117*, 7406; *Angew. Chem. Int. Ed.* **2005**, *44*, 7240. For examples of NHCs bearing *N*-ferrocenyl substituents, see: a) A. Bertogg, F. Camponovo, A. Togni, *Eur. J. Inorg. Chem.* **2005**, 347; b) B. Bildstein, M. Malaun, H. Kopacka, K. Wurst, M. Mitterböck, K.-H. Ongania, G. Oppromolla, P. Zanello, *Organometallics* **1999**, *18*, 4325; c) B. Bildstein, M. Malaun, H. Kopacka, K.-H. Ongania, K. Wurst, *J. Organomet. Chem.* **1999**, *572*, 177.
- 7 U. Siemeling, T.-C. Auch, O. Kuhnert, M. Malaun, H. Kopacka, B. Bildstein, *Z. Anorg. Allg. Chem.* **2003**, *629*, 1334.

- 8 See the Supporting Information for more details.
- 9 a) E. L. Rosen, M. D. Sanderson, S. Saravanakumar, C. W. Bielawski, *Organometallics* **2007**, *26*, 6042; b) R. W. Alder, M. E. Blake, L. Chaker, J. N. Harvey, F. Paolini, J. Schütz, *Angew. Chem.* **2004**, *116*, 6020; *Angew. Chem. Int. Ed.* **2004**, *43*, 5896; c) R. W. Alder, P. R. Allen, M. Murray, A. G. Orpen, *Angew. Chem.* **1996**, *108*, 1211; *Angew. Chem. Int. Ed. Engl.* **1996**, *35*, 1121.
- 10 1,1'-Disubstituted-ferrocenes with bulky *N*-substituents (i.e., mesityl, *neo*-pentyl, and diphenylmethyl) were reluctant to undergo formylative cyclization.
- 11 The propensity of strained ferrocenophanes to undergo nucleophilic ring-opening reactions is well-documented, see: a) F. Jäkle, R. Rulkens, G. Zech, D. A. Foucher, A. J. Lough, I. Manners, *Chem. Eur. J.* **1998**, *4*, 2117; b) R. Rulkens, D. P. Gates, D. Balaishis, J. K. Pudelski, D. F. McIntosh, A. J. Lough, I. Manners, *J. Am. Chem. Soc.* **1997**, *119*, 10976. In addition, NHCs are known to ligate to metallocenes, see: C. D. Abernethy, J. A. C. Clyburne, A. H. Cowley, R. A. Jones, *J. Am. Chem. Soc.* **1999**, *121*, 2329.
- 12 a) D. M. Khramov, V. M. Lynch, C. W. Bielawski, *Organometallics*, **2007**, *26*, 6042; b) M. D. Sanderson, J. W. Kamplain, C. W. Bielawski, *J. Am. Chem. Soc.* **2006**, *128*, 16514; c) W. A. Herrmann, J. Schütz, G. D. Frey, E. Herdtweck, *Organometallics* **2006**, *25*, 2437.
- 13 Values reported are  $\pm 1 \text{ cm}^{-1}$ .
- 14 **8.3b** and **8.4a** were found to have two crystallographically unique complexes in their asymmetric unit cells.
- 15 D. Denk, P. Sirsch, W. A. Herrmann, *J. Organomet. Chem.* **2002**, *649*, 219.
- 16 a) E. S. Chernyshova, R. Goddard, K.-R. Pörschke, *Organometallics* **2007**, *26*, 3236; b) L. Mercs, G. Labat, A. Neels, A. Ehlers, M. Albrecht, *Organometallics* **2006**, *25*, 5648; c) S. Saravanakumar, K. M. Kindermann, J. Heinicke, M. C. Köckerling, *Chem. Commun.* **2006**, 640; d) H. Jacobsen, A. Correa, C. Costabile, L. Cavallo, *J. Organomet. Chem.* **2006**, *691*, 4350; e) X. Hu, I. Castro-Rodriguez, K. Olsen, K. Meyer, *Organometallics* **2004**, *23*, 755; f) D. Nemcsok, K. Wichmann, G. Frenking, *Organometallics* **2004**, *23*, 3640.
- 17 Conditions:  $\text{CH}_2\text{Cl}_2$  as solvent, 1 mM analyte, 0.1 M  $(\text{Bu}_4\text{N})(\text{PF}_6)$  as electrolyte, referenced to  $\text{Fe}(\text{Cp}^*)_2^+/\text{Fe}(\text{Cp}^*)_2$  at -0.13 V versus SCE, scan rate =  $0.1 \text{ V}\cdot\text{s}^{-1}$ . Reported values are  $\pm 0.01 \text{ V}$ . **8.1**, **8.3**, and **8.4** exhibited reversible or quasi-reversible cyclic voltammograms.<sup>8</sup>

- 18 For additional electrochemical studies of Rh-NHC complexes, see: M V. Baker, S. K. Brayshaw, B. W. Skelton, A. H. White, C. C. Williams, *J. Organomet. Chem.* **2005**, *690*, 2312.
- 19 Since the diaminocarbene linkages are orthogonal to the Cp ligands in complexes **8.3** and **8.4**,  $\pi$ -interactions between the Fe and the Rh centers are likely to be minimal.
- 20 Through-space interactions between Fe centers and various heteroatoms have been observed in ferrocenophanes *via* Mössbauer spectroscopy, see: a) J. Silver, D. A. Davies, R. M. G. Roberts, M. Herberhold, U. Dorfler, B. Wrackmeyer, *J. Organomet. Chem.* **1999**, *590*, 71; b) J. Silver, *J. Chem. Soc., Dalton Trans.* **1990**, 3513.
- 21 Recently, we reported a naphthoquinone-annulated NHC and demonstrated its utility in studying  $\pi$ -backbonding interactions in NHC-metal complexes.<sup>[12b]</sup> The difference in reduction potentials of Rh(cod)Cl and Rh(CO)<sub>2</sub>Cl complexes bearing this NHC was found to be 60 mV. For comparison, differences of up to 370 mV were observed in analogous complexes bearing the diaminocarbene reported herein.
- 22 The nearly identical oxidation potentials exhibited by **8.1a** ( $E_{1/2} = +1.03$  V) and **8.1b** ( $E_{1/2} = +1.07$  V) indicate that inductive effects stemming from the *N*-substituents are relatively minimal.
- 23 The Rh<sup>I</sup>/Rh<sup>II</sup> and Fe<sup>II</sup>/Fe<sup>III</sup> redox couples were unresolved in the cyclic voltammogram of **8.4b**.
- 24 a) I. M. Lorkovic, M. S. Wrighton, W. M. Davis, *J. Am. Chem. Soc.* **1994**, *116*, 6220. b) T. M. Miller, K. J. Ahmed, M. S. Wrighton, *Inorg. Chem.* **1988**, *27*, 4326.
- 25 Addition of strong oxidants such as iodine, iodosobenzoic acid, various Ag(I) salts, chloranil, or 1,2-dichloro-4,5-dicyanoquinone to **8.4a** resulted in decomposition. For examples of oxidizing ferrocene derivatives using chemical agents, see: a) J. S. Miller, D. T. Glatzhofer, C. Vazquez, R. S. McLean, J. C. Calabrese, W. J. Marshall, J. W. Raebiger, *Inorg. Chem.* **2001**, *40*, 2058; b) M. Sato, S. Akabori, M. Katada, I. Motoyama, H. Sano, *Chem. Lett.* **1987**, *9*, 1847; c) R. M. G. Roberts, J. Silver, J. Azizian, *J. Organomet. Chem.* **1986**, *303*, 387; d) M. T. Lee, B. M. Foxman, M. Rosenblum, *Organometallics* **1985**, *4*, 539.
- 26 Krejcik, M.; Danek, M.; Hartl, F. *J. Electroanal. Chem.* **1991**, *317*, 179.

- 27 Conditions: CH<sub>2</sub>Cl<sub>2</sub> as solvent, 10 mM **8.4a**, 0.1 M (Bu<sub>4</sub>N)(PF<sub>6</sub>) as electrolyte. Reported values are  $\pm 2 \text{ cm}^{-1}$ .
- 28 For examples of monitoring vCO in carbonyl complexes as a function of oxidation state, see: a) N. Szesni, M. Drexler, J. Maurer, R. F. Winter, F. de Montigny, C. Lapinte, S. Steffens, J. Heck, B. Weibert, H. Fischer, *Organometallics* **2006**, *25*, 5774; b) T. Scheiring, J. Fiedler, W. Kaim, *Organometallics* **2001**, *20*, 1437; c) D. A. Weinberger, T. B. Higgins, C. A. Mirkin, L. M. Liable-Sands, A. L. Rheingold, *Angew. Chem.* **1999**, *111*, 2748; *Angew. Chem. Int. Ed.* **1999**, *38*, 2565.
- 29 Siemeling, U.; Auch, T.-C.; Kuhnert, O.; Malaun, M.; Kopacka, H.; Bildstein, B. *Z. Anorg. Allg. Chem.* **2003**, *629*, 1334.
- 30 Shafir, A.; Power, M. P.; Whitener, G. D.; Arnold, J. *Organometallics* **2000**, *19*, 3978.

## **Chapter 9: N-Heterocyclic carbenes: Deducing $\sigma$ - and $\pi$ - contributions in Rh-mediated hydroboration and Pd-mediated coupling reactions**

### **ABSTRACT**

The effect of tuning the electronic properties of N-heterocyclic carbene (NHC) ligands was evaluated in multiple, mechanistically-distinct, metal-mediated reactions. Hydroboration, Heck, and Suzuki reactions were shown to result in yields that were up to eight times lower when  $\pi$ -withdrawing substituents were incorporated into the NHC backbone relative to analogues bearing  $\sigma$ -withdrawing groups. This demonstrates the significance of the electronic nature of the interaction formed between NHC ligands and transition metals and provides valuable considerations for catalyst design.

### **INTRODUCTION**

Over the past 40 years,<sup>1</sup> N-heterocyclic carbenes (NHCs) (**9.1**)<sup>2</sup> have blossomed into a class of ligands that have proven to be useful for a broad range of transition metals.<sup>3,4</sup> As strong, two-electron donors, they generally coordinate to metals in a fashion that is analogous to phosphines;<sup>5</sup> however, in many instances, they often produce complexes which are more thermally-stable<sup>6</sup> and/or exhibit higher catalytic activities.<sup>3</sup> Prime examples include the Grubbs 2<sup>nd</sup> generation (**9.2**)<sup>7</sup> and PEPPSI<sup>8</sup> catalysts (**9.3**) (see Figure 1), both of which show higher catalytic activities in olefin metathesis and cross-coupling reactions, respectively, than many of their phosphine-ligated counterparts. Considering the number of synthetic methods known to prepare these compounds,<sup>9</sup> NHCs are often the ligand of choice for applications ranging from metal-mediated catalysis to organometallic materials.<sup>3,10</sup>

In view of this breadth of utility, substantial efforts have been directed toward understanding the nature of the interactions formed between NHCs and transition metals.

Like many other ligands,<sup>11</sup> both the steric and electronic components of NHCs can be independently modulated. Sterics are often modified by varying the N-substituents using relatively straightforward processes that typically involve standard alkylation or amination chemistries.<sup>12</sup> In many cases, the size of the NHC's N-substituents have been shown to significantly influence the catalytic activities of their respective NHC-metal complexes.<sup>8</sup> For example, in Pd-mediated coupling reactions, NHC ligands bearing bulky N-substituents have been found to drastically increase the stability and activity of the catalytically-pertinent species.<sup>13</sup> Likewise, in NHC-ligated pre-catalysts, bulky NHCs have been shown to promote the dissociation of ancillary ligands and facilitate the formation of catalytically-active species.<sup>14</sup> This feature is nicely exemplified in Ru-based olefin metathesis catalysts containing sterically-encumbered NHC and phosphine ligands.<sup>4e,15</sup> Ultimately, a broad range of highly active catalysts have resulted from judicious modification and optimization of the steric parameters of NHCs.<sup>3</sup>

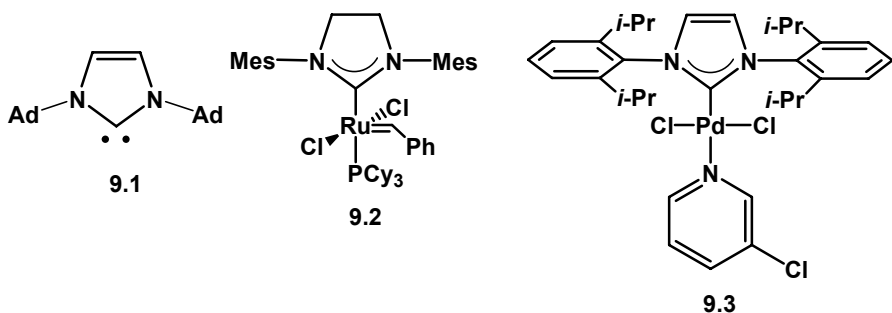


Figure 9.1 Representative examples of an N-heterocyclic carbene (NHC) (**9.1**) and catalytically-active transition metal complexes bearing NHCs (**9.2** and **9.3**). Ad = adamantyl, Mes = 2,4,6-trimethylbenzene, i-Pr = *iso*-propyl.

Tuning the electronic components of NHCs is also of great interest for enhancing the catalytic activities of NHC-metal complexes.<sup>16</sup> Most NHC frameworks offer three distinct options for such purposes: 1) transposition of heteroatoms<sup>17</sup> (e.g., imidazole → oxazole or thiazole), 2) incorporation of additional heteroatoms into the backbone,<sup>18</sup> and 3) attachment of pendant electron-donating or withdrawing groups.<sup>16</sup> With rare exception,<sup>16</sup> varying the N-substituents (particularly, N-aryl substituents) generally has little effect on the electronic properties of NHCs. Regardless, NHC electronics can often be modified without disrupting steric features, which effectively enables separation of these two key components.

The electronic properties of NHCs, particularly their electron donating abilities, are routinely quantified by measuring the CO stretching frequencies ( $\nu_{\text{CO}}$ ) exhibited by their respective Rh carbonyl complexes, (NHC)RhX(CO)<sub>2</sub> (X = Cl, I).<sup>19</sup> Current data indicates that the largest changes in the electron donating abilities of NHCs are achieved by incorporating one or more heteroatoms into their backbones. For example, a Rh carbonyl complex bearing an oxadiazolylidene (**9.4**; see Figure 9.2) exhibited a  $\nu_{\text{CO}} = 2020 \text{ cm}^{-1}$ , which corresponds to the CO ligand *trans* to the NHC and is among highest known frequencies for these types of complexes.<sup>20</sup> While incorporation of additional

heteroatoms into NHC scaffolds likely changes their electronic structures with respect to typical imidazolylidenes, changes in sterics may contribute as well. For example, recent reports revealed that varying the ring size of NHC-type ligands<sup>21</sup> (i.e., **9.5a** → **9.5b** → **9.5c**) had substantial effects on the  $\nu_{\text{CO}}$  exhibited by their respective Rh carbonyl complexes.<sup>22</sup> Hence, to properly study the effects of modifying the electronic components of NHCs, all other structural components should remain identical.

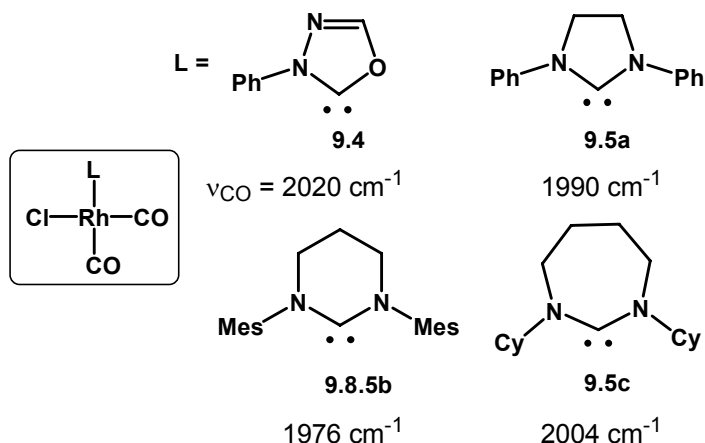


Figure 9.2 Representative complexes used for examining the electron donating properties of N-heterocyclic carbenes. The number listed below each NHC refers to the stretching frequency ( $\nu_{\text{CO}}$ ) exhibited by the *trans*-CO group in their respective (NHC)RhCl(CO)<sub>2</sub> complexes. Ph = phenyl, Mes = mesityl, Cy = cyclohexyl.

Adhering to this criteria, Organ and co-workers prepared a series of 1,3-diadamantyl-benzimidazolylidene precursors that differed only in the functional groups present at the distal 5- and 6-positions.<sup>23</sup> They then studied the ability of their respective NHCs to facilitate Pd-mediated Suzuki cross coupling reactions<sup>24</sup> between various aryl chlorides and boronic acids (see Figure 9.3).<sup>23</sup> This particular reaction was chosen because it is fairly well accepted that its rate limiting step is oxidative addition of Pd<sup>0</sup> species with aryl chlorides;<sup>25</sup> hence, ligand electronics should strongly influence the

outcomes of these reactions. As expected, complexes bearing electron-rich 5,6-dimethoxy-benzimidazolylidenes were generally found to give higher yields of product than their electron-deficient 5,6-difluoro analogues over the same time periods. This seminal contribution effectively paved a new avenue for tuning the activity of Pd-catalysts bearing NHC ligands.

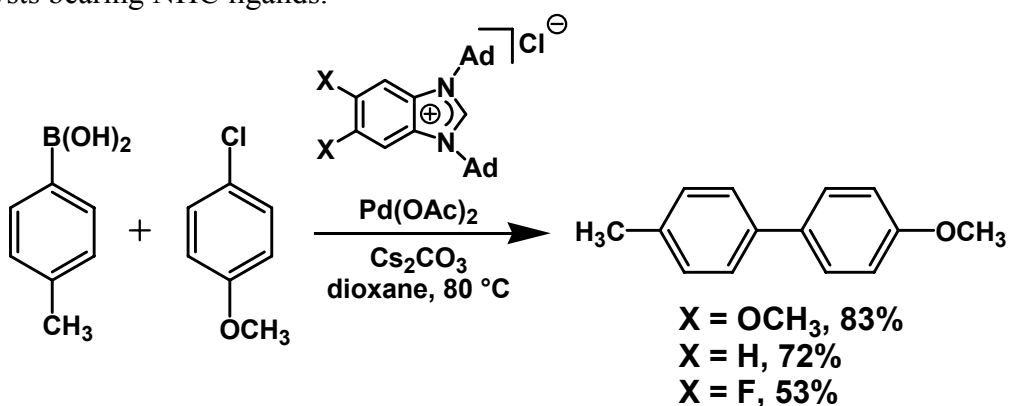


Figure 9.3 Suzuki cross coupling reactions using Pd complexes ligated to electronically-different N-heterocyclic carbenes (generated *in situ*).<sup>23a</sup>

While the installation of pendant functional groups onto NHC ligands clearly influences the electronic and catalytic properties of their respective transition metal complexes, the nature of these effects has not been studied in detail.<sup>26</sup> For example, NHCs are known to form  $\sigma$ - and  $\pi$ -interactions with metals. Because the lone pairs on the nitrogen atom were believed to fill the empty p-orbital of the flanking carbene atom in preference to any ligated transition metal,  $\pi$ -backbonding interactions have historically been considered to be negligible.<sup>27</sup> However, that view has changed considerably over the past several years. For example, Meyer, Frenking, and others employed a combination of computational and crystallographic studies to conclude that  $\pi$ -backbonding interactions contribute up to 30% of the overall bonding character formed between NHCs and certain transition metals.<sup>28</sup> More recently, our group synthesized and characterized a series of Rh

olefin and carbonyl complexes bearing NHCs with different  $\sigma$ - and  $\pi$ -withdrawing groups. Using NMR and FT-IR spectroscopy, we were able to separate their relative electronic effects which lead to the conclusion that  $\pi$ -backbonding interactions were not only present in NHC-Rh complexes but, in some cases, could be finely tuned.<sup>29</sup>

Poised by these results, we sought to build upon Organ's initial investigation and gain insight into how various  $\sigma$ - and  $\pi$ -contributors influence the catalytic activities of NHC-metal complexes. Herein, we compare the abilities of a series of Rh- and Pd-complexes bearing specially-functionalized NHCs to facilitate hydroboration and coupling reactions, respectively. We will show that both  $\sigma$ - and  $\pi$ -interactions are formed between NHCs and transition metals and, in cases where one interaction dominates, can significantly influence reaction yields, rates, and product mixtures. To the best of our knowledge, this is the first study that deduces such  $\sigma$ - and  $\pi$ -effects in reactions catalyzed by metal complexes bearing NHC ligands. On a broader level, the results obtained from this fundamental study should help create new design parameters for optimizing reactions catalyzed by metal complexes containing NHC-type ligands.

## RESULTS

**Synthesis and characterization of Rh complexes ligated to electronically-different NHCs.** In our previous study,<sup>29</sup> we prepared a series of Rh olefin (**9.6**) and carbonyl (**9.7**) complexes ligated to 1,3-dimethylimidazolylidenes bearing various functional groups in their 4- and 5-positions (see Figure 9.4). We benchmarked 1,3-dimethyl-4,5-dichloroimidazolylidene as an NHC possessing predominately  $\sigma$ -withdrawing groups. However, due to known ortho-, para-directing effects of halo substituents in electrophilic aromatic substitutions (EAS), the  $\pi$ -donor abilities of the Cl substituents in this NHC may counteract, at least partially, their  $\sigma$ -withdrawing character. In order to strengthen our hypothesis that  $\pi$ -backbonding interactions are operative in

NHC-Rh complexes and to ensure that the previously observed electronic effects were not due to weakened  $\sigma$ -donation, Rh olefin and carbonyl complexes ligated to 1,3-dimethyl-4-trifluoromethylimidazolylidene were prepared and studied. This particular NHC derivative was chosen because  $\text{CF}_3$  and  $\text{NO}_2$  groups possess identical group electronegativities (3.4).<sup>30,31</sup> Hence, while the electron-withdrawing capabilities of these two functional groups are virtually equal, they can be distinguished by the fact that  $\text{CF}_3$  groups exhibit minimal  $\pi$ -interactions (i.e., they are meta directors in EAS reactions).

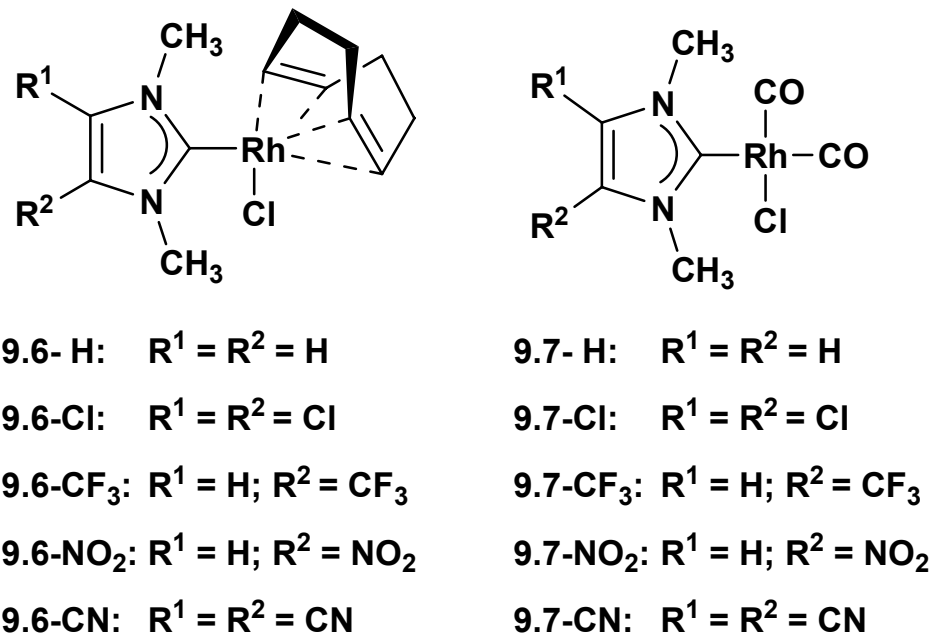


Figure 9.4 Structures of Rh olefin (**9.6**) and carbonyl (**9.7**) complexes synthesized and examined in this study.

Rh complex **9.6-CF<sub>3</sub>** was prepared in accord with our previously reported protocol.<sup>29</sup> 1,3-Dimethyl-4-trifluoromethylimidazolium iodide was treated with  $\text{Ag}_2\text{O}$  followed by transmetalation using  $[\text{Rh}(\text{cod})\text{Cl}]_2$  ( $\text{cod} = 1,5\text{-}cis\text{-}cis\text{-cyclooctadiene}$ ) to obtain pure **9.6-CF<sub>3</sub>** as a yellow solid in 95% yield. Subsequently, pressurizing the

solution of **9.6-CF<sub>3</sub>** with carbon monoxide afforded Rh complex **9.7-CF<sub>3</sub>** in quantitative yield. Analysis of these complexes using <sup>1</sup>H NMR and FT-IR spectroscopy revealed that key signals were in accord with analogues bearing pendant H and Cl groups (see Table 1). Furthermore, despite the identical electronegativities of trifluoromethyl and nitro groups, **9.6-CF<sub>3</sub>** and **9.7-CF<sub>3</sub>** exhibited spectroscopic properties that were significantly different than **9.6-NO<sub>2</sub>** and **9.7-NO<sub>2</sub>**, respectively. In addition, as shown in Figure 9.5, the solid state structure of **9.6-CF<sub>3</sub>** revealed bond distances that were similar to those found in the solid state structures of **9.6-H** and **9.6-Cl**. For example, the C<sub>carbene</sub>-Rh in **9.6-CF<sub>3</sub>** was found to be 2.018(4) Å which is similar to C<sub>carbene</sub>-Rh distances of 2.023(2) and 2.021(2) Å exhibited by **9.6-H** and **9.6-Cl**, respectively. For comparison, the solid state structures of **9.6-NO<sub>2</sub>** and **9.6-CN** revealed shorter C<sub>carbene</sub>-Rh distances of 2.005(3) and 2.006(6) Å, respectively. Collectively these results provide additional support for our notion that π-backbonding interactions are operative in NHC-Rh complexes and may be tuned through derivatization of the NHC.<sup>29</sup> Moreover, comparing metal complexes ligated to NHCs bearing trifluoromethyl groups to those with nitro groups should enable (1) a means to separate σ- and π-interactions formed between NHCs and metals and (2) insight into how each of these fundamental contributors influence catalytic activities.

Complex	$\delta(=CH)$ (ppm) <sup>a</sup>	Complex	$\nu_{CO}$ (cm <sup>-1</sup> ) <sup>b</sup>
<b>9.6-H</b>	5.00	<b>9.7-H</b>	2004
<b>9.6-Cl</b>	5.03	<b>9.7-Cl</b>	2010
<b>9.6-CF<sub>3</sub></b>	5.06	<b>9.7-CF<sub>3</sub></b>	2006
<b>9.6-NO<sub>2</sub></b>	5.12	<b>9.7-NO<sub>2</sub></b>	2012
<b>9.6-CN</b>	5.17	<b>9.7-CN</b>	2017

Table 9.1 Spectroscopic properties of various NHC-Rh complexes. <sup>a</sup>Chemical shifts were determined using  $^1\text{H}$  NMR spectroscopy (solvent =  $\text{CDCl}_3$ ), reported downfield to tetramethylsilane and referenced to residual protio solvent. <sup>b</sup>Carbonyl stretching frequencies ( $\nu_{\text{CO}}$ ) were determined using FT-IR spectroscopy for compounds in solution ( $\text{CDCl}_3$ ). Values reported are  $\pm 0.5 \text{ cm}^{-1}$ . The frequency indicated corresponds to the trans-CO moiety.

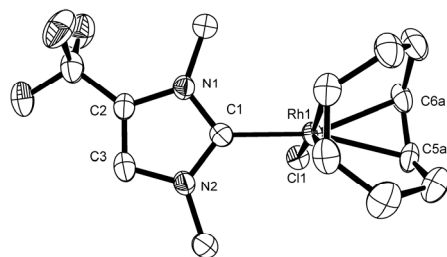


Figure 9.5 ORTEP drawing of **9.6-CF<sub>3</sub>**. Selected bond lengths ( $\text{\AA}$ ) and angles ( $^\circ$ ): C1-Rh1, 2.018(4); C1-N1, 1.359(6); C1-N2, 1.353(3); N1-C2, 1.393(5); N2-C3, 1.373(5); C2-C3, 1.349(6); N1-C1-N2, 104.4(4).

**Deducing  $\sigma$ - and  $\pi$ -contributions in hydroboration reactions catalyzed by Rh-NHC complexes.** With a range of Rh complexes ligated to various functionalized NHCs in hand, attention turned toward exploring their abilities to catalyze hydroboration reactions. The hydroboration of terminal alkynes yields alkenylboronates, which ultimately provides direct access to vinyl boranes, a synthetically useful class of compounds.<sup>24</sup> Although this reaction proceeds uncatalyzed,<sup>32</sup> advantages of known<sup>33</sup> catalyzed variations include decreased reaction times and unique selectivities. In particular, Rh catalyzed hydroborations of terminal alkynes with pinacol or catecholboranes were shown to be greatly facilitated by phosphine ligands and often provided (Z)-1-alkenylboronates in high yields.<sup>34</sup> Since NHC ligands have been shown to have similar metal-activating properties as phosphine ligands,<sup>1-5</sup> we explored the ability of analogous NHC-Rh complexes to catalyze various hydroboration reactions. In

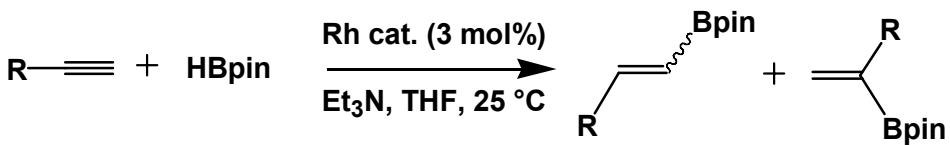
addition, NHC ligands bearing different functional groups were probed to deduce how  $\sigma$ - and  $\pi$ -contributions formed between NHCs and Rh influenced the outcomes of these reactions.

Initial efforts were directed toward studying the hydroborations of phenylacetylene and 1-octyne using pinacolborane and Rh olefin complexes **9.6**. In general, the reactions were performed using a slight modification of a procedure reported by Miyaura.<sup>34</sup> Mixtures of pinacolborane (1.0 equiv.), alkyne (1.2 equiv.), Rh catalyst (3 mol%), and an excess of triethylamine (5 equiv.) were prepared in THF at 25 °C and then monitored over time by  $^1\text{H}$  NMR spectroscopy using an internal standard (mesitylene or 1,3,5-trimethoxybenzene). As a control, hydroborations using  $[\text{Rh}(\text{cod})\text{Cl}]_2$  were also performed. The results of these reactions are summarized in Table 9.2.

As shown in entry 1, Rh complex **9.6-H** was found to catalyze the hydroboration of phenylacetylene, affording a 55% yield of product, under these conditions. To the best of our knowledge, this is the first example demonstrating that Rh-NHC complexes are capable of catalyzing hydroboration reactions.<sup>35</sup> Since increased catalyst loadings, temperature variation, excess alkyne, or the absence of triethylamine did not improve yields (see entries 2 – 5), all subsequent reactions utilized 3 mol% Rh complex and were performed for 14 h at 25 °C using the substrate ratios described above.

After exploring various reaction conditions, our attention shifted towards examining the effects of NHC ligand electronics. Complexes **9.6-Cl** and **9.6-CF<sub>3</sub>** afforded similar yields of products as **9.6-H** (see entries 6 and 7), which suggested to us that the Rh center was not strongly influenced by NHCs bearing strong  $\sigma$ -withdrawing groups. In contrast, significantly lower yields of product were obtained when **9.6-NO<sub>2</sub>** or **9.6-CN**, complexes which contain NHCs bearing  $\pi$ -withdrawing groups, were used as catalysts (see entries 8 and 9). It is noteworthy that the yield of the reaction catalyzed by

**9.6-CF<sub>3</sub>** was nearly twice that of the reaction catalyzed by **9.6-NO<sub>2</sub>**. As mentioned above, the NHCs in these catalysts bear functional groups with identical group electronegativities; hence, we surmise that the observed difference in yields for these two complexes is due to differences in the nature of the interaction ( $\sigma$  versus  $\pi$ ) formed between the NHC and Rh. At any rate, all of the Rh-NHC complexes examined catalyzed hydroborations significantly more efficiently than [Rh(cod)Cl]<sub>2</sub> (c.f., entry 10), which gave very low yields of product under otherwise identical conditions. These results indicate, for the first time, that Rh complexes containing NHCs with  $\sigma$ -withdrawing groups can lead to different product outcomes than analogues bearing  $\pi$ -withdrawing groups.



Entry	R	Rh catalyst	%Yield <sup>b</sup>	E : Z : T <sup>c</sup>
1	Ph	<b>6-H</b>	55	1.5 : 0.8 : 1.0
2	Ph	<b>6-H (10 mol%)</b>	50	1.8 : 1.4 : 1.0
3 <sup>d</sup>	Ph	<b>6-H</b>	47	1.5 : 0.2 : 1.0
4 <sup>e</sup>	Ph	<b>6-H</b>	15 <sup>t</sup>	1.2 : 0.6 : 1.0
5 <sup>g</sup>	Ph	<b>6-H</b>	37	1.2 : 1.6 : 1.0
6	Ph	<b>6-Cl</b>	42	1.3 : 0.0 : 1.0
7	Ph	<b>6-CF<sub>3</sub></b>	50	1.3 : 0.2 : 1.0
8	Ph	<b>6-NO<sub>2</sub></b>	24	1.4 : 1.0 : 1.0
9	Ph	<b>6-CN</b>	24	1.5 : 0.0 : 1.0
10	Ph	[Rh(cod)Cl] <sub>2</sub>	9 <sup>t</sup>	2.2 : 1.1 : 1.0
11	n-Hex	<b>6-H</b>	27	3.8 : 1.4 : 1.0
12	n-Hex	<b>6-H (10 mol%)</b>	45	4.6 : 2.1 : 1.0
13 <sup>d</sup>	n-Hex	<b>6-H</b>	25 <sup>t</sup>	3.7 : 0.8 : 1.0
14 <sup>e</sup>	n-Hex	<b>6-H</b>	8	1.7 : 1.0 : 0.0
15	n-Hex	<b>6-Cl</b>	28	4.5 : 1.5 : 1.0
16	n-Hex	<b>6-CF<sub>3</sub></b>	21 <sup>t</sup>	4.1 : 1.5 : 1.0
17	n-Hex	<b>6-NO<sub>2</sub></b>	18 <sup>t</sup>	3.8 : 0.9 : 1.0
18	n-Hex	<b>6-CN</b>	21 <sup>t</sup>	3.8 : 2.0 : 1.0
19	n-Hex	[Rh(cod)Cl] <sub>2</sub>	10 <sup>t</sup>	4.8 : 0.0 : 1.0
20	Ph	(IMes)Rh(cod)Cl	26	4.5 : 1.6 : 1.0
21	n-Hex	(IMes)Rh(cod)Cl	50	4.3 : 0.7 : 1.0
22	4-MeO-Ph	<b>6-H</b>	60	1.4 : 0.7 : 1.0
23	4-NO <sub>2</sub> -Ph	<b>6-H</b>	30	1.3 : 0.4 : 1.0
24	4-CN-Ph	<b>6-H</b>	33	1.3 : 0.3 : 1.0
25	4-MeO-Ph	<b>6-CF<sub>3</sub></b>	43	1.5 : 0.2 : 1.0
26	4-NO <sub>2</sub> -Ph	<b>6-CF<sub>3</sub></b>	17	1.4 : 0.3 : 1.0
27	4-CN-Ph	<b>6-CF<sub>3</sub></b>	32	1.2 : 0.3 : 1.0
28	4-MeO-Ph	<b>6-NO<sub>2</sub></b>	31	1.9 : 0.8 : 1.0
29	4-NO <sub>2</sub> -Ph	<b>6-NO<sub>2</sub></b>	20	1.7 : 0.4 : 1.0
30	4-CN-Ph	<b>6-NO<sub>2</sub></b>	28	1.2 : 0.4 : 1.0

Table 9.2 Hydroboration of alkynes catalyzed by various Rh complexes. General conditions: [pinacolborane]<sub>0</sub> = 0.33 M (1.0 equiv.), [Et<sub>3</sub>N]<sub>0</sub> = 1.65 M (5.0 equiv.), [alkyne]<sub>0</sub> = 0.4 M (1.2 equiv.), Rh complex (3 mol%), THF, 14 h, 25 °C, unless otherwise noted. All reactions were performed in triplicate.

<sup>b</sup>Combined yield of all possible isomers, as determined from <sup>1</sup>H NMR analysis of crude reaction mixtures using an internal standard (mesitylene or 1,3,5-trimethoxybenzene). Unless otherwise noted, reported yields are ± ≤5%.

<sup>c</sup>Average ratios of the olefin regioisomers found; E: *trans*, Z: *cis*, T: terminal. <sup>d</sup>Reaction was performed at 60 °C. <sup>e</sup>[alkyne]<sub>0</sub> = 1.6 M (4.0 equiv.)

<sup>f</sup>Yield is ± ≤8%. <sup>g</sup>No Et<sub>3</sub>N was added. cod = 1,5-cyclooctadiene. IMes = 1,3-dimesitylimidazolylidene.

Considerably different reaction outcomes were observed for hydroborations of 1-octyne catalyzed by the same set of Rh-NHC complexes. As shown in Table 9.2, preliminary experiments suggested that while **9.6-H** was capable of catalyzing the hydroboration of this substrate under the conditions described above, relatively low yields of product were obtained (see entry 11). However, in contrast to results obtained with phenylacetylene, increased catalyst loadings (10 mol%) lead to higher yields of product (entry 12), although elevated temperature and excess alkyne again did not significantly improve yields (entries 13 – 14). Comparison of entries 11 and 15 – 18 revealed that Rh complexes **9.6** afforded virtually the same yield of product, within experimental error, regardless of the functional group installed the NHC ligand. Furthermore, the activities of these Rh-NHC complexes were found to be only marginally more active than [Rh(cod)Cl]<sub>2</sub> (entry 19). Hence, any influence caused by the pendant functional groups on the NHC ligands in **9.6** appeared to have only a minimal effect on the performance of these particular hydroboration reactions. More broadly, this result suggested to us that the importance of relative  $\sigma$ - and  $\pi$ -contributions to the interactions formed between Rh and NHCs may be substrate dependent.

Although Rh complexes bearing bulky phosphine ligands have been reported to afford hydroboration products with high *cis* contents, very modest stereoselectivities were generally observed in the aforementioned hydroboration reactions catalyzed by **9.6**.<sup>34</sup> However, this disparity may, at least partially, be explained by the difference in sterics between the NHCs explored herein (which contain relatively small N-methyl groups) and the bulky phosphines (i.e., PCy<sub>3</sub>) previously used.<sup>34</sup> This hypothesis is partially supported by the observation that (IMes)Rh(cod)Cl (IMes = 1,3-dimesitylimidazolylidene),<sup>36</sup> a complex that bears bulky N-substituents, exhibited

different (i.e., relatively high *trans*) selectivities, when compared to **9.6-H**, for the hydroboration of both phenylacetylene and 1-octyne (see entries 20 and 21, respectively).

Based on a proposed mechanism of Rh catalyzed hydroboration of alkenes, first reported by Männig and Nöth<sup>37</sup> and later supported by others,<sup>38,39</sup> an analogous mechanism for the hydroboration of alkynes is proposed in Figure 6. There are four key steps in this mechanism: (1) oxidative addition of a borane to Rh-NHC catalyst **A**, (2) alkyne coordination to the resulting Rh hydride **B**, (3) hydride migration (**C** → **D**), and (4) reductive elimination, ultimately leading to an alkenylboronate product and **A**. The structures of the intermediates shown in Figure 6 are supported by analogous Ir hydride and Ir alkyl complexes bearing phosphine ligands, most of which have been characterized spectroscopically or crystallographically.<sup>40</sup>

While each of the steps in the proposed mechanism should be influenced by the electron density residing at the metal center, and therefore amenable to modulation by the coordinated NHC, it has been previously proposed that reductive elimination is the rate limiting step in Rh catalyzed hydroborations of alkenes.<sup>38a,41</sup> Based on all the data shown in Table 9.2, we believe reductive elimination is also the limiting step for hydroboration of alkynes catalyzed by the Rh-NHC catalysts described herein.

In particular, intermediate **D** features an NHC ligand situated *trans* to the alkenyl moiety. Electron withdrawing groups on the carbene ligand are positioned to remove electron density from Rh, resulting in stronger bond formed between the alkene carbon and the metal center. Hence, reductive elimination should be inhibited and result in decreased yields of product in accord with the nature and strength of the electron withdrawing group. Indeed, as shown for phenylacetylene in Table 9.2, a Rh catalyst bearing an electron rich NHC ligand generally afforded higher yields of products than its electron deficient analogues (c.f., entry 1 versus entries 6 – 9). Moreover, the nature of

the interaction formed between NHCs and Rh appears to play an important role. Catalysts ligated to NHCs bearing  $\sigma$ -withdrawing  $\text{CF}_3$  groups affected the outcomes of these reactions to a relatively minor extent compared to analogues bearing  $\pi$ -withdrawing  $\text{NO}_2$  or  $\text{CN}$  groups (c.f., entry 7 versus entries 8 – 9). These results suggested to us that  $\pi$ -withdrawing groups on the NHC ligand are more effective at decreasing electron density at the Rh center and therefore more significantly influencing its reactivity compared to analogues bearing  $\sigma$ -withdrawing groups.

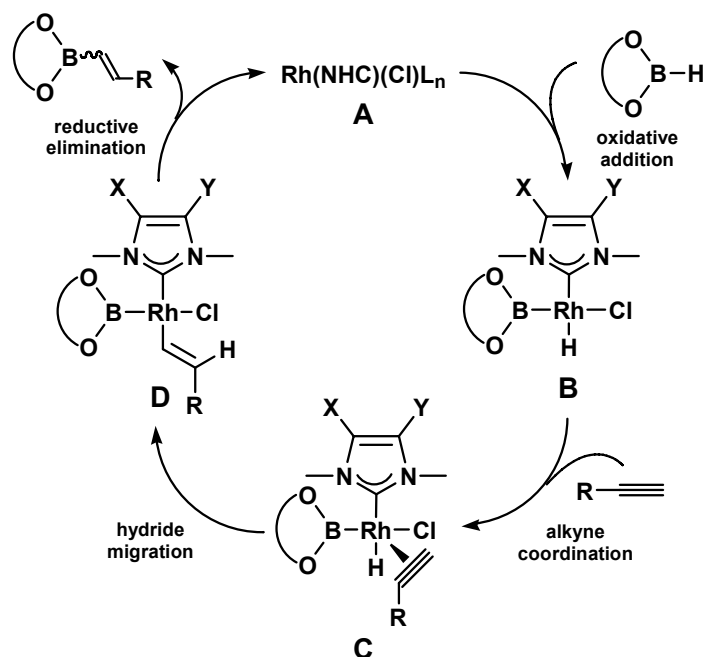


Figure 9.6 Proposed general reaction scheme for the hydroborations of alkynes catalyzed by Rh-NHC complexes.

To gain additional support for the notion that reductive elimination is the rate determining step in Rh-NHC catalyzed alkyne hydroborations, a series of functionalized phenylacetylene derivatives were synthesized and studied for their ability to react with pinacolborane under the conditions described above (entries 22 – 30). Using **9.6-H** as a catalyst, higher yields of hydroboration product were obtained when phenylacetylene

(entry 1) or 4-methoxyphenylacetylene (entry 22) were used as substrates when compared to analogous reactions performed using relatively electron-deficient 4-nitro- or 4-cyanophenylacetylene (entries 23 and 24, respectively). In the former cases, the increased electron density on the substrate may serve to weaken the bond formed between the Rh center and the coordinated alkenyl group, facilitating reductive elimination and resulting in higher yields of product. In contrast, the electron deficient nature of the latter substrates may result in the formation of relatively strong bonds between these two moieties which hinders the reductive elimination process and ultimately product formation. Collectively, these results are consistent with the hypothesis that reductive elimination is the rate-determining step in Rh-NHC catalyzed reactions.

To explore whether the nature of the interaction formed between NHCs and Rh influence the yields of hydroboration products obtained from functionalized phenylacetylenes, the aforementioned reactions were repeated using **9.6-CF<sub>3</sub>** and **9.6-NO<sub>2</sub>** as catalysts (see entries 25 – 30). As expected, lower yields of product were observed in all cases which is likely due to the decreased electron density on the Rh center. However, the relative yields of product obtained from either catalyst were virtually identical. Thus, we conclude that the pendant functional groups on these phenylacetylene derivatives modulate the strength of the Rh-alkenyl bond more strongly than the NHC ligand, thereby diminishing any noticeable effect caused by the latter.

**Synthesis and characterization of Pd complexes ligated to 1,3-dimethyl-imidazolylidenes bearing different pendant functional groups.** Next, attention was directed toward exploring how NHC-based ligands bearing different functional groups influenced Pd-catalyzed Heck and Suzuki cross-coupling reactions.<sup>42</sup> Using previously reported protocols,<sup>9a</sup> (NHC)<sub>2</sub>PdI<sub>2</sub> complexes (**9.8**) bearing the same NHCs as in the

aforementioned Rh complexes (i.e., **9.6** and **9.7**) were prepared from their corresponding imidazolium salts and Pd(OAc)<sub>2</sub> (see Figure 9.7). After 2 h at 80 – 100 °C in DMSO-*d*<sub>6</sub>, NMR scale experiments indicated that the desired complexes formed in quantitative yields with concomitant formation of AcOH. Furthermore, electron deficient imidazoliums qualitatively reacted much faster than their electron rich analogues, supporting the notion that acetate functions as a base in these reactions.<sup>9a</sup> For syntheses performed on preparative scales, a 10 mol% excess of imidazolium salt was used to ensure complete consumption of Pd(OAc)<sub>2</sub>.<sup>43</sup> Ultimately, Pd complexes **9.8** were obtained in excellent yields (90 – 96%) by pouring their corresponding reaction mixtures into excess water upon completion, which caused the precipitation of pale yellow solids that were later collected by filtration. Complexes **9.8** were found to be stable to ambient air and moisture and could be stored for months without any noticeable decomposition.

In addition to NMR and mass spectroscopy, Pd complexes **9.8** were characterized by X-ray crystallography. With the exception of **9.8-CF**<sub>3</sub>, all complexes adopted pseudo-square planar geometries where the NHC ligands were *cis* to each other (an ORTEP of **9.8-Cl** is shown in Figure 8 as a representative example). Although **9.8-CF**<sub>3</sub>, which adopted a *trans* geometry, was different than the other complexes prepared, it has been previously shown that such differences do not influence ultimate product yields of coupling reactions mediated by (NHC)<sub>2</sub>PdX<sub>2</sub>-type pre-catalysts, although initiation rates may vary.<sup>44</sup> Key bond lengths and angles for **9.8** are summarized in Table 3. Complexes **9.8-NO**<sub>2</sub> and **9.8-CN**, exhibited Pd-I and Pd-C<sub>carbene</sub> bond lengths that were shorter than the respective lengths in **9.8-H** and **9.8-Cl**. Similar differences were observed in the series of Rh complexes reported in our previous studies,<sup>29</sup> which were ultimately attributed to π-backbonding interactions.<sup>45</sup>

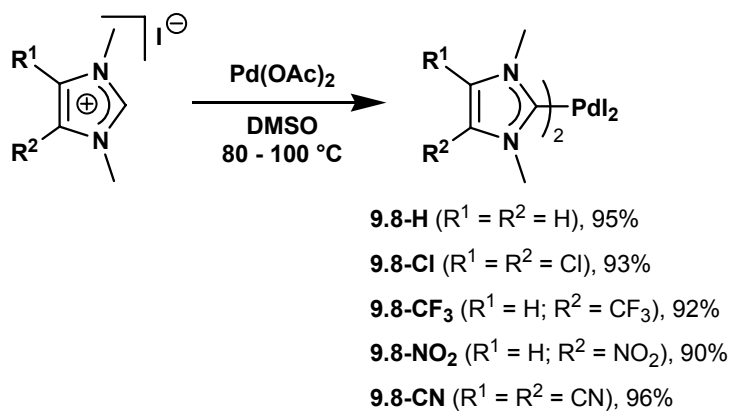


Figure 9.7 Synthesis of Pd-NHC complexes **9.8**.

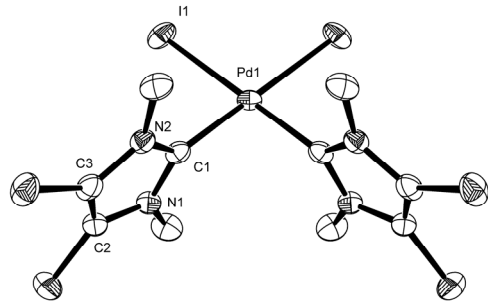


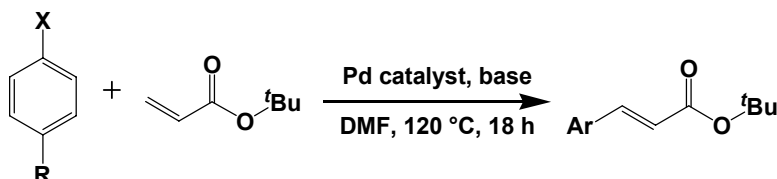
Figure 9.8 ORTEP diagram of **9.8-Cl**. Ellipsoids are drawn at the 50% probability level. Hydrogen atoms have been omitted for clarity. Selected bond lengths are listed in Table 3. The crystal structures of **9.8-CN** and **9.8-NO<sub>2</sub>** were also obtained (not shown) and found to be similar to **9.8-Cl**. The NHCs in the crystal structure of **9.8-CF<sub>3</sub>** (not shown) were found to be *trans*.

Bond	<b>9.8-H<sup>a</sup></b>	<b>9.8-Cl</b>	<b>9.8-CF<sub>3</sub></b>	<b>9.8-CN</b>	<b>9.8-NO<sub>2</sub></b>
Pd1-I1	2.6526(9)	2.6426(3)	2.5965(9)	2.6317(3)	2.6384(7)
Pd1-C1	1.993(3)	2.003(3)	2.006(9)	1.998 (4)	2.002(8)
C1-N1/2	1.351(4)	1.355(4)	1.342(11)	1.341(5)	1.338(10)
C2-C3	1.341(5)	1.340(4)	1.355(14)	1.353(6)	1.368(2)
N1-C1-N2	105.2(3)	105.2(3)	104.5(7)	105.7(3)	104.9(8)

Table 9.3 Selected bond lengths ( $\text{\AA}$ ) and angles ( $^{\circ}$ ) for Pd complexes **9.8**. <sup>a</sup>Data reproduced from ref. 3e.

**Deducing  $\sigma$ - and  $\pi$ -contributions in Heck reactions catalyzed by Pd-NHC complexes.** With a range of Pd complexes in hand, attention turned toward exploring their utilities in catalyzing the Heck reaction. In general, 1 mol% **9.8** was added to a DMF solution containing *tert*-butyl-acrylate (1.4 equiv.) and aryl halide (1.0 equiv.), and then heated to 120  $^{\circ}\text{C}$  for 18 h<sup>46</sup> under nitrogen. Initial studies indicated that 120  $^{\circ}\text{C}$  was the optimal temperature for these coupling reactions. At lower temperatures (i.e., 100  $^{\circ}\text{C}$ ), very low yields of product were obtained for all the Pd-NHC catalyst systems reported herein. At elevated temperatures (i.e., 140  $^{\circ}\text{C}$ ), catalyst decomposition was observed, as evidenced by the formation of  $\text{Pd}^0$ .

In a first set of reactions, NaOAc (1.5 equiv.) was used as base. Product yields were determined by gas chromatography (GC) using an internal standard (mesitylene); results are summarized or noted in Table 4. As expected, 1-iodo-4-methoxybenzene and aryl bromides bearing activating groups (e.g., CHO) afforded the expected products in excellent (>97%) yields. Remarkably, when the reaction was performed using  $\text{Pd}(\text{OAc})_2$  (no NHC ligand), product yields were equally as high. While highly active substrates are useful for determining the mechanism of the reaction,<sup>44</sup> their extreme reactivities without the supporting NHC ligand made them unsuitable for this work.



Ent.	Cat.	R: X: base:	H Br NaOAc	H Br $K_2CO_3$	OMe Br NaOAc	OMe Br $K_2CO_3$	CHO Cl $K_2CO_3$
1	<b>9.8-H</b>		19	100	8	47	1
2	<b>9.8-Cl</b>		11	100	4	42	1
3	<b>9.8-CF<sub>3</sub></b>		76	100	28	75	1
4	<b>9.8-NO<sub>2</sub></b>		8	100	4	22	3
5	<b>9.8-CN</b>		60	100	1	87	10
6 <sup>b</sup>	<b>Pd(OAc)<sub>2</sub></b>		1	100	5	5	0

Table 9.4 Yields of products obtained by coupling *tert*-butyl acrylate with various aryl halides using NHC-Pd complexes **9.8** as catalysts and NaOAc as base. General reaction conditions: catalyst (1 mol%),  $[aryl\ halide]_0 = 0.33\ M$ ,  $[tert\text{-butyl-acrylate}]_0 = 0.47\ M$ ,  $[base]_0 = 0.5\ M$ , [mesitylene]<sub>0</sub> = 0.33 M (internal standard), DMF as solvent, 120 °C, nitrogen atmosphere, 18 h. All reactions were performed in triplicate. Reported yields were determined by GC and are  $\pm 5\%$ . Notes: 4-MeO-PhI and 4-CHO-PhBr afforded 100% yield of product for all catalysts and bases studied. PhCl and 4-CHO-PhCl afforded no yield of product for all catalysts and bases studied. <sup>b</sup>Pd(OAc)<sub>2</sub> was used without any NHC ligand.

As such, attention shifted toward exploring bromobenzene and 4-bromoanisole as coupling partners. These substrates produced very little product when Pd(OAc)<sub>2</sub> was used without ligand. As expected for substrates containing deactivating functional groups, 4-bromoanisole afforded lower yields of product when compared to bromobenzene for all catalysts investigated. Although no universal trend was observed, **9.8-CF<sub>3</sub>** appeared to exhibit significantly higher activities than **9.8-NO<sub>2</sub>**. As described above, trifluoromethyl and nitro groups possess identical electronegativities;<sup>30</sup> hence, the relative activities exhibited by **9.8-CF<sub>3</sub>** and **9.8-NO<sub>2</sub>** may be attributed to  $\sigma$ - and  $\pi$ -contributions formed between their respective NHCs and Pd. The relatively high yields of product obtained when using **9.8-CF<sub>3</sub>** can be explained in terms of its overall donating ability being similar

to benzimidazolylidene, a NHC ligand that has been reported to be highly efficient for Heck couplings.<sup>47</sup> While this underscores the importance of differentiating  $\sigma$ - and  $\pi$ -components in NHCs to optimize yields, the overall activity displayed by these catalysts was disappointingly low, with many substrates, such as aryl chlorides, failing to react.

Since the nature of the base used in Pd-mediated coupling reactions is known to often have a profound effect on reaction rates,<sup>48</sup> we envisioned that the use of stronger bases might facilitate regeneration of active  $\text{Pd}^0$ -species better than  $\text{NaOAc}$  and thus lead to higher yields of product. Indeed, as summarized in Table 9.4, significantly improved yields and a broader scope of substrate reactivity was achieved when coupling reactions were performed using  $\text{K}_2\text{CO}_3$  as base.<sup>49</sup>

Based on the commonly accepted mechanism (see Figure 9.9), the rate liming step of Pd-catalyzed Heck reactions is usually assigned to the oxidative addition of a  $\text{Pd}^0$  species into an aryl halide.<sup>25</sup> Hence, it was surprising that **9.8-CF<sub>3</sub>** and **9.8-CN** were the two most active catalysts studied as they appeared amongst the least likely to undergo rate-limiting oxidative addition. Furthermore, in similar studies, Organ demonstrated that benzimidazolylidenes bearing electron-withdrawing fluorines in their 4- and 5-positions resulted in the lowest yields of product.<sup>23</sup>

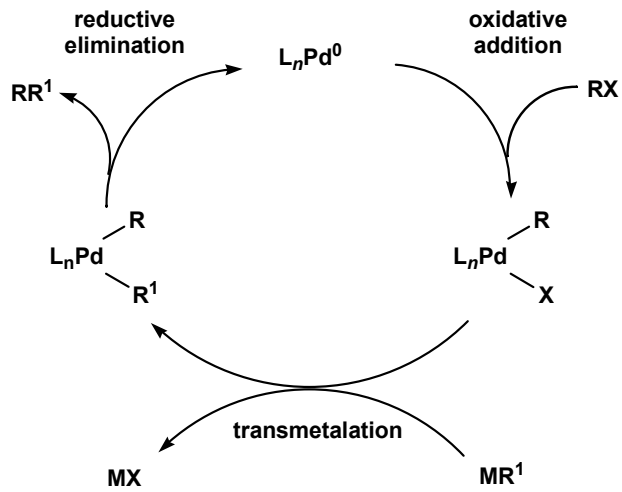


Figure 9.9    Generally accepted mechanism for Pd-catalyzed cross-coupling reactions.

Hence, we surmised that the observed results may be explained by catalyst stability. To gain support for this hypothesis, a kinetic study comparing the activity of **9.8-H** (a Pd complex containing a relatively electron rich NHC that should favor oxidative addition) with **9.8-CN** (a Pd complex containing a relatively electron deficient NHC) over time was performed. The aforementioned catalysts were selected due to their large difference in electronic properties.<sup>29</sup> 4-Bromoanisole and tert-butylacrylate were chosen as coupling partners due to the relatively high yields of products obtained with these catalysts. The reaction conditions were analogous to those described in Table 9.4. As shown in Figure 9.10, it was apparent that while **9.8-H** initiated faster than **9.8-CN**, the former lost all catalytic activity after approximately 1.5 h. In contrast, despite relatively slow initiation kinetics, **9.8-CN** remained active for more than 8 h, which ultimately afforded a higher yield of product. Assuming oxidative addition is the rate limiting step, the resting state of the catalyst is likely to be a NHC Pd<sup>0</sup> complex, where the Pd center is coordinated to one or two NHC ligands.<sup>3</sup> Hence, the enhanced stability of

**9.8-CN** may be explained by the presence of its  $\pi$ -withdrawing cyano groups, which serve to stabilize electron rich  $\text{Pd}^0$ .

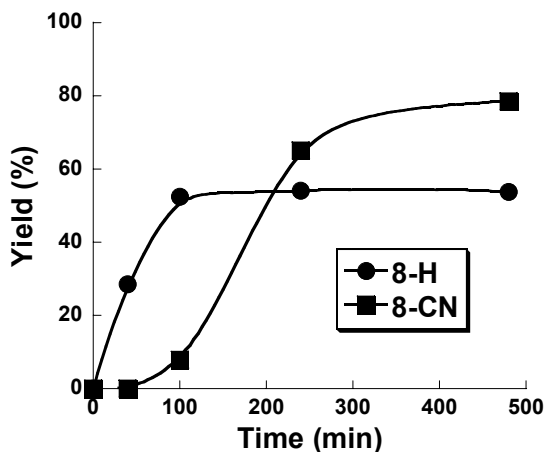


Figure 9.10 Plots of yield versus time for the Heck reaction of tert-butylacrylate with 4-bromoanisole, as catalyzed by **9.8-H** and **9.8-CN**. Conditions: catalyst (1 mol%),  $[4\text{-bromoanisole}]_0 = 0.33 \text{ M}$ ,  $[\text{tert-butyl acrylate}]_0 = 0.47 \text{ M}$ ,  $[\text{K}_2\text{CO}_3]_0 = 0.5 \text{ M}$ ,  $[\text{mesitylene}]_0 = 0.33 \text{ M}$  (internal standard), DMF as solvent,  $120^\circ\text{C}$ , nitrogen atmosphere. Yields were determined by GC.

These results suggest that for catalysts bearing electron withdrawing groups there is a fine balance between stabilizing  $\text{Pd}^0$  intermediates and slowing down the rate of oxidative addition. Indeed, close examination of Table 4 reveals that **9.8-NO<sub>2</sub>** consistently afforded the lowest yields of product; in contrast, **9.8-CF<sub>3</sub>** afforded relatively high yields of product. These subtleties highlight the sensitivity of catalytic activities towards electronic substitution and particularly the relative contributions of  $\sigma$ - and  $\pi$ -interactions present in NHC-Pd complexes.

**Deducing  $\sigma$ - and  $\pi$ -effects in Suzuki reactions catalyzed by Pd-NHC complexes.** Finally, the ability of NHC ligands with various functional groups to influence other Pd-mediating coupling reactions was explored. In particular, the Suzuki cross-coupling of aryl boronates with aryl halides was probed using NHC-Pd complexes

**9.8** as catalysts. Reactions were performed at 120 °C in DMF using 1 mol% of catalyst. In general, reactions were performed using phenylboronic acid (1.1 equiv.), an aryl halide (1.0 equiv.), and K<sub>2</sub>CO<sub>3</sub> (2.0 equiv.) as base; mesitylene (1.0 equiv.) was included as an internal standard. For this study, only the aryl halides were varied because it has been experimentally determined<sup>23</sup> that transmetallation with various derivatives of phenylboronic acid does not have any effect on the reaction rate or yield. The reactions were conducted for 18 h to minimize the effects of potentially different initiation rates exhibited by the catalysts used in this study. Yields were determined by GC analysis of aliquots taken from the crude reaction mixtures; results are summarized in Table 5.

Entry	Catalyst	R =	CH <sub>3</sub>	CH <sub>3</sub>	OCH <sub>3</sub>
		X =	Br	Cl	Br
1	<b>9.8-H</b>		85	15	51
2	<b>9.8-Cl</b>		77	12	60
3	<b>9.8-CF<sub>3</sub></b>		56	15	63
4	<b>9.8-NO<sub>2</sub></b>		32	0	12
5	<b>9.8-CN</b>		52	32	60
6 <sup>b</sup>	<b>9.Pd(OAc)<sub>2</sub></b>		44	0	42

Table 9.5 Yields of products obtained by coupling phenylboronic acid with various aryl halides using NHC-Pd complexes **9.8** as catalysts and K<sub>2</sub>CO<sub>3</sub> as base. General reaction conditions: catalyst (1 mol%), [aryl halide]<sub>0</sub> = 0.5 M, [phenylboronic acid]<sub>0</sub> = 0.55 M, [K<sub>2</sub>CO<sub>3</sub>]<sub>0</sub> = 1.0 M, [mesitylene]<sub>0</sub> = 0.5 M (internal standard), DMF as solvent, 120 °C, nitrogen atmosphere, 18 h. All reactions were performed in triplicate. Reported yields were determined by GC and are ±5%. <sup>b</sup>Pd(OAc)<sub>2</sub> was used without any ligand.

Although close examination of Table 9.5 revealed no obvious general trends, we postulate that the rate determining step of the catalytic cycle may change, depending on the electronic characteristics of the catalyst. In particular, these results suggest that the

reluctance of electron deficient catalysts to undergo oxidative addition may be compensated by enhanced reductive elimination; an opposite trend can be envisioned for catalysts possessing electron rich ligands. Hence, two distinct electronic factors may facilitate opposing processes in the catalytic cycle which ultimately results in similar overall activities. While it is difficult to establish general trends in catalytic activity, the data in Table 6 revealed that **9.8-CF<sub>3</sub>** afforded higher yields of product than **9.8-NO<sub>2</sub>** for all substrates studied. Analogous results were observed in the aforementioned Heck reactions using these same catalysts.

## CONCLUSION

In conclusion, we have synthesized and characterized a series of Rh and Pd complexes ligated to NHC ligands that bear different functional groups. These complexes were explored as catalysts for facilitating three important synthetic reactions: Rh-mediated hydroborations, Pd-mediated Heck reactions, and Pd-mediated Suzuki couplings. Particular attention was directed toward exploring how the nature of the functional group appended to the NHC ligand influenced the outcomes of the aforementioned reactions. In Rh-catalyzed hydroborations involving phenylacetylene, NHCs bearing  $\pi$ -withdrawing groups were found to afford lower yields of products when compared to  $\sigma$ -withdrawing analogues. However, essentially no differences were observed in hydroborations of alkyl acetylenes under otherwise identical conditions. Likewise, diminished effects were observed when functionalized phenylacetylenes were employed as substrates. Similar overall results were observed in Pd-catalyzed Heck reactions between *tert*-butylacrylate and certain aryl halides and, to a lesser extent, in Suzuki couplings. Namely, depending the substrate, significant differences in reaction yield was observed for Pd-catalysts bearing NHCs with  $\pi$ -withdrawing groups as compared to analogues with  $\sigma$ -withdrawing groups.

Collectively, these results provide additional support for the notion that NHCs not only participate in  $\pi$ -interactions with transition metals, an often disputed argument, but such interactions can significantly influence catalytic activities. More specifically, we have demonstrated that the nature of the interaction formed between NHCs and transition metals (i.e.,  $\sigma$  versus  $\pi$ ) often leads to significant differences in the outcomes of reactions catalyzed by NHC-metal complexes. These results should provide useful guidelines for the future design and optimization of metal catalysts bearing NHC ligands.

## EXPERIMENTAL

**General.** All reactions were performed under an atmosphere of nitrogen using standard Schlenk techniques or in a nitrogen filled glove-box. N,N-dimethylformamide (DMF) was dried with molecular sieves and degassed by two freeze-pump-thaw cycles. Tetrahydrofuran and toluene were distilled from Na/benzophenone and degassed by two freeze-pump-thaw cycles. All reagents were purchased from commercial suppliers and were used without further purification.  $^1\text{H}$  NMR spectra were recorded using a Varian Gemini (300 MHz or 400 MHz) spectrometer. Chemical shifts are reported in delta ( $\delta$ ) units, expressed in parts per million (ppm) downfield from tetramethylsilane using the residual protio solvent as an internal standard ( $\text{CDCl}_3$ , 7.24 ppm;  $\text{DMSO}-d_6$ , 2.49 ppm).  $^{13}\text{C}$  NMR spectra were recorded using a Varian Gemini (75 MHz or 100 MHz) spectrometer. Chemical shifts are reported in delta ( $\delta$ ) units, expressed in parts per million (ppm) downfield from tetramethylsilane using the solvent as an internal standard ( $\text{CDCl}_3$ , 77.0 ppm;  $\text{DMSO}-d_6$ , 39.5 ppm).  $^{13}\text{C}$  NMR spectra were routinely run with broadband decoupling. IR spectra were record using Perkin-Elmer Spectrum BX FT-IR system. High-resolution mass spectra (HRMS) were obtained with a VG analytical ZAB2-E or a Karatos MS9 instrument and are reported as m/z (relative intensity). Crystallographic data (excluding structure factors) for the structures in this paper have

been deposited with the Cambridge Crystallographic Data Centre. Copies of the data can be obtained, free of charge, on application to CCDC, 12 Union Road, Cambridge CB2 1EZ, UK, (fax: +44-(0)1223-336033 or e-mail: deposit@ccdc.cam.ac.uk).

**1,3-Dimethyl-4-trifluoromethylimidazolium iodide (9.1-CF<sub>3</sub>)**. A 30 mL vial was charged with 4-trifluoromethylimidazole (1.0 g, 7.35 mmol), NaHCO<sub>3</sub> (0.62 g, 7.35 mmol), 20 mL CH<sub>3</sub>CN, 5 mL CH<sub>3</sub>I, and stir bar. The vial was then sealed and the mixture was stirred at 60 °C. After 24 h, the solvent was removed which afforded the desired product as a 1:1 mixture with NaI in quantitative yield. <sup>1</sup>H NMR (DMSO-*d*<sub>6</sub>): δ 9.42 (s, 1H), 8.61 (s, 1H), 3.92 (s, 3H), 3.88 (s, 3H). <sup>13</sup>C NMR (DMSO-*d*<sub>6</sub>): δ 141.4, 126.5, 121.5 (q, *J*<sub>C-F</sub> = 41.3 Hz), 118.6 (q, *J*<sub>C-F</sub> = 267 Hz), 36.5, 35.1. <sup>19</sup>F NMR (DMSO-*d*<sub>6</sub>): δ -60.28. HRMS: [M]<sup>+</sup> calcd for C<sub>6</sub>H<sub>9</sub>F<sub>3</sub>N<sub>2</sub>: 166.0712; found: 166.0718.

**1,3-Dimethyl-4-trifluoromethylimidazolylidene AgI**. A 30 mL pressure vessel was charged with a mixture of 1,3-dimethyl-4-trifluoromethylimidazolium iodide / NaI (0.44 g of material, containing exactly 1.0 mmol azolium), Ag<sub>2</sub>O (0.23 g, 0.55 mmol), CH<sub>2</sub>Cl<sub>2</sub> (15 mL), and a stir bar. After sealing the vessel, the reaction mixture was stirred at 50 °C for 2 h. Subsequent cooling to ambient temperature caused solids to precipitate which were later removed via filtration. Evaporation of the residual solvent under reduced pressure afforded 0.4 g (90% yield) of desired product as a white powder. <sup>1</sup>H NMR (DMSO-*d*<sub>6</sub>): δ 8.25 (s, 1H), 3.92 (s, 3H), 3.88 (s, 3H). <sup>13</sup>C NMR (DMSO-*d*<sub>6</sub>): δ 189.2, 126.3, 121.5 (m), 37.0. <sup>19</sup>F NMR (DMSO-*d*<sub>6</sub>): -59.76.

**Rh Complex 9.6-CF<sub>3</sub>**. A 20 mL flask was charged with 1,3-dimethyl-4-trifluoromethylimidazolylidene AgI (0.12 g, 0.30 mmol), [Rh(cod)Cl]<sub>2</sub> (73 mg, 0.15 mmol), THF (10 mL), and a stir bar. The resulting mixture was then stirred at 50 °C for 4 h. Afterward, the reaction mixture was cooled to ambient temperature and then filtered through a 0.2 μm PTFE filter. Removal of residual solvent under reduced pressure

afforded 0.12 g (95% yield) of desired product as yellow solid.  $^1\text{H}$  NMR ( $\text{CDCl}_3$ ):  $\delta$  7.19 (s, 1H), 5.06 (s, 2H), 4.17 (s, 3H), 4.10 (s, 3H), 3.27 (s, 2H), 2.39 (br, 4H), 1.96 (br, 4H).  $^{13}\text{C}$  NMR ( $\text{CDCl}_3$ ):  $\delta$  189.6 (d,  $J_{\text{C}-\text{Rh}} = 51.3$  Hz), 123.9, 120.7, 118.1, 99.8 (br), 68.3 (d,  $J_{\text{C}-\text{Rh}} = 12.6$  Hz), 38.3, 36.2, 32.9 (d,  $J_{\text{C}-\text{Rh}} = 11.2$  Hz), 28.8 (d,  $J_{\text{C}-\text{Rh}} = 10.4$  Hz).  $^{19}\text{F}$  NMR ( $\text{CDCl}_3$ ):  $\delta$  -61.58. HRMS:  $[\text{M}-\text{Cl}]^+$  calcd for  $\text{C}_{14}\text{H}_{19}\text{F}_3\text{N}_2\text{Rh}$ : 375.0555; found: 375.0550. Crystals suitable for X-ray analysis were obtained by slow diffusion of hexanes vapor into concentrated acetone solution of **9.6-CF<sub>3</sub>**; CCDC 675951.

**Rh Complex 9.7-CF<sub>3</sub>.** A 5 mL flask was charged with **9.6-CF<sub>3</sub>** (30 mg, 73  $\mu\text{mol}$ ),  $\text{CDCl}_3$  (3 mL), and a stir bar. The resulting reaction mixture was then subjected to slight pressure of CO (balloon). After 1 h, the reaction was complete as determined by NMR spectroscopy. Removal of residual 1,5-cyclooctadiene (and solvent) was not attempted because (NHC) $\text{Rh}(\text{CO})_2\text{Cl}$  type complexes are generally unstable in the solid state.<sup>50</sup>  $^1\text{H}$  NMR ( $\text{CDCl}_3$ ):  $\delta$  7.37 (s, 1H), 4.00 (s, 3H), 3.94 (s, 3H).  $^{13}\text{C}$  NMR ( $\text{CDCl}_3$ ):  $\delta$  184.8 (d,  $J_{\text{C}-\text{Rh}} = 68.4$  Hz), 180.8 (d,  $J_{\text{C}-\text{Rh}} = 59$  Hz), 124.57 (d,  $J_{\text{C}-\text{F}} = 5.1$  Hz), 119.4, (q,  $J_{\text{C}-\text{Rh}} = 355$  Hz), 39.0, 37.0.  $^{19}\text{F}$  NMR ( $\text{CDCl}_3$ ):  $\delta$  -61.51. HRMS:  $[\text{M}-2\text{CO}]^+$  calcd for  $\text{C}_6\text{H}_7\text{ClF}_3\text{N}_2\text{Rh}$ : 301.9305; found: 301.9310.

**Pd Complex 9.8-H.** After charging a 25 mL flask with 1,3-dimethylimidazolium iodide (0.45 g, 2.0 mmol),  $\text{Pd}(\text{OAc})_2$  (0.21 g, 0.95 mmol), 15 mL DMSO, and a stir bar, the resulting reaction mixture was heated to 120 °C for 2 h. Subsequent cooling to ambient temperature followed by the addition of 40 mL of  $\text{H}_2\text{O}$  to the reaction vessel caused solids to precipitate. The solids were collected by filtration, washed with 20 mL of  $\text{H}_2\text{O}$ , and then dried under reduced pressure to afford 0.5 g (95% yield) of the desired product as yellow powder. Spectroscopic data matched literature reports.<sup>51</sup>

**Pd Complex 9.8-Cl.** After charging a 25 mL flask with 1,3-dimethyl-4,5-dichloro-imidazolium iodide (0.59 g, 2.0 mmol),  $\text{Pd}(\text{OAc})_2$  (0.21 g, 0.95 mmol), 15 mL

DMSO, and a stir bar, the resulting reaction mixture was heated to 80 °C for 1 h. Subsequent cooling to ambient temperature followed by the addition of 50 mL of H<sub>2</sub>O to the reaction vessel caused solids to precipitate. The solids were collected by filtration, washed with 20 mL H<sub>2</sub>O, and then dried under reduced pressure to afford 0.61 g (93% yield) of the desired product as a yellow powder. The solution structure of this complex was found to be predominantly (>95%) *cis* by <sup>1</sup>H NMR spectroscopy. <sup>1</sup>H NMR (DMSO-*d*<sub>6</sub>): δ 3.88 (s, 6H). <sup>13</sup>C NMR (DMSO-*d*<sub>6</sub>): δ 162.6, 117.1, 37.5. HRMS: [M]<sup>+</sup> calcd for C<sub>10</sub>H<sub>12</sub>Cl<sub>4</sub>N<sub>4</sub>PdI<sub>2</sub>: 685.6946; found: 685.6946. Crystals suitable for X-ray analysis were obtained by slow cooling of saturated DMSO solution of **9.8-Cl**; CCDC 675948.

**Pd Complex 9.8-CF<sub>3</sub>.** After charging a 25 mL flask with 1,3-dimethyl-4-trifluoromethylimidazolium iodide (0.58 g, 2.0 mmol), Pd(OAc)<sub>2</sub> (0.21 g, 0.95 mmol), 15 mL DMSO, and a stir bar, the resulting reaction mixture was heated to 80 °C for 1 h. Subsequent cooling to ambient temperature followed by addition of 50 mL of H<sub>2</sub>O to the reaction vessel caused solids to precipitate. The solids were collected by filtration, washed with 25 mL of H<sub>2</sub>O, and then dried under reduced pressure to afford 0.60 g (92% yield) of the desired product as a yellow powder. A mixture of complexes with *cis*- and *trans*-geometries were found by <sup>1</sup>H NMR spectroscopy. Likewise, the <sup>19</sup>F NMR spectrum revealed that the product adopted a mixture of various geometrical isomers in an approximately 2:2:2:1 ratio. As noted in the text, X-ray crystallography revealed that **9.8-CF<sub>3</sub>** adopted a *trans* geometry in the solid state. <sup>1</sup>H NMR (DMSO-*d*<sub>6</sub>): δ 8.26 (m, 2), 4.00-3.81 (m, 12H). <sup>13</sup>C NMR (DMSO-*d*<sub>6</sub>): δ 173.7, 168.8, 127.2 (q, *J*<sub>C-F</sub> = 7.7 Hz), 126.6 (m), 122.5-121.7 (m), 119.6 (q, *J*<sub>C-F</sub> = 265 Hz), 119.4 (q, *J*<sub>C-F</sub> = 265 Hz), 38.2, 37.3, 37.1, 36.4. <sup>19</sup>F NMR (DMSO-*d*<sub>6</sub>): δ -59.94 (s, 3F), -60.16 (s, 3F), -60.24 (s, 2F + 0.8F from overlapping minor isomer), -60.34 (s, 0.8F). HRMS: [M]<sup>+</sup> calcd for C<sub>12</sub>H<sub>14</sub>F<sub>6</sub>N<sub>4</sub>PdI<sub>2</sub>:

685.8252; found: 685.8256. Crystals suitable for X-ray analysis were obtained by slow diffusion of water into a concentrated DMSO solution of **9.8-CF<sub>3</sub>**; CCDC 675947.

**Pd Complex 9.8-NO<sub>2</sub>.** After charging a 25 mL flask with 1,3-dimethyl-4-nitroimidazolium iodide (0.54 g, 2.0 mmol), Pd(OAc)<sub>2</sub> (0.21 g, 0.95 mmol), 15 mL DMSO, and a stir bar, the resulting reaction mixture was heated to 80 °C for 1 h. Subsequent cooling to ambient temperature followed by addition of 50 mL of H<sub>2</sub>O to reaction vessel caused solids to precipitate. The solids were collected by filtration, washed with 50 mL of H<sub>2</sub>O, and then dried under reduced pressure to afford 0.58 g (90% yield) of the desired product as a yellow powder. Although the solution structure of this complex was found to be predominantly (>95%) *cis* by <sup>1</sup>H NMR spectroscopy, equimolar quantities of two isomers exhibiting C<sub>2v</sub> and S<sub>2</sub> symmetries were observed. <sup>1</sup>H NMR (DMSO-*d*<sub>6</sub>): δ 8.782 (s, 1H), 8.769 (s, 1H), 4.19 (s, 3H), 3.94 (s, 3H). <sup>13</sup>C NMR (DMSO-*d*<sub>6</sub>): δ 169.4, 139.5, 127.40, 127.34, 39.6, 39.4. HRMS: [M]<sup>+</sup> calcd for C<sub>10</sub>H<sub>14</sub>N<sub>6</sub>O<sub>4</sub>PdI<sub>2</sub>: 641.8201; found: 641.8204. Crystals suitable for X-ray analysis were obtained by slow diffusion of hexanes into a concentrated CHCl<sub>3</sub> solution of **9.8-NO<sub>2</sub>**; CCDC 675951.

**Pd Complex 9.8-CN.** After charging a 25 mL flask with 1,3-dimethyl-4,5-dicyanoimidazolium iodide (0.56 g, 2.0 mmol), Pd(OAc)<sub>2</sub> (0.21 g, 0.95 mmol), 15 mL DMSO, and a stir bar, the resulting reaction mixture was heated to 80 °C for 1 h. Subsequent cooling to ambient temperature followed by addition of 50 mL of H<sub>2</sub>O to reaction vessel caused solids to precipitate. The solids were collected by filtration, washed with 50 mL of H<sub>2</sub>O, and then dried under reduced pressure to afford 0.60 g (96% yield) of the desired product as a yellow powder. The solution structure of this complex was found to be predominantly (>95%) *cis* by <sup>1</sup>H NMR spectroscopy. <sup>1</sup>H NMR (DMSO-*d*<sub>6</sub>): δ 4.04 (s, 6H). <sup>13</sup>C NMR (DMSO-*d*<sub>6</sub>): δ 172.5, 115.9, 107.2, 39.0. HRMS: [M+H]<sup>+</sup> calcd for C<sub>14</sub>H<sub>13</sub>N<sub>8</sub>PdI<sub>2</sub>: 652.8387; found, 652.9391. Crystals suitable for X-ray analysis

were obtained by slow diffusion of diethyl ether into a saturated N,N-dimethylformamide solution of **9.8-CN**; CCDC 675950.

**General procedure used for performing hydroboration reactions.** Rh complex (0.03 mmol) was first weighed into a glass vial and then sealed with a 20/400 TFE/silicone (Alltech) septa followed by a plastic open-centered cap. THF (3 mL), Et<sub>3</sub>N (0.7 mL, 5 mmol), pinacolborane (0.14 mL, 1.0 mmol), an internal standard such as 1,3,5-trimethoxybenzene (61 mg, 0.30 mmol) or mesitylene (0.17 mL, 1.2 mmol), and a stir bar were then added in succession. After stirring at ambient temperature for 30 min, 1-octyne (0.18 mL, 1.2 mmol) or phenylacetylene (0.13 mL, 1.2 mmol) was then added. After stirring the resulting mixture for an additional 14 h at 25 °C, any residual borane was quenched through the addition of excess MeOH (0.5 mL). An aliquot was taken from the crude reaction mixture, diluted with CDCl<sub>3</sub> and then analyzed using <sup>1</sup>H NMR spectroscopy.

**General procedure used for performing Heck coupling reactions.** A stock solution of *tert*-butyl acrylate (0.47 M), aryl halide (0.33 M), and mesitylene (0.33 M) (internal standard) was first prepared in DMF. In a separate vial, base (1.5 mmol), catalyst (0.01 mmol), and 3 mL of the aforementioned stock solution were combined under an atmosphere of nitrogen. The vial was then sealed and placed into an oil bath at 120 °C for 18 h. Afterward, an aliquot was removed, diluted with ethyl acetate, filtered and then analyzed by GC.

**General procedure used for performing Suzuki coupling reactions.** A stock solution of phenylboronic acid (0.55 M), aryl halide (0.5 M), and mesitylene (0.5 M) (internal standard) was first prepared in DMF. In a separate vial, base (1.5 mmol), catalyst (0.01 mmol), and 2 mL of the aforementioned stock were combined under an atmosphere of nitrogen. The vial was then sealed and placed into an oil bath at 120 °C for

18 h. Afterward, an aliquot was removed, diluted with ethyl acetate, filtered and then analyzed by GC.

## REFERENCES

- 1 (a) Wanzlick, H. W.; Schönherr, H. J. *Angew. Chem. Int. Ed.* **1968**, *7*, 141. (b) Öfele, K. *J. Organomet. Chem.* **1968**, *12*, P42. (c) Cardin, D. J.; Çetinkaya, B.; Çetinkaya, E.; Lappert, M. F. *J. Chem. Soc., Dalton Trans.* **1973**, 514.
- 2 Arduengo, A. J., III; Harlow, R. L.; Kline, M. *J. Am. Chem. Soc.* **1991**, *113*, 361.
- 3 For recent reviews of catalytically-active transition metal complexes containing N-heterocyclic carbenes, see: (a) Peris, E.; Crabtree, R. H. *Coord. Chem. Rev.* **2004**, *248*, 2239. (b) Cavell, K. J.; McGuiness, D. S. *Coord. Chem. Rev.* **2004**, *248*, 671. (c) Herrmann, W. A. *Angew. Chem., Int. Ed.* **2002**, *41*, 1290. (d) Hillier, A. C.; Gasa, G. A.; Viciu, M. S.; Lee, H. M.; Yang, C. L.; Nolan, S. P. *J. Organomet. Chem.* **2002**, *653*, 69. (e) Herrmann, W. A.; Elison, M.; Fischer, J.; Köcher, C.; Artus, G. R. *Angew. Chem. Int. Ed.* **1996**, *34*, 2371. (f) Diez-González, S.; Nola, S. P. *Top Organomet. Chem.* **2007**, *21*, 47. (g) Bourissou, D.; Guerret, O.; Gabbaï, F. P. *Chem. Rev.* **2000**, *100*, 39.
- 4 For representative examples, see: (a) Marion, N.; Navarro, O.; Mei, J.; Stevens, E. D.; Scott, N. M.; Nolan, S. P. *J. Am. Chem. Soc.* **2006**, *128*, 4101. (b) Navarro, O.; Marion, N.; Oonishi, Y.; Kelly, R. A., III; Nolan, S. P. *J. Org. Chem.* **2006**, *71*, 685. (c) Louie, J.; Gibby, J. E.; Farnworth, M. V.; Tekavec, T. N. *J. Am. Chem. Soc.* **2002**, *124*, 15188. (d) Jørgensen, M.; Lee, S.; Liu, X.; Wolkowski, J. P.; Hartwig, J. F. *J. Am. Chem. Soc.* **2002**, *124*, 12557. (e) Trnka, T. M.; Grubbs, R. H. *Acc. Chem. Res.* **2001**, *34*, 18.
- 5 Herrmann, W. A.; Mihalios, D.; Ofele, K.; Kipfor, P.; Belmedjahed, F. *Chem. Ber.* **1992**, *125*, 1795.
- 6 Jafarpour, L.; Stevens, E. D.; Nolan, S. P. *J. Organomet. Chem.* **2000**, *606*, 2000.
- 7 Scholl, M.; Ding, S.; Lee, C. W.; Grubbs, R. H. *Org. Lett.* **1999**, *1*, 953.
- 8 O'Brien, C. J.; Kantchev, E. A. B.; Valente, C.; Hadei, N.; Chass, G. A.; Lough, A.; Hopkinson, A. C.; Organ, M. G. *Chem. Eur. J.* **2006**, *12*, 4743.
- 9 (a) Herrmann, W. A.; Schwarz, J.; Gardiner, M. G. *Organometallics* **1999**, *18*, 4082. (b) Voutchkova, A. M.; Feliz, M.; Clot, E.; Eisenstein, O.; Crabtree, R. H. *J. Am. Chem. Soc.* **2007**, *129*, 12834. (c) Lin, I. J. B.; Vasam, C. S. *Coord. Chem. Rev.* **1998**, *251*, 642. (d) Wang, H. M. J.; Lin, I. J. B. *Organometallics* **1998**, *17*, 972.

- 10 (a) Boydston, A. J.; Williams, K. A.; Bielawski, C. W. *J. Am. Chem. Soc.* **2005**, 127, 12496. (b) Khramov, D. M.; Boystron, A. J.; Bielawski, C. W. *Angew. Chem. Int. Ed.* **2006**, 45, 6186. (c) Boydston, A. J.; Bielawski, C. W. *Dalton Trans.* **2006**, 4073. (d) Boydston, A. J.; Rice, J. D.; Sanderson, M. D.; Dykhno, O. L.; Bielawski, C. W. *Organometallics* **2006**, 25, 6087.
- 11 Cotton, F. A.; Wilkinson, G. *Advanced Inorganic Chemistry*, 5<sup>th</sup> Ed.; Wiley-Interscience: New York, 1988.
- 12 (a) Hartwig, J. F. *Angew. Chem., Int. Ed.* **1998**, 37, 2046. (b) Wolfe, J. P.; Wagaw, S.; Marcox, J.-F.; Buchwald, S. L. *Acc. Chem. Res.* **1998**, 31, 805. (c) Prim, D.; Campagne, J.-M.; Joseph, D.; Andrioletti, B. *Tetrahedron* **2002**, 58, 2041. (d) Altenhoff, G.; Goddard, R.; Lehmann, C. W.; Glorius, F. *J. Am. Chem. Soc.* **2004**, 126, 15195.
- 13 Glorius, F. *Top. Organomet. Chem.* **2007**, 21, 1
- 14 Courchay, F. C.; Sworen, J. C.; Coronado, A.; Wagener, K. B. *J. Mol. Cat. A: Chemical* **2006**, 254, 111.
- 15 Fürstner, A.; Ackermann, L.; Gabor, B.; Goddard, R.; Lehann, C. W.; Mynott, R.; Stelzer, F.; Thiel, O. R. *Chem. Eur. J.* **2001**, 7, 3236.
- 16 Leuthaeusser, S.; Schwazr, D.; Plenio, H. *Chem. Eur. J.* **2007**, 13, 7195.
- 17 Alcarazo, M.; Fernández, R.; Alvarez, E.; Lassaletta, J. M. *J. Organomet. Chem.* **2005**, 690, 5979.
- 18 Präsang, C.; Donnadieu, B.; Bertrand, G. *J. Am. Chem. Soc.* **2005**, 127, 10182.
- 19 Herrmann, W. A.; Schütz, J.; Frey, G. D.; Herdtweck, E. *Organometallics* **2006**, 25, 2437.
- 20 For ranking of various carbenes according to their electron donating properties, see: Fürstner, A.; Alcarazo, M.; Krause, H.; Lehmann, C. W. *J. Am. Chem. Soc.* **2007**, 129, 12676.
- 21 (a) Yun, J.; Marinez, E. R.; Grubbs, R. H. *Organometallics* **2004**, 23, 4172. (b) Barinet, P.; Yap, G. P. A.; Richeson, D. S. *J. Am. Chem. Soc.* **2003**, 125, 13314.
- 22 (a) Chianese, A. R.; Li, X.; Janzen M. C.; Faller, J. W.; Crabtree, R. H. *Organometallics* **2003**, 22, 1663. (b) Iglesias, M.; Beetstra, D. J.; Stasch, A.; Horton, P. N.; Hursthouse, M. B.; Coles, S. J. Cavell, K. J. Dervisi, A.; Fallis, I. A. *Organometallics* **2007**, 26, 4800.

- 23 (a) Hadei, N.; Kantchev, E. A. B; O'Brien, C. J.; Organ, M. G. *Org. Lett.* **2005**, *7*, 1991. (b) O'Brien, C. J.; Kantchev, E. A. B; Chass, G. A.; Hadei, N.; Hopkinson, A. C.; Organ, M. G.; Setiadi, D. H.; Tang, T.-H.; Fang, D.-C. *Tetrahedron* **2005**, *61*, 9723.
- 24 For excellent reviews of cross-coupling reactions involving organoboron compounds see: (a) Miyaura, N.; Suzuki, A. *Chem. Rev.* **1995**, *95*, 2457. (b) Suzuki, A. *J. Organomet. Chem.* **1999**, *576*, 147.
- 25 For an excellent review on Pd-catalyzed cross couplings see: Littke, A. F.; Fu, G. C. *Angew. Chem. Int. Ed.* **2002**, *41*, 4176.
- 26 For a theoretical analysis of a NHC-Ir complex where NHC  $\pi$ -donation was found to be significant, see: Scott, N. M.; Dorta, R.; Stevens, E. D.; Correa, A.; Cavallo, L.; Nolan, S. P. *J. Am. Chem. Soc.* **2005**, *127*, 3516.
- 27 (a) Herrmann, W. A.; Köcher, C. *Angew. Chem., Int. Ed.* **1997**, *36*, 2162. (b) Boehme, C.; Frenking, G. *Organometallics* **1998**, *17*, 5801. (c) Green, J. C.; Herbert, B. J. *J. Chem. Soc., Dalton Trans.* **2005**, 1214. (d) Lee, M.; Hu, C. *Organometallics* **2004**, *23*, 976. (e) Heinemann, C.; Müller, T.; Apeloig, Y.; Schwarz, H. *J. Am. Chem. Soc.* **1996**, *118*, 2023. (f) Boehme, C.; Frenking, G. *J. Am. Chem. Soc.* **1996**, *118*, 2039. (g) Arduengo, A. J. III; Dias, H. V. R.; Dixon, D. A.; Harlow, R. L.; Klooster, W. T.; Koetzle, T. F. *J. Am. Chem. Soc.* **1994**, *116*, 6812.
- 28 (a) Tulloch, A. D. D.; Danopoulos, A. B.; Kleinhenz, S.; Light, M. E.; Hursthouse, M. B.; Eastham, G. *Organometallics* **2001**, *20*, 2027. (b) Hu, X.; Castro-Rodriguez, I.; Olsen, K.; Meyer, K. *Organometallics* **2004**, *23*, 755. (c) Nemcsok, D.; Wichmann, K.; Frenking, G. *Organometallics* **2004**, *23*, 3640. (d) Jacobsen, H.; Correa, A.; Costabile, C.; Cavallo, L. *J. Organomet. Chem.* **2006**, *691*, 4350.
- 29 Khramov, D. M.; Lynch, V. M.; Bielawski, C. W. *Organometallics* **2007**, *26*, 6042.
- 30 Group electronegativities: H, 2.1; Cl, 3.0; CN, 3.3; CF<sub>3</sub>, 3.4; NO<sub>2</sub>, 3.4, see: (a) Wells, P.R. *Prog. Phys. Org. Chem.* **1968**, *6*, 111. (b) Anslyn, E. V.; Dougherty, D. A. *Modern Physical Organic Chemistry*; University Science Books: Sausalito, CA, 2006; pg. 16.
- 31 Furthermore, the pKa of 3-trifluoromethylbenzoic acid (5.16) in a 1 : 1 mixture of CH<sub>3</sub>OH : H<sub>2</sub>O is very similar to that of its nitro analogue (4.85), see: De Maria, P.; Fontana, A.; Spinelli, D.; Dell'Erba, C.; Novi, M.; Petrillo, G.; Sancassan, F. *J. Chem. Soc., Perkin Trans. 2*, **1993**, 649.

- 32 (a) Smith, K.; Pelter, A.; Brown, H. C. Borane Reagents; Academic Press: London, 1988. (b) Smith, K.; Pelter, A. In Comprehensive Organic Synthesis; Trost, B. M., Fleming, I., Eds.; Pergamon Press: Oxford, **1991**; Vol. 8, pg. 703. (c) Tucker, C. E.; Davidson, J.; Knochel, P. *J. Org. Chem.* **1992**, *57*, 3482.
- 33 (a) Burgess, K.; Ohlmeyer, M. *J. Chem. Rev.* **1991**, *91*, 1179. (b) Beletskaya, I.; Pelter, A. *Tetrahedron* **1997**, *53*, 4957.
- 34 Ohmura, T.; Yamamoto, Y.; Miyaura, N. *J. Am. Chem. Soc.* **2000**, *122*, 4990.
- 35 Although to the best of our knowledge hydroborations using Rh-NHC complexes are unknown, diborylations of styrene have been demonstrated with Cu-, Pd-, Ag-, Au-, and Pt-NHC complexes and hydroborations mediated by Pt-NHC complexes have been reported. For examples of transition metal mediated diborylations involving NHC ligands, see: (a) Lillo, V.; Fructos, M. R.; Ramírez, J.; Braga, A. A. C.; Maseras, F.; Díaz-Requejo, M. M.; Pérez, P. J.; Fernández, E. *Chem. Eur. J.* **2007**, *13*, 2614. (b) Corberán, R.; Ramírez, J.; Sanaú, M.; Peris E.; Fernandez, E. *Chem. Commun.*, **2005**, 3056. (c) Corberán, R.; Ramírez, J.; Poyatos, M.; Peris, E.; Fernandez, E. *Tetrahedron: Asymmetry*, **2006**, *17*, 1759. (d) Lillo, V.; Mata, J.; Ramírez, J.; Peris E.; Fernandez E. *Organometallics*, **2006**, *25*, 5829. (e) Lillo, V.; Fructos, M. R.; Ramírez, J.; Braga, A. A. C.; Maseras, F.; Díaz Requejo, M. M.; Pérez P. J.; Fernandez, E. *Chem.-Eur. J.*, **2007**, *13*, 2614. For Pt-NHC hydroborations, see: Lillo, V.; Mata, J. A.; Segarra, A. M.; Peris, E.; Fernandez, E. *Chem. Commun.* **2007**, 2184.
- 36 Voutchkova, A. M.; Appelhans, L. N.; Chianese, A. R.; Crabtree, R. H. *J. Am. Chem. Soc.* **2007**, *127*, 17624.
- 37 Mannig, D.; Noth, H. *Angew. Chem., Int. Ed. Eng.* **1985**, *24*, 878.
- 38 For detailed mechanistic studies of hydroboration reactions, see: (a) Evans, D. A.; Fu, G. C.; Anderson, B. A. *J. Am. Chem. Soc.* **1992**, *114*, 6680. (b) Burgess, K.; van der Donk, W. A.; Farstfer, M. B.; Ohlmeyer, M. J. *J. Am. Chem. Soc.* **1991**, *113*, 6139. (c) Widauer, C.; Grützmacher, H.; Ziegler, T. *Organometallics* **2000**, *19*, 2097. For *ab initio* studies of Rh catalyzed hydroborations of alkenes see: Musaev, D. G.; Mebel, A. M.; Morokuma, K. *J. Am. Chem. Soc.* **1994**, *116*, 10693.
- 39 For mechanistic studies of catalyzed hydrometalation of terminal alkynes, see: (a) Ojima, I.; Clos, N.; Donovan, R. J.; Ingallina, P. *Organometallics* **1990**, *9*, 3127. (b) Tanke, R. S.; Crabtree, R. H. *J. Am. Chem. Soc.* **1990**, *112*, 7984. (c) Jun, C.-H.; Crabtree, R. H. *J. Organomet. Chem.* **1993**, *447*, 177. (d) Maruyama, Y.; Yamamura, K.; Nakayama, I.; Yoshiuchi, K.; Ozawa, F. *J. Am. Chem. Soc.* **1998**, *120*, 1421.

- 40 Knorr, J. R.; Merola, J. S. *Organometallics* **1990**, *9*, 3008.
- 41 (a) Musaev, D.G.; Mebel, A.M.; Morokuma, K. *J. Am. Chem. Soc.* **1994**, *116*, 10693. (b) Knorr, J.R.; Merola, J.S. *Organometallics* **1990**, *9*, 3008.
- 42 Baker, M. V.; Skelton, B. W.; White, A. H.; Williams, C. C. *J. Chem. Soc., Dalton Trans.* **2001**, 111.
- 43 Trace Pd(OAc)<sub>2</sub> is known to catalyze these transformations without any ligand, see: de Vries, A. H. M.; Lunders, J. M. C. A.; Mommers, J. H. M.; Henderickx, H. J. W.; de Vries, J. G. *Org. Lett.* **2003**, *5*, 3285.
- 44 For an analysis of difference in reactivity exhibited by *cis* and *trans* bis-NHC Pd complexes, see (a) McGuinness, D. S.; Green, M. J.; Cavell, K. J.; Sketon, B. W.; White, A. H. *J. Organomet. Chem.* **1998**, *565*, 165. (b) Huynh, H. V.; Ho, J. H. H.; Neo, T. C.; Kon, L. L. *J. Organomet. Chem.* **2005**, *690*, 3854.
- 45 For additional evidence of  $\pi$ -backbonding interactions in NHC-Pd complexes see: Hara, K.; Kanamori, Y.; Sawamura, M. *Bull. Chem. Soc. Jpn.* **2006**, *79*, 1781.
- 46 Preliminary studies revealed that all coupling reactions were complete in less than 18 h; see below for additional details on the kinetics of these reactions.
- 47 The relative electron donor abilities of 1,3-dimethyl-benzimidazolylidene ( $\delta = 5.04 - 4.99$  ppm) and 1,3-dimethyl-4,5-ditrifluoromethylimidazolylidene (5.06 ppm) were determined by comparing the chemical shifts of the *trans*-olefins in their respective NHC-RhCl(COD) complexes; see: Baker, M. V.; Brayshaw, S. K.; Skelton, B. W.; White, A. H. *Inorg. Chim. Act.* **2004**, *357*, 2841.
- 48 (a) Shekhard, S.; Hartwig, J. F. *Organometallics* **2007**, *26*, 340. (b) Böhm, V. P. W.; Herrmann, W. A. *Chem. Eur. J.* **2001**, *7*, 4191.
- 49 The use of other bases, such as Na<sub>2</sub>HPO<sub>4</sub>, did not afford appreciably improved yields of product.
- 50 Upon concentration, NHC-Rh carbonyl complexes generally dimerize with concomitant loss of carbon monoxide, see: Sanderson, M. D.; Kamplain, J. W.; Bielawski, C. W. *J. Am. Chem. Soc.* **2007**, *128*, 16514.
- 51 Herrman, W. A.; Fischer, J.; Öfele, K.; Artus, G. R. *J. J. Organomet. Chem.* **1997**, *530*, 259.

## Appendix A: Synthesis of Methyl 2-(trifluoromethyl)acrylate

### EXPERIMENTAL

2-(trifluoromethyl)acrylic acid **A.1** (75 g, 0.54 mol) was dissolved in 500 ml dimethylsulfate and the reaction vessel was heated to 120 °C under atmosphere of nitrogen for 48 hours (figure A.1). The color of the reaction changed to dark brown over 6 hours. After the reaction was cooled to room temperature, a <sup>1</sup>H NMR analysis of an aliquot showed that the ratio of desired product to starting material was 9:1.<sup>1</sup>

The crude reaction was subjected to vacuum distillation by heating the still pot to 120 °C and cooling the receiving flask with dry ice (-78 °C). The pressure was gradually reduced to 100 millitorr over 1 hour, maintaining the temperature of the still head at ~100 °C to obtain 60 grams (73%) of clear liquid. The <sup>1</sup>H NMR analysis of the liquid indicated that the material collected consisted of desired product **A.2** with approximately 6 mol% of dimethyl sulfate impurity. Second distillation with a vigreux column was performed at atmospheric pressure and a fraction boiling at 75-80 °C was collected to obtain 45 grams of the desired product in 55% yield with no detectable impurities.

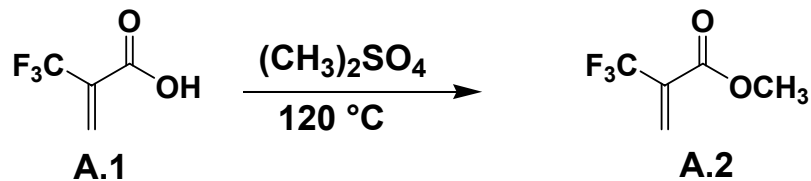


Figure A.1 Esterification of 2-(trifluoromethyl)acrylic acid.

<sup>1</sup>H NMR (CDCl<sub>3</sub>): 6.62 (q, J<sub>H-F</sub> = 1.5 Hz, 1H), 6.34 (q, J<sub>H-F</sub> = 1.2 Hz, 1H), 3.73 (s, 3H) δ. <sup>13</sup>C NMR (CDCl<sub>3</sub>): δ 161.6 (q, J<sub>C-F</sub> = 1.8 Hz), 132.6 (q, J<sub>C-F</sub> = 5.1 Hz), 131.2 (q, J<sub>C-F</sub> = 32.1 Hz), 121.1 (q, J<sub>C-F</sub> = 272.1 Hz), 52.2. <sup>19</sup>F NMR (CDCl<sub>3</sub>): δ -66.73 (s).

## REFERENCES

- 1      Similar reaction using methyl triflate as solvent showed complete consumption of starting material after 1 hour. However due to cost and high volatility of methyl triflate, separation of impurities from the desired product was considered impractical.

## **Vita**

Dimitri Mikhailovich Khramov was born in Novosibirsk, Russia on September 16, 1981. At the age of 13 he moved to San Luis Potosi, Mexico where he spent one year before returning back to Russia. He remained in Russia for one year before moving to Starkville, Mississippi USA where he attended Starkville High School. For the last two years of secondary education, he attended the Mississippi School for Mathematics and Science in Columbus, MS. After graduating from high school in 1999, he attended the Mississippi State University and was awarded a Bachelor of Science degree in Chemistry in May 2002. Later in 2002, he moved to Austin, Texas, and joined the research group of Professor Pagenkopf as a graduate student where he spent two and a half years before joining the research group of Professor Bielawski.

Permanent address: 10285 Sugar Creek dr, Pensacola, FL 32514

This dissertation was typed by the author.